BERGISCHE
UNIVERSITÄT
WUPPERTAL

Effects of Recycling Process on Performance-Related Properties of Recycled Asphalt Mixtures Before and After Ageing

Dissertation

zur Erlangung eines Doktorgrades
(Dr. -Ing.)

in der
Fakultät für Architektur und Bauingenieurwesen
der
Bergischen Universität Wuppertal

vorgelegt von
M.Sc. Haydar Raheem Al-Saaidy
aus Baghdad (IRAQ)

Gutachter:	Univ. -Prof. Dr. -Ing Hartmut Beckedahl
	Univ. -Prof. Dr. -Ing Pahirangan Sivapatham
Dissertation eingereicht:	July, 2019
Tag der mündlichen Prüfung:	06.03.2020

The PhD thesis can be quoted as follows:

urn:nbn:de:hbz:468-20201029-121452-2
[http://nbn-resolving.de/urn/resolver.pl?urn=urn%3Anbn%3Ade%3Ahbz%3A468-20201029-121452-2]

DOI: 10.25926/b91j-sa45
[https://doi.org/10.25926/b91j-sa45]

Tag des Kolloquiums:
06.03.2020
Dekan:
Univ. -Prof. Dr. -Ing Felix Huber

Mitglieder des Prüfungsausschusses:
Univ. -Prof. Dr. -Ing Felix Huber (Vorsitzenden)
Univ. -Prof. Dr. -Ing Hartmut Beckedahl (Berichterstatter)
Univ. -Prof. Dr. -Ing Pahirangan Sivapatham (Berichterstatter)
Univ. -Prof. Dr. -Ing Steffen Anders (Akademischen Mitarbeiter)

Erklärung

Ich erkläre hiermit an Eides statt, dass ich die vorliegende Arbeit selbständig und ohne unerlaubte fremde Hilfe angefertigt sowie andere als die angegebenen Quellen und Hilfsmittel nicht benutzt habe. Die aus fremden Quellen direkt oder indirekt übernommenen Stellen sind als solche kenntlich gemacht. Die Arbeit wurde bisher in gleicher oder ähnlicher Form keinem anderen Prüfungsamt vorgelegt und auch nicht veröffentlicht.

Ort, Datum----------

Dedication

I dedicate this humble effort to the soul of my Mother and to my Father for his continuous and endless support and courage during the course of the study

I would also dedicate this book to my family for their support

Acknowledgment

I would like to show my gratitude to ***Prof. Dr. -Ing H.J. Beckedahl*** for sharing his pearls of wisdom with me during the course of this research.

I would also thank ***Dr. Ian Barnes*** for help in the Chemistry Department. I thank BestLab team of the University of Wuppertal, who provided insight and expertise that greatly assisted the research, even if they may not entirely agree with all of the interpretations/conclusions of this dissertation.

Table of contents

Nomenclature

%	Percent
‰	Per Mille
µm	Micro Meter
BC	Before Christ
CI	Colloidal Index
DSR	Dynamic Shear Rheometer
et al	and others
F	Frequency
Fig.	Figure
H	Hour
Hz	Hertz
IR	Infra-Red
K	Kelvin
KBR	Potassium Bromide
LTA	Long-Term Ageing
LTOA	Long-Term Oven Ageing
M-%	Percent by mass
Max.	Maximum
Min.	Minimum
MPa	Mega Pascal
ºC	Degree Celsius
PAV	Pressure Ageing Vessel
Pen	Penetration
R&B	Ring and Ball
RAP	Reclaimed Asphalt Pavement
RILEM	International Union of Testing and Research Laboratories for Materials and Structures

RTFOT	Rolling Tihn Film Oven Test
STA	Short-Term Ageing
STOA	Short-Term Oven Ageing
T	Temperature
TFOT	Thin Film Oven Test
UV	Ultra Violet
V	Volt
E	Strain

List of tables

List of figures

Abstract

The process of reusing reclaimed asphalt pavement (RAP) has gained much interest due to its proven economic and environmental benefits. It saves natural resources, namely bitumen and aggregates, and reduces the production costs of asphalt mixes. Therefore, many techniques have been developed to enhance production quality regarding the materials used and performance of the final mix. In addition, researchers have focused on accelerating bitumen and asphalt ageing in the lab to simulate bitumen and asphalt ageing in the field during service life.

This study examines both ageing of bitumen in asphalt and reusing of RAP. The first part examines the accelerated ageing of bitumen in asphalt mixes when using a liquid oxidizer (hydrogen peroxide) or a gaseous oxidizer (ozone), in order to study the effect of bitumen oxidation on the performance of aged asphalt as well as to examine the properties of aged bitumen. The results show that ageing by hydrogen peroxide increases the stiffness of aged asphalt by 10% at low temperatures, while the differences in stiffness are marginal at high temperatures compared to the new mix. Furthermore, the results of fatigue resistance show an increase in fatigue resistance at heavy- and light-loadings (0.10‰ and 0.03‰ respectively), of peroxide aged asphalt over unaged asphalt at a rate of 162% and 477% respectively. The results for the physical, chemical, and rheological properties were determined for bitumen aged by hydrogen peroxide. Identical results were obtained regarding long-term aged bitumen after a pressure-ageing vessel (PAV) test. However, the test procedure requires improvements to increase the ageing efficiency of hydrogen peroxide and to meet safety regulations.

The results of ageing by using ozone as oxidizing agent was conducted by subjecting asphalt mixture to a constant stream of ozone and showed an increase in the stiffness of the aged mix. The increase was about 4% at low temperatures as compared to the new mix, while no changes were detected at high temperatures. On the other hand, the recovered bitumen from asphalt aged by ozone shows needle penetration (PEN) values between the penetration values of bitumen after the rolling thin film oven test (RTFOT) and

RTFOT+PAV ageing. However, ageing by ozone (the procedure used in this study) requires additional optimization to achieve better results.

In the second part of this study, the RAP of surface, binder, and base courses as well as three rejuvenating agents were used to produce asphalt mixes. The results of performance tests show that asphalt mixes can be produced using 100% RAP. However, 90% of the RAP was used in the mix, while the rest (10%) was used to correct the RAP's aggregate gradation by new aggregates. The RAP was heated at a temperature of 80 ºC, while the new aggregates were heated at temperature of 160 ºC before mixing. The compaction temperature of asphalt mix was 130 ºC.

The percentages of rejuvenating agents 1, 2, and 3 were 0.60%, 0.29%, and 0.37% of the total mix respectively for the stone mastic asphalt SMA 11 S. The performance properties of the mixes with RAP and rejuvenator, show a reduction in the stiffness modulus of about 48%, 38%, and 42% at high temperatures compared to the asphalt mixes with RAP only. The decrease of stiffness modulus at low temperatures for the variants with rejuvenating agents 1, 2, and 3 was 14%, 8%, and 12% respectively. Asphalt mixes with RAP content and rejuvenators show improvements in fatigue, rutting, and low-temperature behaviour compared to the reference asphalt mix without RAP content.

Several asphalt mixes of AC 16 T D with RAP were produced by using 0.50%, 0.23%, and 0.30% of the total mix of rejuvenating agent 1, 2, and 3 respectively. Compared to the variant with RAP only, at low temperatures, the stiffness modulus of the asphalt mixes with RAP and rejuvenators were decreased by 12%, 8%, and 11% respectively. At high temperatures, the stiffness modulus decreased by 32%, 40%, 41% respectively. The fatigue resistance of asphalt mixtures with RAP was also improved by using the rejuvenating agents. However, the rutting resistances of all variants with rejuvenating agents were less than the reference variant without RAP, indicating that these types of mixes propone to rutting. In addition, aggregate variation in RAP provides another cause for this decrease in rutting resistance. On the other hand, the resistance against low-temperature failure of the asphalt mixes with RAP and rejuvenators were increased compared to the reference.

The percentages of rejuvenating agents 1, 2, and 3 were 0.40%, 0.18%, and 0.25% of the total mix for AC 22 T S respectively. Identical decreases in stiffness modulus were obtained, reaching 8% for the rejuvenator 1 and 10% for both of the rejuvenators 2 and 3 at low temperatures. At high temperatures, the decrease was 27%, 41%, and 29% respectively compared to the variant with RAP only. The fatigue resistance was also comparable to the reference without RAP. Rutting and low-temperature resistance tests were not condcuted for this mixture because this layer is less affected by rutting or low temperatures than surface layer.

The impact of the rejuvenating agents used in this study is presented also through the increase in the needle penetration values and decrease of softening point supported by decrease in complex modulus and increase in phase angle. Furthermore, a decrease in ageing indices of functional groups (sulfoxide and carbonyl groups) of hardened bitumen in RAP was measured as a result of blending and diffusion of the rejuvenators. However, this impact depends on the chemical composition of individual rejuvenator, characteristics of hardened bitumen in RAP content and rejuvenator content. These parameters are important and have to be considered in designing asphalt mix with RAP and rejuvenator to maximize RAP content in the reused mix.

Zusammenfassung

Die Wiederverwendung des Ausbauasphaltes als Asphaltgranulat (Reclaimed Asphalt Pavement - RAP) hat nachweislich wirtschaftliche und ökologische Vorteile, weil dadurch bei der Verwendung von neuen natürlichen Ressourcen wie Bitumen und Gesteinskörnung gespart werden kann. Zusätzlich können die Energiekosten durch die Absenkung der Herstellungstemperatur bei der Asphaltproduktion gesenkt werden. Um die Produktionsqualität des Asphaltmischgutes mit sehr hohem Asphaltgranulatanteil zu verbessern, sind technische Entwicklungen an der Asphaltmischanlage und bei den Prüftechniken des Asphaltmischgutes erforderlich. Im Rahmen dieser Arbeit wurden neue Verfahren zur Simulation der Alterung von Bitumen in situ entwickelt und die Wirksamkeit der zeitraffenden Alterung auf Bitumen- und Asphalteigenschaften mittels gebrauchsverhaltensorientierten Prüfungen im Labor untersucht. Zu diesem Zweck wurde diese Arbeit in zwei Hauptteile unterteilt.

Der erste Teil befasst sich mit der beschleunigten Alterung von Asphalt mit Hilfe der Oxidationsmittel Wasserstoff-Peroxid und Ozon, um den Einfluss der Bitumenoxidation auf die Eigenschaften von gealtertem Asphalt sowie gealtertem Bitumen zu untersuchen. Die Ergebnisse zeigen, dass die Alterung durch Peroxid die Steifigkeit von gealtertem Asphalt im Vergleich zum ungealtern Asphalt bei hohen Temperaturen um 10% erhöht hat. Bei tiefen Temperaturen wurde ein geringerer Steifigkeitsunterschied festgestellt. Darüber hinaus zeigen die Ergebnisse eine Verbesserung der Ermüdungsbeständigkeit bei schwerer und leichter Belastung (0,10 ‰ bzw. 0,03 ‰) von mittels Peroxid gealtertem Asphalt gegenüber nicht gealtertem Asphalt mit einer Rate von 162% bzw. 477%.

Die physikalischen, chemischen und rheologischen Eigenschaften des Bitumens nach der Peroxidalterung, sind identisch mit den Eigenschaften des Druckalterungsgefäß (PAV)-gealterten Bitumens. Dennoch konnte festgestellt werden, dass das Peroxid-Alterungsverfahren verbessert werden müsste, um die Effizienz zu erhöhen und die Arbeitssicherheit zu optimieren.

Beim Ozon-Alterungsverfahren wurde dem granulierten Asphaltmischgut ein konstanter Ozonstrom zugeführt. Mit Hilfe von Ozon gealterter Asphalt zeigt gegenüber dem ungealterten Asphalt eine Steifigkeitszunahme von etwa 4% bei tiefen Temperaturen. Bei hohen Temperaturen konnte eine Veränderung der Asphaltsteifigkeit nicht festgestellt werden. Die Werte der Nadelpenetration des mit Ozon gealterten Bitumens liegen zwischen den Werten des Bitumens nach der Dünnfilm-Prüfofen (RTFOT)- und RTFOT+PAV- Alterung. Das Ozon-Alterungsverfahren ist für praktische Anwendungen noch zu optimieren.

Im zweiten Teil der Studie wurden Asphaltmischgüter mit Asphaltgranulat unter Verwendung von drei Rejuvenatoren für Deck-, Binder- und Tragschichten hergestellt und untersucht. Die ermittelten Ergebnisse zeigten, dass eine Asphaltherstellung mit einem Asphaltgranulatanteil in Höhe von 100% theoretisch möglich ist. Dennoch wurde in dieser Studie die Asphaltgranulatzugabe in den Asphaltmischungen auf 90% begrenzt, um die Korngrößen-Verteilung durch die Zugabe von frischen Gesteinskörnungen in Höhe von 10% zu optimieren. Darüber hinaus wurde die Herstelltemperatur des Asphaltmischgutes auf 130 °C abgesenkt und demzufolge das Asphaltgranulat nur auf 80°C und Gesteinskörnung auf 160°C vortemperiert.

Beim Splittmastixasphalt SMA 11 S mit den Asphaltgranulaten und Rejuvenator 1, 2 und 3 wurden Steifigkeitsabnahmen von etwa 48%, 38%, bzw. 42% bei hohen Temperaturen und von etwa 14%, 8%, bzw. 12% bei tiefen Temperaturen festgestellt. Die Eigenschaften der Ermüdung und der bleibenden Verformung und das Verhalten bei tiefen Temperaturen wurden bei den Varianten mit den Asphaltgranulaten und Rejuvenatoren verbessert. Die Rejuvenatoren 1, 2 und 3 wurden so dosiert, dass sie jeweils einen Anteil von 0,60%, 0,29% und 0,37% der Mischgutmengen ausmachten.

Mehrere Asphaltmischungen von AC 16 T D mit RAP wurden unter Verwendung von Verjüngungsmitteln 1, 2 bzw. 3 mit Anteilen von jeweils 0,50%, 0,23% und 0,30% an der Gesamtmischung hergestellt. Im Vergleich zur Variante nur mit RAP war bei niedrigen Temperaturen der Steifigkeitsmodul der Asphaltmischungen mit RAP und Verjüngungsmitteln um 12%, 8% bzw. 11% verringert. Bei hohen Temperaturen nahm der

Steifigkeitsmodul um 32%, 40% bzw. 41% ab. Die Ermüdungsbeständigkeit der Asphaltmischung mit RAP wurde durch Verwendung der Verjüngungsmittel verbessert. Die Brunftwiderstände aller Varianten mit Verjüngungsmitteln waren jedoch geringer als bei der Referenzvariante ohne RAP, was darauf hinweist, dass diese Arten von Mischungen zur Spurrillenbildung neigen. Darüber hinaus liefert die aggregierte Variation des RAP einen weiteren Grund für die Abnahme des Spurrillenwiderstands. Andererseits wurde die Beständigkeit der Asphaltmischungen mit RAP und Verjüngungsmitteln gegen Tieftemperaturversagen im Vergleich zur Referenzvariante verbessert.

Die Anteile der Verjüngungsmittel 1, 2 und 3 an der Gesamtmischung betrugen 0,40%, 0,18% und 0,25% für AC 22 T S. Die Abnahme des Steifigkeitsmoduls war 8% für die Variante mit dem Verjüngungsmittel 1 und 10% für die anderen beiden Verjüngungsmitteln 2 und 3 bei niedrigen Temperaturen. Bei hohen Temperaturen betrug die Abnahme um 27%, 41% und 29%, verglichen mit der Variante nur mit RAP. Die Ermüdungsbeständigkeit war mit der Referenz vergleichbar. Spurbildung- und Tieftemperatur-Beständigkeitstests wurden für diese Mischung nicht durchgeführt, da diese Schicht weniger von Spurrinnen betroffen ist.

Die Wirkung der verwendeten Verjüngungsmittel wird auch durch die Zunahme der Werte der Nadelpenetration und die Abnahme des Erweichungspunktes bestätigt. Darüber hinaus wird diese, durch die Abnahme des Komplexmoduls und die Zunahme des Phasenwinkels sowie die Abnahme der Alterungsunabhängigkeit der funktionellen Gruppen (Sulfoxid und Carbonylgruppen) unterstützt. Jedoch hängt die Auswirkung von der chemischen Zusammensetzung und Zugabemenge des einzelnen Verjünguugsmittels ab. Die Kenntnisse der Auswirkung vom Verjüngungsmittel sind wichtig und müssen bei der Zusammensetzung des Asphaltmischgutes mit RAP berücksichtigt werden, um den RAP-Gehalt in der wiederverwendeten Mischung maximieren zu können.

Chapter I

Introduction

Ageing of bitumen in asphalt is believed to play the key role in pavement distress and deterioration that may necessitate maintenance, rehabilitation, or even the full removal of old roads. Several factors are involved in the process of initiating bitumen ageing and its development. Ageing during the process of asphalt production at elevated temperatures (up to 190 ºC), along with its transportation, laying down, and compaction is referred to as "short-term ageing". Secondly, climate conditions, oxidation, mechanical stresses and the adsorption of oily bitumen constituents into aggregates are responsible for the "long-term ageing" of bitumen and subsequently the properties of asphalt. Studies have been conducted to simulate bitumen ageing in the lab in order to better understand bitumen characteristics after a certain period of service time.

Worldwide, significant amounts of reclaimed asphalt pavement (RAP) are annually produced. For instance, 10.9 Mio. Metric tons were produced in Germany in 2014. The reuse of this RAP provides economic and environmental advantages. Over the past four decades, this has encouraged researchers to develop many techniques for reusing RAP materials in asphalt mixtures. This accompanied with and without the use of additives and/or specified machines. In most of the literature retrieved by the author, the term "recycling" is used for the reuse of RAP in the production of new asphalt mixtures. The bitumen and aggregates in RAP nearly substitute one to one the raw material - "virgin" bitumen and aggregates - without changing the properties of that asphalt mix. Another form of recycling is the salvage. However, in this study the term of "recycling" means the reuse of RAP to produce an identical material as a "virgin" asphalt mix (new asphalt mix).

In this study, the two issues (namely ageing and recycling) are considered and new methods are developed to simulate asphalt ageing in short- and long-term processes in the field. The use of new approaches to simulate aged asphalt is examined, since most currently applied accelerated ageing methods use high temperatures for bitumen ageing. The use of high

temperatures for ageing, however, leads to differences in the final products compared to the properties of field-aged asphalt. In addition, bitumen is a hydrocarbon compound and its chemical structure and bonds are highly affected and sensitive to temperature variations. The effect of ageing on asphalt properties was evaluated by comparing performance test results determined on the new and aged asphalt. The properties of new bitumen, recovered bitumen from RAP and lab-aged bitumen were also studied. The physical, chemical, and rheological property changes in bitumen due to the ageing process was also determined.

In the second part of the study, several asphalt mixes with and without RAP's obtained from different sites and different pavement layers in combination with rejuvenators were produced. RAP substitutes new bitumen and aggregate in asphalt mixtures and therefore conserves the natural resources. Therefore, almost the maximum dosage of RAP according to the Specification TL AG-StB was added. Performance-related properties of asphalt mixes with RAP were compared to properties of asphalt mixes without RAP (reference variant). In addition, bitumen was extracted from RAP materials and all asphalt mixes. The recovered bitumen was tested and compared to the properties of the bitumen of the reference variant to study the effect of RAP on bitumen properties.

This thesis is organized into seven chapters: Firstly, Chapter 1 contains an overview of the thesis, a problem statement, the objective, and the thesis organization. In Chapter 2, a review of literature relevant to the subject is presented with current research and techniques used in the lab ageing and reusing processes of RAP. Afterward, Chapter 3 illustrates the research methodology, the properties of the used materials, and the specifications followed to achieve the study goals. Moreover, Chapter 4 describes the procedures used in this study to accelerate the ageing process of asphalt. Chapter 5 then summarizes the determined test results of stiffness and the fatigue resistance of the aged asphalt. For the second phase, Chapter 6 contains a study of the impact of RAP and rejuvenators on the performance properties of asphalt. The main conclusions of the study are summarized and presented in Chapter 7 and recommendations for further research are offered. Next, the references used to support the research are cited and the results obtained during the study are presented in the appendix.

Chapter II

Review of Literature

In this chapter, a brief review of selected studies and previous work relevant to the subject of this study is presented. The first section focuses on the composition of bitumen and factors influencing its behavior as the main factor that regulates the performance of asphalt. The second section contains a survey of previous techniques and methods that have been used to accelerate the ageing of asphalt and the results obtained thereby as well as techniques of using RAP in asphalt mixtures.

2.1 Bitumen

Bitumen was initially used to pave roads in Babylon in 620BC (Byrne, 2005), and it has since evolved into the main binder for modern roads due to its ability to bear the loads applied by traffic and variation in climatic conditions. As an organic compound, the main structure of a bitumen molecule is comprised of carbon (82 - 88%) and hydrogen (8 - 11%) with traces of sulfur (< 6%), oxygen (< 1.5%), and nitrogen (< 1%; Airey, 1997). The sources of bitumen differ since it can originate naturally, e.g. in bitumen lakes (Jung, 2006), or can be manufactured by vacuum distillation during the industrial fractionation of crude oil (Jung, 2006). The properties of bitumen may vary according to the origin of the crude oil and/or the method of production, which may cause changes to the complex structure of bitumen molecules and proportions of bitumen constituents.

2.1.1 Chemical Composition of Bitumen

Researchers have developed several methods to analyze the chemical compositions of bitumen. The Corbett method is a widely accepted technique to separate the bitumen (Wu, 2009) into a soluble and insoluble fraction in normal heptane (non-polar solvent), where

the insoluble part of bitumen is referred to as asphaltene. The soluble fraction is referred to as maltenes. Asphaltene is the base fraction of the bitumen molecule and considered to be the most highly polar fraction (strong electronegativity). Other fractions are called maltenes, which are then separated into three parts, according to the different polarity of the solvents used in column chromatography. After several cycles of adsorption and desorption, saturates, aromatics, and resins with different polarities can be precipitated. The acronym for these four components of bitumen is SARA (saturates, aromatics, resins, and asphaltene). Fig. 1 presents a flow chart of the Corbett method, and Fig. 2 shows a sample of SARA components.

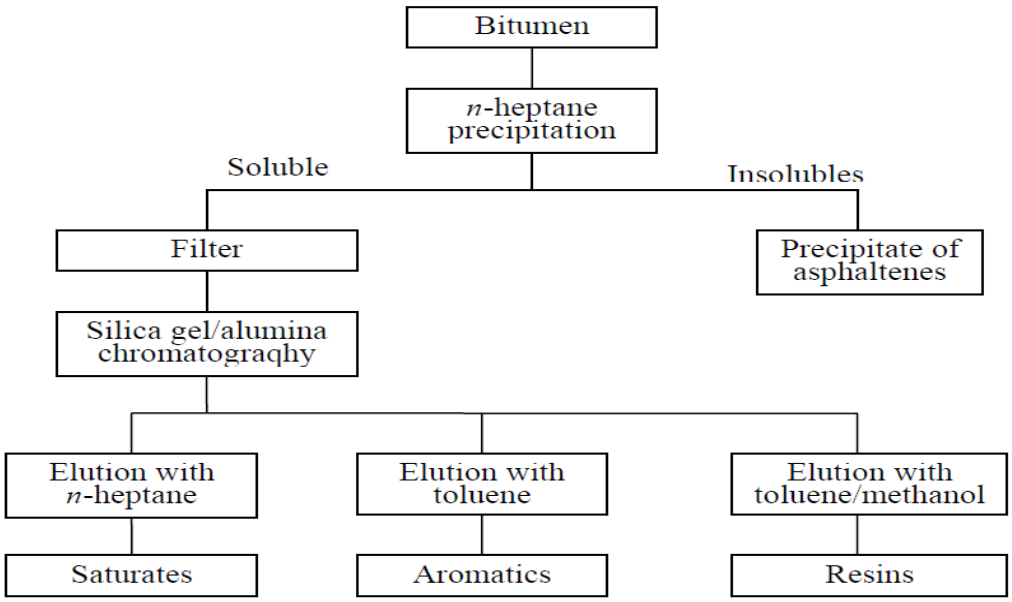

Fig. 1: Corbett adsorption/desorption chromatography (Wu, 2009).

Fig. 2: Chemical compositions of asphalt molecule (http://bmt-rnd.vn/cong-trinh/sara-fraction-and-colloidal-structure/?lang=en, last access 26.12.2018).

2.1.1.1 Asphaltene

Asphaltene represents the hard fraction of bitumen, where the molecules are bonded together strongly to form large molecules. Asphaltene is black or rather dark brown and consists of highly polarized aromatic rings and heteroatoms in addition to nitrogen, oxygen and sulfur. Asphaltene amounts to 5% to 25% of the bitumen molecule (Wu, 2009). The rheological properties of bitumen are highly affected by the proportion of asphaltene, which is less sensitive and more stable at high temperatures during the service life of pavement (Wu, 2009). The molecular weight ranges from 1×10^3 to 1×10^5, with a particle size of 5 nm to 30 nm (Airey, 1997).

2.1.1.2 Saturates

Saturates are non-polar viscous oils which are straw or white in color, with a molecular weight of 3×10^2 to 2×10^3 (Airey, 1997). They comprise straight or branched-chain aliphatic hydrocarbons (Wu, 2009) and amount to 5% to 20% of the bitumen (Wu, 2009).

2.1.1.3 Aromatics

Aromatics have the lowest molecular weight of the components of bitumen (Airey, 1997), amount to 40% to 65% of bitumen and thus represent the major proportion of dispersion medium for the peptized asphaltene (Airey, 1997). They appear as a dark-brown viscous liquid (Wu, 2009).

2.1.1.4 Resins

Resins are dark-brown, can be solid or semi-solid, and are highly polar in nature, which makes them highly adhesive (Airey, 1997). Resins are regarded as dispersing agents or peptizers of asphaltene (Wu, 2009) and therefore, the proportion of resins to asphaltene governs the solution (SOL) or gelatinous (GEL) character of bitumen (Airey, 1997). Resins have a molecular weight ranging from 5×10^2 to 5×10^4 and a particle size of 1 nm to 5 nm (Airey, 1997). Fig. 3 shows structural models of bitumen fractions (SARA).

The aforementioned fractions of bitumen have been used as an index of colloidal instability (CI) developed by Gaestel et al. (1971), which is calculated as follows:

$$\mathrm{CI} = \frac{flocculated\ constituents}{\text{dispersing constituents}} = \frac{Asphaltene+Saturates}{\text{Resins+Aromatics}} \quad \ldots\ldots\ldots\ldots\ldots\ldots\ldots\ldots\ldots\ldots\ldots\ldots\ldots(1)$$

A low CI value means that the asphaltenes are more peptized in the oil-based medium (Airey, 1997) and are thus more durable.

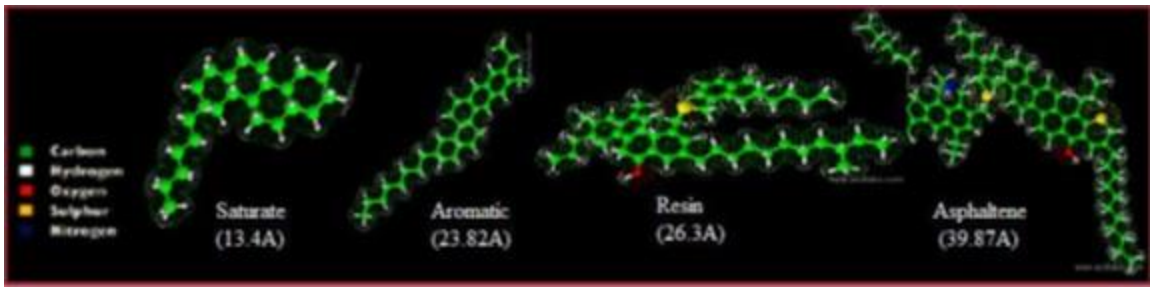

Fig. 3: Structural models of saturates, aromatic, resins, and asphaltene (Behzadfar, 2014).

2.1.2 Bitumen Age Hardening

Although the proportion of bitumen in asphalt is low (around 4% to 7% by weight of the total mix), asphalt performance is highly affected by the properties of bitumen due to their effect on the functional or structural failure of pavement. Age hardening represents the key factor that influences bitumen properties (Wright, 2010; Gawel et al., 2016; Petersen, 2009; Jenkins & Twagira, 2008; Lamontagne et al., 2001). Bitumen is an organic substance and its properties are affected by the presence of oxygen, ultraviolet (UV) radiation (Wu, 2010), ozone produced by the interaction of NOx gas emissions from vehicles (Feng et al., 2015; Liu et al., 2014; Melkonyan et al., 2013; Yi-Qiu et al., 2007; Kurtenbach et al., 2012; Likhterova et al., 1999; Ryer, 1997; Campbell et al., 1964), and changes in temperature (Poulikakos et al., 2016). These external influences cause the bitumen to harden, resulting in substantial rheological changes including an enhancement in viscosity, an increase in the softening point ring and ball (SP R and B), and a reduction in PEN (Bressi et al., 2015; Cheng et al., 2015). The factors involved in the age hardening of bitumen are summarized below:

1. *Oxidation*: the interaction of oxygen within the bitumen molecule, where the rate depends on the binder characteristics. The degree of oxidation is highly dependent on the temperature, duration and film thickness of the bitumen during the interaction.

2. *Volatilization*: the loss of the lighter constituents of the bitumen molecule due to evaporation, primarily a function of temperature.

3. *Polymerization*: a combination of similar molecules to form larger ones, causing progressive hardening.

4. *Thixotropy*: the property of bitumen when a progressive hardening occurs due to the formation of a lattice structure. This formation occurs as a result of hydrophilic suspended particles within the bitumen over a period of time (cyclic loading). However, this impact can be reversed by reheating and working the asphalt.

5. *Syneresis*: the separation or exudation reaction in which the thin, oily liquids are exuded to the surface of the bitumen film. The loss of these oily constituents causes the bitumen to become harder.

6. *Separation*: the removal of the oily constituents, resins or asphaltenes from the bitumen caused by selective absorption of some porous aggregates. (Sharew, 2010).

2.1.2.1 Chemical Changes upon Ageing

During ageing, the oxidation of methylene and degradation of unsaturated chains and/or naphthenic ring structures of benzene systems in the bitumen may lead to the formation of ketones and carboxylic acids and thio-ethers to sulfoxides (Lu & Isacsson, 2002). In addition, the polarity increases due to the structural changes. The increase in polarity leads to a decrease in aromatic content (see section 2.1.1.3) followed by an increase of the resin (see section 2.1.1.4) and asphaltenes (see section 2.1.1.1; Abutalib et al., 2015). Furthermore, in-situ experiments showed that asphaltene content increased by 2% to 10% in 8.5 years (Beale et al., 2014; Hagos, 2008). In addition, the size of asphaltene molecules increases due to oxygen uptake. This was confirmed by environmental scanning electron microscopy (ESEM) taken from unaged bitumen and bitumen aged by the rolling thin film oven test (RTFOT) and the pressure ageing vessel (PAV) test (Zhang et al., 2011a). The results showed that the asphaltene molecular size increased from 0.2 to 0.3 µm to 0.8 to 1.2 µm after ageing. However, almost all artificial ageing techniques use elevated

temperatures, which cause the microstructure to disappear (Fig. 4), and thus do not represent reality adequately.

By ageing thin films of binder in an oven at 163 °C, the RTFOT simulates short-term ageing in the laboratory to represent the ageing of the material in the road. The PAV test uses temperatures of 90 °C to 110 °C and a pressure of 2.10 MPa to simulate long-term ageing in situ (Grosseger, 2015; Zhang & Hu, 2015; Zhang et al., 2011; James & Stewart, 1991). Material that aged artificially is thus completely different from material that aged at a temperature below 80 °C (e.g., roads). Consequently, when developing future standardized ageing tests, it should be noted that deriving useful conclusions from ageing experiments with respect to performance may only be possible while performing such experiments in a temperature range where microstructures are still present (Poulikakos et al., 2016). Fig. 5 shows changes in bitumen constituents (i.e., SARA) during the ageing period (Airey, 1997).

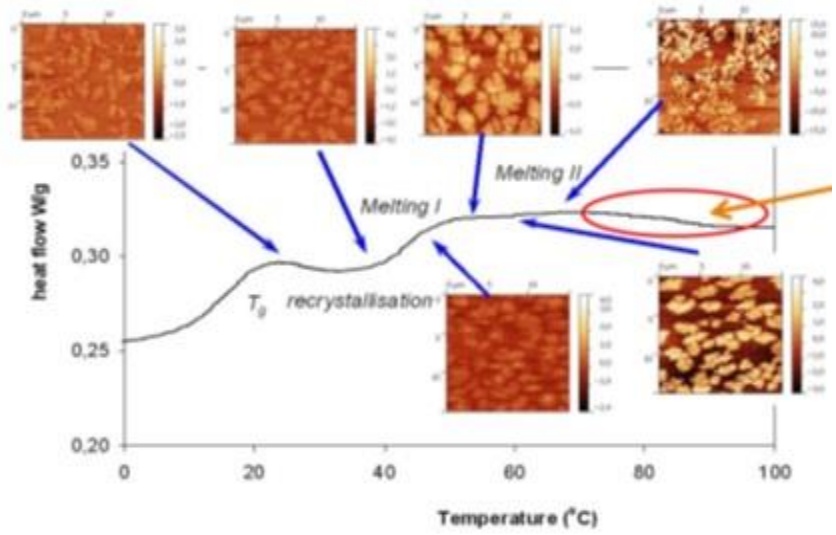

Fig. 4: Changes in bitumen chemical fractions upon ageing (Poulikakos et al., 2016).

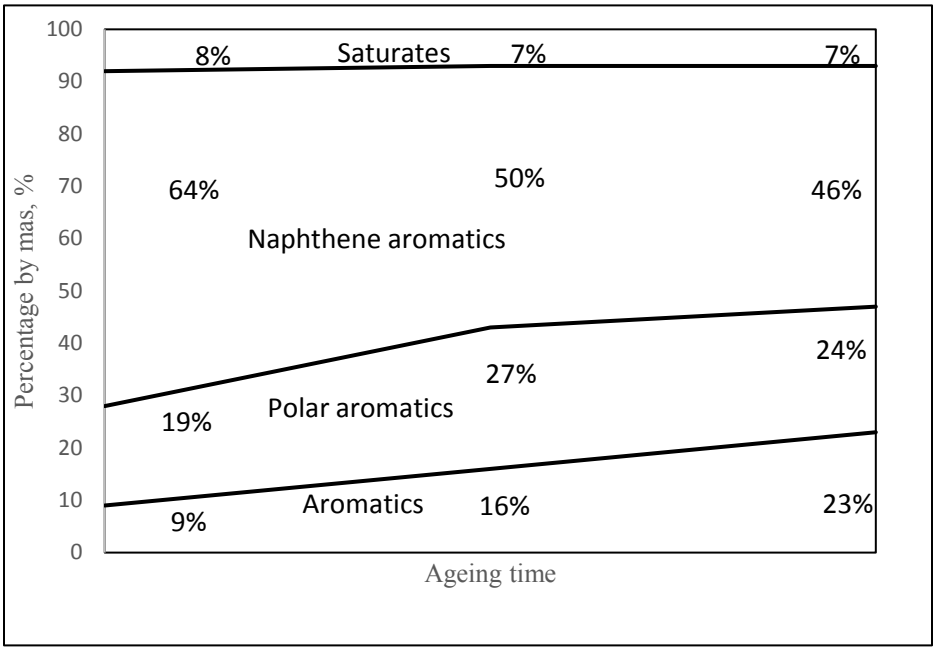

Fig. 5: Fractional changes of bitumen due to ageing time (Airey, 1997)

2.1.2.2 Quantification of Bitumen Age Hardening

Researchers have developed a series of tests and specified material parameters to quantify the effects of ageing on bitumen. These indicators can be classified as physical, rheological, or chemical indices. The physical or empirical index of ageing is derived from standardized tests of bitumen before and after ageing, such as PEN and softening point ring and ball (softening point). In addition, calculating the ratio of change (penetration values) or the difference in softening points of aged and unaged bitumen can serve as indicators.

On the other hand, the ageing index can be measured by studying the change of the rheological parameters of bitumen (complex modulus and phase angle) over a range of different frequencies and temperatures (Yu et al., 2013; AASHTO T315-10, 2010). The ageing increases the complex modulus and decreases the phase angle. In addition, chemical indices can be used for determining bitumen ageing such as CI (previously defined), where

high values of CI indicate an increase in the bitumen ageing (Paliukaite et al., 2014; Subramanian et al., 1996). Another chemical method regards quantifying sulfoxides (S=O) or carbonyl (C=O) groups of bitumen by Fourier transform infrared spectroscopy (FTIR). In this method, the area and peak height of the infrared spectrum at wavenumbers 1030/cm (S=O) and 1700/cm (C=O) are used to quantify chemical changes due to ageing (Reena, 2012; Lucena et al., 2004).

Fig. 6 shows the effect of short- and long-term ageing on the ageing index (viscosity ratio) during the service period of pavement (Shell Bitumen Handbook, 2003). The production of asphalt mixtures obviously has a major effect on the ageing index of bitumen.

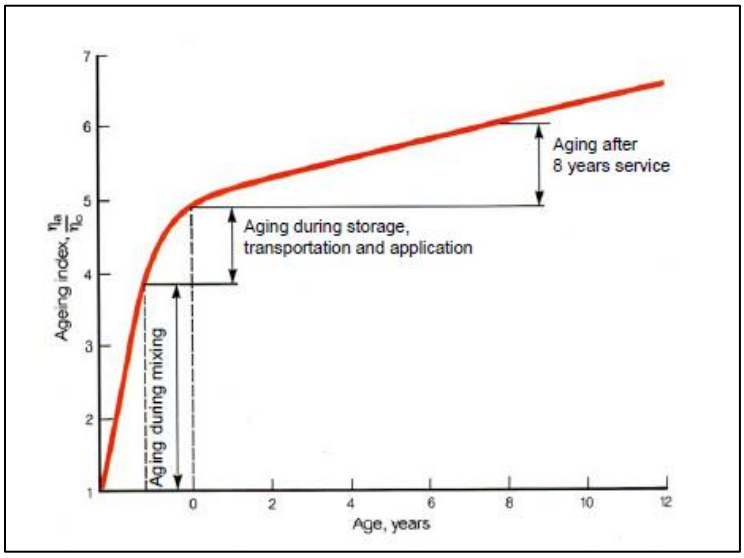

Fig. 6: Effect of ageing (short- and long-term) on ageing index during service period (Shell Bitumen Handbook, 2003).

2.1.2.3 Oxygen Diffusion into Bitumen

Diffusion of oxygen is the main factor responsible for the process of bitumen age hardening (Rad, 2018; Das et al., 2014; Dickinson et al., 1958). Although it was believed that air can only penetrate into the surface layer of the asphalt pavement (top 40mm; Han, 2011). It was found that the majority of air voids regard interconnected air channels, existing from the top to the bottom of the asphalt layer. This finding has been confirmed by using X-ray computed tomography (CT) and image-analysis techniques (Han, 2011).

In addition to oxygen diffusion, oxygen pressure also affects the hardening of aged asphalt. Both the kinetic reaction of the oxidation and the diffusion of oxygen through layers of particles in a maltene media influence such effects. Bitumen hardening increases as temperature and/or oxygen pressure increases (Glover et al, 2002).

2.1.2.4 Simulation of Bitumen Ageing in the Lab

Many test procedures have been developed for both the short- and long-term ageing of bitumen and can be summarized as follows:

1. The Thin Film Oven Test (TFOT)

The combined effects of heat and air on bitumen can be measured using this standard test. In this test, a convection oven is used to age a thin film of bitumen which is placed in a pan at 163 ºC for 5 h. Changes in bitumen characteristics and mass change as a percentage are determined before and after the test to indicate the impact of bitumen hardening. These characteristics include needle penetration, softening point, and dynamic viscosity. The short-term ageing of bitumen due to the production process in the plant can be simulated using this test.

2. The Rolling Thin Film Oven Test (RTFOT)

This test is conducted to simulate the hardening of bitumen in the plant, transportation, and paving, and its severity is about 10% higher than that of the TFOT (Zupanick and Baselice, 1997). The RTFOT (Fig. 7) is used as a standard test under the strategic highway research program (SHRP) binder specification. It is conducted by placing 50g of bitumen in eight cylindrical bottles with openings at one end to inject fresh hot air periodically into the bottles while rotated in a carousel. Compared to the TFOT, the rolling effect reduces skin formation by exposing a fresh bitumen surface. The bottles are placed in an oven at 163 ºC for 75 min or 85 min in the case of SHRP specification. Similar to the TFOT, the bitumen characteristics are measured before and after the test to determine the effect of hardening on bitumen.

Fig. 7: RTFOT ageing apparatus (source: BestLab at the University of Wuppertal).

3. The German Rotating Flask Test (GRFT)

In this test, the bitumen sample is placed in a rotated spherical flask, which is tilted and submerged in an oil bath at 165ºC at a speed of 20 rpm. The test was developed in Germany

as an alternative to the TFOT and RTFOT (Fig. 8). Rotating the vessels allows avoiding skin formation and maintaining the bitumen film during the ageing process. In addition, the oil bath is used to eliminate radiant heating problems associated with certain ovens and to permit rapid bitumen heating. The bitumen sample can be tested in a standard or modified GRFT. In the standard test (GRFT), 100g of bitumen is heated for 150 min with airflow at a rate of 500 cc/min. In the modified GRFT 200g of bitumen is heated for 210 min with an airflow of 2000 ml/min. Controlling the type and volume of gas in contact with the tested bitumen is achieved by conducting the test in a closed vessel. Volatilized components can be collected through certain modifications to the apparatus. Compared with TFOT and RTFOT, the severity of GRFT is almost one-third that of the other tests, indicating less ageing due to less volatiles being produced during the test (Airey, 2003).

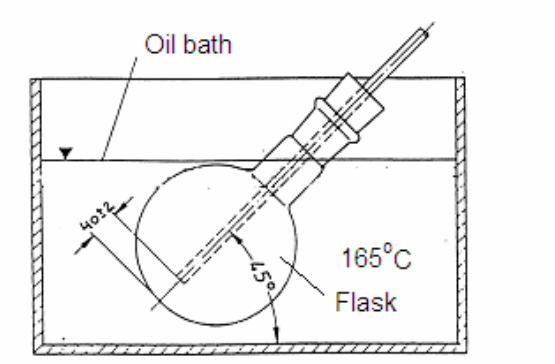

Fig. 8: The German rotating flask Test (GRFT) setup (Hagos, 2008).

4. The Pressure Ageing Vessel (PAV) test

This test is conducted to simulate long-term ageing which represents ageing of bitumen during the service life of the pavement as a second- stage in the ageing process of bitumen. Long-term ageing is following the short-term ageing due to production, transportation, and laying down of asphalt. Short-term ageing represents an important factor that determines the long-term behavior of pavement and influences its performance properties (Francken

et al. 1997). The oxidation of bitumen is the key factor of its long-term ageing in service. Hence, the long-term ageing is defined as a slow oxidation (ageing) process due to the interaction of bitumen with the environment or the air. This ageing is simulated using the PAV test (Fig 9) developed by SHRP. Before conducting this test, bitumen is first aged using the RTFOT (SHRP standard test) method. Different temperatures can be maintained in the ageing vessel during the test, including 85 ºC (PAV 85), 90 ºC (PAV 90), 100 ºC (PAV 100), or 110 ºC (PAV 110) while maintaining the pressure at 2.1 MPa for 20 h. A bitumen sample of 50g with an approximate thickness of 3.2 mm is poured into a preheated 140 mm diameter pan and placed in a shelf rack with a capacity of 10 pans. The recommended temperature of ageing is under 100 ºC to simulate chemical changes in the field. The test apparatus can be used to conduct another long-term testing method at a lower operating temperature and a longer ageing time, which is called high pressure ageing test (HiPAT) and is conducted at 85 ºC for 65 h under 2.1 MPa air pressure.

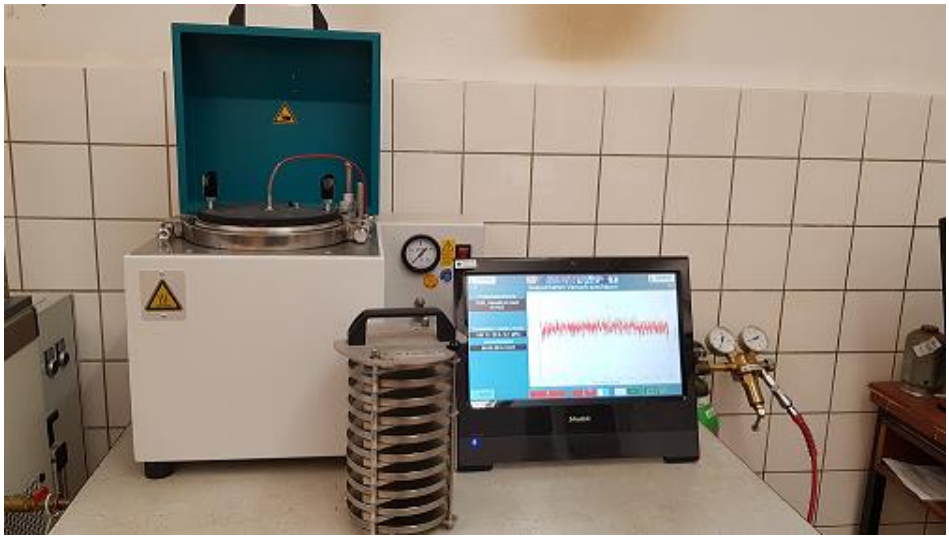

Fig. 9: PAV test apparatus with rack (source: BestLab at the University of Wuppertal).

An important limitation of lab-accelerated tests is that they are performed at temperatures exceeding the existing pavement temperatures, which may result in changes in bitumen

properties that differ from those in reality. In addition, the PAV technique for ageing is a static test and the diffusion of oxygen is inhomogeneous which is considered a drawback since it leads to differences in ageing between the surface and bulk of the sample (Verhasselt 2002). Polymer migration in polymer modified bitumen (PMB) materials has been shown to occur in the PAV ageing through investigating the top and bottom parts of the aged specimens (Verhasselt 2002).

5. The Rotating Cylinder Ageing Test (RCAT)

This test was developed by the Belgian Road Research Center (BRRC; Fig. 10) to accelerate the ageing of bitumen. In addition, it is developed to simulate both the short- and the long-term ageing of bitumen in a single test (Glover, 2007; Verhasselt, 2005). This test differs from the PAV test because it is a dynamic test and a uniform ageing of bitumen is possible. Moreover, sufficient aged bitumen can be obtained for conducting additional investigations to study the properties of bitumen.

Additionally, the impact of ageing on the characteristics of bitumen at various time intervals (reaction time) can be observed. This allows for the study of the development of ageing throughout the testing process. An additional advantage of this test is the combination of the short-term ageing of the RTFOT and long-term ageing of the PAV. This combination reduces the bitumen sample preparation for such tests. The long duration of the testing is considered the RCAT's major limitation (Verhasselt 2002). The RCAT ageing procedure includes the following steps (Hagos, 2008):

a. 500 to 550 g of binder is poured into a stainless-steel cylinder.
b. The cylinder is rotated at a rate of 1 rpm for long-term ageing
c. A grooved stainless-steel roller is inserted to press and distribute about 3mm thick binder film against the inner wall of the cylinder to constantly expose fresh surface and homogenize the binder sample.

d. A constant flow rate of 4.5 l/h of oxygen enriches and renews the atmosphere inside the cylinder
e. The recommended operating temperature is 85 ºC, however a temperature of 90 ºC may be preferred to reduce the test duration.
f. The duration of the test is 240 h at 85 ºC or 144 h at 90 ºC.

The short-term ageing of bitumen is simulated in this test by setting the cylinder at 5 rpm, while in the RTFOT method the apparatus is set at 15 rpm. The airflow rate is 4 L/min. The test duration is 235 ± 5 min (4 h) at 163 ºC. Using this procedure, the degree of ageing is equivalent to that in the RTFOT (Verhasselt 2002).

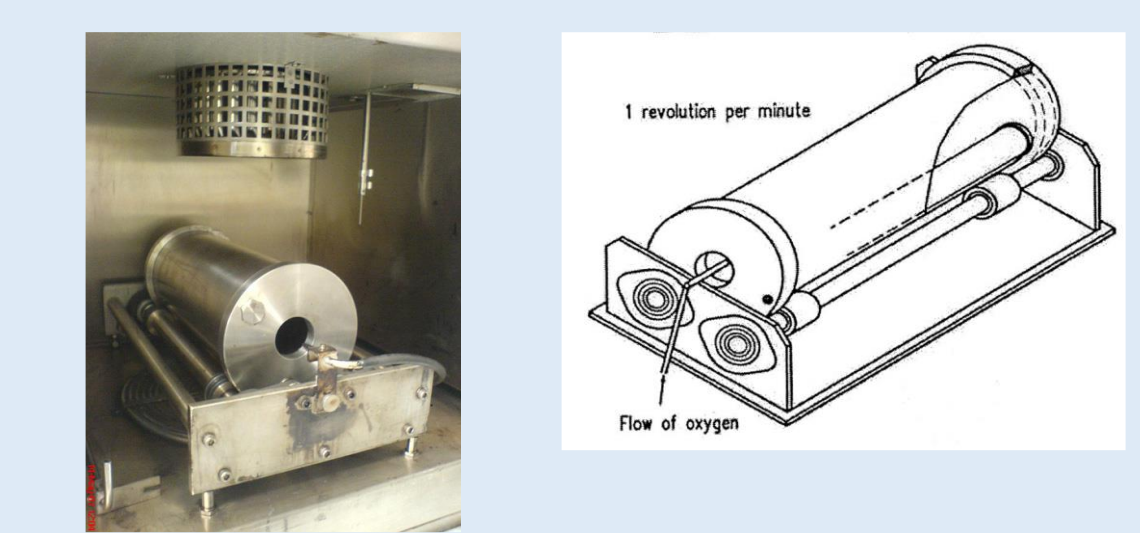

Fig. 10: RCAT device for the accelerated ageing of bituminous binders (Hagos, 2008)

2.1.2.5 Ageing of Asphalt

As previously stated, the ageing of bitumen directly influences asphalt performance. Due to this impact, many techniques have been used to accelerate the ageing of asphalt to predict its final behavior. These techniques comprise heating at elevated temperatures (Kim et al.,

1987). Different time periods of heating were applied to simulate ageing during mixing in the plant, transportation, laying down and compaction, which is called short-term ageing. In addition, there is a need to simulate long-term ageing, which occurs due to varying temperatures during service, mechanical stresses, and other factors (UV light, ozone, etc.) that influence pavement behavior in the field.

- *Short-term ageing*

  The SHRP procedure for short-term oven ageing (STOA) "requires that loose mixtures be heated (aged) in a forced draft oven for four hours at a temperature of 135 ºC prior to compaction. The loose mixture has to be stirred and turned every hour. This was found to represent the condition during mixing and placing and also represents fewer than two years in service for dense mixtures" (SHRP M-007).

- *Long-term ageing*

  The long-term oven ageing (LTOA) procedure "requires that the mixture, previously subjected to STOA, be compacted and reintroduced in an oven at 85 ºC for an additional 120 hours" (SHRP M-007).

In addition, researchers have developed laboratory procedures to simulate the ageing process for both short- and long-term ageing as shown in Table 1. The differences in results can be attributed to the different experiences available with respect to the resources of bitumen and resulting differing viscosity or hardness, thickness of bitumen or mix design.

Another lab-accelerated ageing procedure of asphalt depends on the use of a gaseous oxidant agent which flows into pressure cell that contains a triaxial cell of asphalt (Fig. 11). This method was developed to address the issue of using high temperatures to age asphalt. This method comprises the use of a mix of ozone and nitric oxides as an oxidant agent to increase bitumen oxidation. The test results of stiffness on unaged and lab-aged specimens using this method of ageing have shown that long-term ageing of asphalt may occur at moderate temperatures (60 ºC). In addition, identical results have been obtained using

dynamic shear rheometer (DSR) tests on the recovered binder from aged specimens. The test period is four days and the flow rate of the oxidant agent is 1 L/min (Steiner et al., 2014).

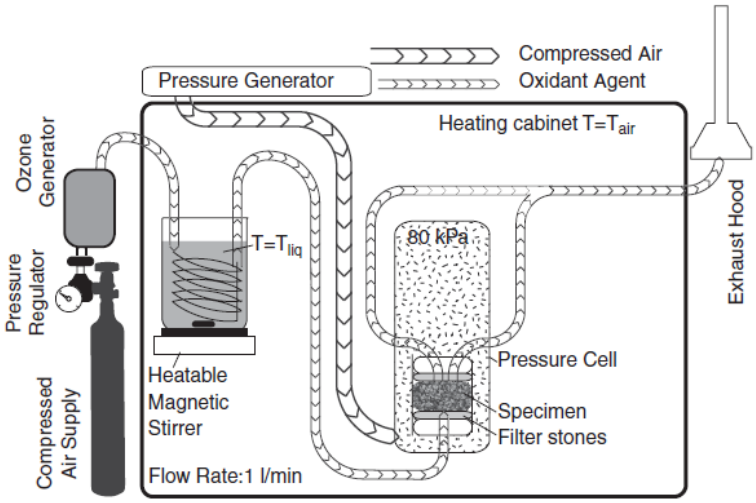

Fig. 11: Setup of ageing process (Steiner et al, 2014).

A new ageing process was recently developed where Marshall specimens were heated at 85ºC for 66h, then kept in cold water at 20 ºC for 6 h. After that, heated at 85 ºC for 42 h and cold water for 6 h, and ending with heating for 66 h at the same temperature (Raab et al., 2017). Performance tests were thereafter performed (stiffness modulus, fatigue resistance, and rutting resistance) according to the German standards. The results showed that, on one hand, the stiffness modulus and fatigue life of aged asphalt specimens were higher than those of unaged asphalt specimens (reference). This perhaps due to the increased hardness of the bitumen and stiffness of the asphalt. On the other hand, the rut depths of aged samples were less than those of the reference samples (Guo et al, 2016; Yousif et al, 2015).

Table 1: Summary of lab-aged asphalt (modified after Van Den Bergh, 2011)

Reference	Material	Short-term	Long-term	In-situ
AAMAS Von Quintas	Compacted		2 days @ 60 ºC + 5days @ 107 ºC	
AASHTO R30-02 (Bell, 1994)	Samples	Loose 2-4 h @ 135 ºC with stirring	Compacted 5 days @ 85 ºC	
BRRC Pierard & Vanelstraete 2009	Loose material 3 cm in oven	1.5h @ 135 ºC	14 days @ 60 ºC	
EMPA	Compacted	3 h @ 135 ºC	16 h @ 110/120 ºC	20 years
Hayicha et al, 2003	Beams	8 h @ 70 ºC	20 days @ 60 ºC	
Hveem 1963	Semi-compacted sand mixes		1000 h @ 60 ºC	
LCPC	Loose material	4 h @ 135 ºC	24 h @ 100 ºC	
Liverpool University	Marshal cores of PA	None	21 days @ 60 ºC (air)	18 months
Mugler, 1970	Compacted with different voids		163ºC during 5 h	
Nottingham University SATS	Compacted	None	Saturated @ 85ºC for 65 h at 2.1MPa	
Ramadan, 2016	Loose material	4 h, 18 h, 40 h, and 64 h @ 135 ºC		
RILEM TG5 DelaRoche et al, 2009	Loose material	4 h @ 135 ºC	7-9 days	
SHELL	Loose	2 h @ mixing temperature	7 days @ 80 ºC	PAV
Tia et al, 1988	Compacted with and without UV		60 ºC for 90 days	
TRL	Pavement cores	None	48 h @ 60 ºC	397 days
Van Gooswilligen 1989	Loose hot mix in sealed tin		16 h @ 160 ºC	

2.2 Recycling of Asphalt

Asphalt is one of the most reusable materials, and the reclaimed material from deteriorated asphalt pavement, known as reclaimed asphalt pavement (RAP), is reused in fresh asphalt

mix production. This process provides many benefits such as energy savings, environmental preservation, reduced construction costs, aggregate and binder conservation, and the preservation of existing pavement geometrics (when used in the maintenance of existing roads). Although asphalt pavements have been recycled since 1915 (Fig. 12), global interest in this process has increased considerably since the 1970s (Kandhal & Mallick, 1997). The process of recycling comprises the use of RAP at different percentages, rejuvenators to restore the properties of aged bitumen, and optimize the virgin bitumen, aggregate, and filler to produce recycled asphalt. The performance of asphalt with RAP content is depend on the properties of RAP used, particularly the effect of aged bitumen in RAP. Another factor regards the efficiency of the rejuvenating agent, whose main role is to restore the certain bitumen properties (decreasing the viscosity and softening point as well as increasing the needle penetration) to meet the requirements of guidelines and standards of new mixes.

In Germany, approximately 15 million tons of RAP are produced every year, while 45 million tons are produced every year in Europe (Willis, 2016; Table 2). This shows that the RAP produced in Germany alone represents around 30% of the total RAP produced in Europe. Although there was an increase in the reused RAP in asphalt mixes (Fig. 13), the rate remains low. The rate of reusing RAP in 2001 was 20%, which slightly increased in 2014 to 26%.

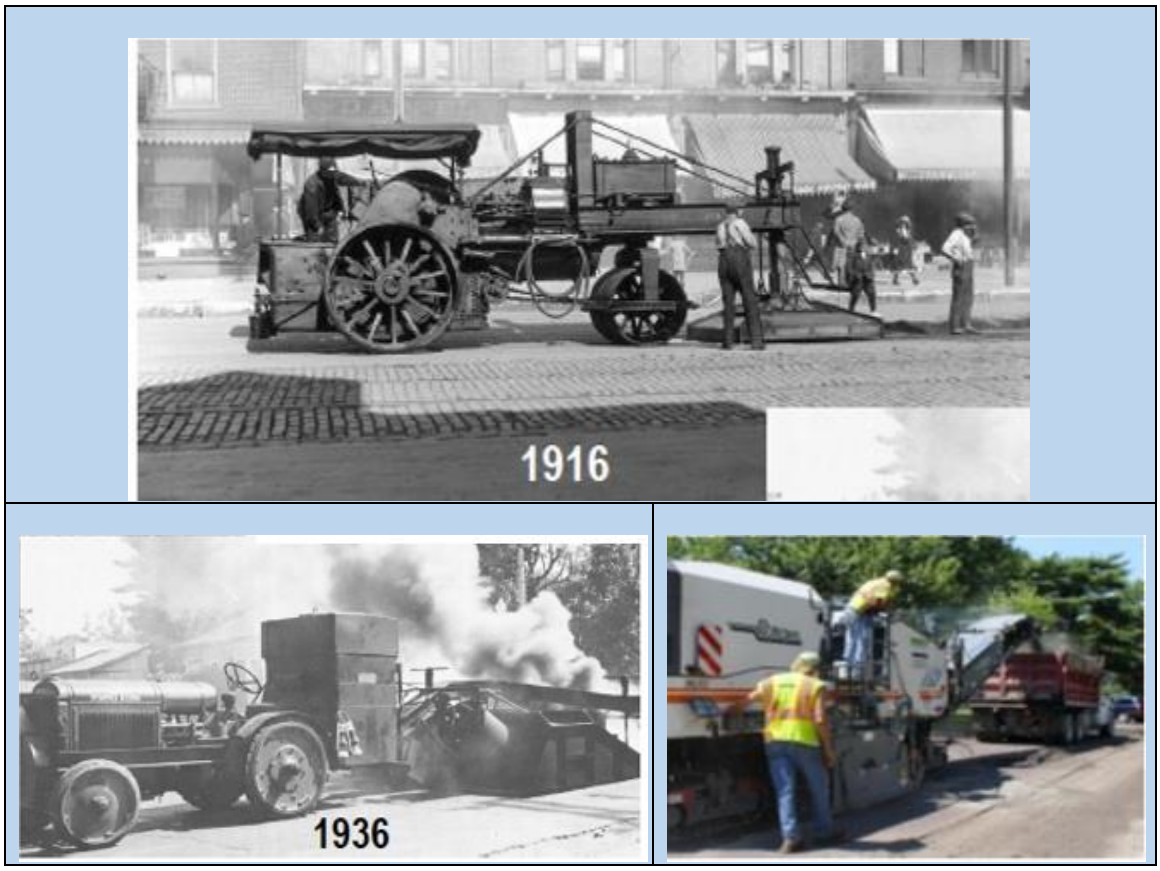

Fig. 12: Pavement recycling at different times (Willis, 2016).

Cold recycling is used in certain cases such as constructing at remote regions, high polycyclic aromatic hydrocarbons (PAH) which are hazardous compounds in natural tar bitumen, highly softened bitumen, or with over capacity of tar/teer. However, the use of cold asphalt is limited. Both tables show that RAP was 100% used in different types of recycled asphalt mixes, which can be attributed to the high volume of asphalt pavements produced every year (40 to 60 million tons). In all countries in the study except Germany, the rate of RAP used still needs to be increased. In Table 3 and Table 4, the quantities of recycled asphalt are shown for hot and warm asphalt and in cold recycled asphalt respectively.

Table 2: Total available reclaimed asphalt pavement in millions of tons (Willis, 2016)

Country	**2001**	**2002**	**2003**	**2004**	**2005**	**2006**	**2007**	**2008**	**2009**	**2010**	**2011**	**2012**	**2013**	**2014**
Denmark	0.22	0.24	0.29	0.271	0.22	0.24	0.48	0.41	0.31	0.35	0.60	0.58	0.79	1.30
Finland	0.20	0.37						0.50	0.50	1.00	1.00	1.00	0.86	1.00
France	5.00	5.00	5.10	6.50	6.5.00	6.50	6.50	6.50	7.05	7.08	7.08	6.50	6.90	9.24
Germany	**15.00**	**150**	**14.00**	**14.00**	**14.00**	**14.00**	**14.00**	**14.00**	**14.00**	**14.00**	**14.00**	**11.50**	**11.50**	**10.90**
Great Britain	5.00		5.00	5.00	4.50	5.00	4.00	4.00	4.00	4.00	4.50	4.50	4.50	3.35
Italy	13.00	130	14.00	14.00	14.00	14.00	14.00	13.00	12.00	11.00	11.00	10.00	10.00	9.00
Netherlands	3.50	3.50	4.00	3.80	3.00	3.40	3.50	3.50	4.50	4.00	4.00	4.00	4.50	4.50
Norway	0.52	0.47	0.26	0.28	0.41	0.59	0.61	0.72	0.76	0.75	0.72	0.78	0.68	0.83
Spain				1.63	2.25	0.69	1.20	1.15	1.85	1.59	1.35	0.36	0.21	0.39
Sweden	1.00	0.90	0.75	0.80	0.75	0.65	0.90	1.00	1.00	1.10	1.10	1.00	0.90	1.20
Switzerland	1.75	1.90	2.10	2.30	0.90	0.94	0.98	1.10	1.20	1.45	1.75	1.57	1.37	1.00
Total	45.19	40.37	45.51	48.59	46.52	46.01	46.22	45.88	47.17	46.32	47.11	41.81	42.21	42.72

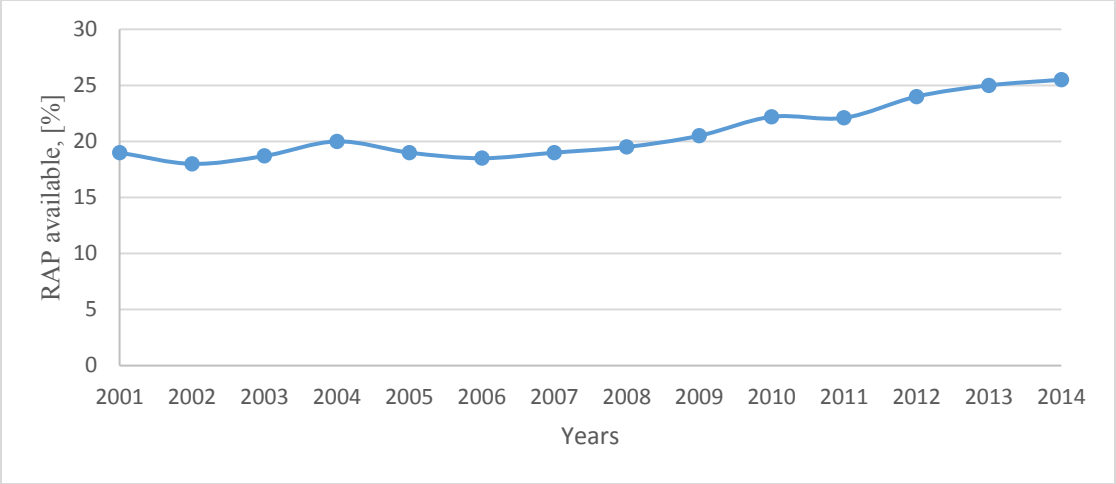

Fig. 13: Percentage of RAP used in recycled mixes (Willis, 2016).

Table 3: Percentage of total RAP used in hot and warm recycled mixes (Willis, 2016).

Year/Country	Denmark	France	Germany	Italy	Netherlands	Norway	Spain	Sweden	Switzerland
2007	57.0	13.0	**82.0**	20.0	90.0	08.0	45.0	60.0	50.0
2008	59.0	23.0	**82.0**		83.0	11.0	48.0	65.0	50.0
2009	55.0	41.0	**82.0**	20.0	74.0	12.0	52.0	75.0	50.0
2010	56.0	40.0	**82.0**	20.0	75.0	15.0	56.0	70.0	52.0
2011	80.0	45.0	**84.0**	20.0	83.0	18.0	73.0	70.0	51.0
2012	77.0	62.0	**87.0**	20.0	80.0	18.0	66.0	75.0	52.0
2013	83.0	64.0	**90.0**	20.0	76.0	21.0	85.0	80.0	48.0
2014	54.0	64.0	**90.0**	20.0	70.0	20.0	97.0	80.0	62.0

Table 4: Percentage of total RAP used in cold recycled mixes (Willis, 2016).

Year/Country	Denmark	France	Germany	Italy	Netherlands	Norway	Spain	Sweden	Switzerland
2007	43.0	2.0	**18.0**	0.0	10.0	80.0	55.0	40.0	50.0
2008	41.0	4.2	**18.0**	0.0	0.5	73.0	62.0	35.0	50.0
2009	45.0	0.0	**18.0**	0.0	0.0	70.0	48.0	25.0	50.0
2010	44.0	0.0	**18.0**	0.0	0.0	85.0	44.0	30.0	48.0
2011	20.0	0.0	**16.0**	0.0	15.0	62.0	27.0	25.0	47.0
2012	23.0	0.0	**13.0**	0.0	15.0	68.9	17.0	20.0	45.0
2013	17.0	0.0	**10.0**	0.0	0.0	10.0	15.0	20.0	40.0
2014	11.0	0.0	**10.0**	0.0	15.0	50.0	3.0	20.0	36.0

The criteria for using RAP in Germany are determined according to TL AG-StB 09/13. The uniformity of RAP is the necessary condition for using RAP granules. Uniformity can be determined using a range of characteristics. The characteristics according to TL AG-SBtB 09 include the following:

- Softening point [°C]
- Binder content [M.-%]
- Filler < 0.063 mm [M.-%]
- Fine aggregate 0.063 – 2 mm [M.-%]
- Coarse aggregate > 2 mm [M.-%]

The percentage of RAP content in the asphalt mix can be calculated using the following formula:

$$Zi = \frac{0.5 \times Tzul,i}{ai} \times 100 \quad \text{.....(2)}$$

where:

Zi is the allowable percentage of RAP, M-%,

Ai is the value of the specific property (softening point, binder content, filler content, fine, or coarse aggregate); and

Tzul,i is the total tolerance of the specific property (according to Table 5).

This equation can be applied for asphalt base course mix (AC T) and asphalt full depth layer (AC T D S) mixes with all properties mentioned above. For asphalt binder course mix (AC B) and asphalt wearing course mixes (AC D mixes), it can be applied only with the values of the softening point, and for other properties, the constant of the equation is 0.33 instead of 0.5.

Table 5: Tolerance of specific values for calculating RAP content

Property	Tzul	
	AC D, AC B, and AC T D	AC T
Softening point (R&B), ºC	8.0	8.0
Binder content, M.-%	0.8	1.0
Filler < 0.063 mm, M.-%	6.0	10.0
Fine aggregate 0.063 to 2 mm, M.-%	16.0	16.0
Coarse aggregate > 2 mm, M.-%	16.0	18.0

2.2.1 Techniques of Asphalt Recycling

Several techniques have been employed in the process of reusing RAP in asphalt. These methods were developed according to the maintenance or rehabilitation required for roads

and can be classified as follows: hot in-situ, hot in-plant, cold in-situ, or cold in-plant (Byrne, 2005).

2.2.1.1 Hot In-Place Recycling Technique

This technique is used in the surface correction of distressed pavements through the gradual heating of distressed surface of pavement. The following step is scarifying and then mixing with bitumen. New aggregate may be used as required (Schvallinger, 2011).

In this process, three techniques can be recognized:

a) *Heater-scarification (reshape):* This method involves the use of surface heating to 120 ºC -130 ºC to a depth of 3-6 cm. After that, scarifying the pavement and laying it without the addition of new aggregates or bitumen. This process eliminates surface irregularities and restores the original line and grade of the pavement. The drawback is that it does not always produce a smooth and flat surface.

b) *Repaving:* This method combines the use of heater-scarification with a new asphalt overlay.

c) *Remixing (remix compact):* This method is used when adding new materials such as aggregates or asphalt with one of the previous processes. Remixing represents the most common technique and includes the following steps:

- Heating the pavement surface using preheaters. The minimal area of the preheater unit is 200-300 m^2 based on the depth and weather conditions.
- The heating/milling unit then continues to heat the surface and removes the softened pavement.
- The heating/mixing unit agitates the loosened material and adds new materials such as RAP, virgin aggregate or new asphalt to create a homogeneous mix.
- Laying down and compaction by conventional paver and rollers (Figs. 14 and 15) (Schvallinger, 2011). However, this method is uncommon in Germany.

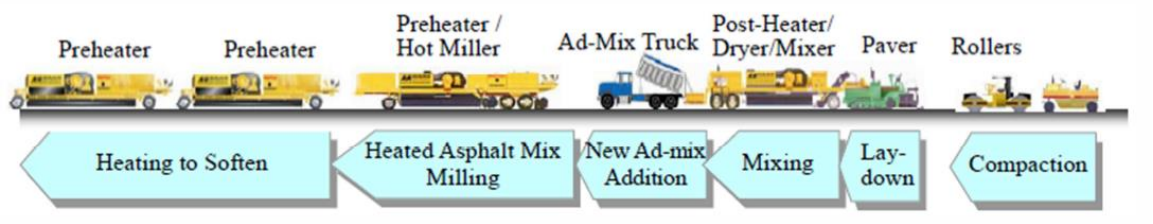

Fig. 14: Composition of HIPR train in remixing method (Schvallinger, 2011).

Fig. 15: Hot in-place recycling using remixing process. (http://martec.ca/benefit/. Last accessed 26.09.2018).

2.2.1.2 Hot In-Plant Recycling

This technique is used to produce an asphalt mix with reused RAP in a quality equal to new asphalt. This method includes milling of asphalt from old roads (Fig. 16), preparation by means of crushing at the plant (Fig. 17) and storage for later use in producing asphalt mix. Different methods are used to produce the asphalt mixes with RAP including the use of batch or drum-mixer plants. The insertion of RAP can be accomplished in several ways for a batch plant. These includes the insertion at the bottom of the hot elevator, in the mixing unit, in the dryer, or by using a double-drum. In a drum-mix plant, RAP can be inserted in either a parallel flow (Fig. 18) or a counter-flow. Plant configuration and technology may limit the addition of maximum RAP content in the asphalt mix; however,

100% of RAP using in asphalt is possibly by means of using specific technology (Schvallinger, 2011).

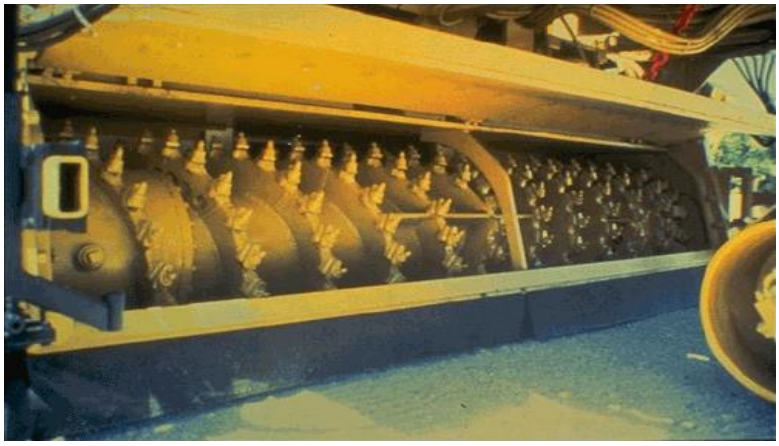

Fig. 16: Teeth of cold milling machine (fhwa.dot.gov/pavement/recycling/98042/05.cfm last accessed 26.09.2018).

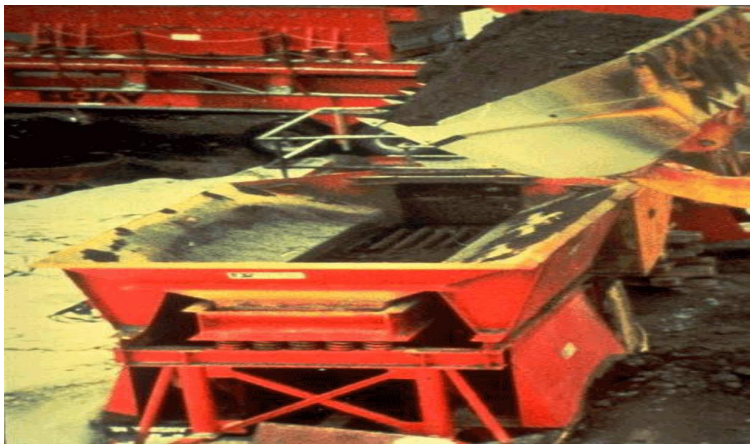

Fig. 17: Reclaimed asphalt pavement (RAP) crusher (fhwa.dot.gov/pavement/recycling/98042/05.cfm last accessed on 26.09.2018)

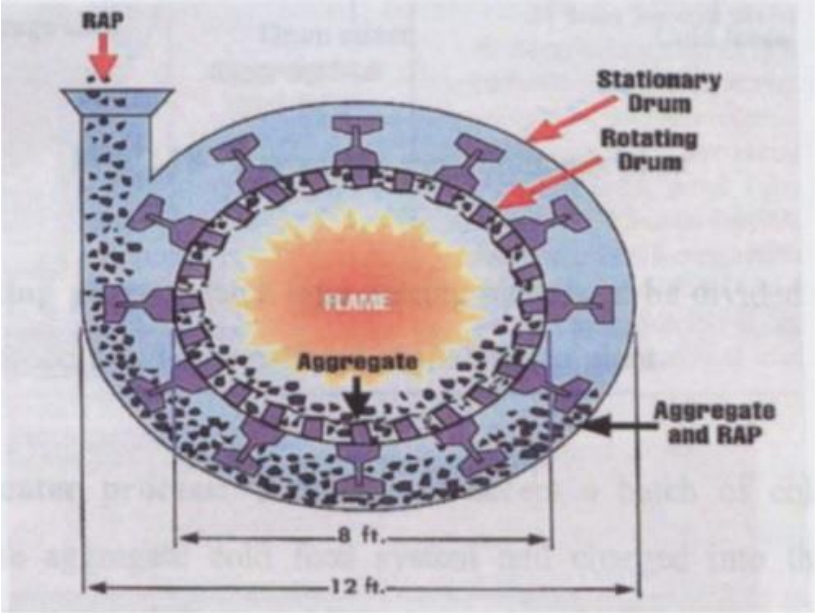

Fig. 18: Parallel flow drum mixer (Byrne, 2005).

2.2.1.3 Cold In-Situ Recycling

In this technique of recycling RAP, no heating or transportation is needed except for rejuvenating agents (Schvallinger, 2011). Cold in-situ recycling of RAP consists of milling, adding new aggregates or water (Schvallinger, 2011), and mixing with new emulsified or foamed bitumen as shown in Fig. 19 (Byrne, 2005). This type of recycling is suitable when it is not possible to use hot in-situ recycling such as in remote construction sites or when the RAP material fails to meet the requirements of hot recycling.

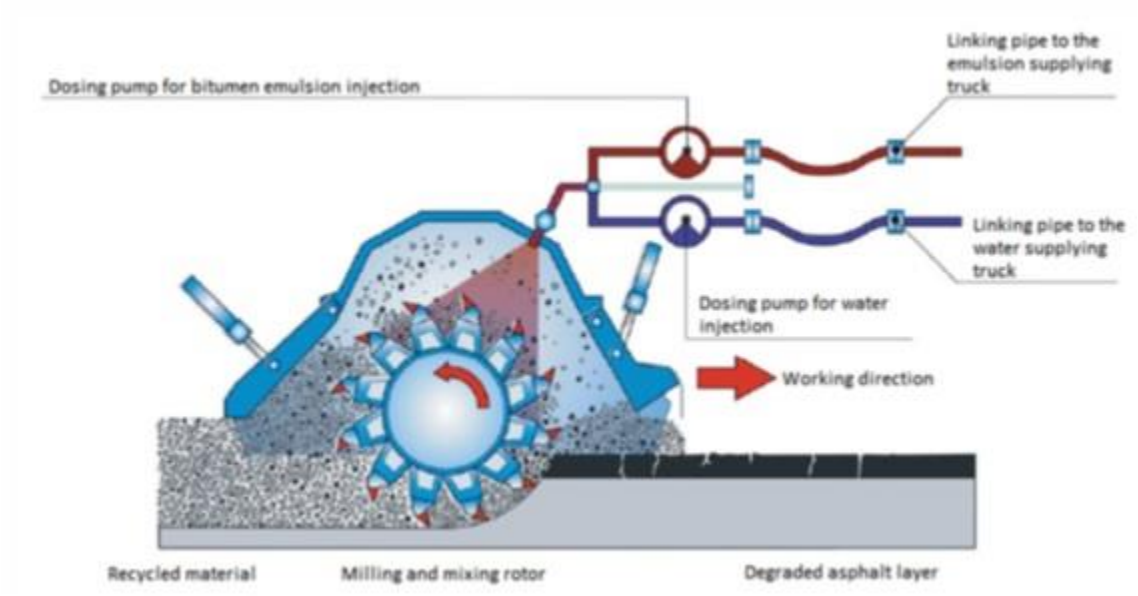

Fig. 19: Cold in-situ recycling process (Schvallinger, 2011).

2.2.1.4 Cold In-Plant Recycling

This method is less commonly used in Europe and involves mixing RAP with emulsified bitumen. Most cold-recycling plants are consequently mobile and can be transported to the construction site. The preparation of RAP for mixing is similar to that in hot in-plant recycling, where after milling and screening, the RAP is introduced to a scaling hopper and inserted in the mixer. To avoid the segregation of the mix, the coarse and fine aggregates are inserted at different times. The coarse aggregates are first wetted and coated with emulsified bitumen. Thereafter, fine aggregates are introduced, coated with emulsion, and mixed. Finally, the coarse and fine aggregates are mixed together. Paving can be performed using conventional machinery, while compaction requires a high amount of energy (FHWA-HIF-17-042, 2018; Schvallinger, 2011).

2.2.1.5 Warm and Half -Warm Recycling

This technique is new and is based on mixing RAP at reduced temperatures, between 70 ºC-100 ºC for half-warm mix asphalt recycling and 120 ºC-130 ºC for warm mix asphalt. This process has been found most appropriate for the rehabilitation of pavement from both economic and environmental perspectives (Almeida et al., 2010; Punith et al., 2013).

2.2.1.6 Disadvantages of In-Situ and In-Plant Recycling

Although the process of recycling includes several advantages, the disadvantages of in-situ recycling include the following:

- Less homogenous recycled pavement
- Possible appearance of longitudinal cracks if adjacent strips of pavement are not correctly bonded
- Longer rehabilitation time than that required for a simple overlay of hot-mix asphalt

The disadvantages of in-plant recycling include the following:

- A lower production rate of the plant due to the elevated humidity
- Additional space is required for stockpiling RAP materials
- A high level of inconsistency of RAP materials, since they are milled from different locations and stockpiled in one place
- The RAP needs to be ventilated to avoid reduced plant production due to the gaseous emissions from drying RAP (Heneash, 2013)

2.2.2 Blending of Aged and New Bitumen

The bitumen in RAP materials is aged due to several factors and hence might perform differently from the virgin binder. The solubility of aged and new bitumen is consequently affected by their chemical compatibility, difference in molecular weight, blending

proportion, and mixing temperature (Hassan, 2017). It is well known that RAP's impact on the characteristics of asphalt mix can be neglected when the RAP content is low (15% to 20%). When RAP content between 20% to 40% of the whole asphalt however, the impacts of the hardened bitumen of RAP can be compensated for using a virgin binder one grade softer on both the high- and low- temperature grades. The RAP's binder stiffens the blended binder. If the stiffness of the recovered bitumen from RAP is not too high, higher amount of RAP content can be used. Furthermore, binders in RAP can be tested by employing the same testing procedures for new bitumen (McDaniel et al., 2000). These findings have been supported to determine the stiffness and fatigue resistance of the asphalt with different RAP contents by indirect tensile tests (McDaniel et al, 2000; Carlson, 2014).

2.2.3 Gradation of Aggregates' in the RAP

The particle size and gradation of aggregates in the RAP may limit the using of high amount of RAP in asphalt mix if there is a difference between the gradation of aggregates in the RAP and in the final mix. Therefore, the gradation of aggregates in the RAP may need to be corrected by blending with proper virgin aggregates in order to meet the gradation limits of the final mix (McDaniel et al., 2000). This correction can be achieved by sorting RAP according to particle size after preparation by means of crusher and dosage in different amounts or, with the use of new aggregates if needed.

Another aspect to examine regards the high percentage of fines in RAP aggregates due to the crushing and milling processes (but not the fines of the asphalt mix). However, the high percentage of fines can be removed by the dust collector system or by screening the RAP (Hassan, 2017). The fines generated due to crushing coarse aggregates can be eliminated by dust removal, however the fines of RAP material contain considerable amounts of bitumen, and it is therefore important to use these fines in the asphalt mix with reused RAP. Bitumen absorption by the aggregates in the RAP should also be considered, especially at high RAP contents and when the aggregates have high levels of absorption (Hassan, 2017).

2.2.4 Effect of Rejuvenating Agents

Rejuvenators have been used to soften the aged bitumen in RAP or to compensate for the stiffness of aged binders, especially at using of high RAP contents (> 50%; Seferoglu et al., 2018; Zaumanis et al., 2014). It has also been found that rutting and fatigue performance are improved in asphalt samples with RAP and rejuvenating agents from different sources (Bankowski, 2018; Zaumanis et al., 2016; Zaumanis et al., 2014; Fig. 20). The results of virgin mix may be due to the use of softer bitumen and the bitumen used is not known.

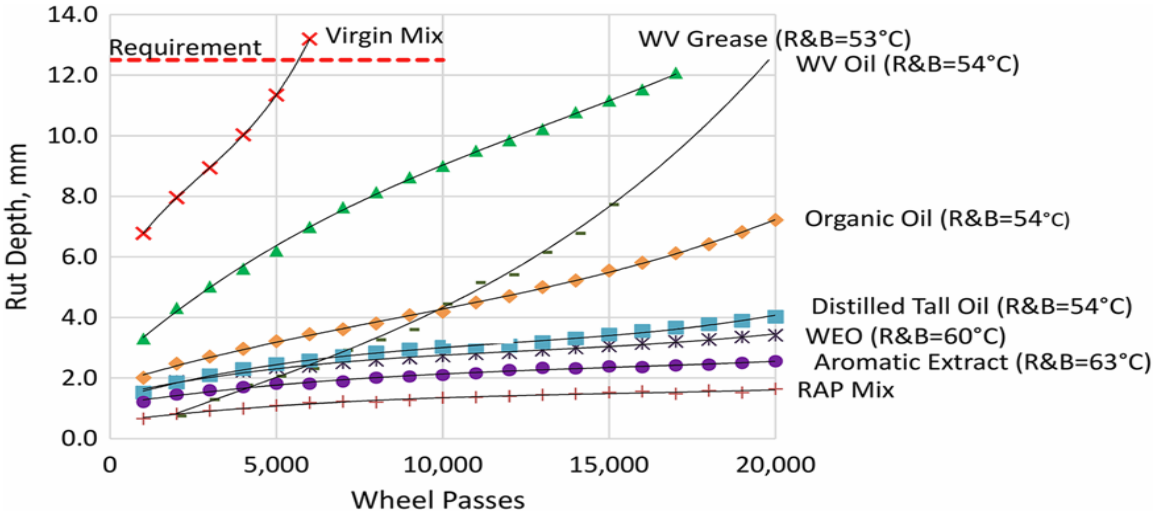

Fig. 20: Hamburg wheel tracking test results of recycled mixes by different rejuvenating agents. All recycled mixes results were within requirements, while the virgin mix exceeded limits (Zaumanis, et al., 2014).

Furthermore, rejuvenating agents provide some advantages over softer binders:

- Cheap storage, in some cases because they do not need to be heated
- Simple handling; can be added to the mixture using a pump or liquid additive dosage system
- Easy control of dosage

- Ability to be applied directly on RAP (the rejuvenating agent can diffuse into the aged binder)
- Ability to maximize the RAP -content in the asphalt mix up to 100%
- Cost effectiveness (Zaumanis et al., 2014). However, such advantages may not be applicable in certain cases.

Chapter III

Materials and Research Methodology

This chapter contains details regarding the materials used to achieve the research plan and objectives, the test plan developed to cover the different research aspects, and the procedures of experiments.

3.1 Research Aims and Objectives

3.1.1 Research Aims

This research has the following aims:

- To develop a procedure of accelerated asphalt ageing which simulates the ageing process during the service life of pavement

- To maximize the RAP content in the recycled asphalt without affecting the performance properties of the asphalt

3.1.2 Research Objectives

Asphalt specimens will be prepared in the lab by employing different bitumen grades and aggregate sizes. Following this preparation, this research pursued the following objectives:

- Utilizing potent oxidizing agents to accelerate the ageing process of asphalt

- Collecting RAP of different types of layers for extracting bitumen to study its chemical and rheological properties

- Investigating the performance properties of aged asphalt and asphalt with RAP content

- Measuring the impact of the ageing using new methods and processes of reusing of RAP on the properties of the extracted bitumen characteristics

- Determining the changes in asphalt performance before and after ageing or reusing of RAP

3.2 Materials

3.2.1 Bitumen

Three types of bitumen have been chosen for this research: two are unmodified bitumen (penetration grade bitumen 30/45 and 50/70) while the third is polymer modified bitumen (SBS modified bitumen, PMB 25/55-55 A). Bitumen was brought to the laboratory in sealed metal containers holding about 5 kg each. The bitumen grades and delivery times were marked on each container, and then samples were tested to specify the basic properties of the delivered bitumen. The bitumen samples were also aged in the lab for both short- and long-term ageing using the RTFOT and PAV tests according to DIN EN 12607-1 and DIN EN 14769 respectively. The results of the short- and long-term ageing will be used to compare with site-aged bitumen extracted from old asphalt (RAP) with lab-aged samples of asphalt. The properties of the bitumen used and related specifications are below shown in Table 6 for virgin bitumen and for extracted bitumen from RAP of surface (RAP,S), binder (RAP,B), and base (RAP, T) layers.

Table 6: Properties of binders used in the study

Bitumen type	Penetration, 0.1 [mm]	Softening point, [°C]	Fraas breaking point, [°C]	Density, [g/cm^3]	Viscosity @60 °C [Pa.S]
Specification	DIN EN 1426	DIN EN 1427	DIN EN 12593	DIN 52004	DIN EN 13702-1
30/45	37	54.8	-12.0	1.031	666.45
After RTFOT	24	60.2	-	-	-
After PAV	15	73.1	-	-	-
50/70	59	49.4	-13.5	1.030	-
After RTFOT	38	55.7	-12.0	-	-
After PAV	21	65.5	-	-	-
PMB	54	55.3	-15.0	1.029	-
After RTFOT	34	63.7	-	-	-
RAP, S	19	68.6	-	-	-
RAP, B	21	63.5	-	-	-
RAP, T	17	71.8	-	-	-

3.2.2 Aggregate, RAP and Filler

The aggregate type used in this study was diabase while the filler was limestone dust. Before use, the aggregate was dried overnight at 110 °C, then sieved and stored in groups

according to grain size. The fine aggregate was distributed twice in a rotary distributor and then stored for later use in the study. The aggregate gradation was selected according to standard specifications namely TL Asphalt-StB 07/13, Fassung 2013 (FGSV 797). The reclaimed asphalt RAP was obtained from different locations in North Rhine Westphalia in Germany and from different types of layers. The RAP's were milled separately in each layer and were classified into three categories: surface layer, binder layer mixed partially with base course, and base layer. After delivery to the lab, the RAP was dried at 25 °C for 72 h in oven then labeled and stored for later use in the study. Five samples were randomly chosen from each batch of layer and investigated for classification. Thereby, binder was extracted to determine bitumen properties (Table 6) and gradation of aggregate was determined (Tables 7-11).

Four mixtures representing three layers of pavement were selected as follows:

1) *Surface layer mix*: SMA 11 S, stone mastic asphalt with maximum aggregate size of 11 mm and for the specificity of highly stressed pavement "S"
2) *Full-depth layer:* AC 16 T D, maximum aggregate size 16 mm, where "T D" denotes base- and surface layer (Tragdeckschicht)
3) *Binder layer*: AC 16 B S, maximum aggregate size 16 mm, where "B" denotes binder layer (Binderschicht)
4) *Base layer*: AC 22 T S, maximum aggregate size 22 mm, where "T S" denotes base layer (Tragschicht)

Tables 7- 11 show the gradation limits and the percentages of coarse aggregate (crushed diabase), fine aggregate (diabase chippings) and limestone filler for the four types of mixes used. The tables contain also the gradation of aggregate from RAP (RAP,S [Table 8], RAP,B [Table 10], and RAP,T [Table 11] of surface, binder, and base layers respectively). The gradation of aggregate needed to correct the gradation of the reused mixture so that producing a mix of 90/10 (aggregate from RAP / virgin aggregate) that meets the gradation of the selected virgin aggregate. Figs. 21, 22a, 22b, and 23 show the grading curves of aggregates used in this study for the surface, binder, full-depth, and base layers respectively. The mixture was designed using dedicated pre-programmed software.

Table 7: Properties of aggregate and filler used in the study

Agg. Type	Agg. Group [mm]	Bulk Specific Gravity [g/cm^3]	Specification
Diabase	16-22 (16/22)	2.837	DIN EN 1097-6, Anhang A
Diabase	11-16 (11/16)	2.823	DIN EN 1097-6, Anhang A
Diabase	8-11 (8/11)	2.836	DIN EN 1097-6, Anhang A
Diabase	5-8 (5/8)	2.825	DIN EN 1097-6, Anhang A
Diabase	2-5 (2/5)	2.831	DIN EN 1097-6, Anhang A
Diabase	0-2 (0/2)	2.831	DIN EN 1097-6, Anhang A
Limestone filler	0-0.063 (0/0.063)	2.835	By Manufacturer

Table 8: Gradation limits and selected percentages of SMA 11 S, RAP and corrections

Sieve size, [mm]	Specification limits passing, [%]		Selected, [%] passing	RAP, S, [%]	Correction [%]
	Lower	Upper			
16.000	100.0	100.0	100.0	100.0	100.0
11.200	90.0	100.0	100.0	100.0	100.0
8.000	50.0	65.0	65.0	71.4	7.0
5.600	35.0	45.0	45.0	49.3	6.0
2.000	20.0	30.0	28.5	31.6	1.0
0.063	8.0	12.0	10.0	11.1	0.0

Table 9: Gradation limits and selected percentages of AC 16 B S

Sieve size, [mm]	Specification limits passing, [%]		Selected, [%] passing
	lower	Upper	
22.400	100.0	-	
16.000	90.0	100.0	100.0
11.200	65.0	80.0	80.0
2.000	25.0	30.0	29.2
0.125	5.0	10.0	8.5
0.063	3.0	7.0	6.5

Table 10: Gradation limits and selected percentages of AC 16 T D, RAP, and corrections

Sieve size, [mm]	Specification limits passing, [%]		Selected, [%] passing	RAP, B [%] passing	Correction [%]
	Lower	Upper			
22.400	100.0	100.0	100.0	100.0	100.0
16.000	90.0	100.0	98.0	99.1	88.0
11.000	80.0	90.0	90.0	96.7	29.0
2.000	30.0	50.0	43.4	47.0	11.0
0.125	8.0	20.0	14.0	15.0	5.0
0.0635	6.0	11.0	10.9	11.5	5.0

Table 11: Gradation limits and selected percentages of AC 22 T S

Sieve size, [mm]	Specification limits passing, [%]		Selected, [%] passing	RAP, T [%] passing	Correction [%]
	Lower	Upper			
31.500	100.0	100.0	100.0	100.0	100.0
22.400	90.0	100.0	100.0	100.0	100.0
16.000	75.0	90.0	89.9	89.0	98.0
2.000	25.0	40.0	37.6	35.5	56.5
0.125	4.0	14.0	11.2	6.8	50.8
0.063	2.0	9.0	8.6	5.7	34.7

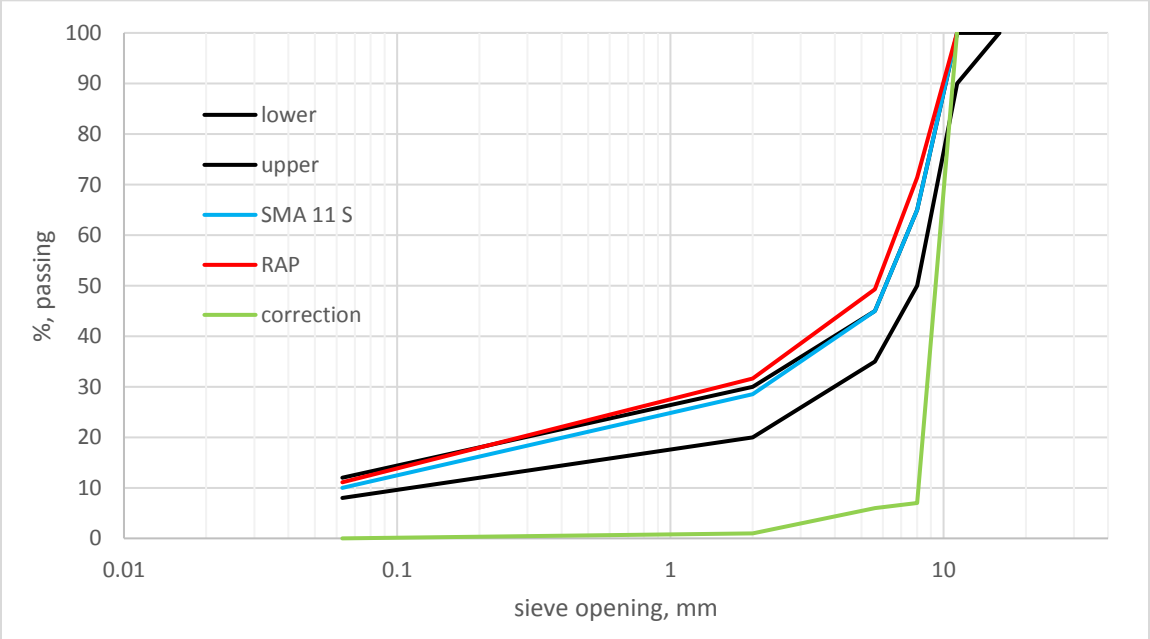

Fig. 21: Grain size distribution curve of SMA 11 S, RAP of surface course, and corrections.

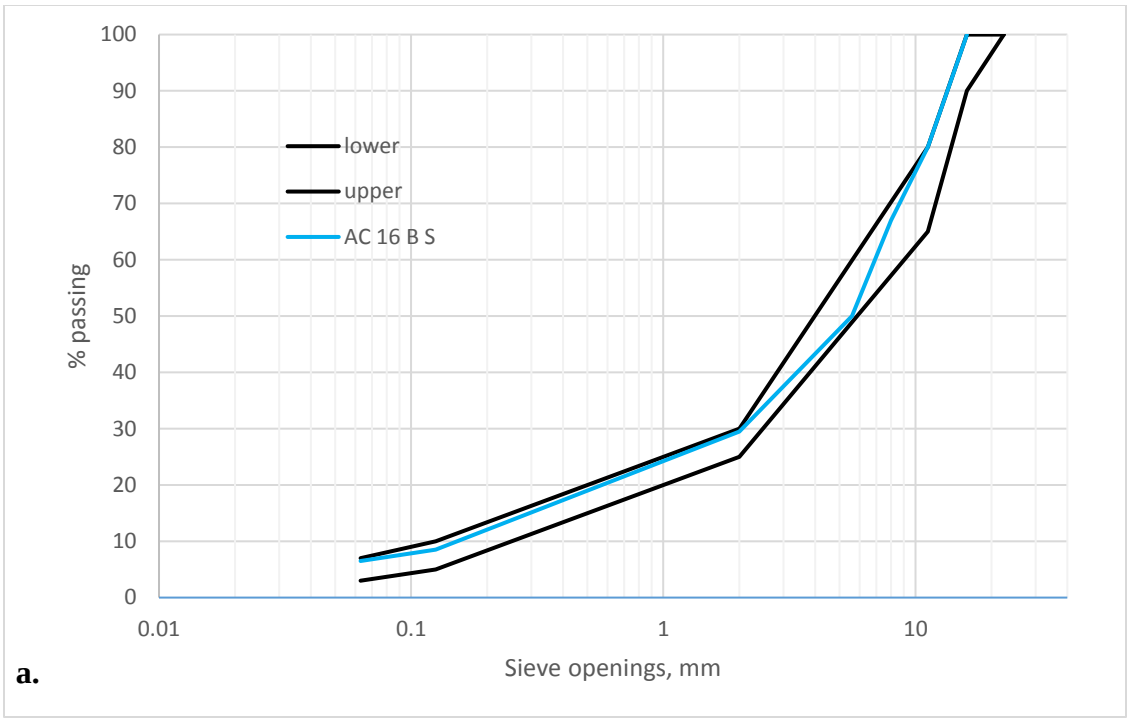

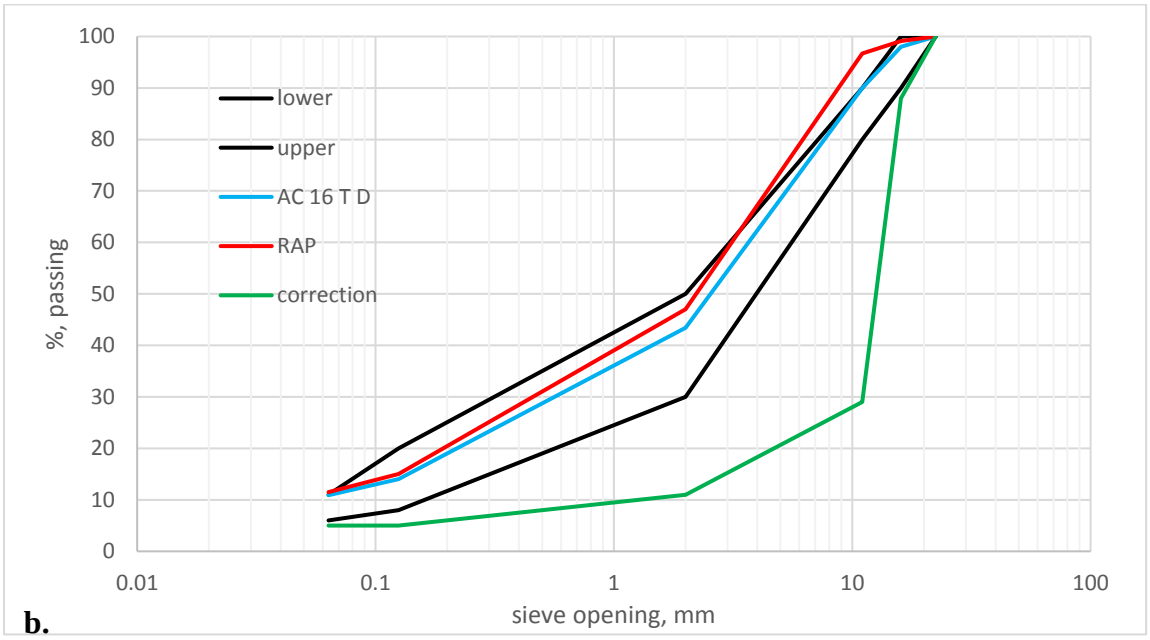

Fig. 22: Grain size distribution curve of (**a.**) AC 16 B S and (**b.**) AC 16 T D, RAP of binder layer and corrections.

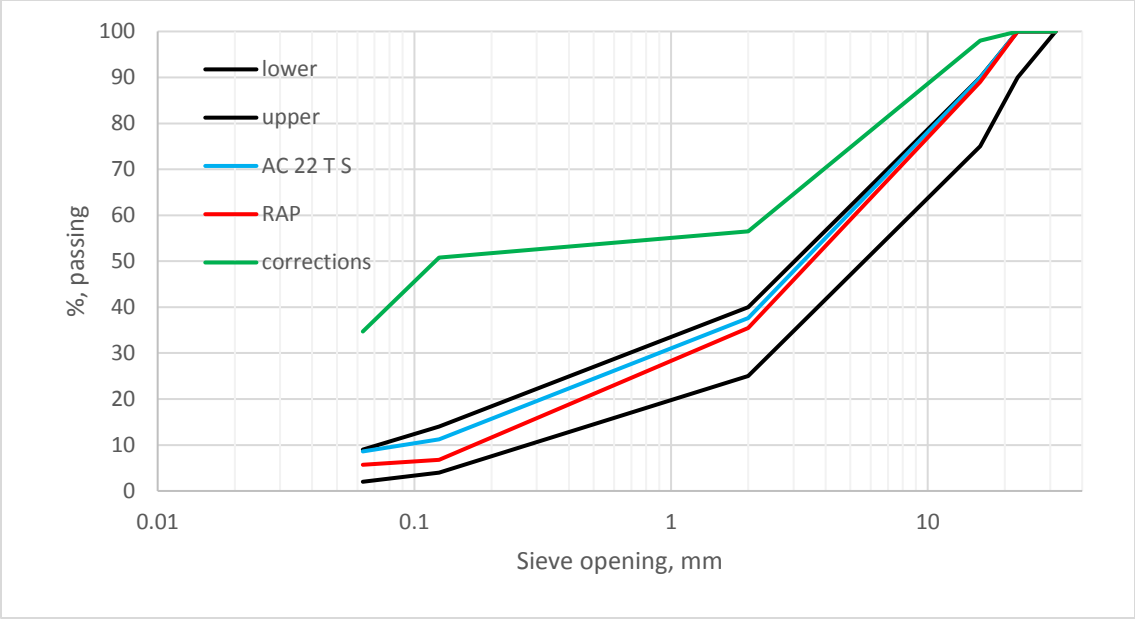

Fig. 23: Grain distribution curve of AC 22 T S and corrections.

Marshall specimens (Ø = 101.6 ± 0.1 mm, height 63.5 ±2.5 mm) were then prepared using three systematic selected bitumen contents to determine optimum bitumen subject to volumetric parameter (air void contents and density) to meet relevant specifications. Table 12 shows properties of mixtures used in the study. The selected fiber content for SMA 11 S was 0.3% of the total mix, and the detailed results are shown in Appendix A.

Table 12: Values of Marshall specimens for different mix types

Asphalt type	Bitumen type	Min. binder content [%]	Air voids limit, [%]	Obtained air voids, [%]	Optimum binder, [%]
SMA 11 S	30/45	6.6	2.5 to 3.0	2.7	7.2
SMA 11 S	25/55-55 A	6.6	2.5 to 3.0	2.5	7.2
AC 16 BS	30/45	4.4	3.5 to 6.5	5.7	5.0
AC 16 TD	50/70	5.4	1.0 to 3.0	1.7	5.7
AC 22 TS	30/45	3.8	5.0 to 7.0	6.2	4.5
AC 22 TS	50/70	3.8	5.0 to 7.0	5.4	4.5

3.2.3 Ozone (O3)

Ozone was selected as a gaseous oxidizing agent and is classified as one of the most powerful oxidizers. In addition, ozone traces in the air can be generated as an interaction product between vehicles' exhaust fumes and ultraviolet radiation (UV).

3.2.4 Hydrogen Peroxide (H_2O_2)

As an aqueous oxidizing agent hydrogen peroxide was obtained from the department of chemistry at the University of Wuppertal. Its properties are presented below in Table 13, as supported from the chemistry department of the University.

3.2.5 Rejuvenating Agents

Three types of rejuvenating agents were used in this study and chosen from three different sources. The first is wax based and denoted as agent 1, while the other two agents are oil based and denoted as agents 2 and 3. The properties of these agents, as supplied by manufacturers, are listed in Tables 14, 15, and 16 respectively.

Table 13: Properties of H_2O_2 used in the study

Property	Unit	Value
Formula		HOOH
Molar mass	[g/mol]	34.01
Concentration	[%]	35.00
Density, @ 20 ºC	[g/cm^3]	1.13
Boiling Temperature	[ºC]	150.20
Melting Temperature	[ºC]	-0.43
Oxidation Potential	[V]	1.80

Table 14: Properties of rejuvenating agent no. 1

Parameter	Unit	Typical values	Method
Pour point*	[°C]	85-105	DIN ISO 2207
Dyn. Viscosity @ 120 °C	[mPas]	35-55 **	Brookfield
Flash point, COC	[°C]	>300	DIN ISO 2599
Pin penetration, 25 °C	1/10 [mm]	25-35	DIN 51580
Water content	[%]	< 1	DIN ISO 3733
PCB *polychlorinated biphenyls)	[mg/kg]		DIN 51527-1
PAH to EPA (polycyclic aromatic hydrocarbons benzo(a)pyrene	[mg/kg] [mg/kg]	< 10 < 0.5	Gas chromatography

* on a rotating thermometer

** kin. Viscosity due to higher viscosity and darker color is not possible

COC: Cleveland open cup.

Table 15: Properties of rejuvenating agent no. 2

Parameter	Unit	Value
Density at 25 °C	[g/mL]	0.932
Viscosity 40°C	[cSt]	55.000
Viscosity 60 °C	[cSt]	30.000
Flash point (closed cup)	[°C]	269.000
pH-value	[-]	7.600
Oligomer Content	[%]	15.00

Table 16: Properties of rejuvenating agent no. 3

Parameter	Unit	Min	Max	Typical	Method
Density, 15 °C	[kg/dm^3]	0.910	0.925	0.917	EN 15326
Viscosity, 0 °C	[mm^2/s]	3000.000	5000.000	4000.000	EN 12595
Viscosity, 20 °C	[mm^2/s]	450.000	600.000	530.000	EN 12595
Viscosity, 60 °C	[mm^2/s]	30.000	40.000	36.000	EN 12595
Flash point, PM	[°C]	206.000		212.000	EN ISO 2719
Pour point	[°C]		-15.000	30.000	ASTM D 97

3.3 Testing Methods

To achieve the goal of this study, the testing consisted of evaluating the performance properties of aged and asphalt mixes with RAP along with standard asphalt mixes as a control mix (reference mix). Marshall specimens were produced at different bitumen contents to determine the optimum bitumen content that meets relevant specifications. A novel ageing method in the laboratory was then applied to simulate the real ageing process.

In the second part of the study, asphalt samples with RAP were prepared and evaluated against performance tests. The laboratory tests were divided into two groups, one for bitumen and the other for asphalt. The samples were cored or cut from laboratory-produced

slabs and dried before the dimensions and bulk specific gravity were determined. The specimen diameters and thicknesses were determined according to the maximum aggregate size or test requirement. Specimens were placed into the testing machine in the same direction of compaction to avoid an influence of compaction direction on the test results.

3.3.1 Tests of Asphalt

3.3.1.1 Stiffness Modulus

This test is a fundamental performance test and was performed to determine or simulate the performance of asphalt under traffic at different climatic conditions and load patterns. It was performed according to Standard DIN EN 12697-26 (2012_06) at four temperatures: -10 °C, 0 °C, 10 °C and 20 °C. Three load frequencies were applied - 0.1, 1 and 10 Hz - and three specimens were tested for every test parameter. The specimen dimensions for this test were 100 mm diameter by 40 mm height for SMA 11 S and AC 16 B S and 150 mm diameter by 60 mm height for AC 22 T S. The test was applied and controlled using the GEOsys8.7.8 software. A template Excel sheet was used for interpretation, and results for every load frequency were calculated using the software. The results were then combined, and master curves of stiffness modulus versus reduced frequency were created using regression analysis and the solver feature of Excel.

3.3.1.2 Fatigue Test

The ability of asphalt mix to resist accumulations of damage was evaluated using this test, according to Standard DIN EN 12697-24 (2012_06). The sample dimensions were the same as the stiffness tests. However, the samples were tested at one temperature, 20 °C, and one frequency, 10 Hz. According to the specifications, three sets of specimens with three specimens each were tested at three different loading magnitudes. Thereafter, the initial strain to failure and number of load cycles were recorded for each set and combined

in one graph. This graph describes the linear relationship between the numbers of load cycles to failure versus the initial strain.

3.3.1.3 Dynamic Creep Test

This test was conducted at 50 ºC according to Standard DIN EN 12697-25 (2016_12). All specimens had dimensions of 150 mm diameter by 60 mm height, regardless of maximum aggregate size.

3.3.1.4 Low Temperature Test

Performance at low temperature was assessed using this test in two ways according to Standard DIN EN 12697-46 (2012_07). The test specimen is a prism with a square cross-section of 40 mm for SMA 11 S and 50 mm for AC 16 T D, while the length of the prism was 160 mm for all. The specimens were first tested by setting the test specimen between fixed ends. The test started from 20 ºC by reducing the temperature by a rate of 10 K/h until failure due to cryogenic stresses, while the specimen length was kept constant. The second method was a direct tension test at a rate of 1 mm/min performed at four temperatures: 20 °C, 5 °C, -10 °C, and -25 °C. This test was not performed with AC 22 T S since the effect of low temperature is a surface phenomenon and thus the base layer is less affected.

3.3.2 Tests of Bitumen

In addition to the standard empirical tests (needle penetration, softening point, breaking point, RTFOT and PAV test), the bitumen was evaluated using two additional tests.

3.3.2.1 Dynamic Shear Rheometer (DSR) Test

The DSR test was performed to determine and analyze the rheological properties of bitumen by applying torque stress to bitumen samples at different temperatures (-5 °C up to 100 °C) and different frequencies (0.1, 1, 1.59, 5, and 10 Hz), with continuous recording of complex shear stiffness (G*) and phase angle (δ) of binders. Two diameters were used in this test (8 mm and 25 mm), which was applied according to Standard DIN EN 14770.

3.3.2.2 Fourier Transform Infra-Red Spectrometer (FTIR) Test

This test was performed to quantify functional groups consisting of bitumen molecules and the chemical changes during ageing. It was conducted at the Department of Chemistry of Wuppertal University using a Nicolet machine. The bands were calculated and analyzed using the OMNIC 7 software by Thermo Fisher. The testing protocol was in accordance with the BRRC ME 85/13. The testing cells were omni cells with KBr window, and both were purchased from Sigma-Aldrich Company. A sample of solubilized bitumen (tetrachloroethylene) was briefly fitted in the cell between an infrared light source and a detector before subjecting infrared light to the sample and measuring the light absorbed. Depending on the chemical groups and bonds constituting the bitumen molecules, the absorption measurements at different frequencies resulted in a spectrum of absorption as a function of wavenumber. The wavenumber is the unit used and represent the number of waves per centimeter. This test is usually used to identify bitumen's types and to evaluate its ageing properties by measuring changes in chemical bonds at certain bands compared un-aged bitumen of the same bitumen grade. The main frequencies used for this purpose are the carbonyl group (C=O) and the sulfides group (S=O) at 1702 and 1020 cm^{-1} respectively. Polymer-modified bitumen can also be identified using this technique as follows:

1) Styrene butadiene styrene (SBS) at 966 and 698 cm^{-1}
2) Ethylene vinyl acetate) at 1736 and 1242 cm^{-1}

Before taking a spectrum measurement, the device was brought to -180°C using liquid nitrogen and calibrated. A background scan (with the cell filled only with the solvent) was then performed to detect the influence of the solubilizing agent and the effect of cell window. After that, 32 scans at a resolution of 4^{-1} were taken for each sample. All scans were conducted between 400 and 4000 cm^{-1}.

3.4 Research Plan

The steps used in this study can be divided into two main parts: first is maintaining the performance properties within accepted limits and regulations; and to study the effects of the ageing of asphalt mixes in the lab. This was achieved using a new approach to ageing asphalt and bitumen by employing high oxidation chemicals in the form of liquid or gas to accurately simulate the real ageing of pavement in the field. To assess the rate of ageing, reference mixes of new bitumen and aggregate were prepared. Then, the results were analyzed and compared by applying the performance tests for both the new and aged mixtures.

A flow chart of the test plan for the ageing and reusing processes are shown in Figs. 24 and 25, respectively.

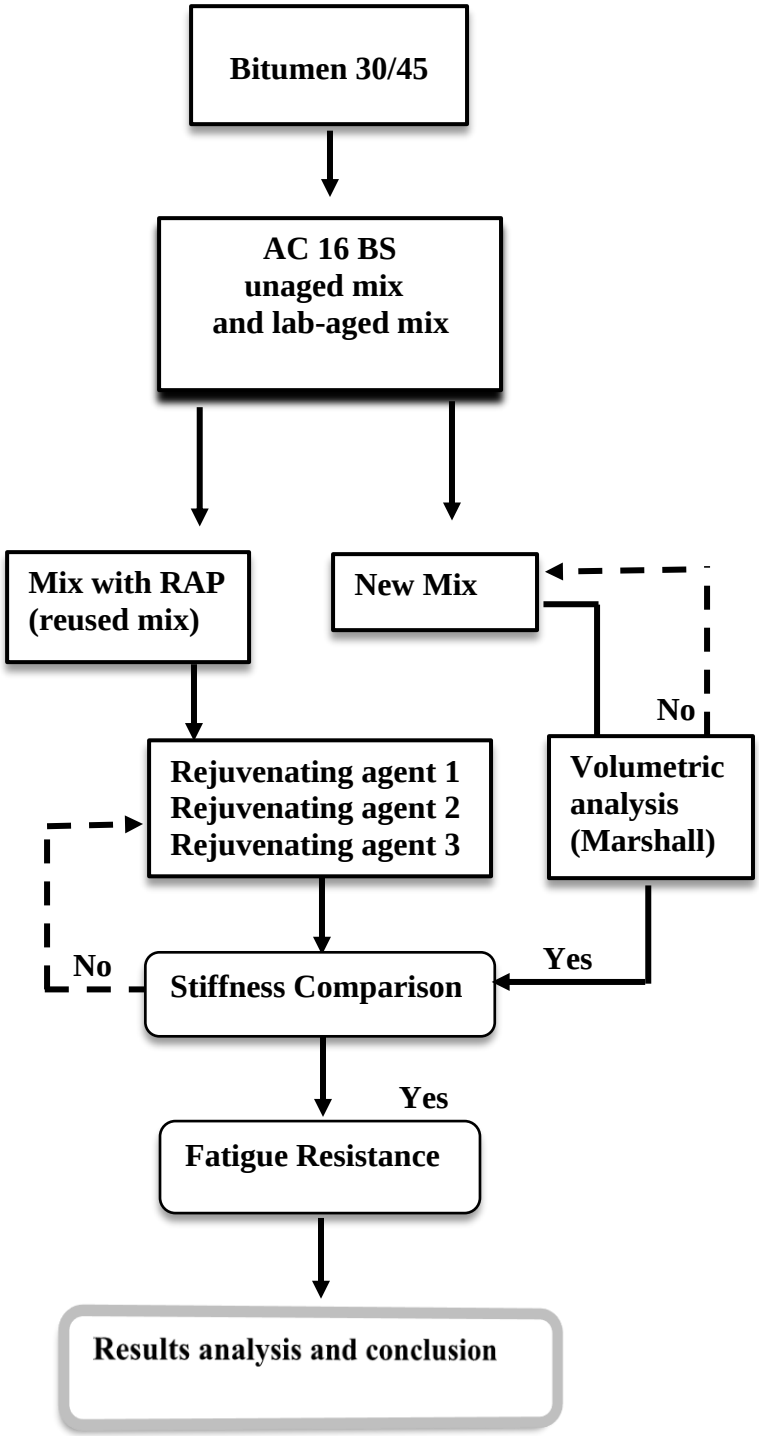

Fig. 24: Flow chart of lab-aged and reused asphalt

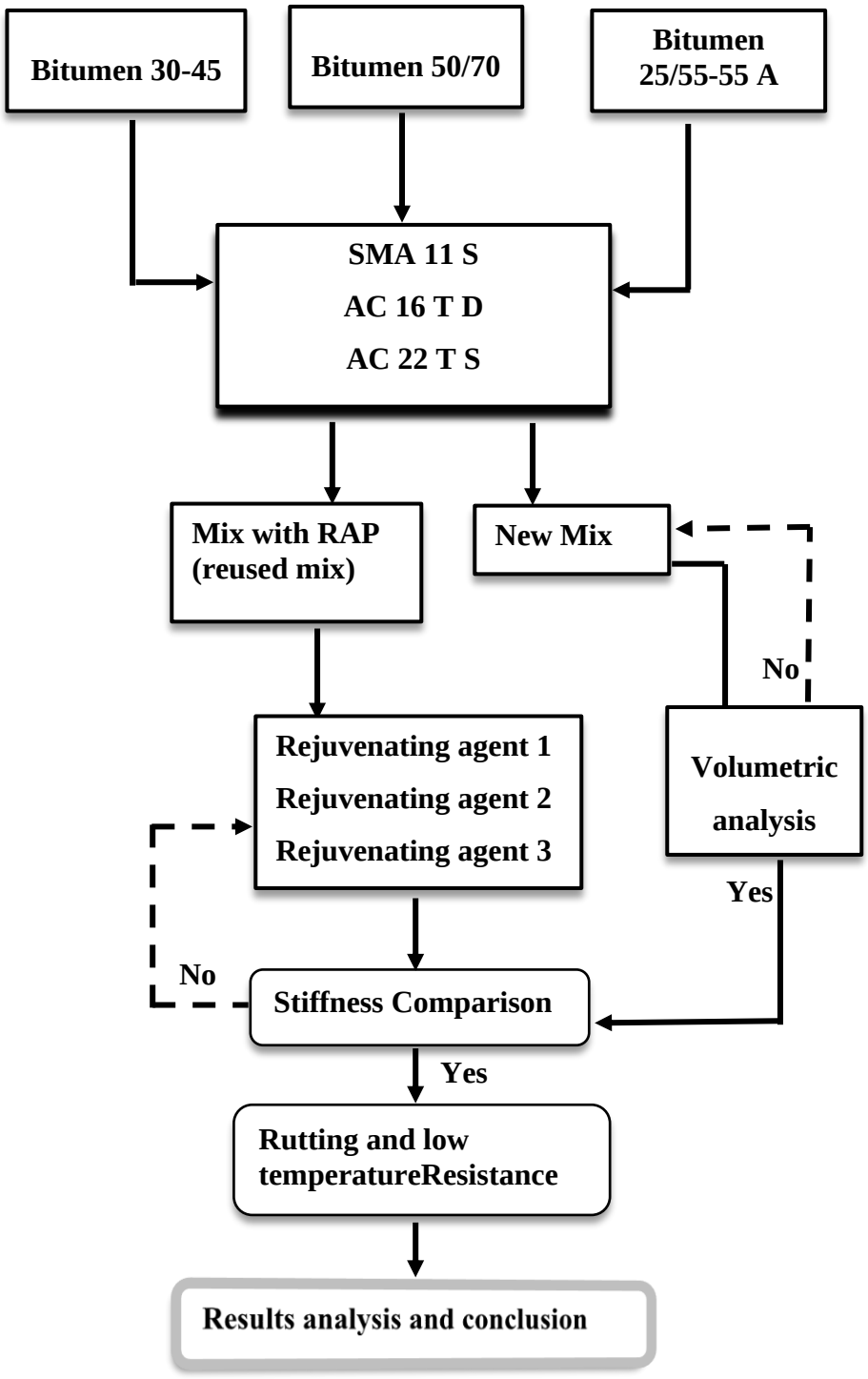

Fig. 25: Flow chart of reused RAP materials

Chapter IV

Ageing of Asphalt Mixtures

The accelerated ageing methods of asphalt mixes in laboratories currently depend on heating asphalt mixtures in ovens at different temperatures and durations. However, the chemical bonds between hydrocarbon atoms and bitumen functional groups are sensitive to temperature magnitude, variation and duration of exposure. For these reasons, new approaches have been developed in this study. This was achieved by employing chemical species or oxidative agents to accelerate oxidative ageing as a predominant cause of asphalt hardening and subsequent ageing. Hydrogen peroxide (H_2O_2) as an aqueous and ozone (O3) as a gaseous oxidative agent have been used.

4.1 Ageing of Asphalt-Mix by Hydrogen Peroxide (H_2O_2)

Asphalt mixtures were prepared according to the Standards of asphalt mixtures EN 12697-35 in the lab of the type AC 16 B S, but without compacting. After mixing, the asphalt mix was prepared to granulates. The granulates were spread to cool to a temperature of 35 ºC and particles were prevented from stick with each other. Then, the granulated asphalt was immersed in H_2O_2 with a concentration of 35%. The process is performed under the hood for safety considerations and to avoid the harmful effects of the excess oxygen emitted from the peroxide after reacting with the bitumen of asphalt, as shown in Fig. 26. The asphalt was immersed for 168 h. Then, asphalt granulates were removed, dried, and again heated to the compacting temperature of 140 ºC. Finally, the compacted specimens were evaluated in order to determine stiffness modulus and fatigue resistance. New asphalt mixtures were prepared without this ageing pathway in order to compare results and identify the extent of accelerated ageing of this approach.

a. Side view

b. Top view

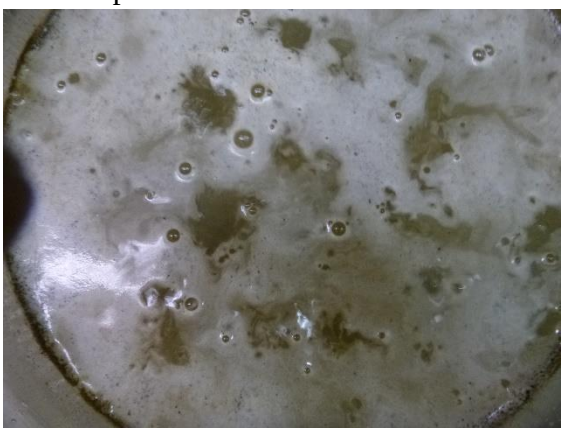

Fig. 26: H_2O_2 chamber of ageing asphalt, (a) side view and (b) top view

4.2 Ageing of Asphalt-Mix by Ozone (O3)

Ozone is a highly oxidizing gas and is produced as a side product of vehicle gases' interaction with UV light. For this reason, it is used in this study to accelerate the asphalt ageing in the lab and to simulate the real ageing process in the field. However, the number of samples was limited to two since this test was performed in the test chamber (shown in Fig. 27), which is specialized for testing rubber products in the automobile industry. This test was conducted in the lab of the testing company, and the granulated asphalt was subjected to a stream of ozone gas at a concentration of 20 ppm for 300h and at 50% humidity.

Fig. 27: Ozone ageing testing machine

(http://www.argentox.com/de/ozonpruefschraenke/index.php)

4.3 Ageing of Asphalt-Mix by Current Ways (Heating Method)

For comparison purposes, the asphalt mixes were further aged using the current used method of ageing by heating. For short-term ageing, the asphalt mix was stored at 135 ºC for 4 h in an oven. The long-term ageing consists of the same procedure of short-term ageing followed by ageing by storing the asphalt mix for 288 h at 75 ºC in the oven. This temperature was chosen after reviewing previous relevant work (EPA, 2008) and since it does not exceed the temperature of pavement in the field.

4.4 Ageing of Bitumen by RTFOT and PAV Test

A neat bitumen of grade 30/45 was evaluated using standard evaluation methods along with dynamic and chemical analysis, and bitumen extracted from new or aged mixes were likewise evaluated.

4.5 Pros and Cons of Different Ageing-Methods (General Aspects)

The use of peroxide as an oxidizing agent of asphalt has the advantage of simulating the oxidation process of asphalt in the field. Thus, there is no need to elevate temperatures to obtain aged asphalt. Furthermore, this process is simple, does not require specialized equipment or tools. In addition, it can be easily integrated with asphalt-specimens preparation where it can be applied after mixing asphalt granules, and can be applied on loose or compacted asphalt. However, safety should be reconsidered due to the fumes emitted during the test, as shown previously in Fig. 26, to avoid skin or eye irritation. This issue can be addressed by applying the test under a ventilating hood.

One advantage of using ozone as a gaseous oxidizing agent concerns ability to simulate asphalt conditions in the field because the ozone can occur naturally as a product of the interaction between vehicles fumes and UV light. Safety is another advantage of this process since it is applied in a closed chamber and can be applied on loose or compacted asphalt. The main disadvantage regards the need for a specialized stain-less steel chamber, because ozone is a highly corrosive gas.

Chapter V

Changes of Asphalt Specimens' Properties and Bitumen-Properties

The performance properties of asphalt were evaluated by measuring the stiffness modulus and fatigue resistance for un-aged and aged asphalt specimens. This achieved by using different methods of ageing, as previously described in Chapter 4. The determined test results were evaluated to compare the effectiveness between different ageing methods used. In addition, the bitumen properties were measured for the un-aged bitumen and bitumen extracted from aged asphalt. This included measuring the conventional, rheological and chemical properties of bitumen. The test results were analyzed to determine the change due to ageing using the methods employed in the study.

5.1 Stiffness of Asphalt Specimens

This test is a common method to measure the stiffness modulus of mixtures at different temperatures and load frequencies and hence to evaluate asphalt's resistance to different types of loadings. At low temperatures, the asphalt mixture becomes stiffer (since bitumen viscosity is high at these temperatures) and more susceptible to cracking. At high temperatures however, the stiffness modulus of the asphalt mixture is low since bitumen is less viscous. The decrease in viscosity leads to the problem of pavement rutting, especially in the wheel path. For the lab samples aged by peroxide, Fig. 28 shows the stiffness modulus for new and aged asphalt (AC 16 B S). At high temperatures or low vehicle speed (which is expressed by log reduced frequency) there was no significant difference in the stiffness modulus since both were less than 5×10^3 MPa. At low temperatures or high vehicles speeds, there was an increase in the stiffness modulus of about 3×10^3 MPa for the oxidized bitumen compared to the new mix. An increase of about 10% in the stiffness modulus of asphalt was obtained by using peroxide as an oxidizing agent according to the specified method. Additional results are shown in Appendix B.

To further study the effect of high temperature on the stiffness modulus of aged asphalt, asphalt granules were aged in an oven for 4 h at 135 ºC and then aged by peroxide (Fig. 29). They also were aged by peroxide first and then by oven for 4 h at 135 ºC (Fig. 30).

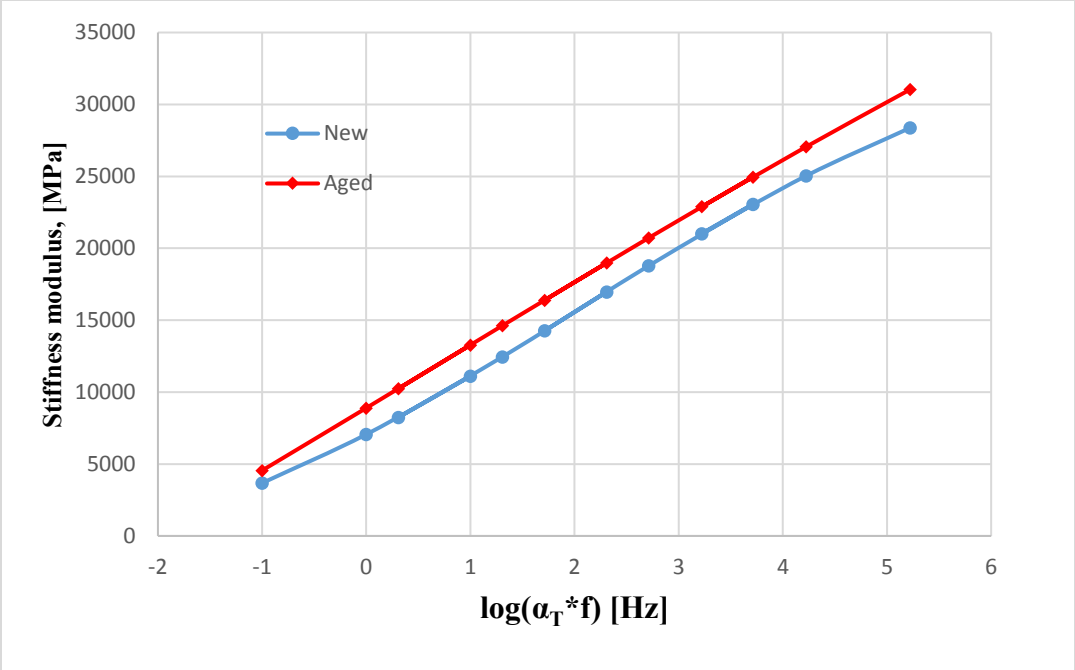

Fig. 28: Stiffness modulus of aged asphalt mix by H_2O_2 and compared to new mix of binder layer, AC 16 B S

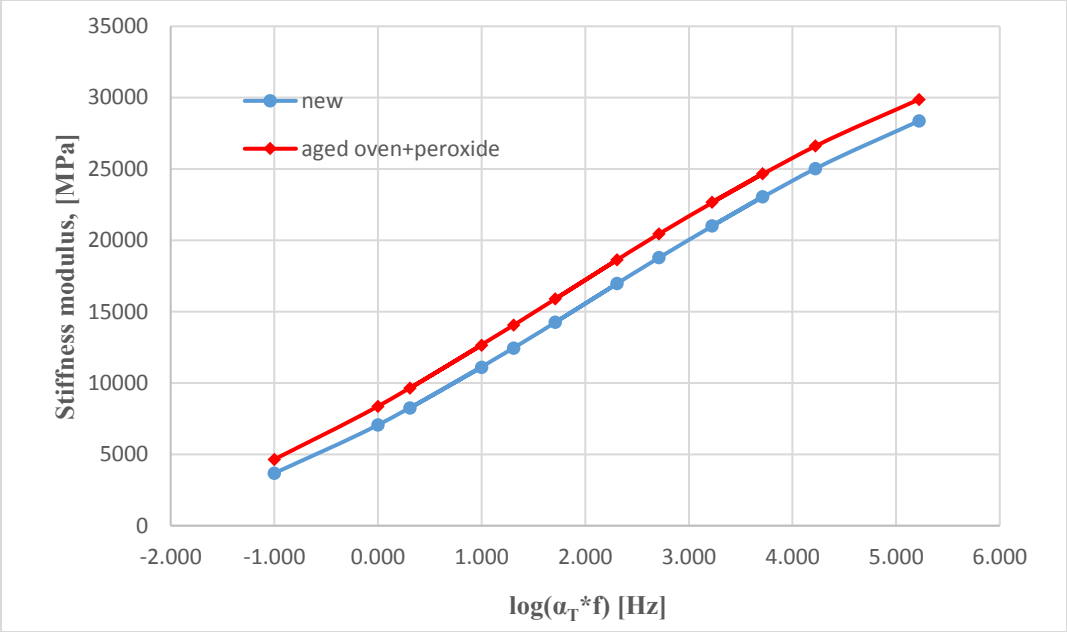

Fig. 29: Stiffness modulus of aged asphalt mix by oven for 4 h at 135 ºC + H_2O_2 and compared to new mix of binder layer, AC 16 B S

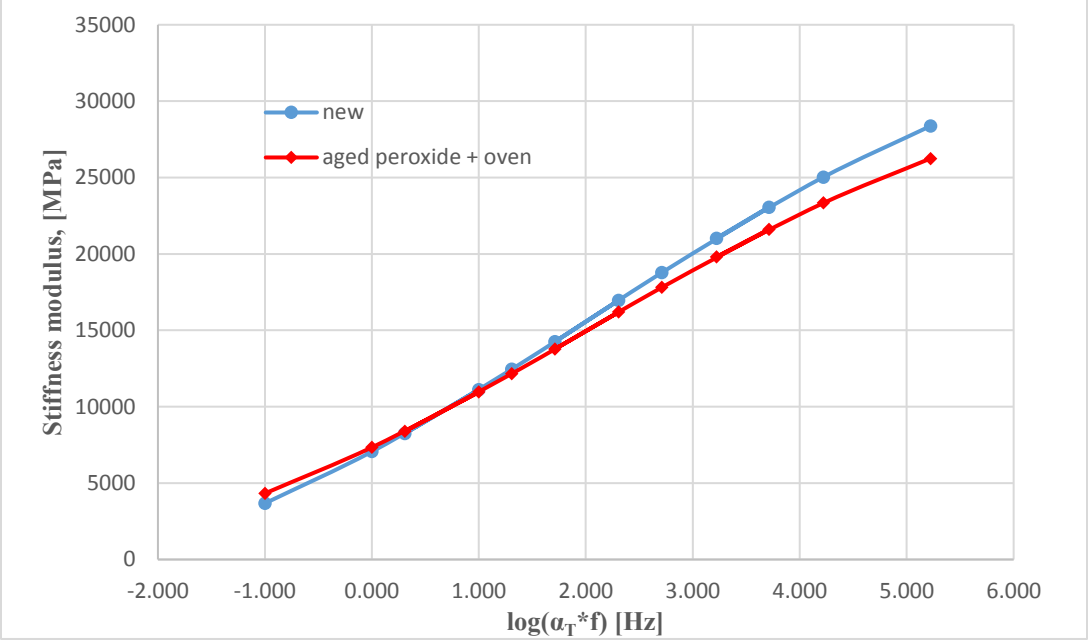

Fig. 30: Stiffness modulus of aged asphalt mix by H_2O_2 + oven for 4 h at 135 ºC and compared to new mix of binder layer, AC 16 B S

The enhanced stiffness modulus of the oven-aged- specimens, before and after ageing by peroxide, unexpectedly revealed that the results of both methods were less than the increase obtained using peroxide alone. Moreover, when the peroxide-aged samples overheated (H_2O_2 + oven), there was also a reduction in stiffness, which may be attributed to the impact of peroxide on the molecular structure of bitumen.

The test using ozone was not performed under ideal conditions since asphalt granulates were accumulated in the testing chamber. This accumulation limits the exposure to ozone stream to only the bitumen film on the top layer, with less exposure to the binder at lower layers. However, there was a marginal increase in stiffness of about 700 MPa (4%) at low temperatures or high loading frequency, as shown in Fig. 31. At high temperatures or low loading frequency, there was no difference in stiffness between the control and ozone-aged specimens. This may be due to the limited number of specimens. Additional results are presented in Appendix B.

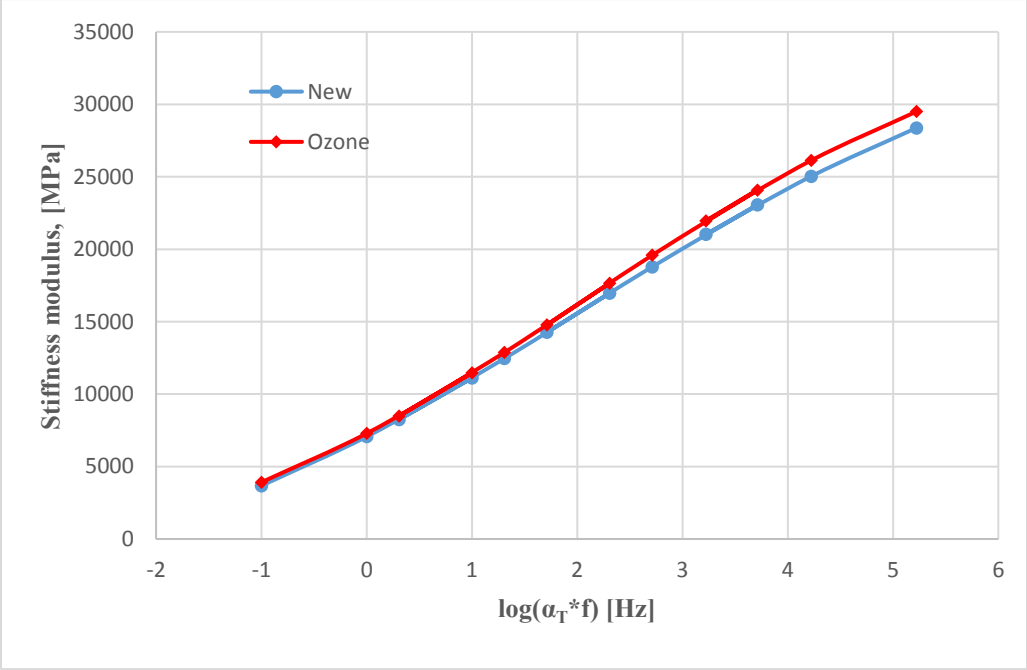

Fig. 31: Stiffness modulus of ozone-aged asphalt compared to new asphalt

The results of the short- and long-term ageing of asphalt are shown in Fig. 32 (previously described in Chapter four). Incremental decrease is shown in stiffness as the frequency increases. This means that the stiffness of aged asphalt decreases at low temperatures compared to the new asphalt. This unusual behavior may be explained as an effect of the ageing procedure which weakens the bonding and compaction potential of loose asphalt and workability due to the use of high temperatures. Additional results are shown in Appendix B.

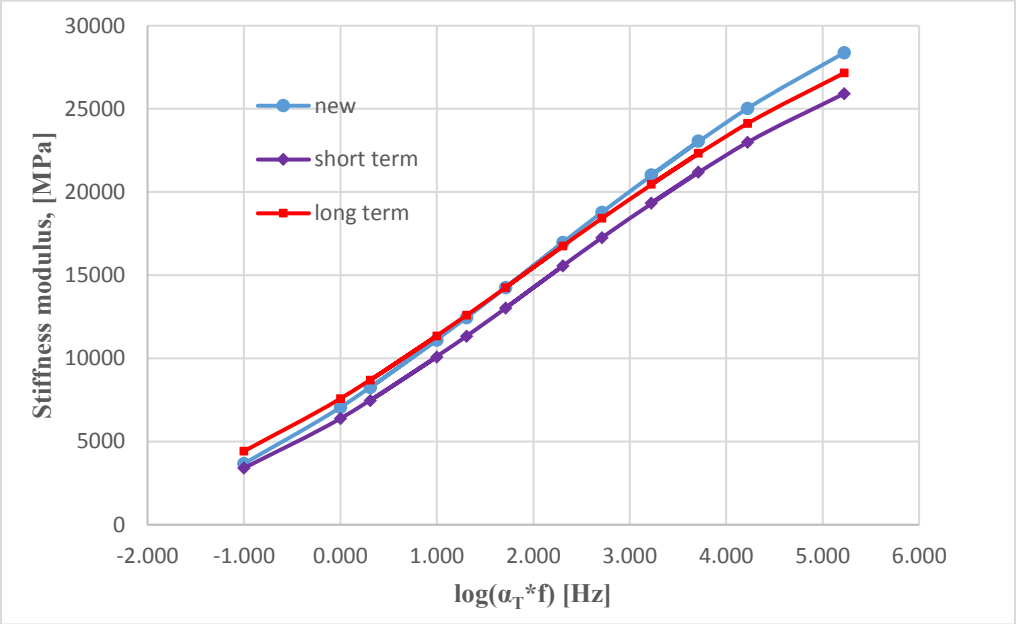

Fig. 32: Stiffness modulus of aged asphalt by short-term and long-term ageing methods as compared to new asphalt

Finally, the stiffness results obtained from above mentioned ageing methods were normalized to the unaged (new) mix. Moreover, results presented as a rate of change to the unaged mix (Fig. 33) at high and low temperatures. The results confirm the role of peroxide in accelerating the ageing of bitumen in the asphalt where, stiffness of peroxide aged mix is higher than other mixes and nearly comparable to short-term and peroxide aged mix (ST+per).

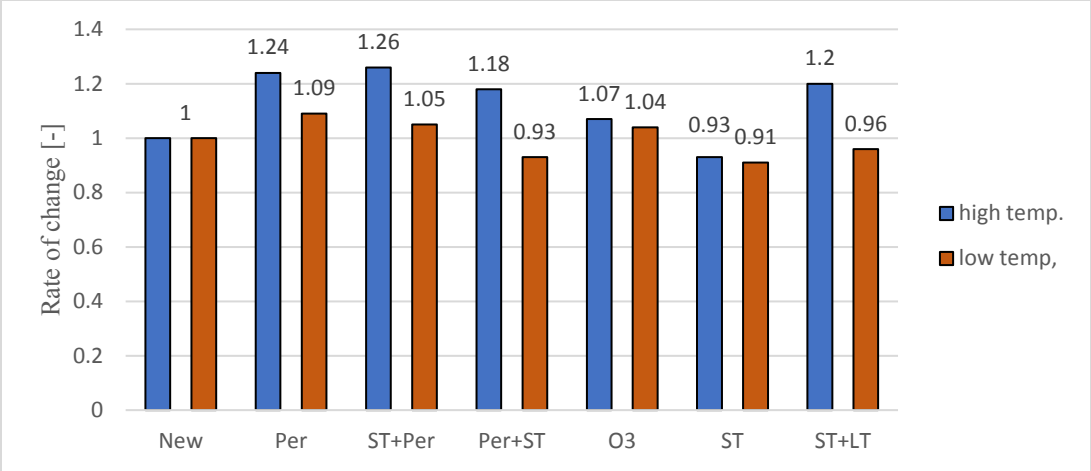

Legend:

New = new / control mix Per = peroxide-aged mix ST+per = short-term + peroxide Per+ST = peroxide-aged + short-term O3 = ozone-aged mix and ST = short-term ageing LT = long-term aged

Fig. 33: Effect of ageing method on stiffness as a rate of change of aged to control (new) mix

5.2 Fatigue of Asphalt Specimens

This test is performed to evaluate asphalt's resistance to load repetitions of magnitudes below failure loads at the same load frequency. Three load categories (high [σ = 0.8 MPa], middle [σ = 0.35 MPa], and low [σ = 0.2 MPa]) were used to simulate different vehicles' capacities. The selected load categories were kept constant for all variants tested (Table 17). The measured results of fatigue behavior are taking the form of power equation as shown in Fig. 34 for the unaged mix. The calculated values of load cycles are obtained through applying the equation derived from measured results. The calculated values are used in the comparison between different variants because the measured results are composed of two variables (initial elastic strain and load cycles). Initial elastic strain is selected at two different points (0.03‰ for light loadings and 0.10‰ for heavy loadings) as shown in the same figure while, the load cycles are calculated according to the equation. The calculated values are reliable because they are statistically significant as the squared error is less than 5% (R^2 = 0.97). Measured results and calculated values are shown in Table 17 for all variants involved in the fatigue test.

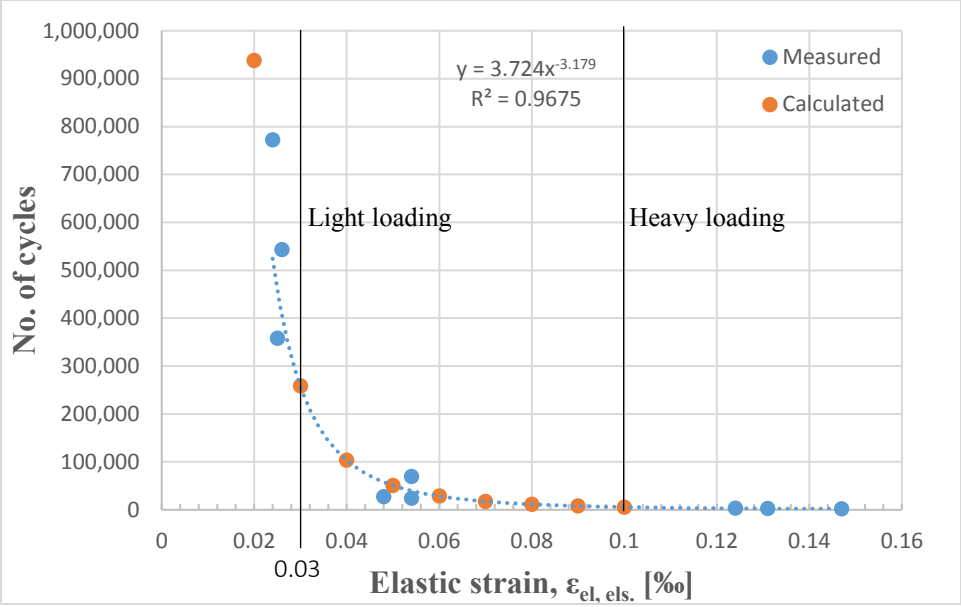

Fig. 34: Measured results and calculated values of fatigue behavior of the new mix

The measured results of the unaged and aged samples by peroxide, Fig. 35 (log-log scale) illustrates that the failure occurred for unaged mix at initial elastic strain of 0.134‰ (2.50×10^3 load cycles) and of 0.025‰ (5.58×10^5 load cycles) for heavy- and light-loadings, respectively. Peroxide aged mix failed at initial elastic strain of 0.109‰ (6.59×10^3 load cycles) and of 0.055‰ (1.02×10^5 load cycles) for heavy- and light-loadings, respectively. Calculated values revealed an increase in the fatigue behavior at heavy loadings (initial elastic strain of 0.10‰) of 162% in the aged mix compared to the new mix (according to the relevant equation). At light loadings (initial elastic strain of 0.03‰), the increase is significant and reaching 477% (Table 17) indicating the impact of ageing using peroxide on asphalt performance. Due to safety considerations and limited test chamber availability, the test parameters such as peroxide concentration or test durations were limited in this study. These concerns resulted a limited number of produced samples.

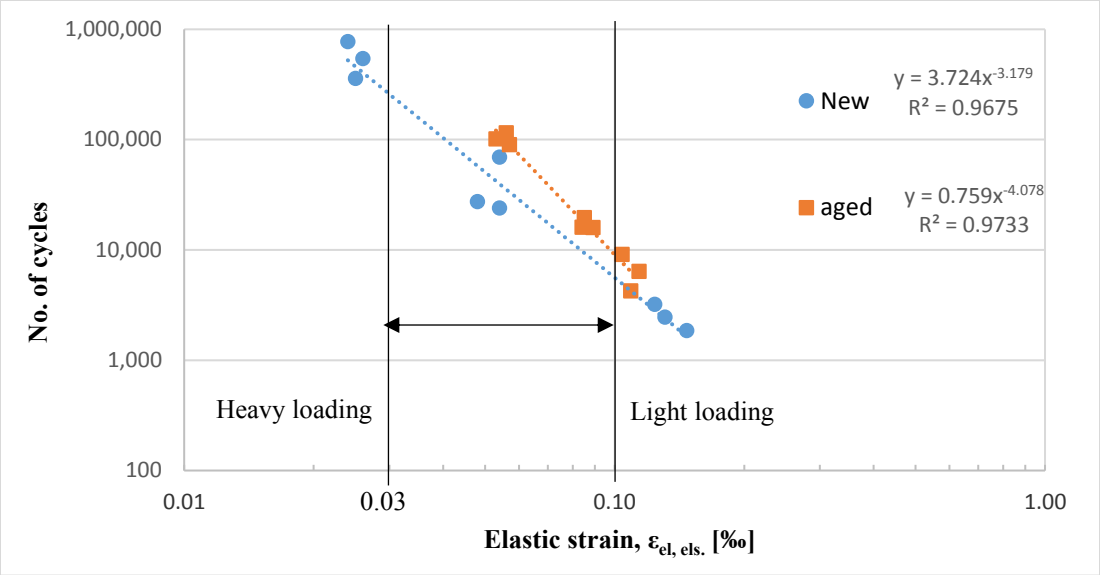

Fig. 35: Fatigue results comparison between new and aged asphalt by peroxide

The fatigue resistances of aged asphalt by combining oven and peroxide-aged samples are shown in Figs. 36 and 37 for oven-aged before and after peroxide ageing, respectively. The use of heating with peroxide-aged samples before and after ageing did not significantly affect the resistance of compacted samples to fatigue compared to the results of ageing using peroxide. Calculated values of load cycles for STB mix at heavy loadings (initial elastic strain of 0.10‰) showed a decrease of 28% while, peroxide aged mix showed an increase of 162%. Similarly, the increase at light loadings (initial elastic strain of 0.03‰) is 290% for STB mix and 477% for peroxide aged mix. Identical behavior is shown for STA mix where, at heavy- and light-loadings, the increase is 119% and 345%, respectively (Table 17). The fatigue results of ozone-aged asphalt exhibited identical resistance for both new and aged mixes, indicating no effect of ageing on fatigue resistance compared to the reference mix (Fig. 38). The limited effect may be attributed to the limited number of available samples (only two specimens) which may cause insignificant results in addition to restricted test conditions. The fatigue results for short- and long-term aged asphalt (Fig. 39) showed an increase in the number of loading cycles until the occurrence of fatigue. However, the results are lower than peroxide aged mix where, short-term aged asphalt (ST) showed an increae at heavy- and light- loadings of 118% and 268% respectively, and long-

term aged asphalt (LT) exhibited an increase at heavy- and light- loadings of 127% and 335% respectively (Table 17). Additional results are found in Appendix C.

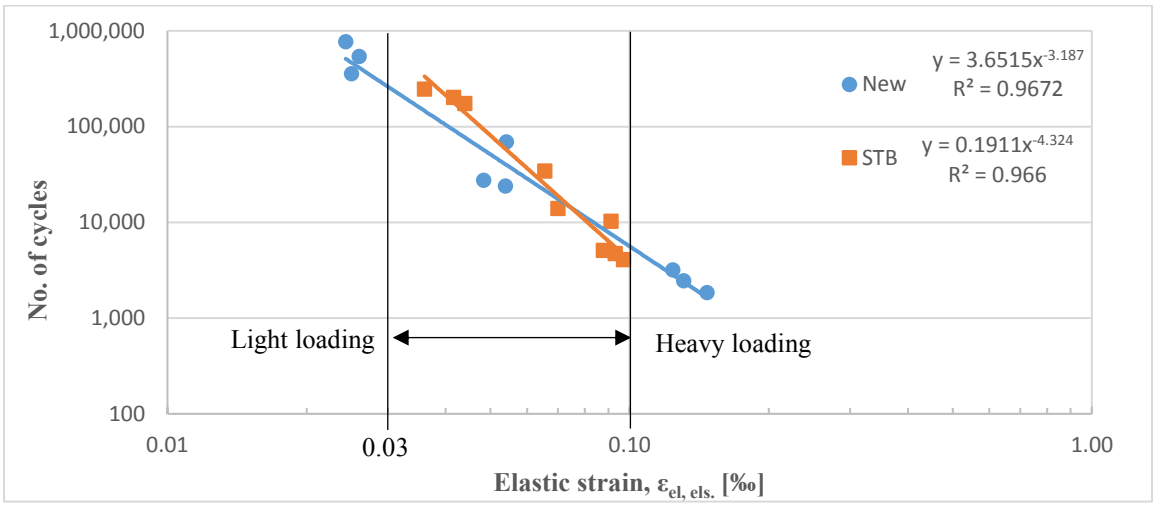

Fig. 36: Fatigue results comparison between new and aged asphalt by oven-aged granulates for 4 h at 135 ºC + peroxide (STB)

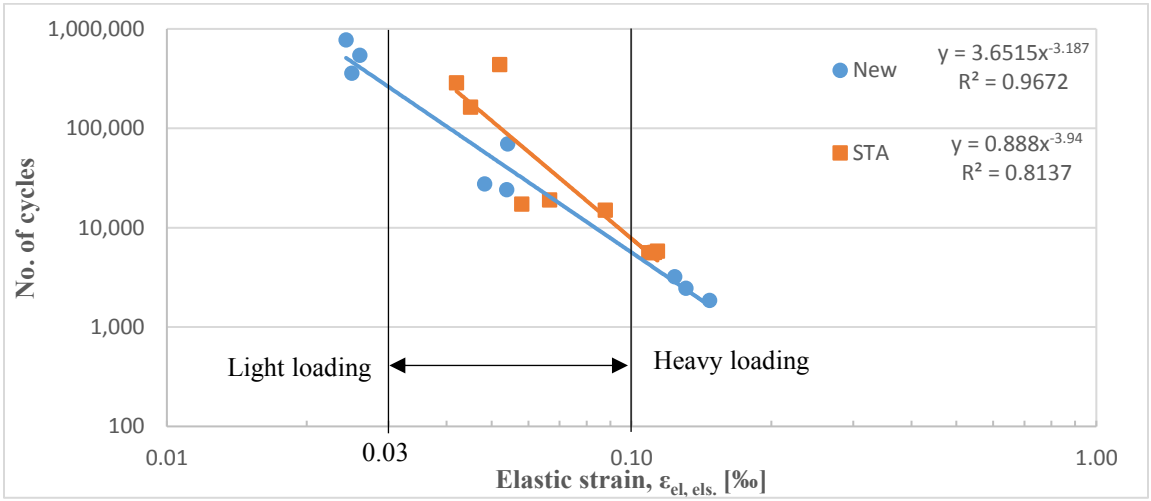

Fig. 37: Fatigue results comparison between new and aged asphalt by peroxide- + oven-aged granules for 4 h at 135 ºC (STA).

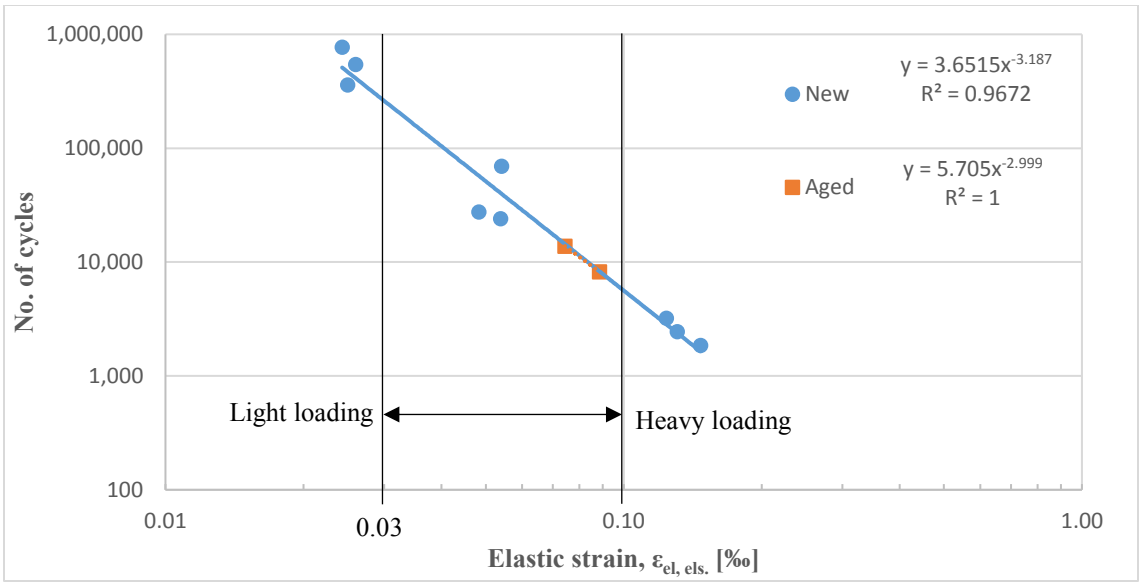

Fig. 38: Fatigue results comparison between new and aged asphalt by ozone

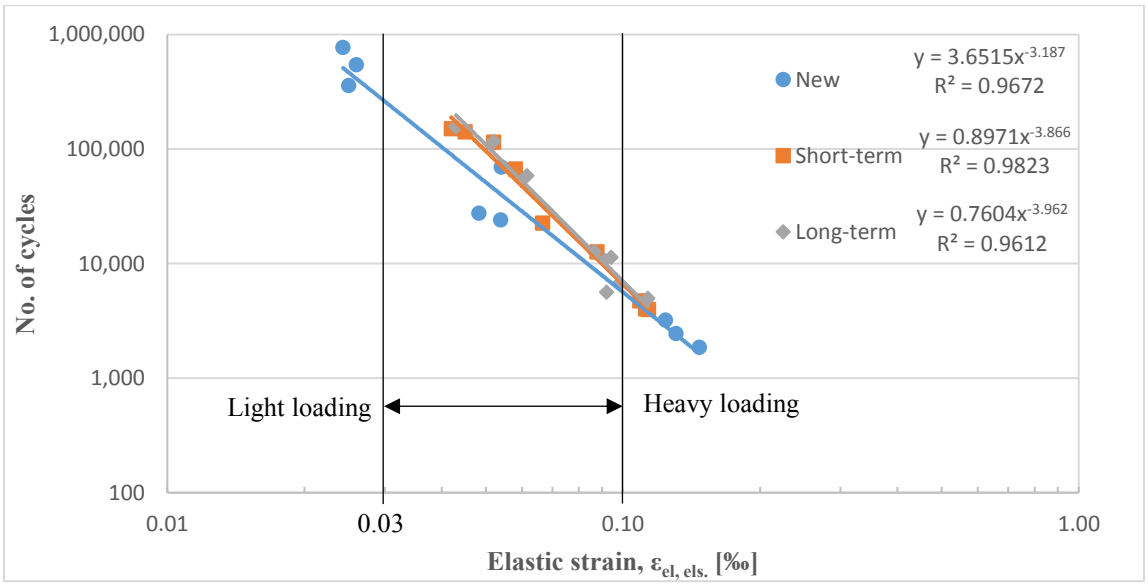

Fig. 39: Fatigue results comparison between new, short- and long term-aged asphalt

Table 17: Test parameters of fatigue behavior for new and aged AC 16 B S mixes

T, [ºC]	20								
f [Hz]	10								
μ [-]	0.2984								
$\sigma_{u,[}$MPa]	0.035			0.035			0.035		
$\sigma_{o,[}$MPa]	0.80	0.80	0.80	0.35	0.35	0.35	0.20	0.20	0.20
	N_{Makro} [-]								
New*	1,853	2,453	3,206	24,007	27,500	69,509	542,854	772,020	358,194
Peroxide*	4,257	9,108	6,405	16,001	19,625	16,038	90,004	101,568	115,421
Ozone*	8,204	13,805							
ST*	3,960	4,710	4,009	12,601	22,503	67,002	141,066	114,494	150,195
STA*	5,802	5,602	5,617	15,000	19,006	17,225	163,510	436,505	286,882
STB*	5,102	4,725	4,105	10,310	14,000	34,500	202,506	175,030	247,084
LT*	4,958	5,622	6,659	10,659	12,608	11,307	58,507	116,294	156,202
	εel, anf [‰]								
New*	0.147	0.131	0.124	0.054	0.048	0.054	0.026	0.024	0.025
Peroxide*	0.109	0.104	0.114	0.089	0.085	0.084	0.057	0.053	0.056
Ozone*	0.089	0.074							
ST*	0.114	0.109	0.112	0.088	0.067	0.058	0.045	0.052	0.042
STA*	0.102	0.106	0.103	0.083	0.078	0.080	0.043	0.037	0.040
STB*	0.088	0.093	0.097	0.091	0.070	0.066	0.042	0.044	0.036
LT*	0.113	0.092	0.098	0.091	0.087	0.094	0.062	0.052	0.043
Equations derived from the test results (Y= cycles to failure and X = initial elastic strain)									
		New	Peroxide	Ozone	ST	STA	STB	LT	
constant	a	3.724	0.759	8.949	0.917	0.582	0.186	0.733	
constant	b	-3.179	-4.078	-2.820	-3.860	-4.061	-4.337	-3.987	
Regression	R^2	0.97	0.97	1.00	0.98	0.99	0.96	0.96	
Y	0.10‰	5,624	9,083	5,913	6,641	6,701	4,043	7,117	
	0.03‰	258,369	1,231,803		692,690	890,343	748,982	864,966	
Rate*, [%]	0.10‰	100	162	105	118	119	72	127	
	0.03‰	100	477		268	345	290	335	

*) New: new mix by using new bitumen of the grade 30/45
Peroxide: AC 16 B S mix aged by using peroxide at a concentration of 35% for 168 h.
Ozone: AC 16 B S mix aged by using ozone at a concentration of 20 ppm and 50% humidity for 300 h.
ST: AC 16 B S mix aged for short-term at 135 ºC for 4 h.
STA: peroxide-aged + short-term aged mix.
STB: short-term-aged + peroxide-aged mix.
LT: short-term-aged + ageing at 75 ºC for 244 h.
Rate: Rate of change calculated as a ratio of aged to new.

5.3 Physical Properties of Bitumen

Fig. 40 shows a comparison of conventional properties, needle penetration at 25 ºC, and softening point (SP ring and ball) for bitumen 30/45 to evaluate temperature susceptibility. The comparison comprises new, lab-aged bitumen by both the RTFOT and PAV tests, and bitumen extracted from new, peroxide-aged, and ozone-aged asphalt mixes. There was a decrease in penetration of about 35% and 59% due to ageing for lab-aged bitumen by RTFOT and RTFOT+PAV (PAV) test respectively compared to unaged bitumen. There was a reduction of about 46%, 57%, and 41% for bitumen extracted from new, peroxide-aged, and ozone-aged asphalt mixes respectively compared to unaged bitumen.

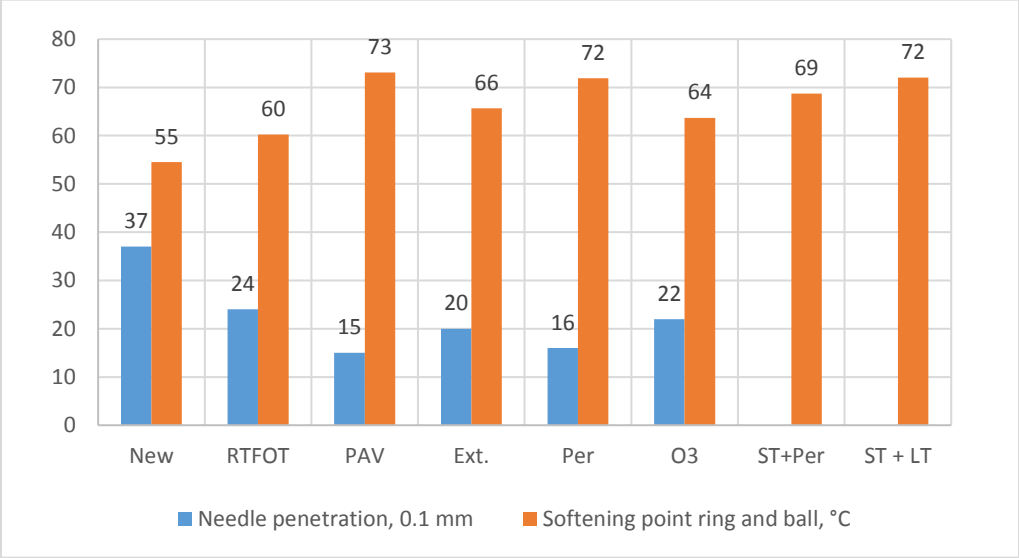

Legend:

New = new / control mix RTFOT= short-term aged bitumen PAV= long-term aged bitumen

*Ext. = extracted from new mix *ST+ per = short-term + peroxide-aged mix *O3 = ozone-aged mix

*Per = peroxide-aged mix *ST+ LT = short-term +long-term aged mix

*, bitumen was extracted from these mixes.

Fig. 40: Penetration and softening point values of bitumen at different conditions of ageing.

Results of penetration for (ST+per) and (ST+LT) were unavailable due to the limited amount of bitumen obtained during the extraction process. Furthermore, the penetration index (PI) is used to evaluate the bitumen response to temperature variations. Equation 3 is used to calculate the penetration index:

$$PI = \frac{1952 - 500.\log(pen) - 20T(R\&B)}{50.\log(pen) - T(R\&B) - 120} \quad \text{.....(3)}$$

where:

PI is penetration index

Pen is penetration at 20 ºC, dmm, and

T(R&B) is softening point ring and ball, ºC

Fig. 41 compares penetration indices for bitumen in the study, where long- term lab-aged bitumen by the PAV test and peroxide-aged bitumen exhibited comparable susceptibility to temperature variations. The penetration indices for peroxide-aged asphalt and PAV-aged bitumen are 0.67 and 0.73 respectively and are higher than the penetration indices of other bitumen, revealing that they are less sensitive to temperature change or are more hardened.

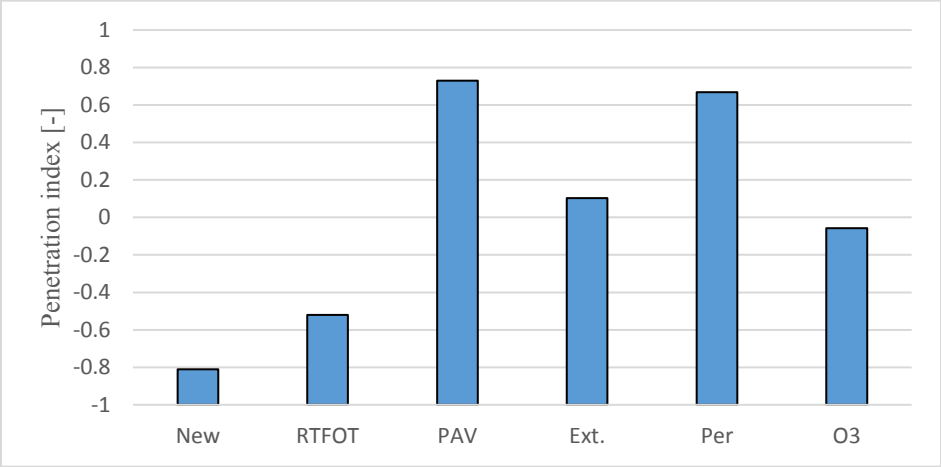

Legend:

New = new / control mix RTFOT= short-term aged bitumen PAV= long-term aged bitumen

*Ext.= extracted from new mix *Per = peroxide-aged mix *O3 = ozone-aged mix

*, bitumen was extracted from these mixes.

Fig. 41: Penetration index of bitumen at different conditions of ageing

The ageing index (Fig. 42) is a ratio of aged to unaged bitumen results regarding needle penetration at 25 ºC or softening point. The results showed that the ageing indices (for needle penetration and softening point) of PAV and peroxide- aged bitumen are comparable. The ageing indices by penetration and softening point for RTFOT and O3-aged bitumen are also nearly comparable. This was in line the with performance results of asphalt. Results of ageing index by penetration for (ST+per) and (ST+LT) were unavailable due to the limited amount of bitumen obtained during the extraction process. These results confirm the impact of peroxide as candidate oxidizing agent for accelerating asphalt ageing in the lab without the need of using elevated temperatures.

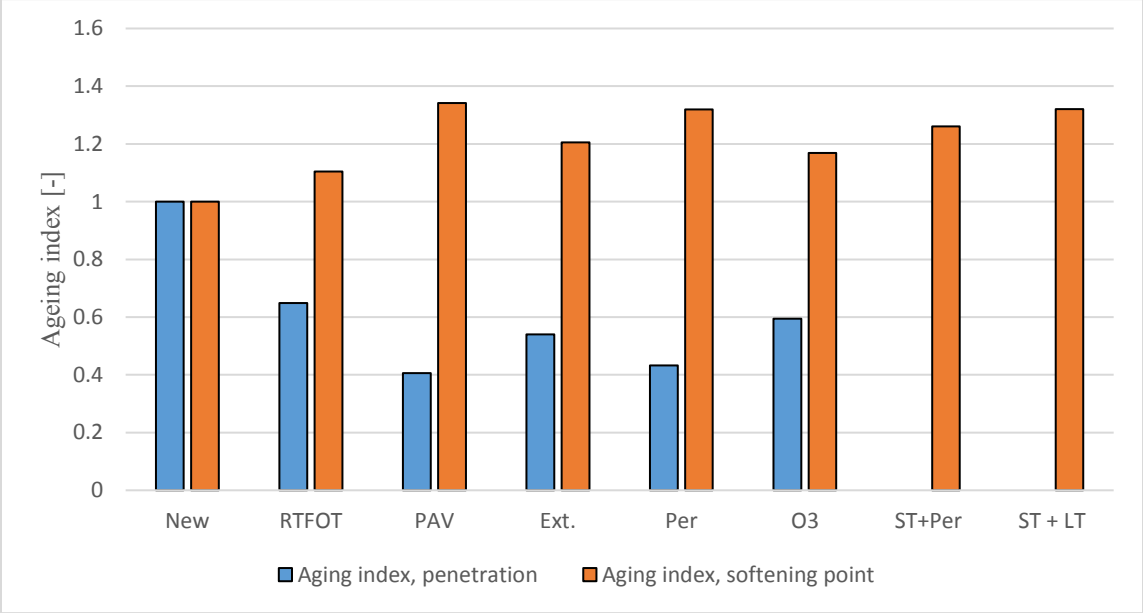

Legend:

New = new / control mix RTFOT= short-term aged bitumen PAV= long -term aged bitumen

*Ext.= extracted from new mix *Per = peroxide-aged mix *O3 = ozone-aged mix

*ST + per = short-term+peroxide-aged mix *ST+ LT = short-term aged +long-term aged mix.

*, bitumen was extracted from these mixes.

Fig. 42: Ageing index of new, lab-aged and extracted bitumen from aged asphalt

5.4 Rheological Properties of Bitumen

The complex modulus and phase angle of bitumen 30/45 were determined for unaged and aged bitumen at different temperatures. Dynamic shear rheometer tests were conducted to demonstrate the influence of the ageing method on the rheological properties of bitumen. It is well known that bitumen's physical, chemical, and rheological properties greatly affect the performance of asphalt such as fatigue or rutting resistance and susceptibility to temperature variations. For this purpose, new and lab-aged bitumen for short- and long-term ageing expressed by RTFOT and PAV tests were evaluated using the DSR test. In this test, complex modulus, G*, and subsequently storage and loss modulus beside the phase angle (δ) were determined at different temperatures, frequencies, and plate geometry. In addition, the bitumen extracted from slabs of new and lab-aged mixes prepared using different ageing methods were evaluated in the same manner. The results were then compared with new, RTFOT, and PAV aged bitumen. The results are shown in Fig. 43. The test was conducted at a frequency of 1.59 Hz. There is an obvious enhancement in complex modulus of aged bitumen by different ageing methods relative to the unaged bitumen. At low temperatures, bitumen exhibits glass-like behavior but has fluid-like behavior while at high temperatures. However, an incremental difference appears as the temperature increases. On the other hand, at low temperatures there is a difference in phase angle due to the structural change of bitumen molecules as a result of ageing. The phase angle in new bitumen is higher than that of aged bitumen. The difference contracts as temperature increases until 70 ºC. At which temperature, all kinds of bitumen except for PAV show an increase in phase angle. Peroxide-aged bitumen showed behavior between the RTFOT and PAV-aged bitumen. For ozone-aged bitumen (Fig. 44), the results show that the complex modulus and phase angle are nearly comparable to those of RTFOT-aged bitumen. This reflects the characteristics of short-term- aged asphalt, which is a measure of changes that may occur to asphalt during mixing, transportation, laying down, and first year in service. Ozone is a potent oxidizing gas, and this limited effect may be attributed to the test conditions as previously described.

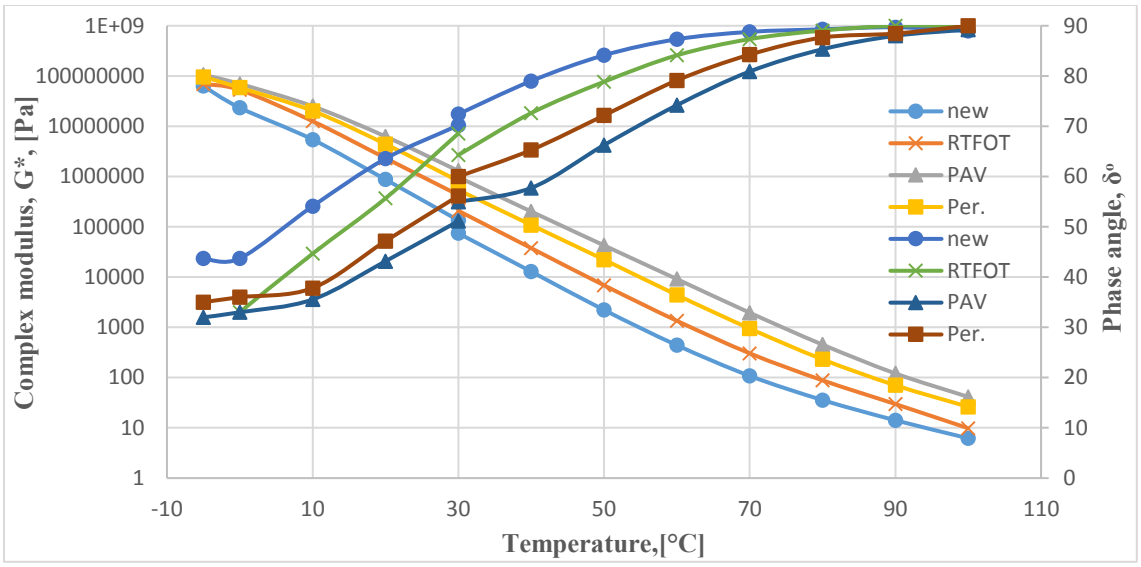

Legend:

New = new / control bitumen RTFOT= short-term aged bitumen PAV= long-term aged bitumen

Per = peroxide-aged mix

Fig. 43: Effect of ageing by peroxide on complex modulus, and phase angle, at 1.59 Hz

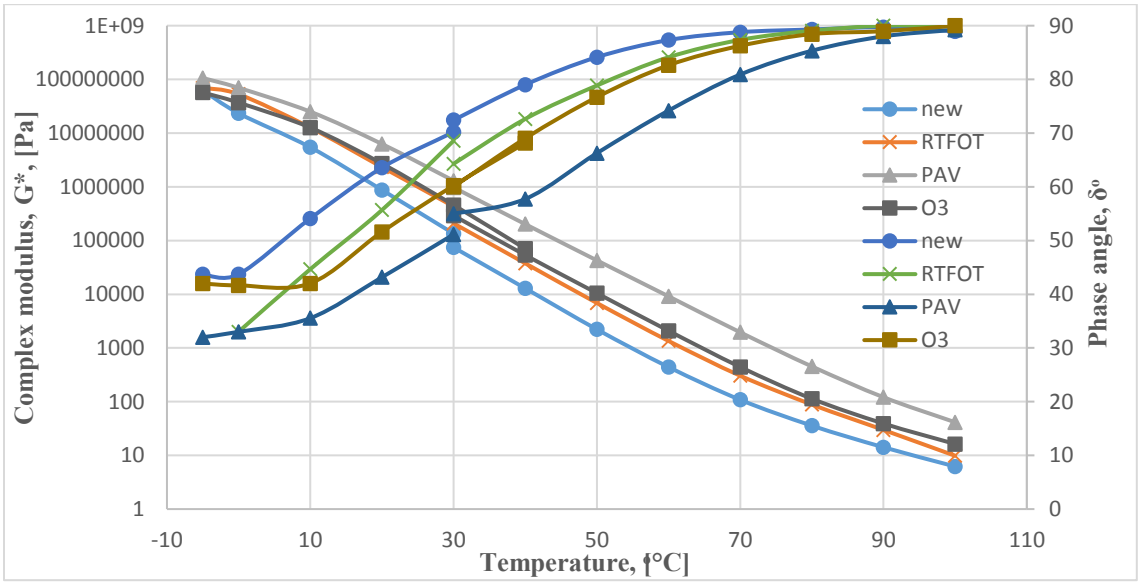

Legend:

New = new / control bitumen RTFOT= short-term aged bitumen PAV= long -term aged bitumen

O3 = ozone-aged mix

Fig. 44: Effect of ageing by ozone on complex modulus, and phase angle, at 1.59 Hz.

The results of long term-aged asphalt (Fig. 45) for 4 h at 135 ºC followed by 288 h at 75 ºC showed G* results identical to PAV-aged bitumen and highly equivalent results for the phase angle at the range of test temperatures. The results of peroxide-aged asphalt and long term-aged asphalt exhibited nearly similar dynamic parameters of extracted bitumen. Ageing by the PAV test describes the properties of bitumen after 10-15 years in service (Erkens et. al., 2016; Lu et. al., 2008). Therefore, peroxide-aged and long-term aged asphalt may provide accurate reference cases for asphalt performance after a long period in service.

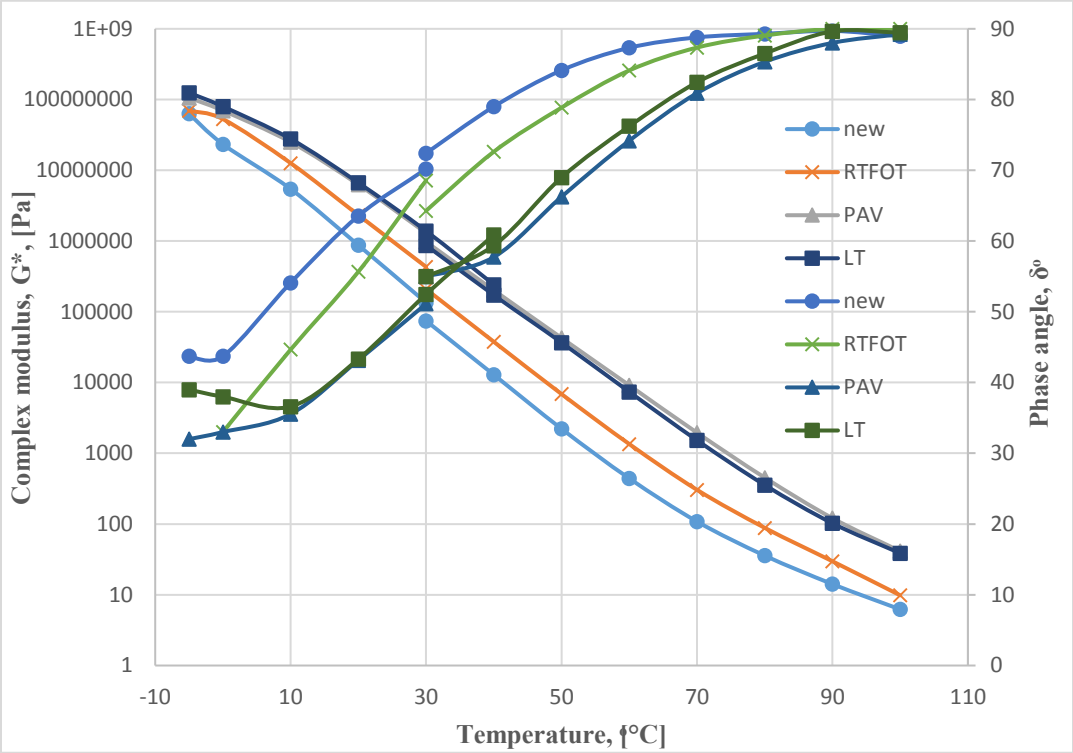

Legend:

new = new / control bitumen RTFOT= short-term aged bitumen PAV= long -term aged bitumen

LT= long-term aged asphalt

Fig. 45: Effect of ageing long-term ageing method on complex stiffness modulus, G*, and phase angle, δ º at 1.59 Hz

5.5 Chemical Designation of Bitumen

The FTIR test was utilized to determine the effect of different ageing processes on chemical groups and changes in the structure of bitumen molecules. The indices of ageing were defined as changes in area under the peak 1030/cm wavenumber (sulfoxide group; Fig. 46) and the wavenumber of 1705/cm which represent the carbonyl group (Fig. 47). The results were normalized to two peaks, 1360 and 1475/cm wavenumbers (Dony et al., 2016; Fig. 48). Areas under these two peaks were used to normalize the calculations of sulfoxide and carbonyl groups to indicate ageing.

The indices of sulfoxide (Iso) and carbonyl (Ico) were calculated according to the following equations (Dony et. al. 2016):

$$\text{Ico} = \frac{A1}{A0} \quad \text{.....(4)}$$

$$\text{Iso} = \frac{A2}{A0} \quad \text{.....(5)}$$

where:

A0 is the area of reference peaks at wavenumbers 1460/cm and 1375/cm

A1 is the peak area of the carbonyl group at wavenumber 1700/cm, and

A2 is the peak area of the sulfoxide group at wavenumber 1030/cm

The summarized results of Iso and Ico indices are presented in Fig. 49. The Ico indices for bitumen aged by different methods are converged and even identical for long-term, peroxide- and ozone-aged bitumen. However, there is a recognizable difference regarding the Iso indices for different bitumen. Where, the peroxide- and ozone-aged asphalt showed higher indices while asphalt aged by high temperature in different ways (STB, STA, ST, and LT) showed similar indices. As expected, new bitumen showed fewer indices than other types since it is not yet subjected to ageing, unlike other types (ST, STA, STB, LT, Per., and O_3) of bitumen.

Sulfides were found to be more susceptible to oxidation (Green et al., 1993) and is therefore, considered an indication of short-term ageing during the mixing and compacting of asphalt. In contrast, the carbonyl group is time- dependent and related to ageing during the service period or long-term ageing at relatively low temperatures compared to mixing and compacting temperatures. The low values of Ico thus indicate that the formation of a carbonyl group is initiated for all bitumen types under consideration in this study. However, peroxide- and ozone-aged bitumen proved to have a higher rate of ageing.

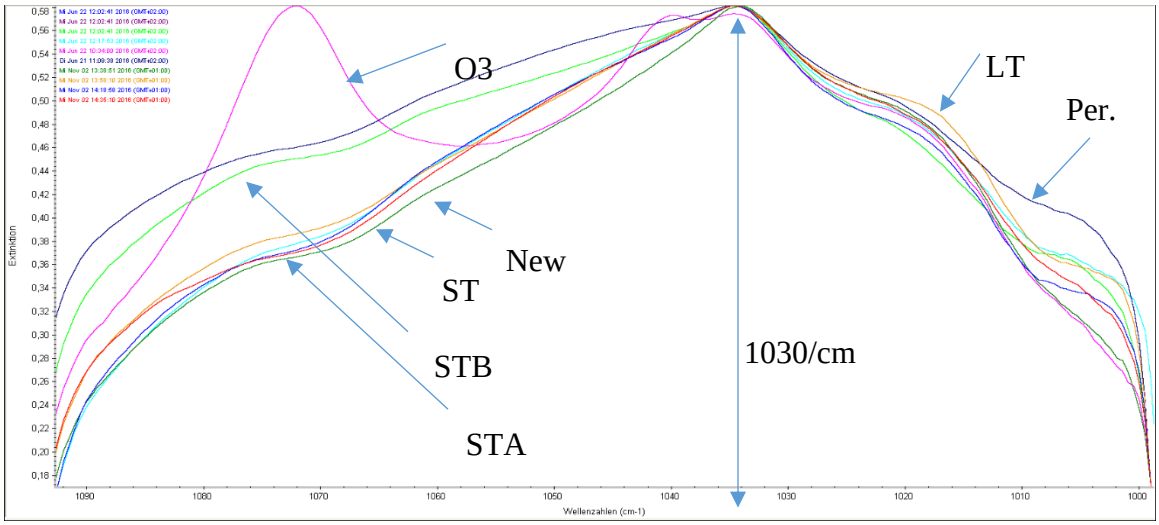

Legend:
new = new bitumen
*Per = peroxide-aged asphalt
*O3 = ozone-aged mix
*ST &LT = short- & long-term aged asphalt
*STA =peroxide+short-term aged asphalt
*STB=ST+per.
*, bitumen was extracted from these mixes.

Fig. 46: Spectrum of sulfoxide group of different bitumen at wavenumber 1030/cm of Fourier transform infrared spectroscopy (FTIR)

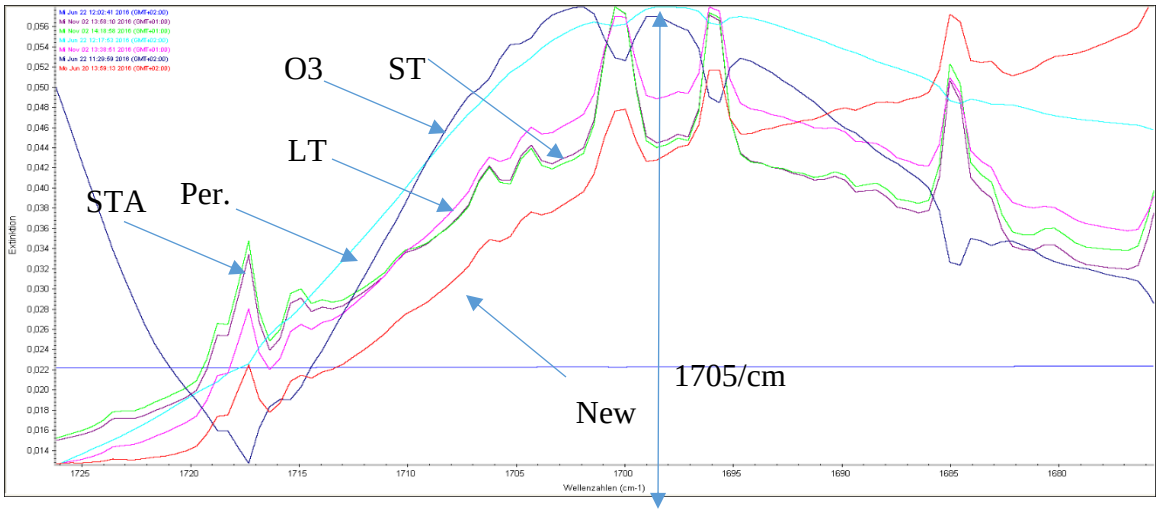

Legend:

new = new bitumen *Per = peroxide-aged asphalt *O3 = ozone-aged mix
*ST = short-term aged asphalt *LT = long-term aged asphalt STA= short-term+peroxide
*, bitumen was extracted from these mixes.

Fig. 47: Spectrum of carbonyl group of different bitumen at wavenumber 1705/cm of Fourier transform infrared spectroscopy (FTIR)

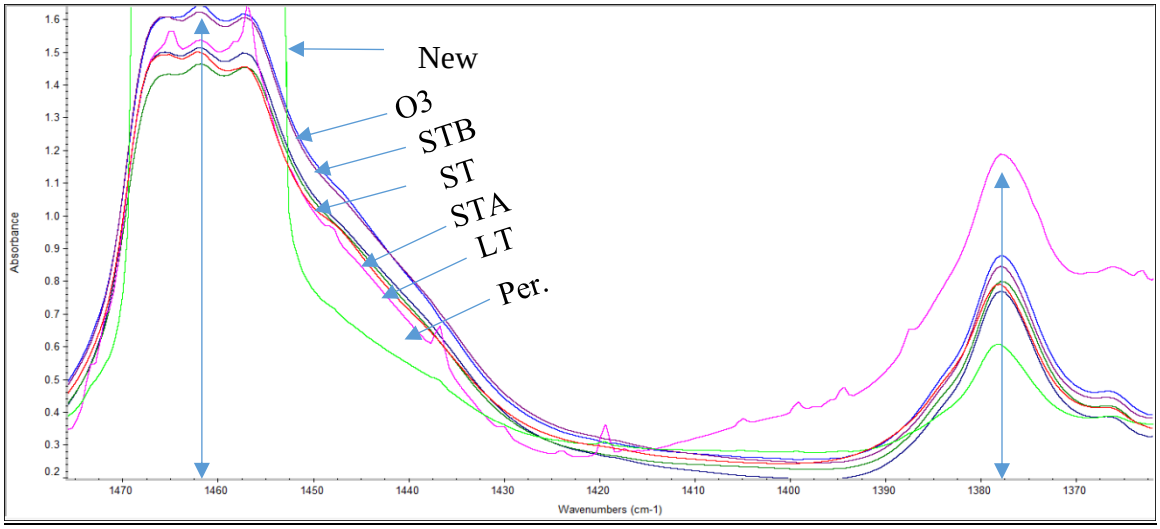

Legend:

new = new bitumen *Per = peroxide-aged asphalt *O3 = ozone-aged mix
*ST = short-term aged asphalt *LT = long-term aged asphalt *STA=peroxide+short-term
*STB=short-term+peroxide
*, bitumen was extracted from these mixes.

Fig. 48: Fourier transform infrared spectroscopy (FTIR) spectrum for reference peaks at wavenumbers 1375/cm and 1460/cm.

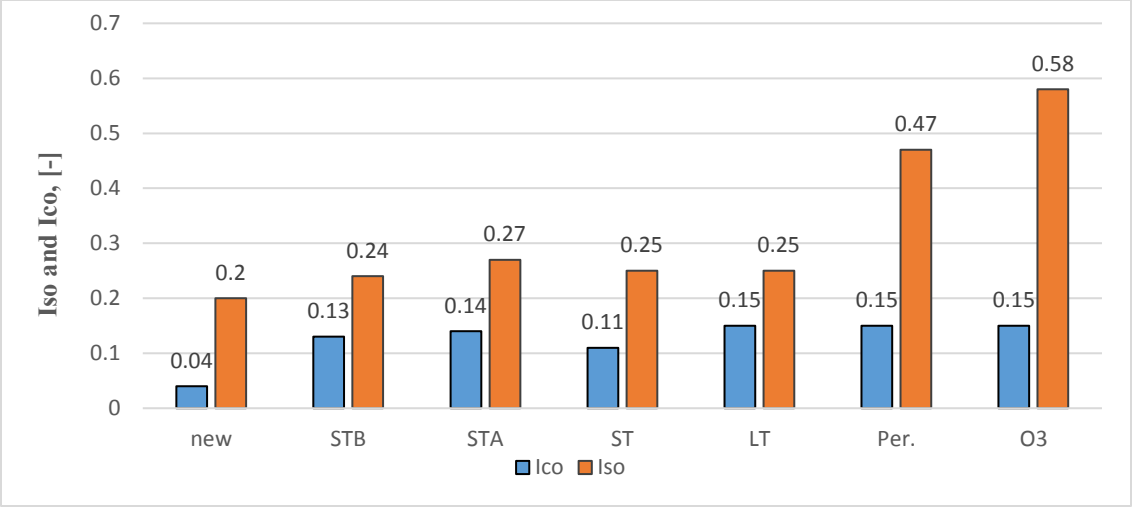

Legend:
new = new bitumen *STB= short-term+peroxide-aged *STA=peroxide+short-term aged
*ST = short term aged asphalt *LT = long-term aged asphalt *Per = peroxide-aged asphalt
*O_3 = Ozone-aged bitumen
*, bitumen was extracted from these mixes.

Fig. 49: Index of sulfoxide (Iso) and Index of carbonyl (Ico) as normalized to reference peaks

5.6 Pros and Cons of Different Ageing Methods (Asphalt and Bitumen Properties)

Ageing using peroxide provides the advantage of increasing the stiffness modulus and fatigue resistance of asphalt- specimens more than the current method of ageing (oven ageing). Moreover, combining peroxide ageing with oven ageing produced a marginal effect of oven heating on the stiffness of asphalt- specimens. This indicates the principal role of peroxide in accelerated ageing. Furthermore, the ozone-aged asphalt- specimens showed an enhancement in stiffness modulus. However, the oven-aged specimens showed reduced stiffness as compared to un-aged asphalt despite the long testing period, indicating a limitation of this method; however it is to mention that this behavior is uncommon.

The physical properties of bitumen were changed in response to the ageing process. The change in the peroxide, ozone, RTFOT, PAV, and long term-aged bitumen results of needle penetration (decrease) and softening point ring and ball (increase). Such results are

obtained as compared to the results of new bitumen, but to different extents. This indicates the advantage of using these ageing methods. The rheological properties of bitumen were similarly changed, suggesting an increase in the complex modulus and a decrease in phase angle. The chemical analysis of bitumen has the benefit of determining the cause of ageing. The peroxide and ozone results showed a steep increase in the formation of the sulfoxide (which is responsible for the short-term ageing of bitumen) and the carbonyl groups (responsible for the long-term ageing of bitumen).

Chapter VI

Impact of RAP and Rejuvenators on the Properties of Asphalt Specimens

To study the effect of reuse of RAP on the performance of the asphalt, several asphalt mixes with high percentage of RAP in combination of using different types of rejuvenating agents were produced and tested. Reclaimed asphalt was obtained from different sites. Three RAP sources were selected from three types of pavement layers: surface, binder, and base course. It was noted that the binder layer contained slight aggregates from the base course due to the milling process. This was also noted for the surface-layer RAP but to a lower extent. Lab-aged asphalt was obtained using a new asphalt mix prepared in the lab (standard mix) which was then aged using peroxide (as described in section 4.1.1).

Three types of asphalt mixes were produced: SMA 11 S with surface layer RAP, AC 16 T D with binder-layer RAP, and AC 22 T S with base-layer RAP. The RAP characteristics were presented in section 3.2.1 (extracted bitumen) and in 3.2.2 (aggregates). Three different types of rejuvenators were used and the properties of the rejuvenators are described in section 3.2.5. To study the impact of the rejuvenator in the asphalt mix with high amount of RAP content, specimens were prepared with and without using rejuvenating agents. Table 18 summarizes the details of the new, RAP, and asphalt mixes. In addition, performance tests were conducted to evaluate the impact of the highest content of RAP in the asphalt mix (90% of total mix). This will preserve the natural resources of aggregate and bitumen. The performance tests comprised the stiffness modulus, fatigue, cyclic creep, and low-temperature resistance tests (Table 19). The specimens representing the base layer (T1, T2, and T3) were excluded from the cyclic creep and low-temperature resistance tests because the base layer is less affected by cyclic loading or low-temperature. Lab-aged asphalt by peroxide was reused in combinatios with rejuvenators to study the effect of the reusing process on such mixes with controlled parameters (aggregate distribution and bitumen). However, the asphalt mixes with rejuvenators of lab-aged

asphalt were only evaluated regarding stiffness and fatigue due to less available asphalt mix. Otherwise, the process requires large quantities of peroxide and that was because of safety considerations not possible.

The asphalt mixes were prepared by heating RAP or lab-aged asphalt to 80 ºC at a content of 90% of the total asphalt mix and the new aggregates were heated to 160 ºC. Afterwards, the RAP or lab-aged asphalt, new aggregate, rejuvenating agent, and the new bitumen (if needed) were mixed at 130 ºC and compacted at 120 ºC using a roller compactor to produce the slabs. The mixing and compacting temperatures were determined according to the manufacturer's instructions and after testing trial mixes. Compared to conventional asphalt mixes, the reduction in mixing and compacting temperatures represents one benefit of impact of rejuvenating agents. The amount of rejuvenator was determined according to the manufacturer's instructions, bitumen content in RAP, and volumetric analysis. These criteria were applied to prepare the asphalt mix with RAP to meet the requirements of the reference mix (Table 20). The new aggregate was used to correct the gradation of the asphalt mix (if needed) and to heat the total mix to the mixing temperature. Table 20 shows that the RAP provides about 90%, 86%, 95%, and 76% of bitumen to the asphalt mix for B, S, D, and T mixes respectively, which is calculated as a ratio of bitumen from RAP to the required bitumen. The use of RAP bitumen results in a sizable conservation of the new bitumen in addition to saving 90% of the aggregate. The energy required to heat the aggregate is consequently reduced (because only 10% of aggregate is heated) compared to the energy required to produce new asphalt. The mixes S0, D0, and T0 were prepared by heating the RAP to the mixing and compacting temperatures of new mix without using new bitumen to study the performance of RAP and to determine the impact of reusing process on asphalt properties before and after reusing.

Table 18: Sources and designation of the asphalt mixes

Source	Mix type	Agent no.	New bitumen	Asphalt mix (RAP + Agent)	No.
Virgin	AC 16 B S	No agent	30/45	-	B, New
Lab-aged	AC 16 B S	No agent	30/45	-	aged
Lab-aged	AC 16 B S	1	30/45	AC 16 B S	B1
Lab-aged	AC 16 B S	2	30/45	AC 16 B S	B2
Lab-aged	AC 16 B S	3	30/45	AC 16 B S	B3
Virgin	SMA 11 S	No agent	30/45	-	S, New 30/45
Virgin	SMA 11 S	No agent	55/55-25 A	-	S, New PMB
RAP	Surface	No agent	-	-	S0
RAP	Surface	1	30/45	SMA 11 S	S1
RAP	Surface	2	30/45	SMA 11 S	S2
RAP	Surface	3	30/45	SMA 11 S	S3
Virgin	AC 16 T D	No agent	50/70	-	D, New
RAP	Binder	No agent	-	-	D0
RAP	Binder	1	50/70	AC 16 T D	D1
RAP	Binder	2	50/70	AC 16 T D	D2
RAP	Binder	3	50/70	AC 16 T D	D3
Virgin	AC 22 T S	No agent	30/45	-	T, New 30/45
Virgin	AC 22 T S	No agent	50/70	-	T, New 50/70
RAP	Base	No agent	-	-	T0
RAP	Base	1	30/45	AC 22 T S	T1
RAP	Base	2	30/45	AC 22 T S	T2
RAP	Base	3	30/45	AC 22 T S	T3

Table 19: Performance tests employed in the study for evaluating the asphalt specimens

Asphalt mix	Stiffness resistance	Fatigue resistance	Cyclic creep test	Low- temperature resistance
B, New	X	X	-	-
aged	X	X	-	-
B1	X	X	-	-
B2	X	X	-	-
B3	X	X	-	-
S0	X	X	-	-
S, New 30/45	X	X	X	X
S, New PMB	X	X	X	X
S1	X	X	X	X
S2	X	X	X	X
S3	X	X	X	X
D0	X	X	-	-
D, New	X	X	X	X
D1	X	X	X	X
D2	X	X	X	X
D3	X	X	X	X
T0	X	X	-	-
T, New 30/45	X	X	-	-
T, New 50/70	X	X	-	-
T1	X	X	-	-
T2	X	X	-	-
T3	X	X	-	-

Table 20: Details of the components of mixes with RAP and rejuvenator

Mix type	RAP, [%]	New agg., [%]	Required bit. [%]	RAP*, bit., [%]	Agent**, [%]	New bit, [%]
B1	90	10	5.0	4.50	0.40	0.10
B2	90	10	5.0	4.50	0.20	0.30
B3	90	10	5.0	4.50	0.25	0.25
S1	90	10	7.2	6.23	0.60	0.37
S2	90	10	7.2	6.23	0.29	0.68
S3	90	10	7.2	6.23	0.37	0.60
D1	90	10	5.7	5.40	0.50	0.00
D2	90	10	5.7	5.40	0.23	0.00
D3	90	10	5.7	5.40	0.30	0.00
T1	90	10	4.5	3.40	0.40	0.68
T2	90	10	4.5	3.40	0.18	0.90
T3	90	10	4.5	3.40	0.25	0.83

* amount of bitumen from RAP

** agent content in the asphalt mix of the three rejuvenators used was determined according to the manufacturer's instructions and by preparing trial mixes.

The peroxide-aged asphalt was first prepared (see section 4.1) and then used to produce asphalt mix at a content of 90% of the total mix. Three types of rejuvenating agents (one solid and two fluid) were employed to produce three mixes with RAP and rejuvenator. Initial mixes were prepared to determine the optimum agent content, after which the stiffness (see section 5.1) and fatigue (see section 5.2) resistances were determined for the specimens. The results obtained were compared with relevant results for new and aged specimens.

This research phase also comprises studying the performance properties of the asphalt mixes with RAP, which was obtained from different regions in North Rhine Westphalia in Germany. Samples were dried at 25 ºC for 72 h before being used in the lab (see section 3.2.2). For initial testing, Marshall specimens were prepared to determine the proper dosage of rejuvenator (according to the manufacturer's instructions).

6.1 Stiffness of Asphalt Specimens

By means of the stiffness of asphalt, several properties of asphalt can be described:

- The ability to distribute loads
- The ability of asphalt to resist fatigue failure
- To resist low-temperature cracking
- The resistance against accumulation of rutting at high temperatures

The stiffness results of the specimens with RAP and rejuvenator are shown in the sections below for the three mixtures produced using RAP.

6.1.1 Lab-aged Asphalt-Specimens

The stiffness modulus for the samples with RAP and rejuvenator (Fig. 50) was lower than that of unaged or aged samples. Less stiffness at low temperatures is preferred to avoid the consequences of the glass-like behavior of bitumen. The different rejuvenators seemingly caused the same lowering effect (compared to new or aged mixes) at temperatures tested. However, the amount of decrease in stiffness at low temperatures differed according to the rejuvenating agent type. The mixtures produced with rejuvenating agent 1 clearly showed higher stiffness than the mixtures prepared with the other two rejuvenating agents. This may be due to the effect of the rejuvenating agent's chemical composition since it is a wax-based agent. Because this mix is lab-aged, the aged mix represents a mix with no rejuvenator. Additional results are presented in Appendix B.

Fig. 51 differentiates the stiffness modulus between high and low temperatures for aged, unaged, and asphalt with RAP in combination with the three rejuvenating agents used. Compared to the aged mix, the decrease of stiffness modulus at low temperatures was higher than the reduction at high temperatures. Where, the decrease in stiffness at low temperatures was about 19%, 44%, 64% and 53% for asphalt mixes without rejuvenator (B, New), B1, B2, and B3 respectively. The decrease in stiffness at higher temperatures was about 9%, 28%, 37%, and 31% for asphalt mixes without rejuvenator (B, New), B1,

B2, and B3 respectively. This reduction can be attributed to the effect of the rejuvenating agent used in the asphalt mix with RAP, which softened the aged bitumen and substituted the deficiency of bitumen in the asphalt mix with RAP.

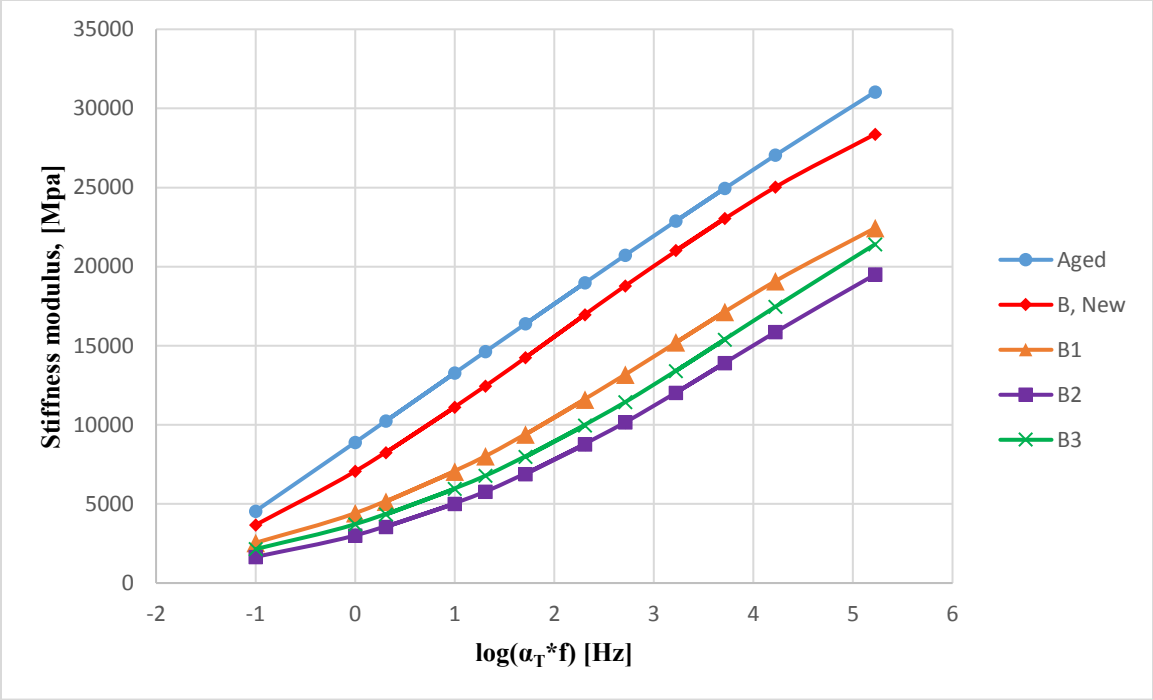

Legend:

B, New = new asphalt without RAP Aged = peroxide-aged asphalt B1 = asphalt with RAP + rejuvenator no.1

B2 = asphalt with RAP + rejuvenator no.2 B3= asphalt with RAP + rejuvenator no.3

Fig. 50: Stiffness modulus of AC 16 B S mixes

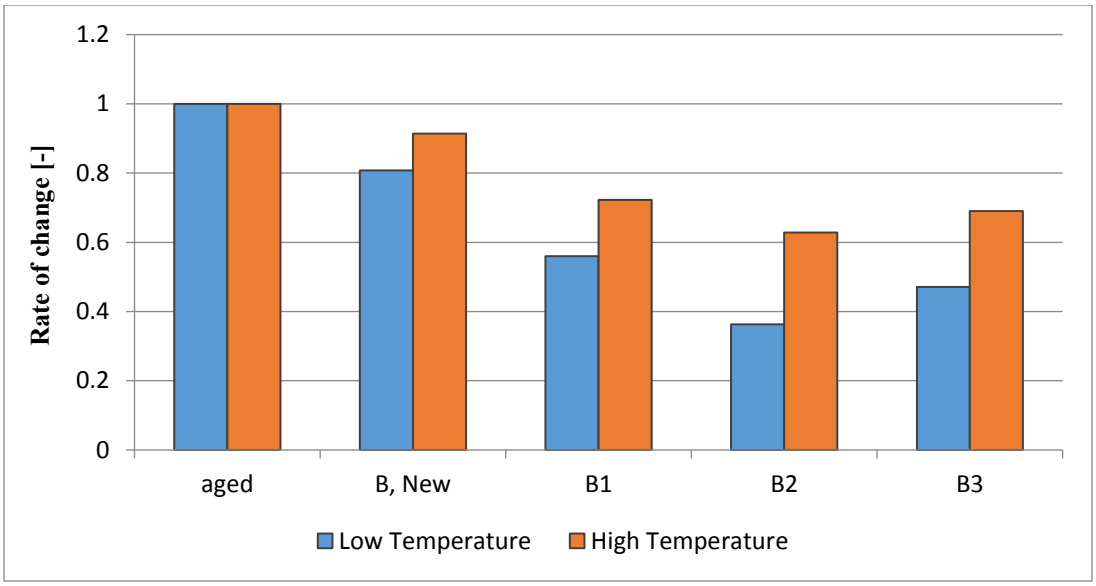

Legend:

B, New = new asphalt without RAP Aged = peroxide-aged asphalt B1 = asphalt with RAP + rejuvenator no.1

B2 = asphalt with RAP + rejuvenator no.2 B3= asphalt with RAP + rejuvenator no.3

Fig. 51: Effect of rejuvenators used, on stiffness modulus as normalized to aged mix, at low and high temperatures for AC 16 B S mixes

6.1.2 Stone mastic asphalt (SMA 11 S)

Two grades of bitumen (30/45 and PMB) were used to prepare new specimens (S, 30/45) and (S, PMB), and the asphalt mix with RAP and without rejuvenator or new bitumen (S0). Three asphalt mixes with RAP (S1, S2, and S3) were prepared (as previously described) using the three rejuvenators as shown in Fig. 52. Compared to the mix S0, the asphalt mixes S1, S2, and S3 showed a decrease in stiffness modulus of 14%, 8% and 12% respectively at low temperatures (Fig. 53). In addition, a decrease of about 48%, 38% and 42% for mixes S1, S2, and S3 respectively was detected at high temperatures. The rejuvenators used influenced the stiffness at high, average and low temperatures tested.

In addition, the mix S0, which does not contain the rejuvenating agent, shows a significant increase in stiffness modulus of about 33% compared to the new mix with bitumen grade 30/45 (S, new 30/45) at high temperatures. This is due to the hardened bitumen in RAP

(needle penetration is 19 and softening point is 69 °C). At low temperatures, both mixes showed identical stiffness since bitumen rheological characteristics tend to perform as glass-like at low temperatures and has a steady-state flow at high temperatures.

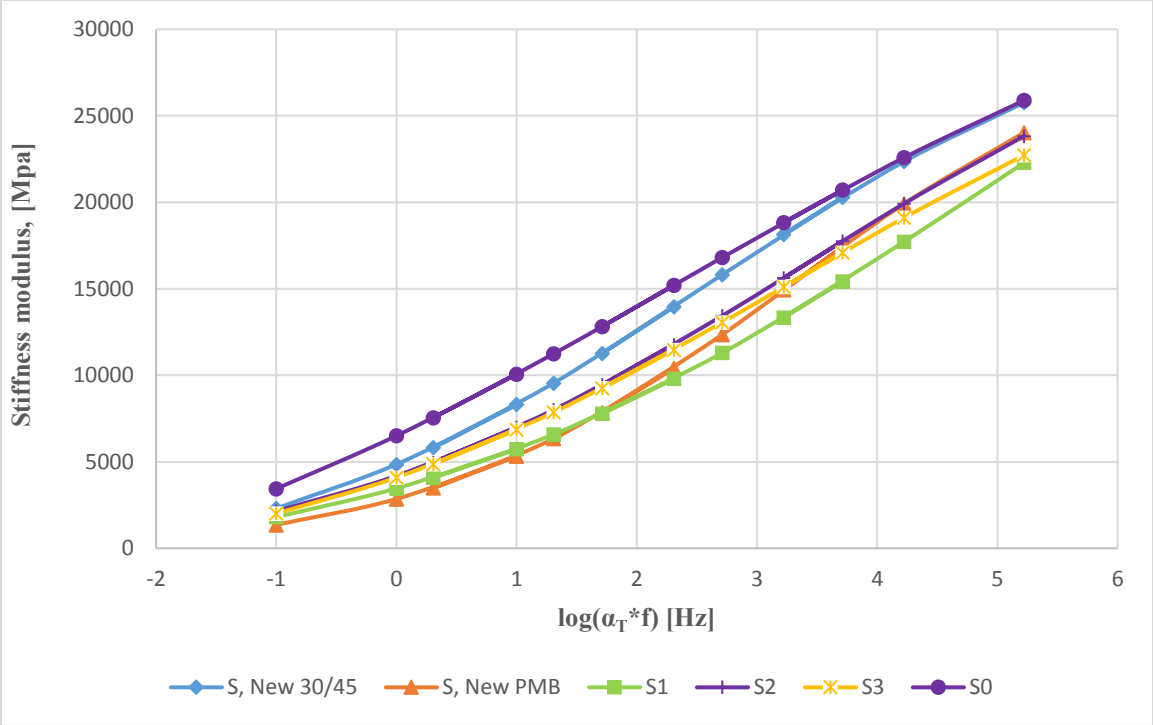

Legend:

S, New 30/45 = asphalt with virgin bitumen 30/45

S, New PMB = asphalt with virgin bitumen PMB

S1 = asphalt mix with RAP+rejuvenator no. 1

S2 = asphalt mix with RAP+rejuvenator no. 2

S3 = asphalt mix with RAP+rejuvenator no. 3

S0 = asphalt mix with RAP, no rejuvenator

Fig. 52: Stiffness modulus of SMA 11 S mixes

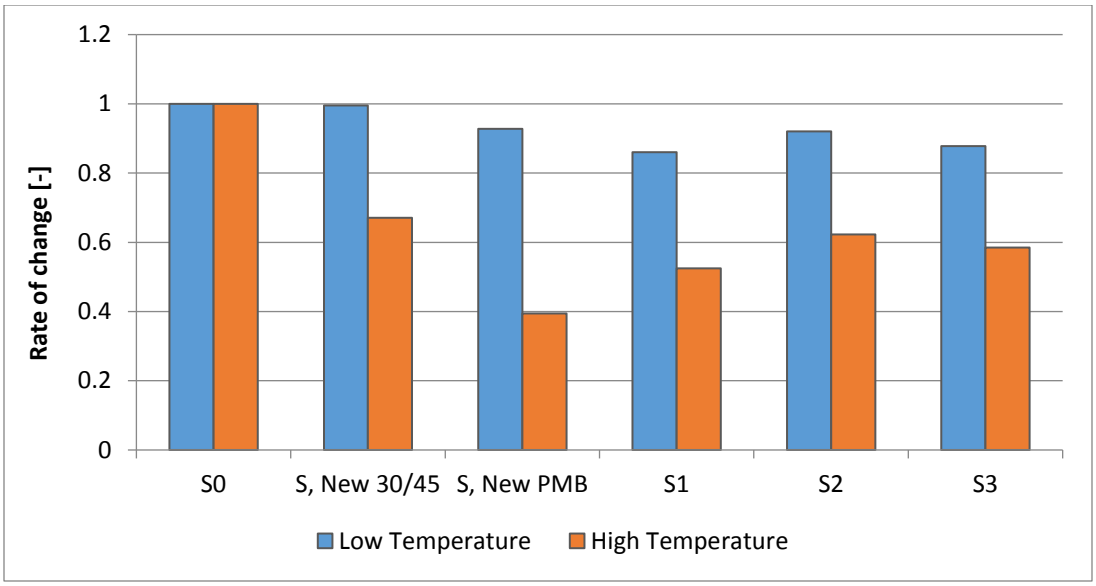

Legend:

S, New 30/45 = asphalt with virgin bitumen 30/45

S, New PMB = asphalt with virgin bitumen PMB

S1 = asphalt mix with RAP+rejuvenator no. 1

S2 = asphalt mix with RAP+rejuvenator no. 2

S3 = asphalt mix with RAP+rejuvenator no. 3

S0 = asphalt mix with RAP, no rejuvenator

Fig. 53: Effect of rejuvenators used on stiffness modulus as normalized to asphalt without rejuvenator, at low and high temperatures for SMA 11 S mixes

6.1.3 Asphalt full-depth layer (AC 16 T D)

Bitumen with grade 50/70 was selected to produce the new mix (according to the applied norms), in which new asphalt mixes were prepared and evaluated by determining the stiffness modulus (D, New 50/70). In addition, asphalt mixes with RAP were prepared with rejuvenating agents D1, D2, and D3 as well as a mix without a rejuvenating agent (D0).

The tested mixtures were prepared in different conditions (unaged, and mixes with rejuvenators) and different rejuvenating agents (three types of agents). However, there were no observed differences in the stiffness modulus at high temperatures (except the variant D0) as shown in Fig. 54 (reduced frequency -1). The mixes showed nearly similar behavior. However, a difference was noticeable at low temperatures, as shown in the same figure.

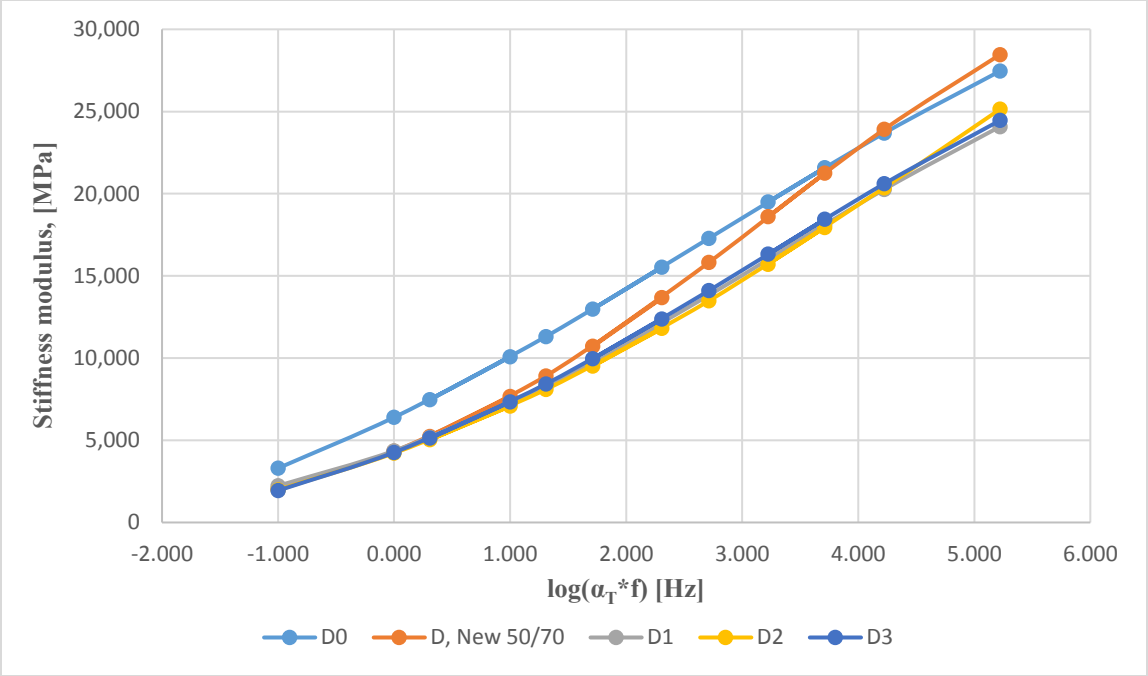

Legend:

D, New 50/70 = asphalt with virgin bitumen 50/70

D1 = asphalt mix with RAP+rejuvenator no. 1

D2 = asphalt mix with RAP+rejuvenator no. 2

D3 = asphalt mix with RAP+rejuvenator no. 3

D0 = asphalt mix with RAP, no rejuvenator

Fig. 54: Stiffness modulus of AC 16 T D mixes

Fig. 55 shows that at extremely low temperatures, the stiffness moduli of the mixes with RAP were decreased by 12%, 8% and 11% for the variants D1, D2, and D3 respectively. At high temperatures, D1 specimens showed a decreased stiffness of about 32% compared to the RAP mix (D0), while D2 and D3 specimens showed a decrease in stiffness modulus of about 40% and 41% respectively. This indicates the role of rejuvenating agents in restoring the RAP performance by lowering the stiffness of hardened bitumen. The stiffness decreased at high and low temperature to a range, which is comparable to that of new asphalt. On the other hand, asphalt mix without RAP and rejuvenator (D, new) showed a marginal increase in stiffness modulus at low temperatures of about 3% and a noticeable decrease at high temperatures of about 38%. Although the decrease in stiffness of the mix D0 is low (3%) however, this result is unexpected because old asphalt mixes with highly hardened bitumen (needle penetration 21 and softening point 64 ºC) is commonly showing

higher stiffness than new mixes as shown in the section of ageing. Many factors may have contributed to such an unusual result, one of which is the brittleness of bitumen due to the hardening (as shown in the results of bitumen extracted from RAP of binder layer). The decrease occurred at low temperatures only. Bitumen behavior is glass-like at very low temperatures, which worsens if hard bitumen is used. In this case, both factors account for lowering the asphalt stiffness. In addition, hardened bitumen of RAP requires very high temperatures to soften. The D0 mix is produced at 130 ºC, which seems insufficient to soften the hardened bitumen in RAP. This resulted in weak bonding potential between aggregate particles. The testing variability and mix design may provide a further explanation of such behavior.

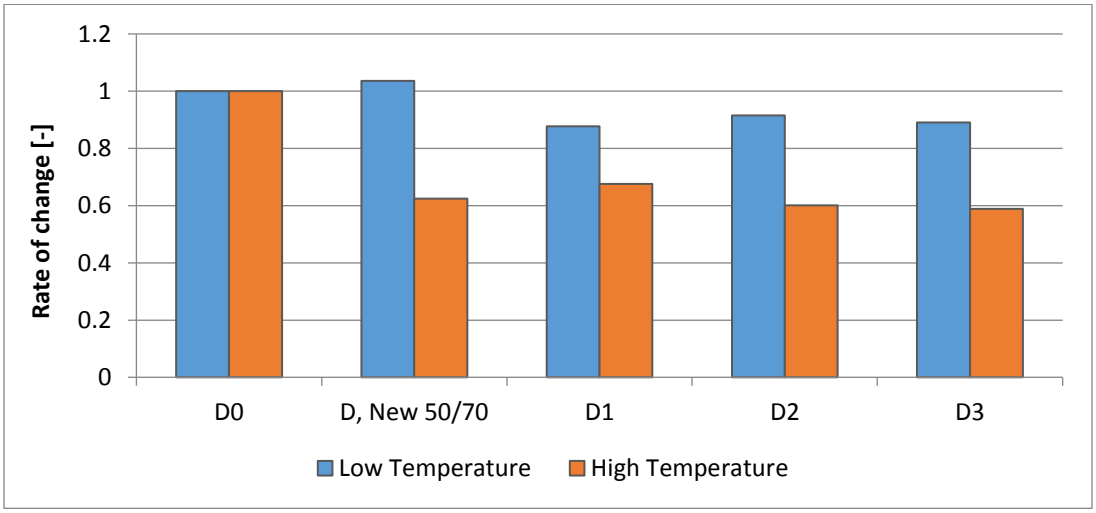

Legend:

D, New 50/70 = asphalt with virgin bitumen 50/70

D1 = asphalt mix with RAP+rejuvenator no. 1

D2 = asphalt mix with RAP+rejuvenator no. 2

D3 = asphalt mix with RAP+rejuvenator no. 3

D0 = asphalt mix with RAP, no rejuvenator

Fig. 55: Effect of rejuvenators used, on stiffness modulus as normalized to asphalt mix without rejuvenator, at low and high temperatures for AC 16 T D mixes

6.1.4 Asphalt base course (AC 22 T S)

Two grades of bitumen (30/45 and 50/70) were employed to prepare new mixes (T, New 30/45 and T, New 50/70), and the specimens without rejuvenator (T0). Asphalt mixes with RAP T1, T2, and T3 were prepared by the three rejuvenating agents, as shown in Fig. 56. The differences in stiffness modulus between the new asphalt mixes are expected because of the harder bitumen (30/45 grade) used in one mix and the softer bitumen used in the other mix (50/70 grade) for new mixes. The impact of rejuvenators for mixes T1, T2, and T3 is also obvious. The variant T0 exhibited a significant decrease in stiffness modulus at low temperatures compared to new mixes. The same factors affecting the unexpected result of D0 mix maybe applied to T0 mix because, both mixes were prepared under similar conditions. The stiffness modulus of the new mixes and mixes with RAP were normalized to the mix (T0) which is shown in Fig. 57. The asphalt mixes with RAP responded differently to the applied stresses during the test. The stiffness modulus was reduced by 8% for T1 specimens and 10% for both T2 and T3 specimens at low temperatures. The stiffness moduli of these mixes were decreased by 27%, 41%, and 29% at high temperatures respectively. These results indicate the role of the rejuvenators in decreasing the stiffness of asphalt.

The mixes used in this test showed different stiffness modulus values. The SMA 11 S mix showed a range of stiffness values of 1.4×10^3 MPa to 3.4×10^3 MPa at high temperatures and a range of 22.3×10^3 MPa to 25.9×10^3 MPa at low temperatures. For AC 16 T D mixes, the range was 1.9×10^3 MPa to 3.3×10^3 MPa at high temperatures and 24.5×10^3 MPa to 28.5×10^3 MPa at low temperatures. While for AC 22 T S, it was 3.0×10^3 MPa to 5.1×10^3 MPa at high temperatures and 25.5×10^3 MPa to 32.2×10^3 MPa at low temperatures. These differences can be attributed to the changes in aggregate size and distribution. The using of larger aggregates increases the stiffness modulus of the total mix, as shown in the AC 22 T S mix. Another reason for this difference is the bitumen content and grade. The use of a higher percentage of bitumen reduces also the stiffness modulus of the mix, as shown in the SMA 11 S mix. The effect of air voids also represents an influencing factor on the stiffness modulus of the mix.

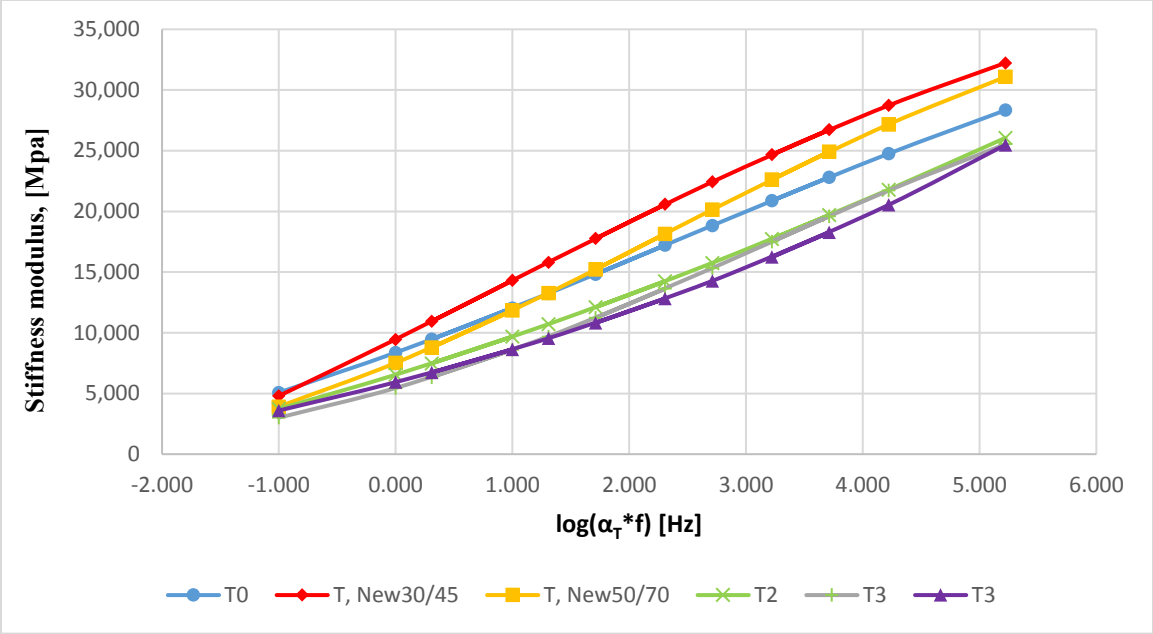

Legend:

T, New 30/45 = asphalt with virgin bitumen 30/45

T, New 50/70 = asphalt with virgin bitumen 50/70

T1 = asphalt mix with RAP+rejuvenator no. 1

T2 = asphalt mix with RAP+rejuvenator no. 2

T3 = asphalt mix with RAP+rejuvenator no. 3

T0 = asphalt mix with RAP, no rejuvenator

Fig. 56: Stiffness modulus of AC 22 T S mixes

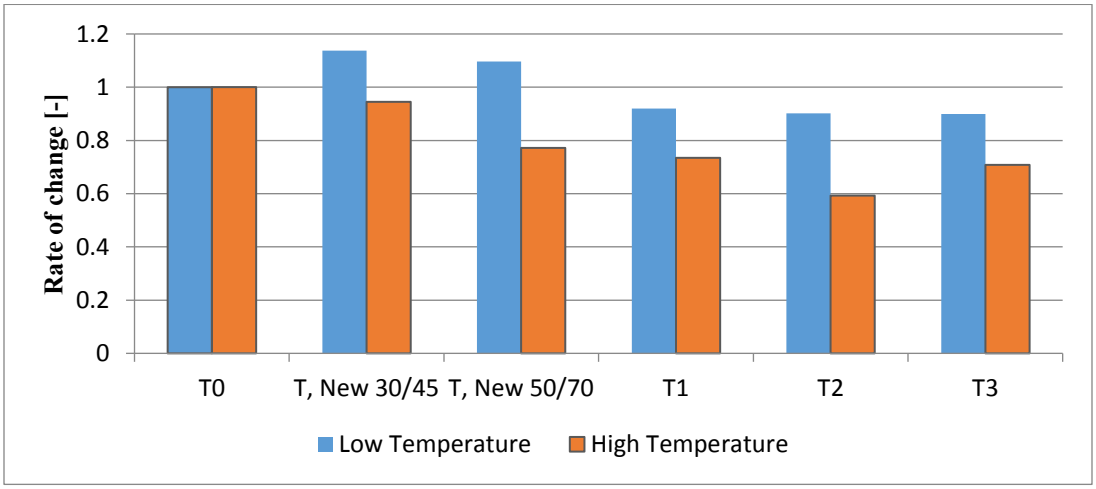

Legend:

T, New 30/45 = asphalt with virgin bitumen 30/45

T, New 50/70 = asphalt with virgin bitumen 50/70

T1 = asphalt mix with RAP+rejuvenator no. 1

T2 = asphalt mix with RAP+rejuvenator no. 2

T3 = asphalt mix with RAP+rejuvenator no. 3

T0 = asphalt mix with RAP, no rejuvenator

Fig. 57: Effect of rejuvenators used, on stiffness modulus as normalized to asphalt mix without rejuvenator, at low and high temperatures for AC 22 T S mixes

6.2 Fatigue of Asphalt-Specimens

Two types of fatigue, bottom-up as classical distress, can be recognized in asphalt pavement at the thin layer. The top-down cracking can be recognized at thick layers (Mackiewicz, 2018). Fatigue cracking initiates in areas where the tensile stress is highest at the wheel path and worsens with asphalt ageing and repeated loads. It starts with longitudinal cracks that connect to form pieces similar to those on the back of an alligator (another name for this is "alligator cracking"). This process occurs as a consequence of high traffic at stresses lower than failure stresses or the yielding point of the mix.

This test was performed at a constant temperature of 20 ºC according to the specifications explained in section 3.3.1.2. The test was conducted at three levels of loadings: short-term loads (heavy) for simulating trucks loads, intermediate loads, and long-term loads (light) for simulating light-weight vehicles. Measured results (average of three independent test results) are presented in the figures below. The values of load cycles were calculated according to the derived equations of measured results. The calculated values were used in the comparison between the different variants as applied previously in section 5.2.

6.2.1 Lab-Aged Asphalt-Specimens

Asphalt binder layer mix AC 16 B S were tested for heavy (σ = 0.80 MPa), intermediate (σ = 0.35 MPa), and light loadings (σ = 0.20 MPa). The levels of loading were kept constant for all variants tested. The results of unaged (B, New), aged, and mixes with RAP in combination with rejuvenating agents B1, B2, and, B3 (Fig. 58 and Table 21), responded differently to macro-crack initiation. At heavy loadings, load cycles to failure occurred at 2.50×10^3 (initial strain of 0.134‰), 6.59×10^3 (0.109‰), 4.05×10^3 (0.111‰), 8.12×10^3 (0.103‰), and 3.45×10^3 (0.144‰) of the variants (B, New), aged, B1, B2, and B3 respectively of measured results. The behavior of different mixtures at decreased loadings differed also, as the failure of unaged mixtures occurred at load cycles of 5.58×10^5 (initial strain of 0.025‰). The failure occurred at lower load cycles (about 1.02×10^5) but at higher initial strain around 0.055‰ for the aged mixture. The measured failure of the variants B1,

B2, and B3 occurred in the range between unaged and aged samples for light loading. Where, load cycles of 4.46 × 10^5 and an initial strain of 0.035‰ was measured for the variant B1. In addition, failure occurred at 1.65 × 10^5 and 1.55 × 10^5 load cycles and an initial strain of around 0.034‰ and 0.039‰ for the variants B2 and B3 respectively (Table 21). Compared to the variant (New) and at high loadings (initial elastic strain of 0.10‰), calculated values of load cycles showed an increase of 102%, 157%, and 119% for the variants B1, B2, and B3 respectively. At light loadings (initial elastic strain of 0.03‰), a decrease in load cycles of 12% occurred for the variant B2 while, an increase calculated of 270% and 149% for the variants B1 and B3 respectively (Fig. 59).

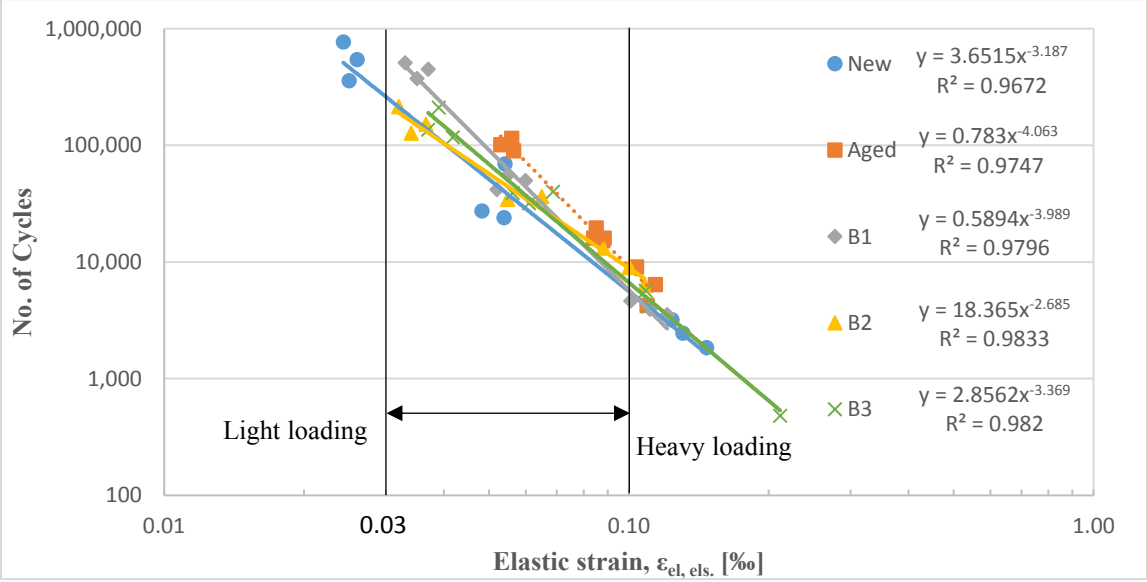

Legend:

New = new asphalt | Aged = aged asphalt by peroxide | B1 = asphalt mix with rejuvenator no.1

B2 = asphalt mix with rejuvenator no.2 | B3 = asphalt mix with rejuvenator no.3

Fig. 58: Measured results of fatigue resistance of AC 16 B S mixes

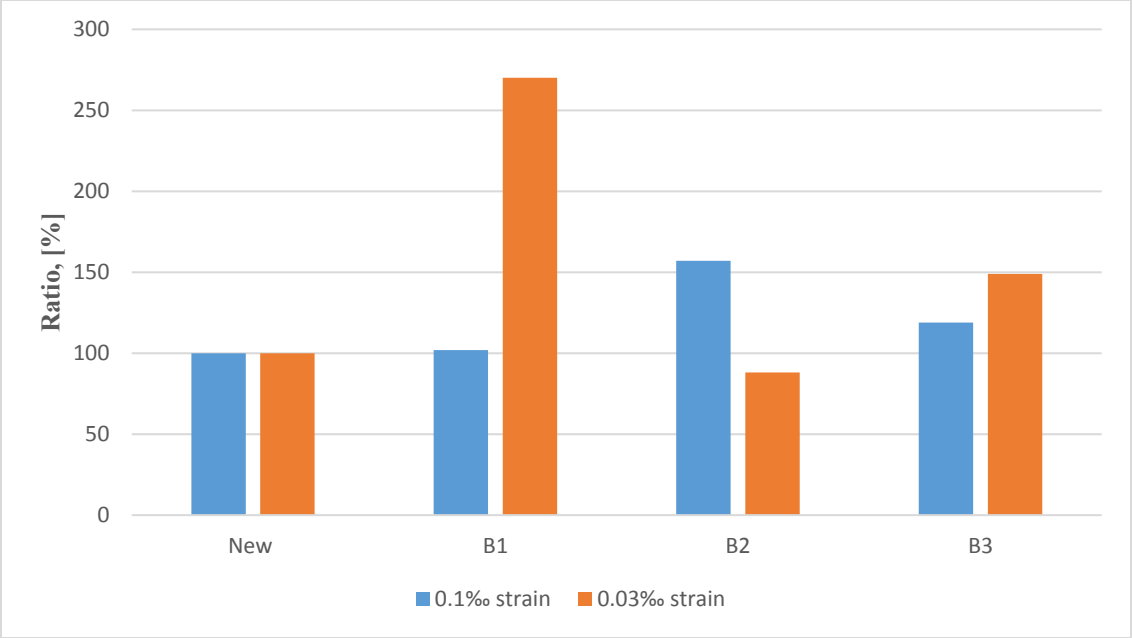

Legend:

New = new asphalt Aged = aged asphalt by peroxide B1 = asphalt mix with rejuvenator no.1

B2 = asphalt mix with rejuvenator no.2 B3 = asphalt mix with rejuvenator no.3

Fig. 59: Calculated values of fatigue resistance of AC 16 B S mixes

Table 21: Test parameters of fatigue for AC 16 B S mixes

T, [°C]	20								
f [Hz]	10								
μ [-]	0.2984								
$\sigma_{u,}$ [MPa]	0.035			0.035			0.035		
$\sigma_{o,}$ [MPa]	0.80	0.80	0.80	0.35	0.35	0.35	0.20	0.20	0.20
	N_{Makro} [-]								
B, New*	1,853	2,453	3,206	24,007	27,500	69,509	542,854	772,020	358,194
B1*	3,550	4,656	3,948	42,000	50,008	55,886	451,503	374,984	510,996
B2*	8,956	9,009	6,395	13,206	34,504	36,485	151,504	126,920	215,324
B3*	482	5,706	4,158	39,003	40,000	32,000	117,019	210,988	136,558
	εel, anf [‰]								
B, New*	0.147	0.131	0.124	0.054	0.048	0.054	0.026	0.024	0.025
B1*	0.121	0.101	0.111	0.052	0.060	0.055	0.037	0.035	0.033
B2*	0.100	0.100	0.108	0.088	0.055	0.065	0.037	0.034	0.032
B3*	0.212	0.109	0.110	0.056	0.069	0.061	0.042	0.039	0.037

Equations derived from the test results (Y= cycles to failure and X = initial elastic strain)

$Y = a \times X^b$		New*	B1*	B2*	B3*				
constant	a	3.724	0.5923	17.742	2.886				
constant	b	-3.179	-3.987	-2.698	-3.366				
Regression	R^2	0.97	0.98	0.98	0.98				
Y	0.10‰	4,942	5,748	8,851	6,704				
	0.03‰	227,038	698,649	227,892	385,764				
Rate, [%]	0.10‰	100	102	157	119				
	0.03‰	100	270	88	149				

*) B, New: AC 16 B S new mix by using virgin bitumen of the grade 30/45 without RAP.
B1: AC 16 B S asphalt mix by using RAP + rejuvenating agent 1
B2: AC 16 B S asphalt mix by using RAP + rejuvenating agent 2
B3: AC 16 B S asphalt mix by using RAP + rejuvenating agent 3
Rate: Rate of change calculated as a ratio of aged to new.

6.2.2 Stone mastic asphalt (SMA 11 S)

The results of fatigue resistance to repetitive loadings for high (σ = 0.60 MPa), intermediate (σ = 0.40 MPa), and light loadings (σ = 0.25 MPa) for the surface layer are shown in Fig. 60 and Table 22. The levels of loadings were kept constant for all variants of SMA 11 S mix. The measured results of the new mixes (S, New 30/45 and S, New PMB) showed less resistance to fatigue cracking. The variant S0 was more resistant to the formation of macro cracking before failure. The mixes with RAP and rejuvenators (S1, S2 and S3) performed in the range between the new and S0 variants.

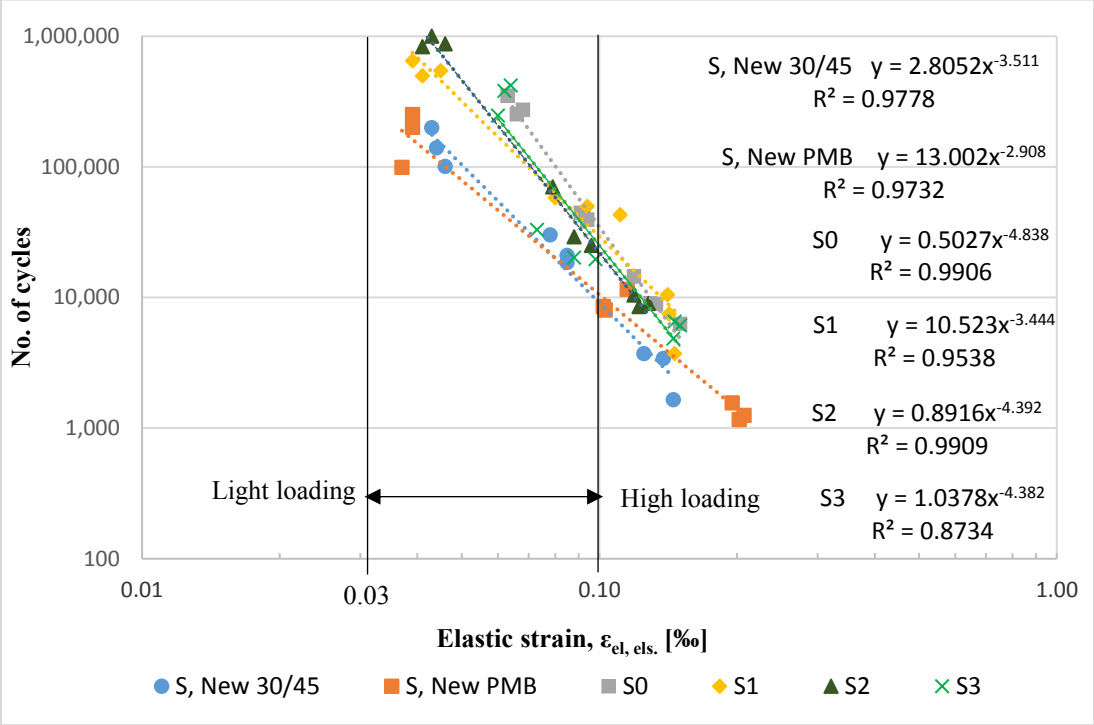

Legend:

S, New 30/45 = asphalt with virgin bitumen 30/45

S, New PMB = asphalt with virgin bitumen PMB

S1 = asphalt mix with RAP+rejuvenator no. 1

S2 = asphalt mix with RAP+rejuvenator no. 2

S3 = asphalt mix with RAP+rejuvenator no. 3

S0 = asphalt mix with RAP, no rejuvenator

Fig. 60: Measured results of fatigue resistance of stone mastic asphalt SMA 11 S

To compare the responses of different mixes to fatigue crack formation, two elastic strains at failure were randomly chosen at certain points. One of which, for light-weight loadings (0.03‰) and the second for heavy weight-loadings (0.10‰). For clearly demonstration of impact of the test results gained, strains with high span were selected. The number of load cycles until macro-crack formation was then computed according to the corresponding equation of the fatigue line of the relevant mix. The calculated values were then normalized to the reference mix (S, New 30/45) and compared (Fig. 61). S0 represents specimens' fatigue resistance without rejuvenator to show the impact of the rejuvenating agent in the reuse of RAP.

At heavyweight loadings, the variant with polymer-modified asphalt mix (S, New PMB) showed an increase of about 116%. The variants with rejuvenators showed different patterns of responses. The mixture S1 showed a vast increase in the number of load cycles of about 322%, compared to the new mix (S, New 30/45). While, mix S2 showed a significant increase of about 242%. Additionally, mix S3 increased by 275%. Finally, an increase of about 381% was measured for the mix S0. The effect of using different rejuvenating agents can be detected. The use of the same mix type and reusing-process conditions while varying the rejuvenator type resulted in different patterns of crack formation resistance. The impact of rejuvenators is also detected through the increase in load cycles of the variants S1, S2, and S3 at lightweight loadings. The increase of 297%, 698%, and 785% in mixes S1, S2, and S3 respectively. A decrease of about 44% occurred in the load cycles until the formation of macro-cracks in the case of the variant new PMB (S, New PMB).

These results indicate that the mix (S1) showed better resistance to fatigue cracking in the category of high loading while, the other two mixes (S2 and S3) at light loading. The mix (S0) exhibited higher resistance as well as at high (381 %) and light loadings (1880%), which may be due to the hardening of the bitumen in RAP.

Table 22: Test parameters of fatigue for SMA 11 S mixes

T, [°C]	20								
f [Hz]	10								
μ [-]	0.2984								
$\sigma_{u,}$ [MPa]	0.035			0.035			0.035		
$\sigma_{o,}$ [MPa]	0.60	0.60	0.60	0.40	0.40	0.40	0.25	0.25	0.25
	N_{Makro} [-]								
S, New* 30/45	1,651	3,401	3,702	21,007	18,508	30,006	100,501	139,303	199,509
S, New *PMB	1,554	1,250	1,159	8,003	8,506	11,502	99,005	250,505	200,000
S0*	6,252	9,004	8,888	14,410	44,410	39,500	273,003	251,547	349,747
S1*	3,709	10,502	7,453	42,869	58,007	49,785	648,002	542,367	496,977
S2*	9,007	10,406	8,500	24,952	70,109	29,000	999,009	870,010	831,498
S3*	6,105	6,510	4,826	19,557	32,960	20,159	246,722	419,877	381,184
	εel, anf [‰]								
S, New* 30/45	0.145	0.138	0.125	0.085	0.085	0.078	0.046	0.044	0.043
S, New* PMB	0.195	0.207	0.202	0.103	0.102	0.115	0.037	0.039	0.039
S0*	0.150	0.129	0.133	0.119	0.091	0.094	0.068	0.066	0.063
S1*	0.146	0.141	0.142	0.111	0.080	0.094	0.039	0.045	0.041
S2*	0.128	0.119	0.122	0.096	0.079	0.088	0.043	0.046	0.041
S3*	0.150	0.146	0.145	0.098	0.073	0.088	0.060	0.064	0.062

Equations derived from the test results (Y= cycles to failure and X = elastic strain)

Y = a × Xb		S, New	S, New PMB	S0	S1	S2	S3
constant	a	2.805	13.002	0.503	10.523	0.892	1.038
constant	b	-3.511	-2.908	-4.838	-3.444	-4.392	-4.382
Regression	R2	0.98	0.97	0.99	0.95	0.99	0.87
Y	0.10‰	9,098	10,520	34,619	29,251	21,987	25,010
	0.03‰	623,435	348,772	11,721,853	1,848,987	4,351,646	4,890,670
Ratio, [%]	0.10‰	100	116	381	322	242	275
	0.03‰	100	56	1,880	297	698	785

*) S, New 30/45: SMA 11 S mix using virgin bitumen of the grade 30/45 without RAP
S, New PMB: SMA 11 S mix using virgin bitumen of the grade PMB without RAP
S0: asphalt mix only with RAP of the surface layer (RAP, S)
S1: SMA 11 S mix by using RAP + rejuvenating agent 1
S2: SMA 11 S mix by using RAP + rejuvenating agent 2
S3: SMA 11 S mix by using RAP + rejuvenating agent 3

a. 0.10‰ strain

b. 0.03‰ strain

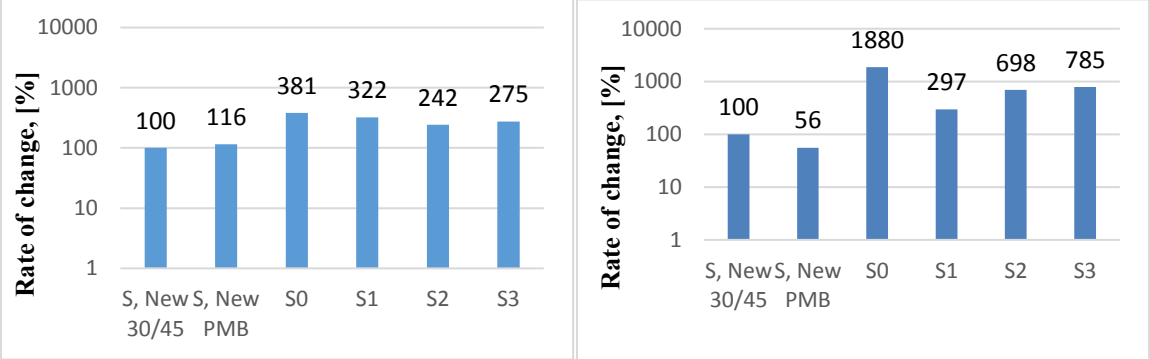

Legend:

New 30/45 = new asphalt with bitumen 30/45 New PMB = new asphalt with PMB

S1 = asphalt mix with rejuvenator no. 1 S2 = asphalt mix with rejuvenator no. 2

S3 = asphalt mix with rejuvenator no. 3 S0 = asphalt mix with no rejuvenator

Fig. 61: Calculated values of fatigue resistance of SMA 11 S mix

6.2.3 Asphalt full-depth layer AC 16 T D

The full-depth layer showed different responses to the applied loads in the three categories of light, intermediate, and heavy loadings at a constant frequency of 10 Hz and temperature of 20 ºC. The slope of the new asphalt's (D, New 50/70) resistance was steeper than that of the variants with RAP. This indicates that with more repetitions of light loads, macro-cracks initiate at higher levels of initial elastic strain. However, with the repetition of heavy loads, failure occurs at lower values of the initial elastic strain (Fig. 62 and Table 23).

According to the equations derived from the mixes' responses Fig. 63 shows a comparison of calculated values of load cycles to failure determined at two strain levels that may occur in pavement due to heavy or light loading. To compare the results, the calculated load cycles to failure were normalized to the reference mix (New 50/70). At 0.10‰ strain (Fig. 63a), an increase of 337%, 230%, and 363% was calculated for the asphalt mixes D1, D2, and D3 respectively. The load repetitions increased following the formula at 0.03‰ initial elastic strain (Fig. 63b) reaching 296% for the variant D1 while, decreased to 32% and 52% for the variants D2 and D3 respectively. D0 represents specimens' fatigue resistance without rejuvenator to show the impact of the rejuvenating agent in the reusing process of

RAP. The results of this variant showed an increase in the calculated values of load cycles of 501% and 308% at high and low loadings respectively. The results showed clearly the influence of rejuvenators in decreasing the fatigue behavior of RAP.

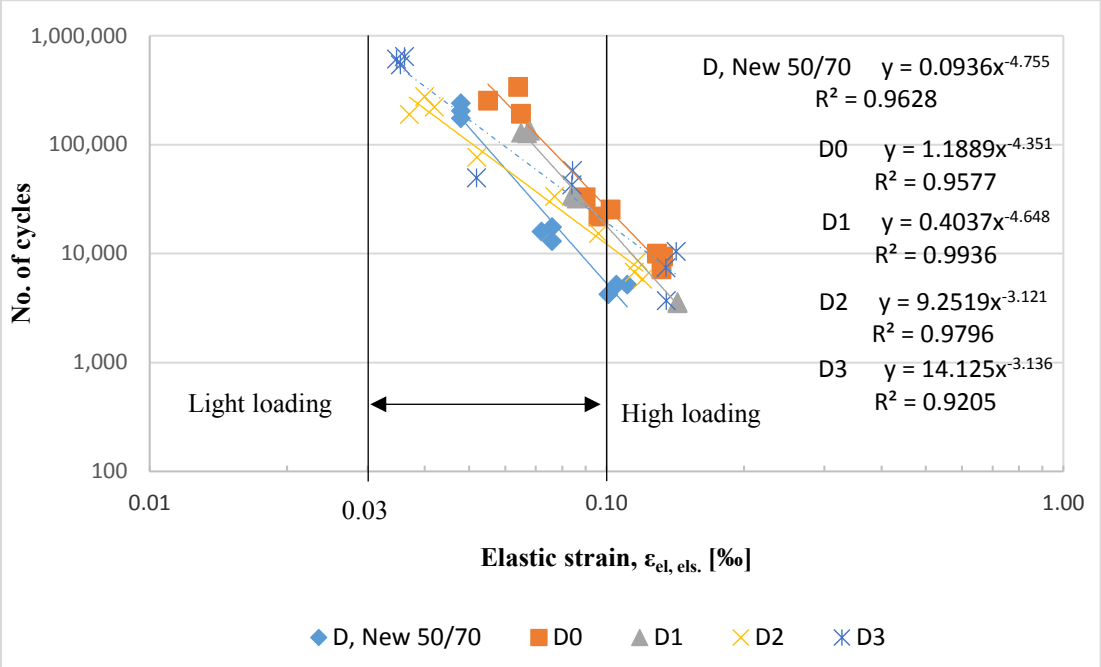

Legend:

D, New 50/70 = asphalt with virgin bitumen 50/70

D1 = asphalt mix with RAP+rejuvenator no. 1

D2 = asphalt mix with RAP+rejuvenator no. 2

D3 = asphalt mix with RAP+rejuvenator no. 3

D0 = asphalt mix with RAP, no rejuvenator

Fig. 62: Measured results of fatigue resistance of AC 16 T D mixes

Table 23: Test parameters of fatigue for AC 16 T D mixes

T, [°C]	20								
f [Hz]	10								
μ [-]	0.2984								
σ_u, [MPa]	0.035			0.035			0.035		
σ_o, [MPa]	0.50	0.50	0.50	0.36	0.36	0.36	0.30	0.30	0.30
	N_{Makro} [-]								
D, New 50/70*	5,208	5,202	4,253	17,500	13,003	16,001	240,502	175,503	204,003
D0*	7,200	9,410	10,010	33,000	25,509	22,000	192,009	340,044	253,555
D1*	3,601	3,502	3,550	34,000	32,148	33,458	127,507	134,685	129,504
D2*	6,759	8,654	5,832	15,355	76,502	33,666	222,005	190,272	277,669
D3*	3,709	10,502	7,453	42,869	58,007	49,785	648,002	542,367	610,548
	εel, anf [‰]								
D, New 50/70*	0.111	0.105	0.101	0.076	0.076	0.072	0.048	0.048	0.048
D0	0.132	0.133	0.129	0.090	0.102	0.096	0.065	0.064	0.055
D1	0.143	0.143	0.143	0.084	0.086	0.085	0.067	0.068	0.065
D2	0.115	0.117	0.120	0.096	0.052	0.077	0.042	0.037	0.040
D3	0.135	0.142	0.135	0.084	0.084	0.052	0.036	0.035	0.035

Equations derived from the test results (Y= cycles to failure and X = elastic strain)

Y = a × Xb		D, New 50/70	D0*	D1*	D2*	D3*		
constant	A	0.094	1.189	0.403	9.252	14.125		
constant	B	-4.755	-4.351	-4.648	-3.121	-3.136		
Regression	R2	0.96	0.96	0.99	0.98	0.92		
Y	0.10‰	5,324	26,678	17,950	12,224	19,319		
	0.03‰	1,631,414	5,025,633	4,835,030	523,764	842,823		
Ratio, [%]	0.10‰	100	501	337	230	363		
	0.03‰	100	308	296	32	52		

*) D, New 50/70: AC 16 T D mix using virgin bitumen of the grade 50/70 without RAP
D0: asphalt mix only with RAP of the binder layer (RAP, B)
D1: AC 16 T D mix by using RAP + rejuvenating agent 1
D2: AC 16 T D mix by using RAP + rejuvenating agent 2
D3: AC 16 T D mix by using RAP + rejuvenating agent 3

a. 0.10‰ strain

b. 0.03‰ strain

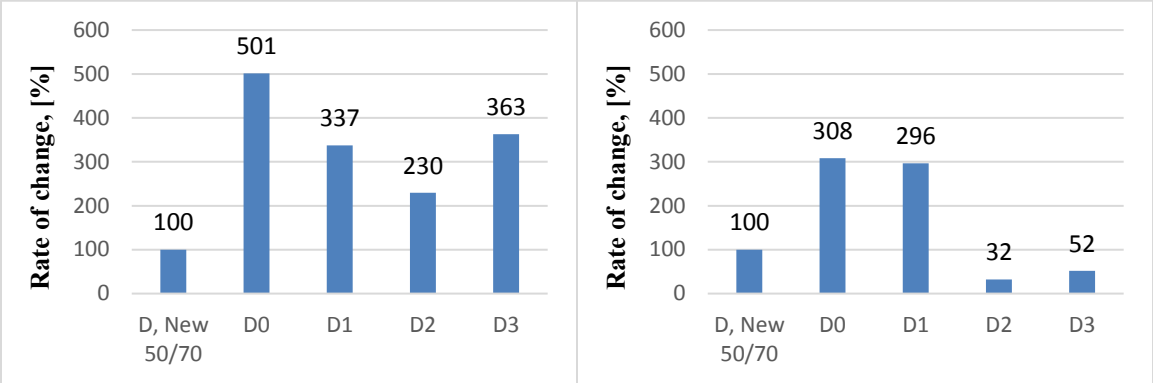

Legend

D, New 50/70 = asphalt with virgin bitumen 50/70

D1 = asphalt mix with RAP+rejuvenator no. 1

D2 = asphalt mix with RAP+rejuvenator no. 2

D3 = asphalt mix with RAP+rejuvenator no. 3

D0 = asphalt mix with RAP, no rejuvenator

Fig. 63: Calculated values of fatigue resistance of AC 16 T D mixes

6.2.4 Asphalt base course (AC 22 T S)

The responses of AC 22 T S asphalt mixes (T1, T2, and T3) were measured at heavy (σ = 0.90 MPa), intermediate (σ = 0.65 MPa), and light (σ = 0.35 MPa) loadings where, these loading levels were kept constant for all variants of this mix. Calculated values were normalized and compared to those of the new mix which was produced with the bitumen grade (T, New 30/45), and the bitumen with grade 50/70 was used to prepare the new mixes (T, New 50/70). The variant with RAP (T0) was prepared without using the rejuvenating agent. Fig. 64 and Table 24 show these mixtures' resistances to fatigue cracking at different loading categories.

Fig. 65 compares the calculated values of the responses to fatigue distress expressed as normalizations of cycles until the formation of macro-cracks between different mixes and the reference mix (T, New 30/45). At heavy loading (Fig. 65a), the new mix (T, New 50/70) showed a decrease of about 42% and 39% for the variant T1 while, the mixes T2, and T3 displayed increases of 132%, and 113% respectively, as well as of 283% for the T0 mix.

On the other hand, the new mix (T, New 50/70) decreased at lightweight loadings to 15% of the reference mix. While, the mixes T1, T2, and T3 reduced to 9%, 19%, and 79% respectively, as well as to 35% for the asphalt mix T0. The decrease in fatigue behavior of the T1, T2, and T3 mixes is in response to the decrease in stiffness modulus as previously shown.

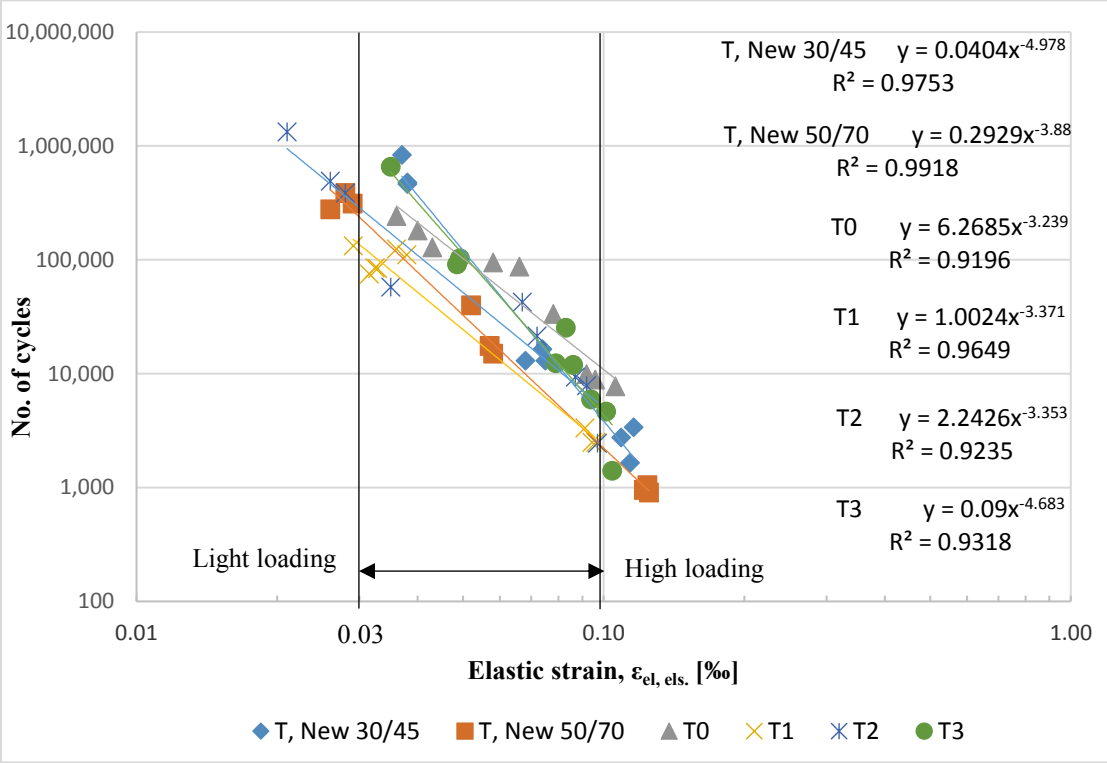

Legend:

T, New 30/45 = asphalt with virgin bitumen 30/45

T, New 50/70 = asphalt with virgin bitumen 50/70

T1 = asphalt mix with RAP+rejuvenator no. 1

T2 = asphalt mix with RAP+rejuvenator no. 2

T3 = asphalt mix with RAP+rejuvenator no. 3

T0 = asphalt mix with RAP, no rejuvenator

Fig. 64: Measured results of fatigue resistance of AC 22 T S mixes

Table 24: Test parameters of fatigue for AC 22 T S mixes

T, [°C]	20								
f [Hz]	10								
μ [-]	0.2984								
$\sigma_{u,}$ [MPa]	0.035			0.035			0.035		
$\sigma_{o,}$ [MPa]	0.90	0.90	0.90	0.65	0.65	0.65	0.35	0.35	0.35
	N_{Makro} [-]								
T, New* 30/45	3,404	1,659	2,758	16,508	13,002	13,010	478,104	463,502	837,005
T, New* 50/70	906	1,053	953	15,010	17,510	40,002	313,502	388,504	279,005
T0*	9,953	7,777	8,888	33,501	95,109	87,254	129,004	181,374	242,814
T1*	2,501	2,504	3,351	75,423	84,001	85,017	111,000	124,812	133,505
T2*	2,454	9,359	7,851	21,405	42,756	57,760	1,333,506	492,373	386,975
T3*	1,405	5,942	4,654	25,447	12,405	12,005	91,501	103,510	657,198
	εel, anf [‰]								
T, New* 30/45	0.116	0.114	0.109	0.074	0.068	0.075	0.038	0.038	0.037
T, New* 50/70	0.125	0.124	0.122	0.058	0.057	0.052	0.029	0.028	0.026
T0*	0.092	0.106	0.096	0.078	0.058	0.066	0.043	0.040	0.036
T1*	0.096	0.095	0.091	0.032	0.033	0.032	0.038	0.036	0.029
T2*	0.097	0.087	0.092	0.072	0.067	0.035	0.021	0.026	0.028
T3*	0.104	0.094	0.101	0.083	0.079	0.086	0.049	0.049	0.035

Equations derived from the test results (Y= cycles to failure and X = elastic strain)

$Y = a \times X^b$		T, New 30/45*	T, New 50/70*	T0*	T1*	T2*	T3*
constant	A	0.040	0.293	6.269	1.002	2.243	0.090
constant	B	-4.978	-3.880	-3.238	-3.371	-3.353	-4.683
Regression	R^2	0.98	0.99	0.92	0.96	0.92	0.93
Y	0.10‰	3,840	2,222	10,868	2,355	5,055	4,338
	0.03‰	1,539,117	237,404	536,745	136,353	286,394	1,218,663
Ratio, [%]	0.10‰	100	58	283	61	132	113
	0.03‰	100	15	35	9	19	79

*) T, New 30/45: AC 22 T S mix using virgin bitumen of the grade 30/45 without RAP
T, New 50/70: AC 22 T S mix using virgin bitumen of the grade 50/70 without RAP
T0: asphalt mix only with RAP of the base course (RAP, T)
T1: AC 22 T S mix by using RAP + rejuvenating agent 1
T2: AC 22 T S mix by using RAP + rejuvenating agent 2
T3: AC 22 T S mix by using RAP + rejuvenating agent 3

a. 0.10‰ strain

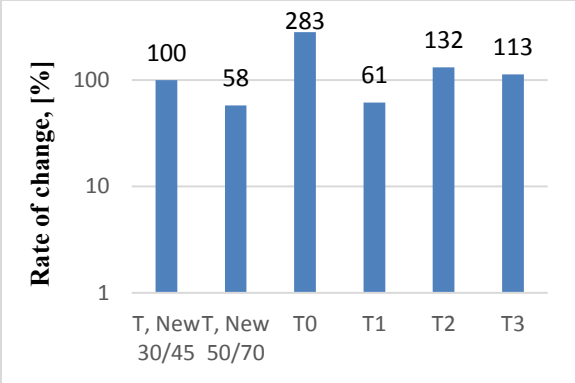

b. 0.03‰ strain

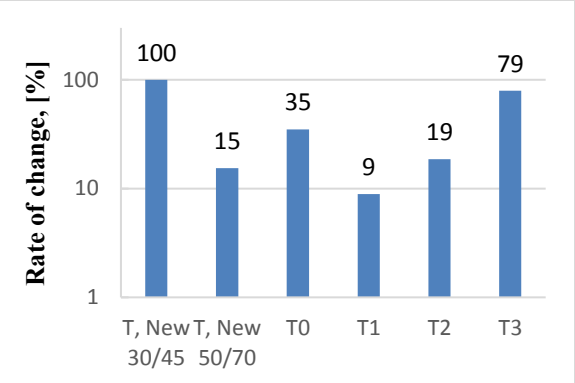

Legend:

T, New 30/45 = asphalt with virgin bitumen 30/45

T, New 50/70 = asphalt with virgin bitumen 50/70

T1 = asphalt mix with RAP+rejuvenator no. 1

T2 = asphalt mix with RAP+rejuvenator no. 2

T3 = asphalt mix with RAP+rejuvenator no. 3

T0 = asphalt mix with RAP, no rejuvenator

Fig. 65: Calculated values of fatigue resistance of AC 22 T S mixes

The results of fatigue resistance revealed that, failure occurred at a higher load repetitions and initial elastic strain for the SMA 11 S mix, and at lower load repetitions and less initial elastic strain for the AC 22 T S mix. The effect of the rejuvenating agents and of the changes in grain size provide reasons for this response in SMA 11 S and a high percentage of bitumen in addition to filler and low air voids. These factors all affect the overall response and behavior of the asphalt mixes. The bitumen type and grade also influence the asphalt mixes' resistance to fatigue distress and thus the performance of pavement. Fig. 66 illustrates fatigue cracks in two types of asphalt mixes, SMA 11 S (Fig. 66a) and AC 22 T S (Fig. 66b). The extension in the SMA 11 S mix can be clearly recognized, while the AC 22 T S mix showed sudden cracking. Furthermore, the crack in the SMA 11 S mix took a longer path than the crack in the AC 22 T S mix did due to the differences in the aggregate size.

a. SMA 11 S b. AC 22 T S

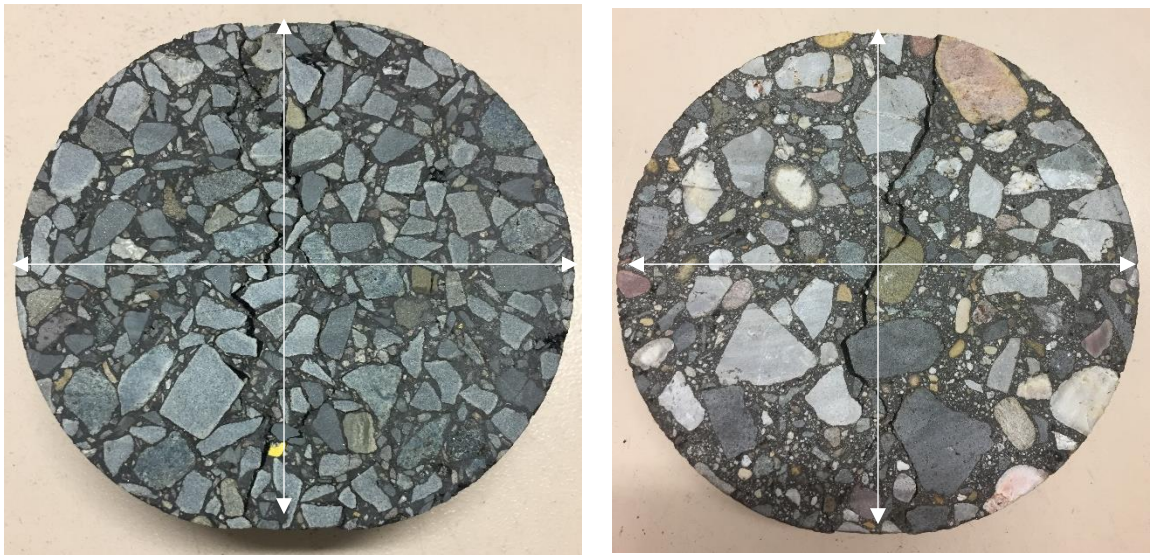

Fig. 66: Failure shape and path of different mixes, (a) SMA 11 S and (b) AC 22 T S mix

6.3 Permanent Deformation of Asphalt-Specimens

The asphalt specimens were evaluated to measure resistance to permanent deformation by subjecting vertical compressive loads at a temperature of 50 ºC. The loading took the pattern of one second of loading followed by a rest period for one second until 1×10^4 cycles of loading and unloading are reached. This test measures the resistance of asphalt mixes to rutting that may occur in pavement at high temperatures. Rutting is a surface phenomenon and due to that, this test was applied on speciemens of asphalt wearing course mixes SMA 11 S and AC 16 T D. This test was only conducted for asphalt variants produced with RAP materials, and therefore the lab-aged mix was excluded.

Several configurations can be applied in this test. A quasi-lateral confinement was selected since it more closely represents pavement condition during service than other configurations did (Fig. 67). The loading in this configuration occurs on a 100 mm diameter plate while the diameter of the sample is 150 mm.

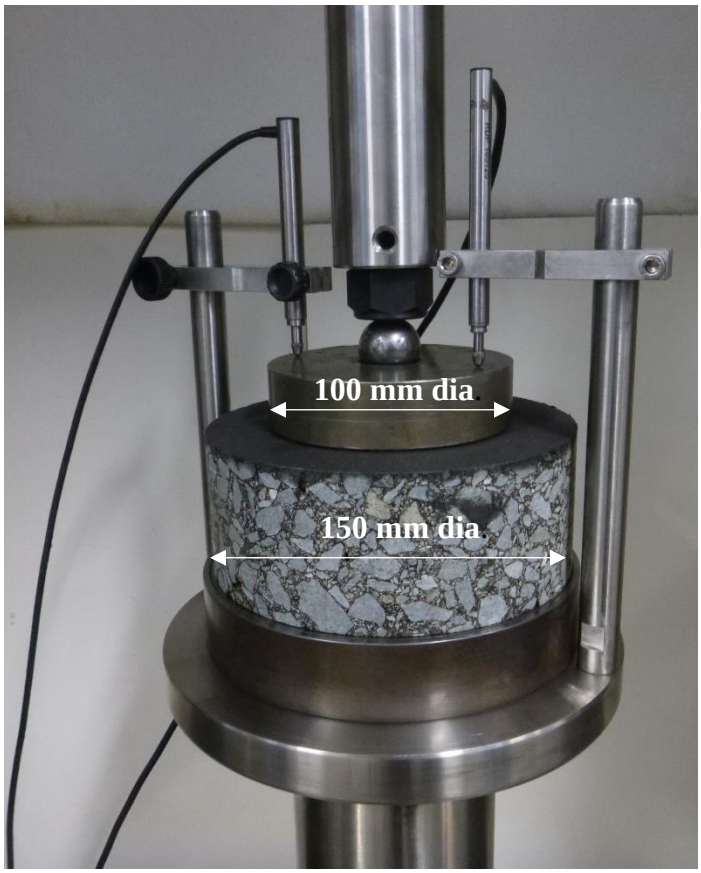

Fig. 67: Configuration of sample prepared for creep test

6.3.1 Stone mastic asphalt (SMA 11 S)

The surface layer is most subjected to the influence of thermal damage through the development of rutting in the wheel paths during hot season, because the stiffness of asphalt surface layer significantly decreases due to high temperature. Consequently, the resistance of asphalt layer to permanent deformation reduces as the temperature increases and thus, asphalt layer prone to rutting.

Cumulative axial strain in percent ε_n [%] is plotted as a function of load cycles as presented in Fig. 68. The detected creep compliances of the asphalt mixes SMA 11 S for the variants new (S, New 30/45 and S, New PMB) and with the RAP (S1, S2 and S3) are slightly different. The major part of the permanent deformation occurred at the first 1×10^3 load

cycles. After that, a lower rate of increase occurs between the cycles 1×10^3 to 5×10^3 before the slope flattens (Fig. 68). Table 25 demonstrates certain parameters derived from this test. Cumulative axial strain curves generally follow a root function until plastic failure occurs. Fig. 69 shows a comparison of cumulative axial strain after 1×10^4 cycles of loadings, where the average strain of new mixes was 3.8% and 3.3%, 4.1%, and 4.2% for the variants S1, S2 and S3, respectively. The lower the value of permanent strain, the higher is the resistance of the tested asphalt against permanent deformation.

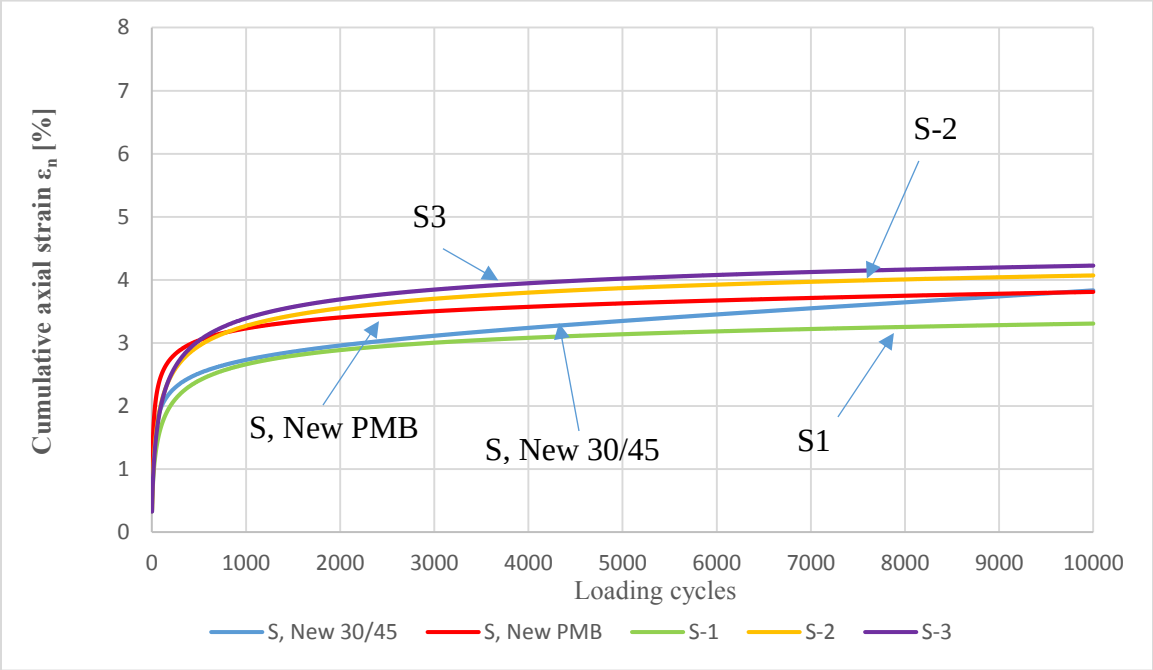

Legend:

S, New 30/45 = asphalt with virgin bitumen 30/45

S, New PMB = asphalt with virgin bitumen PMB

S1 = asphalt mix with RAP+rejuvenator no. 1

S2 = asphalt mix with RAP+rejuvenator no. 2

S3 = asphalt mix with RAP+rejuvenator no. 3

Fig. 68: Cumulative axial strain of SMA 11 S mixes

Table. 25: Creep test parameters for different SMA 11 S mixes

Mix		S New	S PMB	S1	S2	S3
Stiffness at 3600 cycles, [MPa]	Avg.*	3.166	2.825	3.279	2.660	2.616
	Std.*	0.354	0.132	0.141	0.107	0.555
Stiffness at 10000 cycles, [MPa]	Avg.*	2.647	2.630	3.027	2.460	2.422
	Std.*	0.359	0.125	0.135	0.114	0.520
Creep rate, [µm/m/cycle]	Avg.*	0.100	0.028	0.024	0.028	0.030
	Std.*	0.029	0.002	0.001	0.004	0.019
Axial strain, [%]	Avg.*	3.833	3.809	3.307	4.070	4.226
	Std.*	0.513	0.179	0.147	0.189	0.906

* Avg.= average and Std.= Standard deviation.

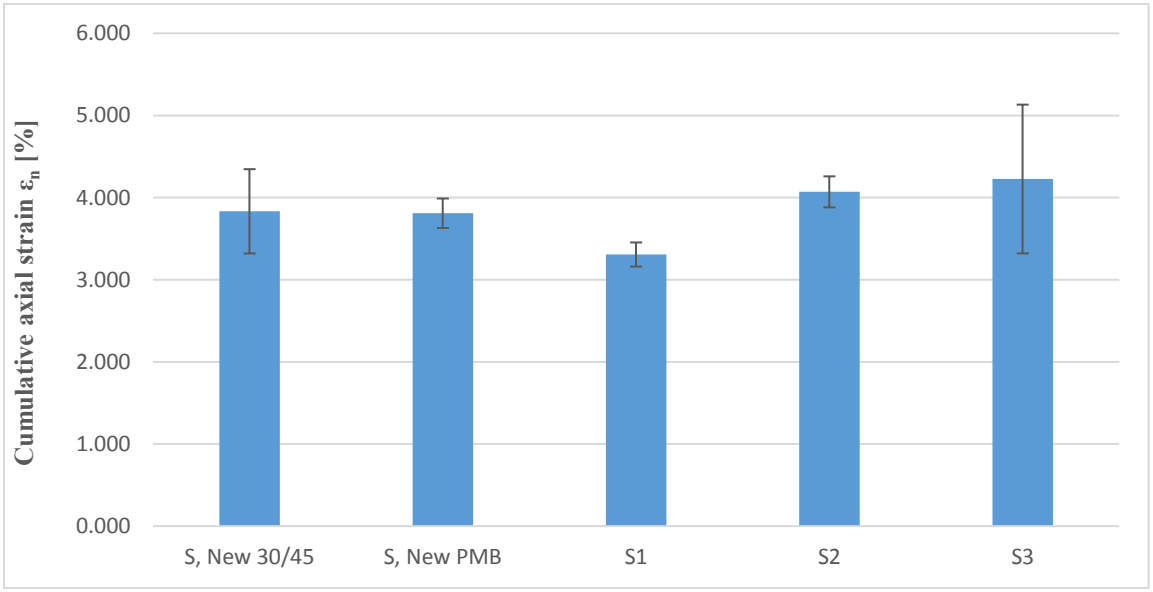

Legend:

S, New 30/45 = asphalt with virgin bitumen 30/45

S, New PMB = asphalt with virgin bitumen PMB

S1 = asphalt mix with RAP+rejuvenator no. 1

S2 = asphalt mix with RAP+rejuvenator no. 2

S3 = asphalt mix with RAP+rejuvenator no. 3

Fig. 69: Cumulative axial strain of SMA 11 S mixes at the end of test

6.3.2 Asphalt full-depth layer (AC 16 T D)

The asphalt mixes of the full-depth layer with RAP showed high rate of permanent deformation (Fig. 70) compared to the new mix (New 50/70). The variant D1 with the rejuvenator 1 shows the highest permanent strain compared to the variant D2 and D3, although the variants of SMA 11 S illustrate the opposite. Many factors may contribute in such result (Saffiuddin et al., 2014). These factors include asphalt mix design and aggregate gradation of this type of layer since it takes over the functions of the base and surface layers. It is to mention that this mix is not designed for heavy load area and it is well known that this asphalt mix is susceptible to rutting. Air voids and filler content are also regarded as determinantal factors. Additionally, the diffusion of rejuvenators in aged asphalt is a key factor affecting final viscosity and thus the performance of asphalt. However, the impact of rejuvenator is not likely playing a role in reducing the resistance of these mixes to permanent deformation since it has shown that the stiffness was kept at allowable limits. In addition, a factor may play a role is the preparation method of the asphalt mix (RAP heating at 80 ºC and aggregate at 160 ºC). However, this factor is also less considered here because similar method of asphalt mix preparation was followed with SMA 11 S mix. In addition, stiffness results of the variants D1, D2, and D3 showed comparable behavior compared to the variant (D, New 50/70) which indicate an added benefit of the rejuvenators used (reducing mixing temperature of RAP to minimize fume emissions). The most influencing factor that may affect permanent deformation resistance is aggregate gradation as shown by some researchers (Lira et al., 2019; Hoang and Hai Le, 2018; and Golalipour et al., 2012). The aggregate variation in RAP may be the most probable factor affecting the results of D1, D2, and D3 mixes. Although AC 16 T D mix was designed according to similar conditions (aggregate gradation, bitumen content and air voids), aggregate in RAP was determined as the average of five random samples which may not representing the actual aggregate distribution. Aggregate variation in RAP did not affect the results in SMA 11 S mixes due to the differences in aggregate size and distribution (see section 3.2.2). In conclusion, knowing that the most parameters affecting the performance of AC 16 T D mix were comparable to the reference mix (D, New 50/70). The aggregate variation in RAP is still the uncontrolled factor, which is likely participated in increasing the cumulative

permanent strain of D1, D2, and D3 variants. Table 26 outlines the parameters of different mixes involved in this experiment, where stiffness, creep rate, and permanent deformation for mixes with RAP and rejuvenator were higher than those for the new mix. While the new mix showed 3.8% of cumulative axial strain after 1×10^4 loading and unloading cycles, the mixes with RAP showed a cumulative axial strain of 7.5% for D1 mix and 7.2% for both of D2, and D3 mixes (Fig. 71).

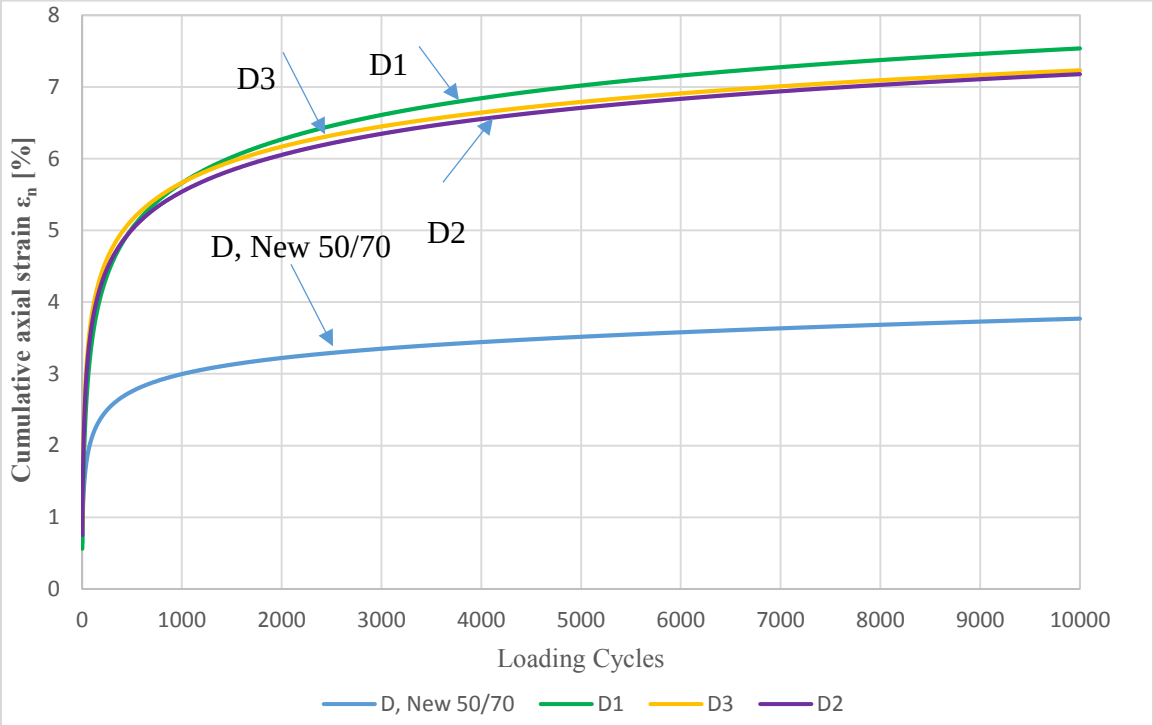

Legend:

D, New 50/70 = asphalt with virgin bitumen 50/70

D1 = asphalt mix with RAP+rejuvenator no. 1

D2 = asphalt mix with RAP+rejuvenator no. 2

D3 = asphalt mix with RAP+rejuvenator no. 3

Fig. 70: Cumulative axial strain of AC 16 T D mixes

Table 26: Creep test parameters for different of AC 16 T D mixes

Mix		New	D1	D2	D3
Stiffness after 3600 cycles, [MPa]	Average	2.934	1.485	1.578	1.554
	Std.*	0.297	0.103	0.327	0.316
Stiffness after 10000 cycles, [MPa]	Average	2.653	1.331	1.422	1.412
	Std.*	0.281	0.086	0.287	0.286
Creep rate, [µm/m/cycle]	Average	0.040	0.072	0.070	0.062
	Std.*	0.006	0.010	0.006	0.013
Permanent strain, [%]	Average	3.809	7.537	7.178	7.231
	Std.*	0.460	0.488	1.448	1.464

* Std.= standard deviation.

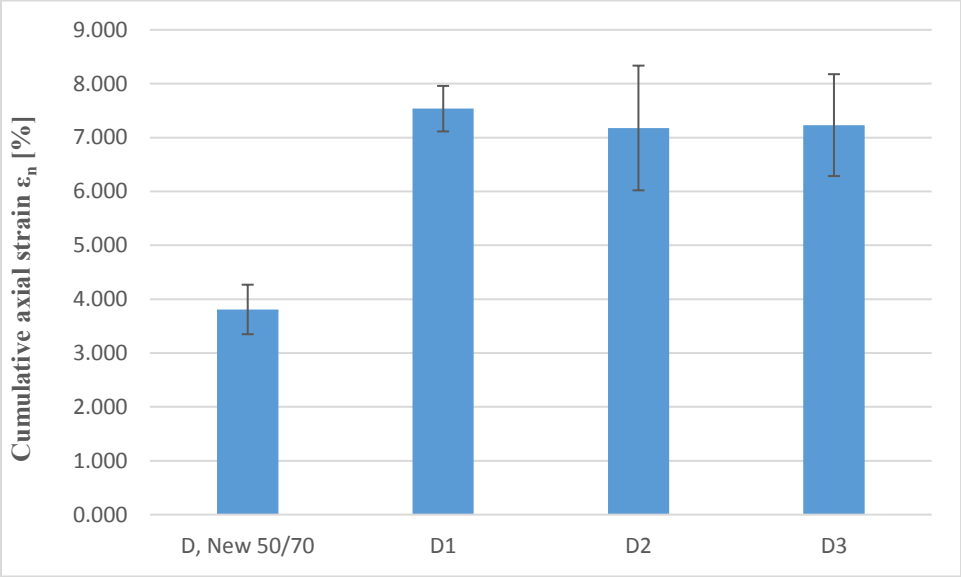

Legend:

D, New 50/70 = asphalt with virgin bitumen 50/70

D1 = asphalt mix with RAP+rejuvenator no. 1

D2 = asphalt mix with RAP+rejuvenator no. 2

D3 = asphalt mix with RAP+rejuvenator no. 3

Fig. 71: Cumulative axial stray of AC 16 T D mixes at the end of test

6.4 Low Temperature Behavior of Asphalt Specimens

This test measures the resistance of asphalt to thermal cracking at low temperatures and is applied using two methods. The first one is the thermal stress restrained specimen test (TSRST) and the second one is the uniaxial tension stress test (UTST). In the TSRST, the length of the sample is held constant by fixing the two ends of the prism of asphalt mix. The tensile strength is measured by lowering the temperature inside the test chamber until failure. This accompanied with continuous recording of the induced stresses until the fracture point. As test results, cryogenic stress over the temperature σ_{cry} (T), failure stress $\sigma_{cry,failure}$ and failure at the failure temperature $T_{failure}$ have been determined. The second method applies constant strain rate on the prism at constant temperatures to determine the maximum tensile stress at the selected temperatures until failure and while recording the stress at the rupture point (Fig. 72). Results of this test are the maximum stress (tensile strength) β_t (MPa) and the corresponding tensile failure strain $\varepsilon_{failure}$ at the test temperature.

6.4.1 Stone mastic asphalt (SMA 11 S)

The surface layer is affected at low temperatures by cracks developing due to the high internal tensile stresses of contracted asphalt. Fig. 73 shows the effect of lowering temperatures on the developed stresses in new asphalt (new 30/45; Fig. 73a). The tensile strength increased as temperature decreased to reach a peak stress at -10.0 ºC (β_t= 5.6 MPa) and then decreased at -25.0 ºC. In the fixed-length sample of TSRST, lowering temperatures increased the internal contraction stresses until the fracture at failure temperature $T_{failure}$= -25.0 ºC ($\sigma_{cry,failure}$ = 4.2 MPa). The new asphalt which prepared using PMB bitumen (Fig. 73b) exhibited a failure temperature of $T_{failure}$= -31.5 ºC ($\sigma_{cry,failure}$ = 4.4 MPa). This may be due to the use of polymer-modified bitumen with high penetration compared to the variant with conventional bitumen 30/45. In addition, an increase in the applied tensile strength at -10.0 ºC (0.6 MPa) was achieved in the new mix using PMB compared to (New 30/45). For the variants with RAP (Figs. 73c, 73d, and 73e), the increase in tensile strength were 0.7 MPa, 0.8 MPa, and 1.2 MPa for S1, S2, and S3 respectively compared to the (New 30/45) mix. This indicates the asphalt mix's with RAP increased

resistance to low-temperature-induced stresses for the three types of rejuvenator used. The failure temperature due to internal stresses of freezing were at $T_{failure}$ = -27.9 ºC ($\sigma_{cry,failure}$ = 5.0 MPa), $T_{failure}$ = -25.6 ºC ($\sigma_{cry,failure}$ = 4.6 MPa), and $T_{failure}$ = -25.4 ºC ($\sigma_{cry,failure}$ = 4.5 MPa) for S1, S2, and S3 respectively. The reference mix (New, 30/45) shows a failure temperature of $T_{failure}$ = -25.0 ºC. Fig. 74 summarizes these results, where the asphalt mixes with RAP and rejuvenators showed better resistance to freezing stresses compared to the reference (New 30/45). With decreasing failure temperature, the resistance against low temperature crack increases.

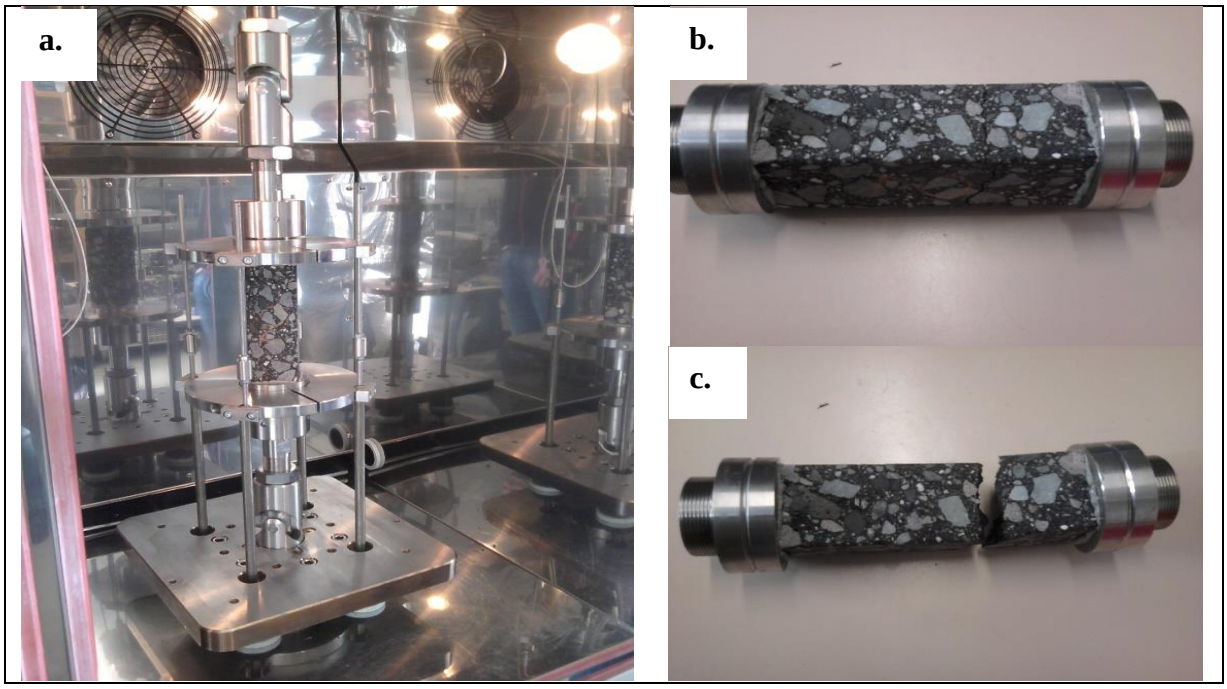

Fig. 72: Test of resistance of asphalt mixes to thermal cracking at reduced temperatures. (a) Sample after being set inside testing chamber, (b) sample prepared for test and (c) sample after the test.

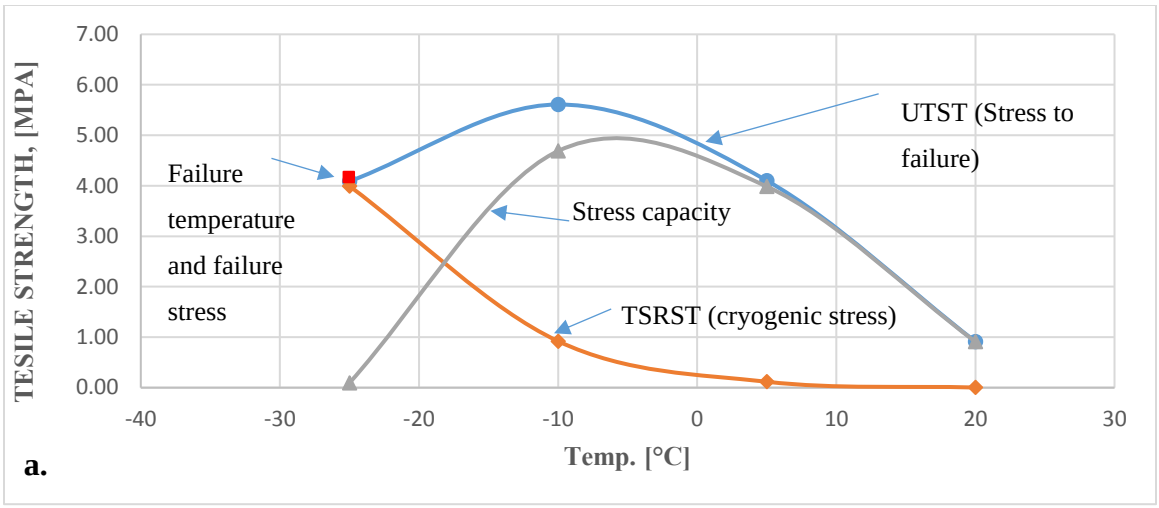
TESILE STRENGTH, [MPA]
7.00
6.00
5.00
4.00
3.00
2.00
1.00
0.00
-40
-30
-20
-10
0
10
20
30
Temp. [°C]
Failure temperature and failure stress
UTST (Stress to failure)
Stress capacity
TSRST (cryogenic stress)
a.

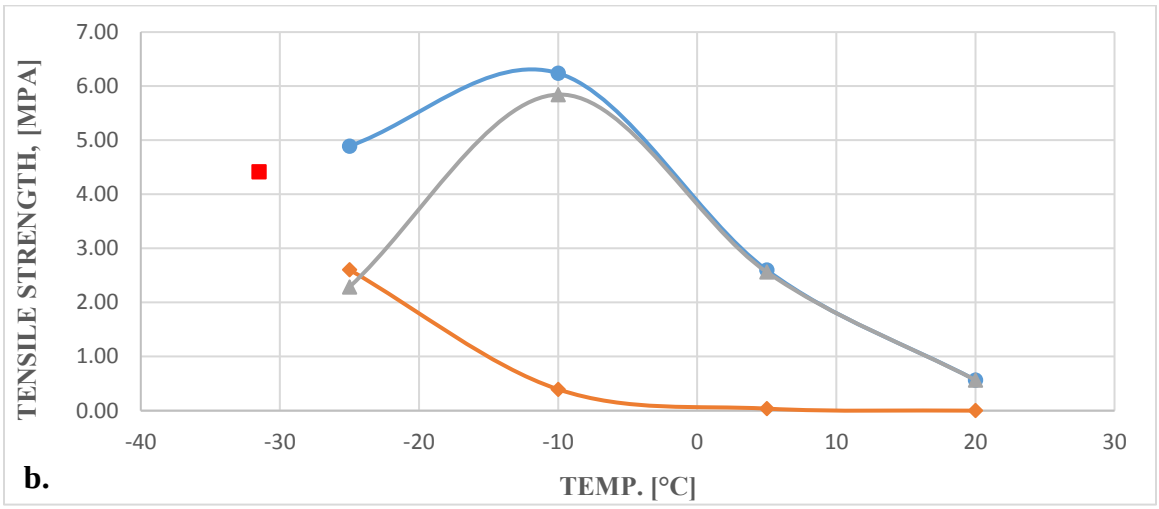
TENSILE STRENGTH, [MPA]
7.00
6.00
5.00
4.00
3.00
2.00
1.00
0.00
-40
-30
-20
-10
0
10
20
30
TEMP. [°C]
b.

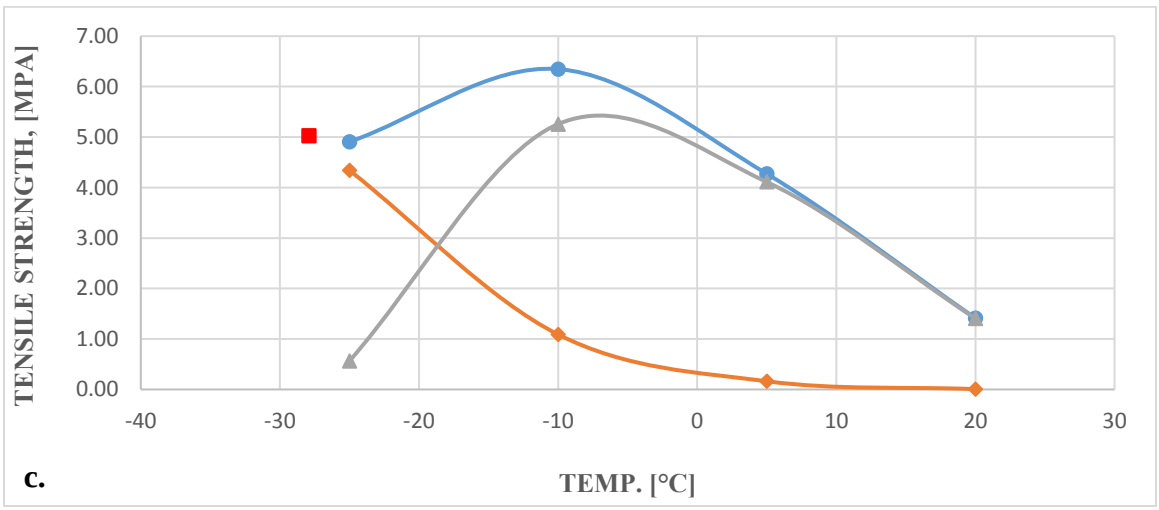
TENSILE STRENGTH, [MPA]
7.00
6.00
5.00
4.00
3.00
2.00
1.00
0.00
-40
-30
-20
-10
0
10
20
30
TEMP. [°C]
c.

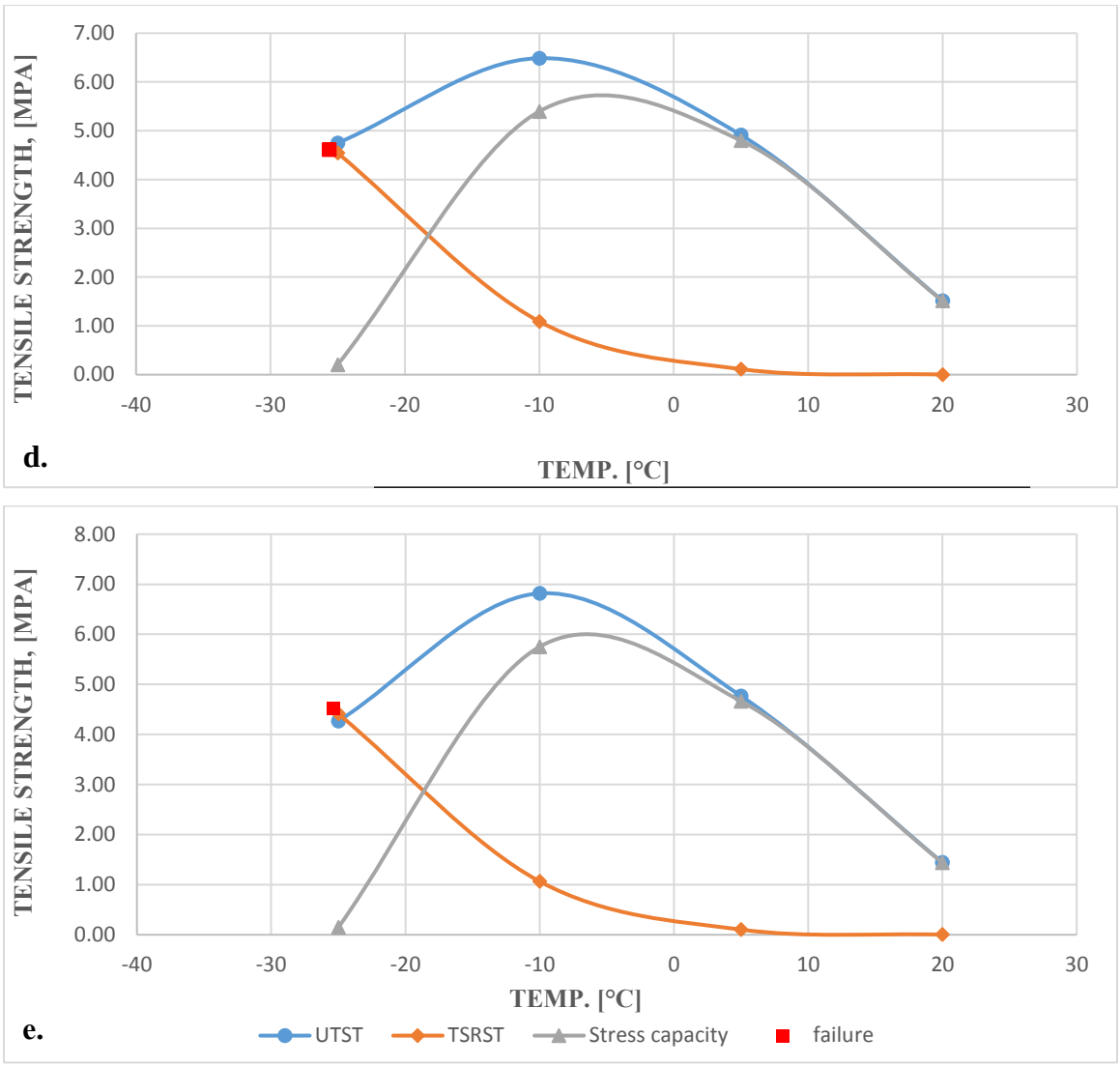

Legend:

a = asphalt with virgin bitumen 30/45 b = asphalt with virgin bitumen PMB

c = asphalt mix with RAP+rejuvenator no. 1 (S1) d = asphalt mix with RAP+rejuvenator no. 2 (S2)

e = asphalt mix with RAP+rejuvenator no. 3 (S3)

Fig. 73: Effect of low temperature in SMA 11 S mixes.

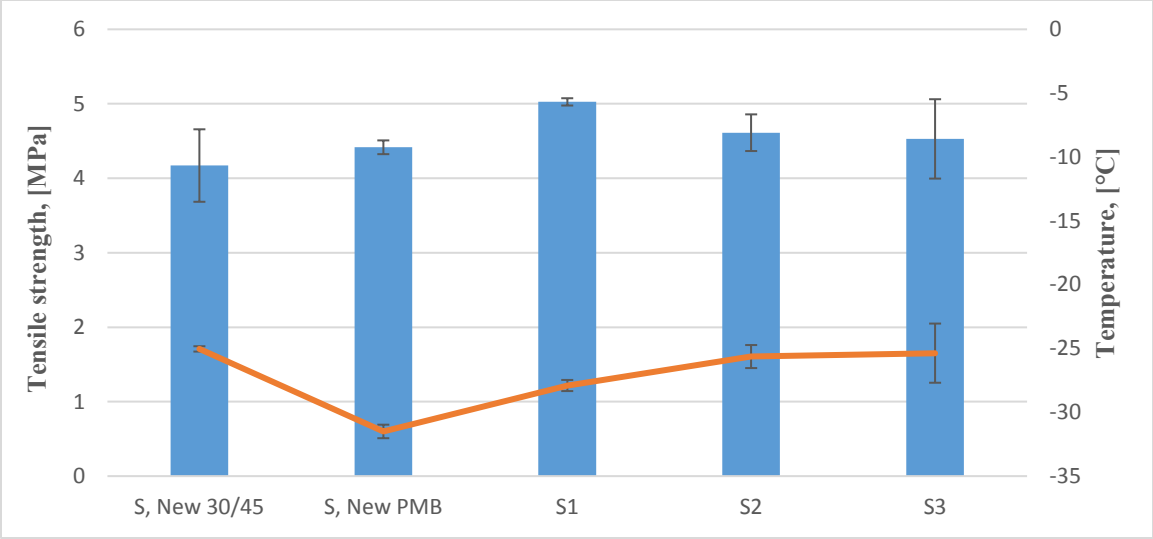

Legend:

S, New 30/45 = asphalt with virgin bitumen 30/45 S, New PMB = asphalt with virgin bitumen PMB

S1 = asphalt mix with RAP+rejuvenator no. 1 S2 = asphalt mix with RAP+rejuvenator no. 2

S3 = asphalt mix with RAP+rejuvenator no. 3

Fig. 74: Failure temperatures due to cryogenic tensile strengths for SMA 11 S mixes

6.4.2 Asphalt full-depth layer (AC 16 T D)

The full-depth asphalt layer is influenced by freezing stresses like the surface layer. Therefore, different mixes of asphalt with RAP using the three rejuvenating agents and new mix using the bitumen grade 50/70 as a reference mix (New, 50/70) were examined. The effect of freezing stresses on asphalt are shown in Fig. 75a, 75b, 75c, and 75d for new 50/70, D1, D2, and D3 respectively.

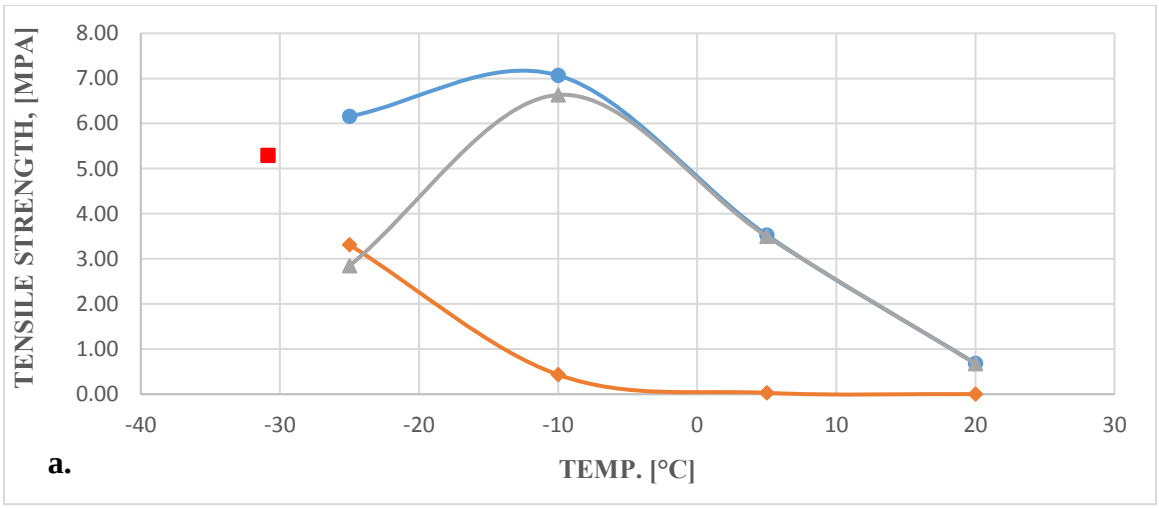
TENSILE STRENGTH, [MPA]
8.00
7.00
6.00
5.00
4.00
3.00
2.00
1.00
0.00
-40
-30
-20
-10
0
10
20
30
TEMP. [°C]

a.

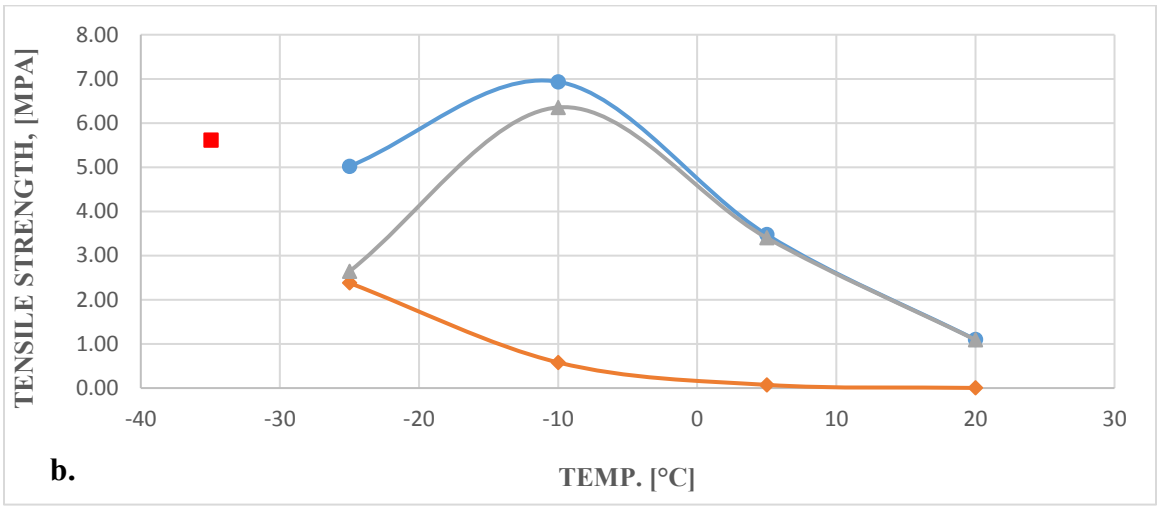
TENSILE STRENGTH, [MPA]
8.00
7.00
6.00
5.00
4.00
3.00
2.00
1.00
0.00
-40
-30
-20
-10
0
10
20
30
TEMP. [°C]

b.

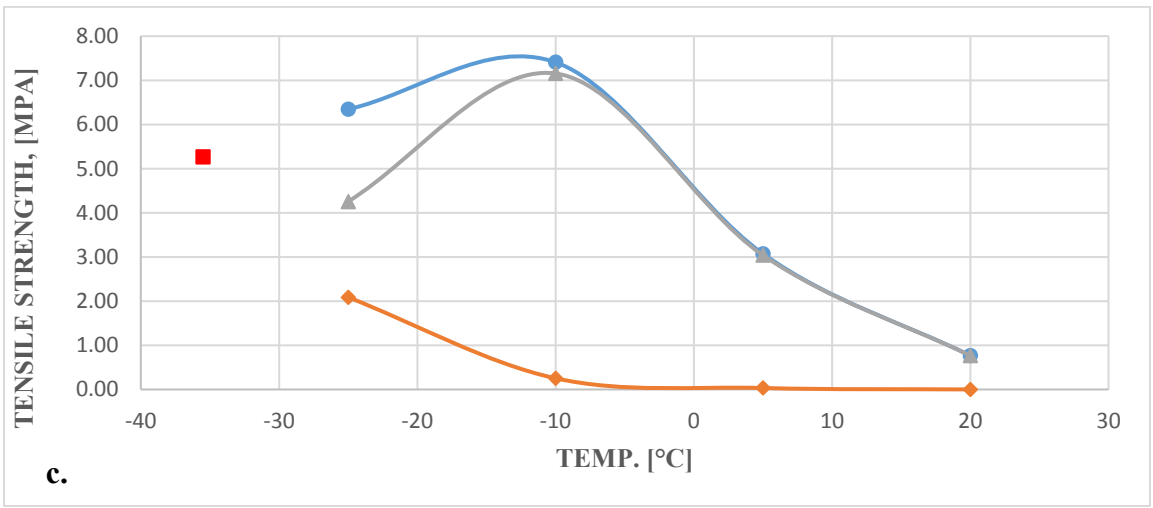
TENSILE STRENGTH, [MPA]
8.00
7.00
6.00
5.00
4.00
3.00
2.00
1.00
0.00
-40
-30
-20
-10
0
10
20
30
TEMP. [°C]

c.

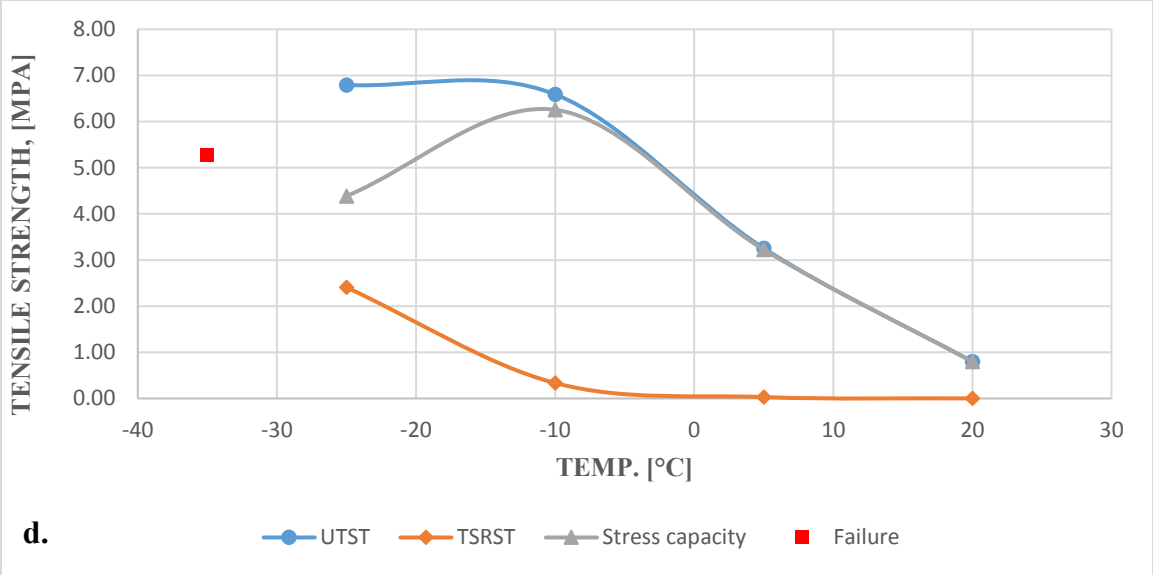

Legend:

a = asphalt with virgin bitumen 50/70 (New, 50/70)

b = asphalt mix with RAP+rejuvenator no. 1 (D1)

c = asphalt mix with RAP+rejuvenator no. 2 (D2)

d = asphalt mix with RAP+rejuvenator no. 3 (D3)

Fig. 75: Effect of low temperature in AC 16 T D mixes

The maximum stresses (β_T) applied to the mix D1 were comparable to those of the new mix at -10.0 ºC (β_T = 6.9 MPa). While, the stress increased in D2 (β_T =7.4 MPa) and D3 (β_T = 6.6 MPa). This indicates nearly similar resistance to tensile strengths at low temperatures compared to the reference mix. At extremely low temperatures (-25.0 ºC), the asphalt mix with RAP exhibited lower cryogenic stresses (σ_{cry}) of 2.4 MPa for D1 and D3, and 2.1 MPa for D2 variants compared to the reference mix which showed higher cryogenic stresses of about 3.3 MPa. The failure stress $\sigma_{cry.failure}$ of the asphalt mixes with RAP were comparable to those of new asphalt ($\sigma_{cry.failure}$ = 5.3 MPa) for reference (New, 50/70), D2, and D3 with a slightly higher stresses of 5.6 MPa for D1 mix. However, the failure temperature of the new mix (New, 50/70; $T_{failure}$ = -30.9 °C) was higher than those for the asphalt mixes with rejuvenators D1, D2, and D3 mixes ($T_{failure}$ = -35.0 ºC, -35.5 ºC, and -35.0 ºC respectively; Fig. 76). This enhancement can be attributed to the effect of rejuvenating agents used in the asphalt mix with RAP. With decreasing failure temperature, the resistance against low temperature crack increase. Due to that, the asphalt mixes with

RAP and rejuvenators show better low temperature behaviors compared to the reference variant (New, 50/70). Additional results are shown in Appendix D.

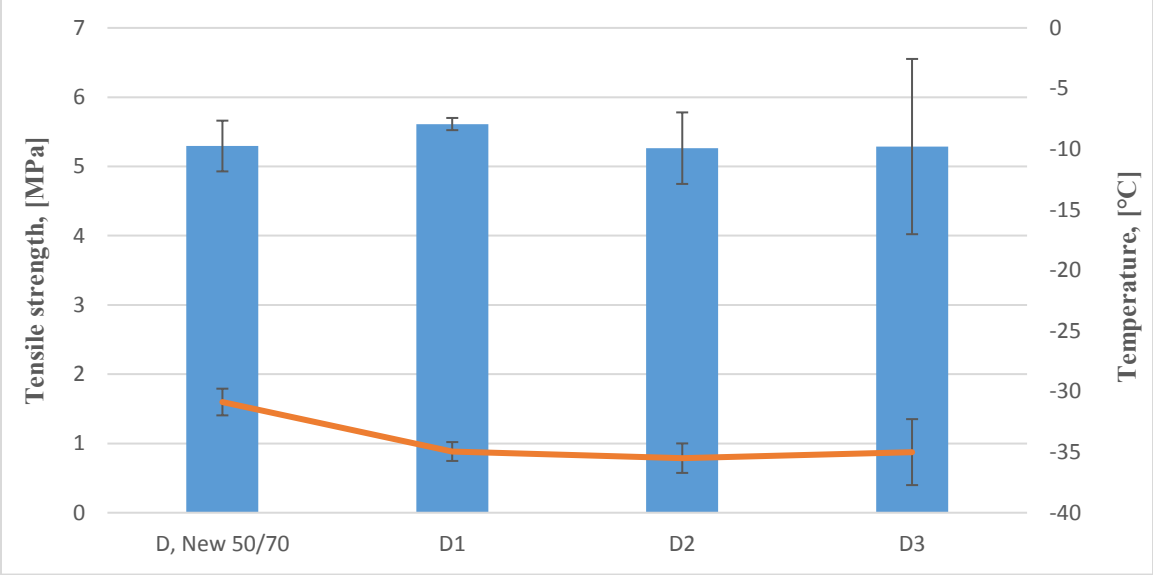

Legend:

D, New 50/70 = asphalt with virgin bitumen 50/70

D1 = asphalt mix with RAP+rejuvenator no. 1

D2 = asphalt mix with RAP+rejuvenator no. 2

D3 = asphalt mix with RAP+rejuvenator no. 3

Fig. 76: Failure temperatures due to cryogenic tensile strengths for AC 16 T D mixes

6.5 Physical Properties of Bitumen

Different kinds of bitumen were investigated using empirical tests (needle penetration and softening point ring and ball). Results were compared with respective bitumen recovered from mixes with RAP and rejuvenator (S1, S2, S3, T1, T2, and T3) or RAP only (S0 and T0). The bitumen 30/45 was used as the reference. Similarly, bitumen 50/70 was tested and compared with recovered bitumen from mixes with RAP and rejuvenator (D1, D2, and D3) or RAP only (D0). Reference bitumen results comprise the virgin, RTFOT, and PAV values of needle penetration and softening point ring and ball. Ageing index was also considered to study the impact of rejuvenators used and reusing process on the properties of bitumen. The target of the rejuvenators is to decrease the viscosity of the hardened bitumen in RAP to reach comparable properties of new (reference) bitumen. Ageing index

was calculated as a ratio of aged to unaged bitumen (using penetration or softening point results), the unaged bitumen is the reference (bitumen 30/45, or 50/70) and other types were regarded as aged bitumen. Fig. 77 illustrates the results of bitumen used in the mix SMA 11 S. The influence of rejuvenator is detected through the shift in penetration and softening point results of bitumen S1, S2, and S3. The properties of hardened bitumen (S0) changed to comparable properties of RTFOT bitumen. However, the rate of impact depends on the rejuvenator type. Compared to S0, bitumen S1 and S3 show an increase in ageing index by penetration (Fig. 77b) of about 14% which is comparable to RTFOT properties. While, bitumen S2 showed an increase of 33% of the same index. The increase in ageing index by penetration is preferred since it indicate the transition from hardened bitumen to softer bitumen while, the decrease in ageing index by softening point is preferred for the same reason. The impact of rejuvenator is obvious also in the results of ageing index by softening point since the decrease of bitumen S1, S2, and S3 is 6%, 19%, and 5% respectively.

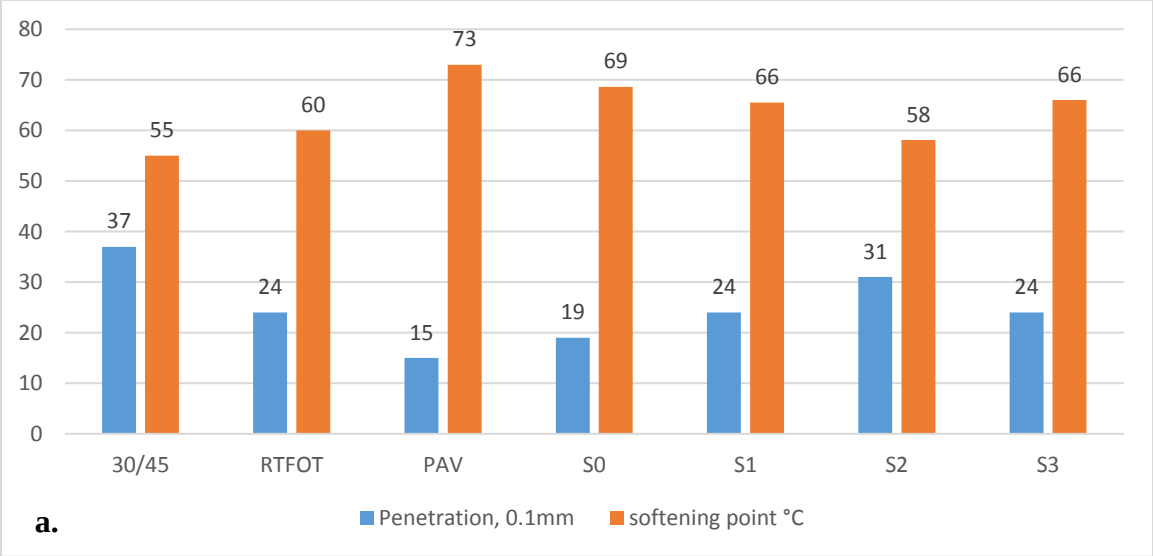

a.

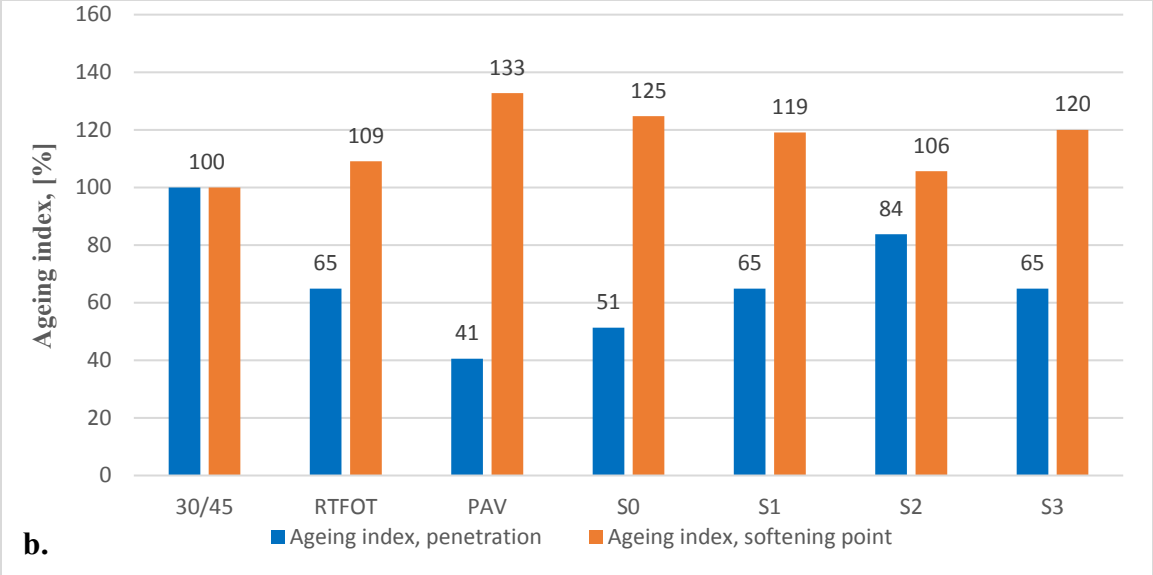

Legend:

30/45 = virgin bitumen grade 30/45 RTFOT = short-term aged bitumen

PAV = long-term aged bitumen S0 = extracted bitumen from RAP only mix

S1, S2, and S3 = extracted bitumen from mix of RAP and rejuvenators 1, 2, and 3 respectively

Fig. 77: **a**. Needle penetration and softening points ring and ball, and **b.** ageing index of new, lab-aged and extracted bitumen from SMA 11 S mixes

Fig. 78 presents the results of new bitumen (50/70) which was used in AC 16 T D mix (reference), extracted bitumen from mixes with RAP and rejuvenators (D1, D2, and D3) and bitumen extracted from the mix of only RAP (D0). Comparable properties of the variant D0 and PAV regarding ageing index by penetration (Fig. 78 b) with nearly identical properties of ageing index by softening point. The influence of rejuvenators is high as shown in the results of variants D1, D2, and D3 compared to the variant D0. The increase was 50%, 37%, and 23% respectively. Whereas, the decrease in ageing index by softening point for the variants D1, D2, and D3 was 19%, 15%, and 10% respectively, compared to the variant D0.

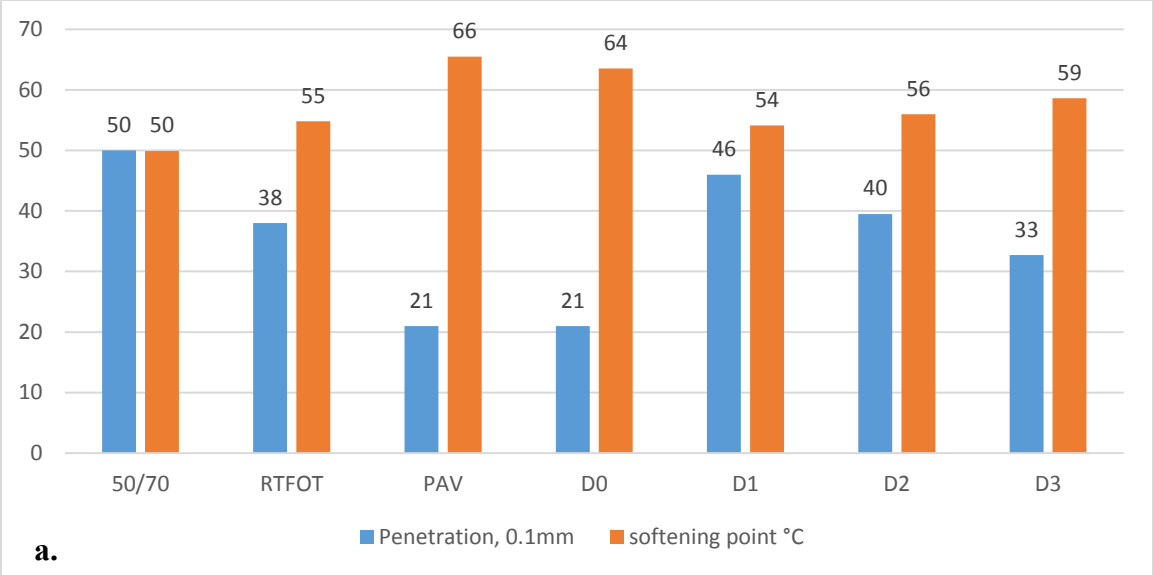

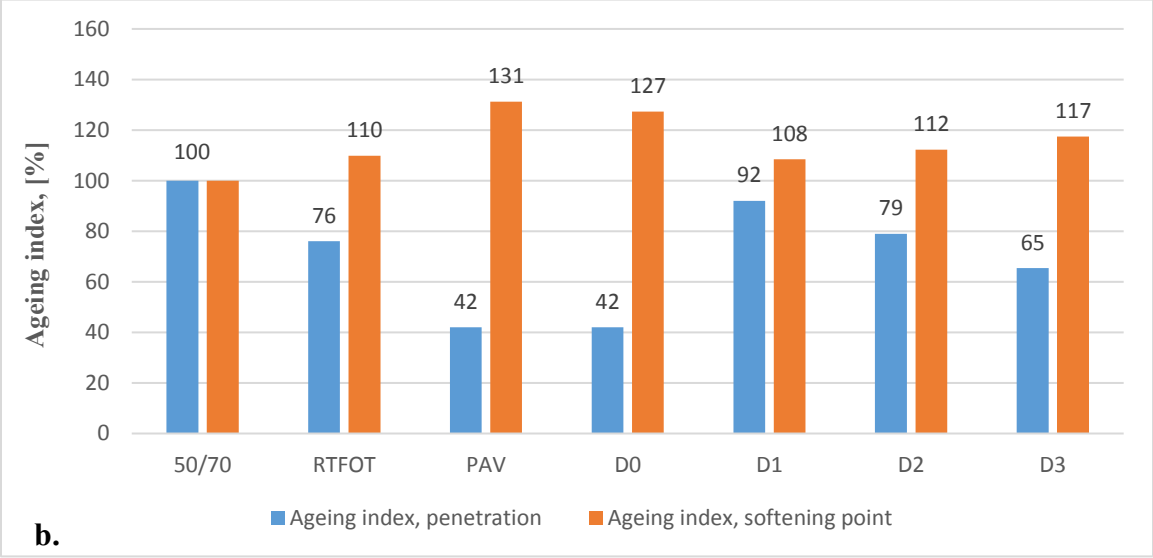

Legend:

50/70 = virgin bitumen grade 50/70 RTFOT = short-term aged bitumen

PAV = long-term aged bitumen D0 = extracted bitumen from RAP only mix

D1, D2, and D3 = bitumen extracted from mix of RAP and rejuvenators 1, 2, and 3 respectively

Fig. 78: **a**. Needle penetration and softening points ring and ball, and **b.** ageing index of new, lab-aged and extracted bitumen from AC 16 T D mixes

Results of new bitumen (30/45), which were used as reference in AC 22 T S mix, bitumen extracted from asphalt mixes with RAP and rejuvenator (T1, T2, and T3), and bitumen extracted from the mix of only RAP (T0) are shown in Fig. 79. It is obvious that the used rejuvenators have increased the ageing index by penetration (Fig. 79b) of T1, T2, and T3 variants compared to the variant T0 to reach an increase of 62%, 68%, and 62% respectively, which are comparable to or slightly exceed the results of virgin bitumen (30/45). The ageing index by softening point showed a noticeable decrease in the ageing index of the variants T1, T2, and T3 compared to the variant T0. The measured decrease is 28%, 30%, and 28% respectively.

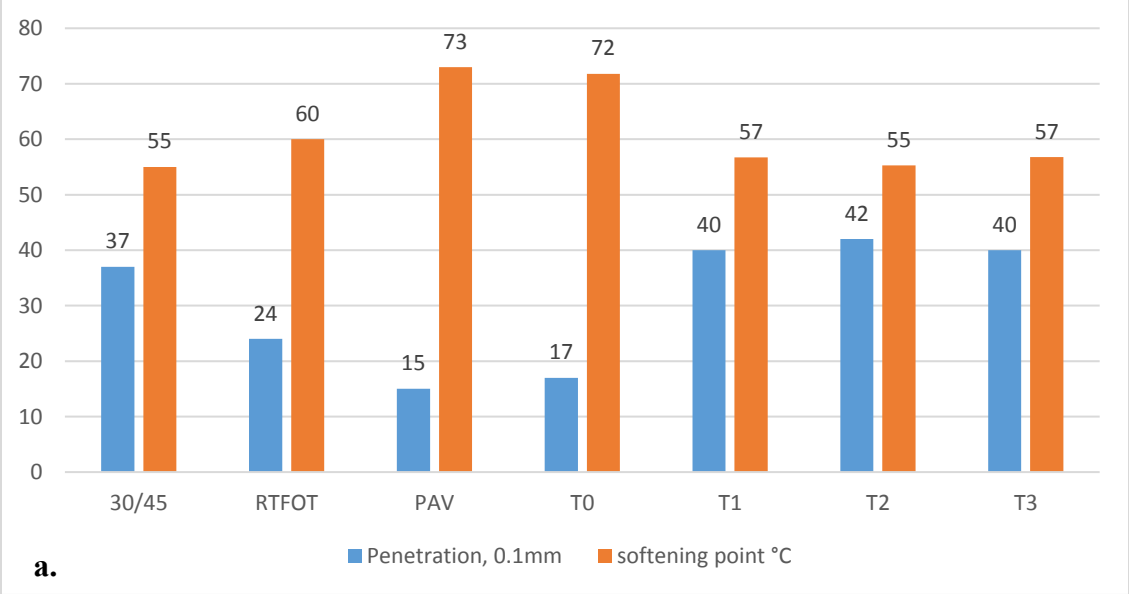

a.

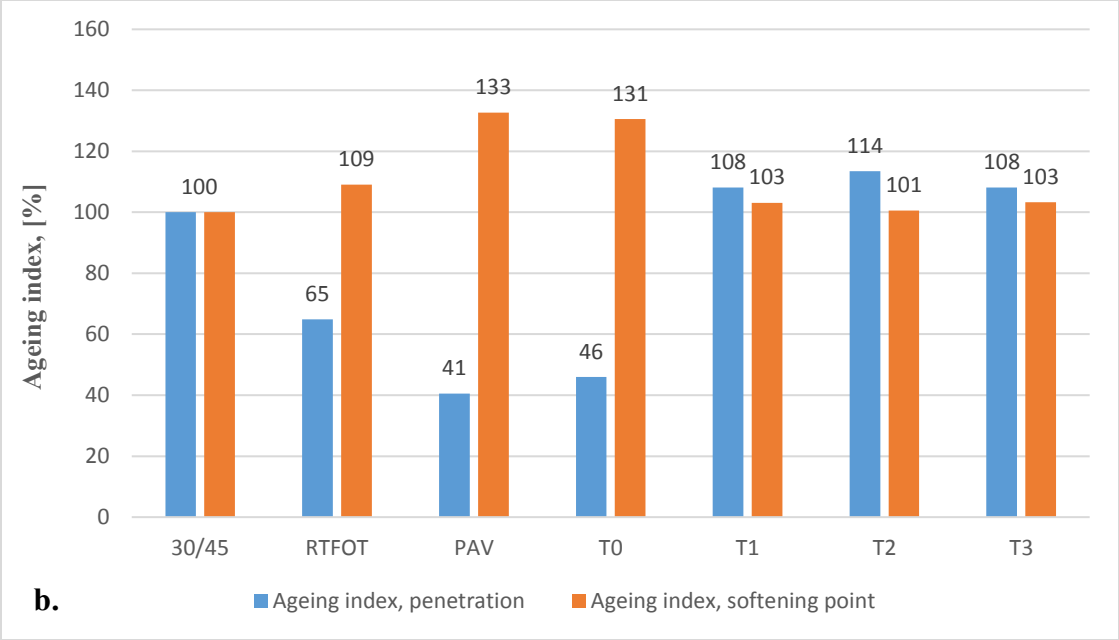

Legend:

30/45 = virgin bitumen grade 30/45 RTFOT = short-term aged bitumen

PAV = long-term aged bitumen T0 = extracted bitumen from RAP only mix

T1, T2, and T3 = extracted bitumen from mix of RAP and rejuvenators 1, 2, and 3 respectively

Fig. 79: **a**. Needle penetration and softening points ring and ball, and **b.** ageing index of new, lab-aged and extracted bitumen from AC 22 T S mixes

Although the rejuvenators used in the study have softened the hardness of bitumen in RAP of the three mixes used (SMA 11 S, AC 16 T D, and AC 22 T S), the rates of impact are different as shown previously. Such differences maybe attributed to the ratio of rejuvenator to hardened bitumen in RAP. This ratio can be calculated from Table 20 where, for the variants S1, S2, and S3, the ratio is 9.63%, 4.65%, and 5.94% respectively. For the variants T1, T2, and T3, the ratio is 11.76%, 5.29%, and 7.35% respectively. This increase may affect the characteristics of bitumen, as demonstrated from the results of the bitumen (T0) which showed lower penetration and higher softening point results (penetration 17 and softening point 72 °C). Bitumen (S0) showed characteristics of less viscous bitumen (penetration 19 and softening point 69 °C). The comparison between the bitumen of S type and T type was held because they were compared to the same reference (30/45). In addition, bitumen content in RAP of S type is 6.23% while it is 3.40% in T type bitumen. These

factors (rejuvenator content, bitumen content in RAP, and properties of each bitumen) maybe participated in such different responses as shown in ageing index results. This applies also in the case of bitumen D0 where, results of penetration and softening point were 21 and 64 °C respectively and the content was 5.40% in RAP. The ratio of each rejuvenator to the hardened bitumen in the variants D1, D2, and D3 was 9.26%, 4.26%, and 5.56% respectively. Finally, it is also noticed that the properties of each rejuvenator are a detreminantal factor due to the differences in composition of these agents which affected the dosage of individual agent in the same mix as shown in Table 20. For instance, the ratio of increase in penetration is calculated for S0 with rejuvenator 1 ([penetration of S1 × 100] ÷ [Penetration of S0 × hard bitumen content in S0]). The rejuvenator 1 increased the penetration of the variants S0, D0, and T0 by 20%, 41%, and 69% respectively, per 1% of hardened bitumen in RAP of relevant variant. The same rejuvenator decreased the softening point for S0, D0 and T0 by 15%, 16%, and 23% respectively, per 1% of hardened bitumen in RAP. Similarly, the impact of rejuvenator 2 is shown to increase the penetration of the variants S0, D0, and T0 by 26%, 35%, and 73% respectively, per 1% of hardened bitumen in RAP. The softening point decreased for the same variants by 13%, 16%, and 22% respectively. The variants S0, D0, and T0 show an increase in penetration due to the impact of rejuvenator 3 of 20%, 29%, and 69% respectively, per 1% of hardened bitumen in RAP of respective variant. The decrease in softening point was 15%, 17%, and 23% for the same variants respectively, per 1% of bitumen in RAP of relevant variant. Blending between the rejuvenator and hard bitumen in RAP, and diffusion of the rejuvenator may provide a probable explanation of the different impact of rejuvenators on penetration and softening point. Where, as shown by the ratios of change per 1% of bitumen in RAP, the variant S0 with higher bitumen content (6.23%) than the variants D0 and T0 (5.40% and 3.40% respectively). With decreased bitumen content, the film thickness of bitumen decreases which allows for increased impact due to blending and diffusion of the rejuvenator with the hardened bitumen. This factor (blending and diffusion) is the reason of using different rejuvenator content to bitumen in RAP.

6.6 Rheological Properties of Bitumen

The rheological properties of virgin bitumen (30/45) is determined here as reference. The lab-aged bitumen using RTFOT and PAV, the extracted bitumen of surface layer with RAP (S0), and in combination with rejuvenators 1 and 2 (S1 and S2) are shown in Fig. 80a. Compared to the reference bitumen (30/45), the variants S1 and S2 exhibited rheological properties between RTFOT and PAV. Fig. 80b demonstrates the impact of rejuvenators used on rheological properties of bitumen at low (-5 °C) and high (60 °C) temperatures as a ratio of complex modulus of the variants RTFOT, PAV, S0, S1, and S2 to the reference (30/45). The impact of rejuvenators at low temperatures compared to the variant S0 is shown through the decrease in complex modulus of the variants S1 and S2 (29% and 37% respectively). At high temperatures (60 °C), the decrease in complex modulus of the variants S1 and S2 is 338% and 243% respectively. Compared to S0, the variants S1 and S2 at low temperature show an increase in phase angel (Fig. 80c) of 11% and 15% respectively. Marginal impact shown at high temperature. It can be noted that at extremely low temperatures the impact of the rejuvenator is lower than that at high temperature. This can be attributed to the glass-like behavior of bitumen at low temperatures. The results of rheological properties support the results derived from physical tests which are previously shown. The variant S3 was not shown due to the limited amount of recovered bitumen after extraction.

For the virgin bitumen 50/70 (reference), RTFOT, bitumen extracted from RAP (D0), and bitumen extracted from asphalt mixes with RAP in combination with rejuvenator (D2) the results are shown in Fig. 81. Fig. 81b shows the complex modulus of the variants at low (-5 °C) and high (60 °C) temperatures. Compared to the variant D0, the complex modulus of the variant D2 decreased at low and high temperatures by 91% and 386% respectively due to the impact of rejuvenating agent. Phase angle results (Fig. 81c) compared to D0 showed a decrease at low temperature of 5% and an increase of 4% at high temperature.

Both figures show that the use of rejuvenators have affected the rheological properties of aged bitumen in RAP by reducing the complex modulus and increasing the phase angle.

These changes are beneficial in restoring the rheological properties of hardened bitumen in RAP and thereby enhance the performance of asphalt with RAP. In addition, these results appear to be in line with the physical results and support the influence of the rejuvenators. The effect of temperature is also obvious as shown in the same figures.

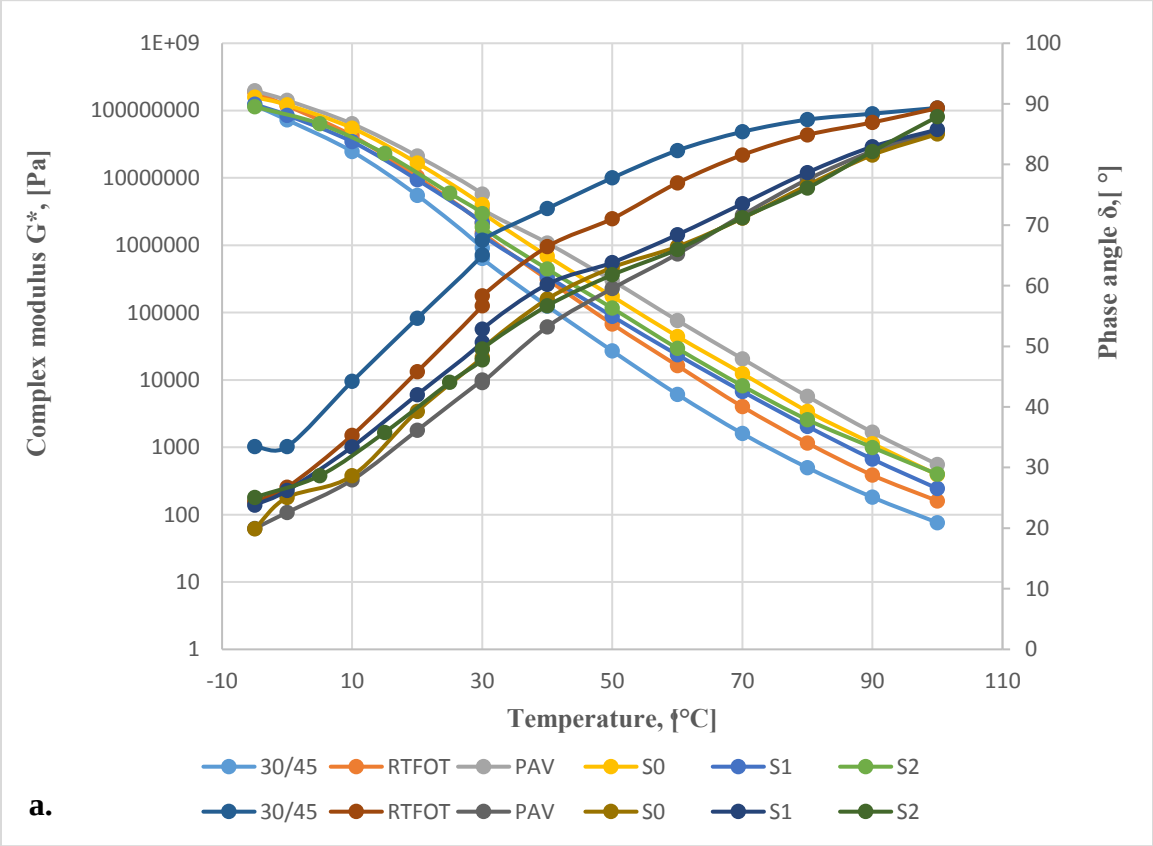

a.

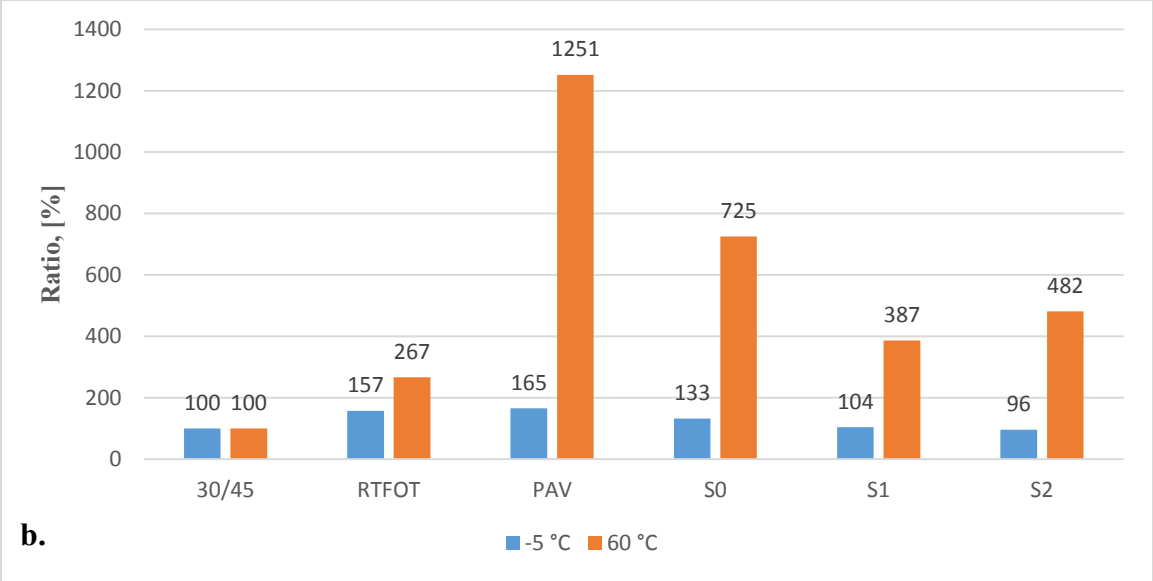

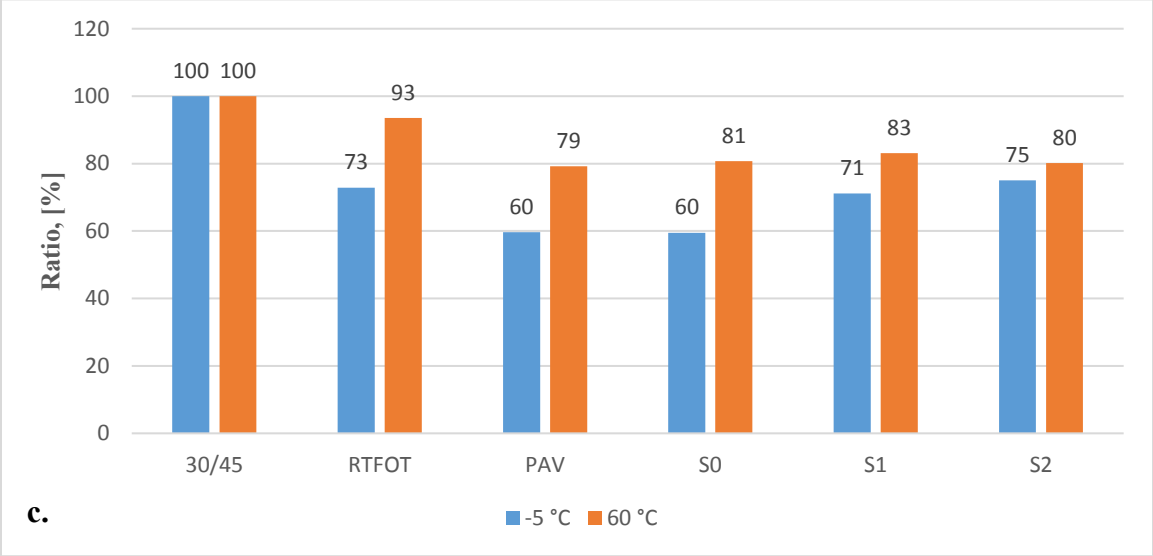

Legend:

30/45 = virgin bitumen grade 30/45 RTFOT = short-term aged bitumen

PAV = long-term aged bitumen S0 = extracted bitumen from RAP only mix

S1 and S2 = extracted bitumen from mix of RAP and rejuvenators 1 and 2respectively

Fig. 80: **a.** Complex modulus and phase angle at different temperatures, **b.** Ratio of complex modulus, and **c.** Ratio of phase angle for new, lab-aged and extracted bitumen from SMA 11 S mixes

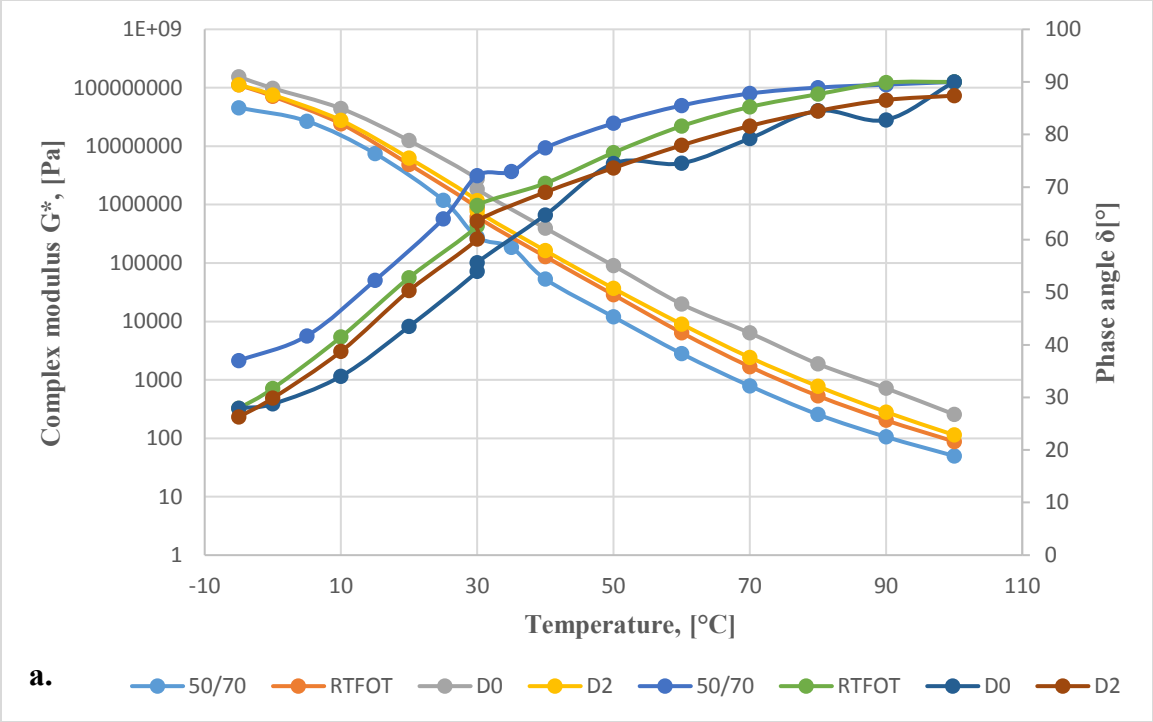
1E+09
100000000
10000000
1000000
100000
10000
1000
100
10
1
Complex modulus G*, [Pa]
100
90
80
70
60
50
40
30
20
10
0
Phase angle δ[°]
-10
10
30
50
70
90
110
Temperature, [°C]
a.
50/70
RTFOT
D0
D2
50/70
RTFOT
D0
D2

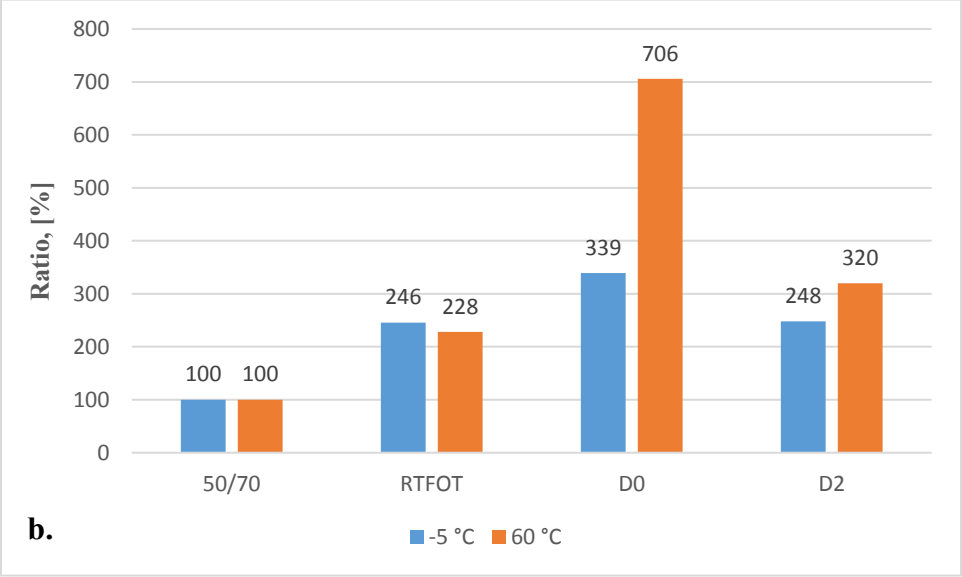
800
700
600
500
400
300
200
100
0
Ratio, [%]
100
100
246
228
339
706
248
320
50/70
RTFOT
D0
D2
b.
-5 °C
60 °C

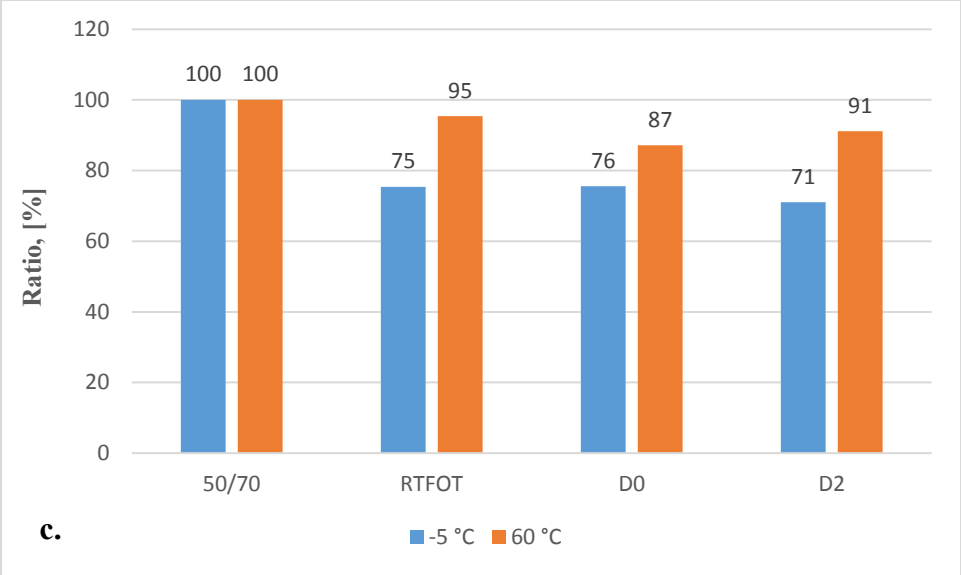

Legend:

50/70 = virgin bitumen grade 50/70 RTFOT = short-term aged bitumen

D0 = extracted bitumen from RAP only mix

D2 = extracted bitumen from mix of RAP and rejuvenators 2

Fig. 81: **a.** Complex modulus and phase angle at different temperatures, **b.** Ratio of complex modulus, and **c.** Ratio of phase angle for new, lab-aged and extracted bitumen from AC 16 T D mixes

6.7 Chemical Designation of Bitumen

Functional groups of the new (reference) 50/70 bitumen grade, aged, and extracted bitumen (asphalt with RAP + rejuvenators) are shown in Fig. 82a for the sulfide group (wavenumber at 1030/cm). In addition, Fig. 82b shows the spectrum for the carbonyl group (wavenumber at 1705/cm). Many peaks occur along the S1 curve, which is likely due to the impact of the rejuvenator. The reference peaks are shown in Fig. 82c at 1375/cm and 1460/cm wavenumbers. The Iso and Ico ageing indices are shown in Fig. 83 as ratio to the reference (new) bitumen to demonstrate the impact of rejuvenator on chemical structure characteristics of bitumen. Where, the impact is obvious through the reduction in the index of long-term ageing (Ico) of the variants S0 and S1 (262% and 74% respectively). This

decrease can be attributed to the use of rejuvenator 1 because the variant S0 was extracted from a mix composed of RAP only while, the variant S1 was extracted from the mix of RAP and rejuvenator. Moreover, results of the index of short-term ageing (Iso) showed also a decrease but to less extent in the variants S0 and S1 (130% and 110% respectively) due maybe to the same impact of rejuvenator 1. These results suggest an impact of the rejuvenator on the chemical structure elements of bitumen in the reusing process of RAP along with the aforementioned impact on physical and chemical characteristics of bitumen in RAP. The test was not conducted to other variants due to limited amounts of extracted bitumen.

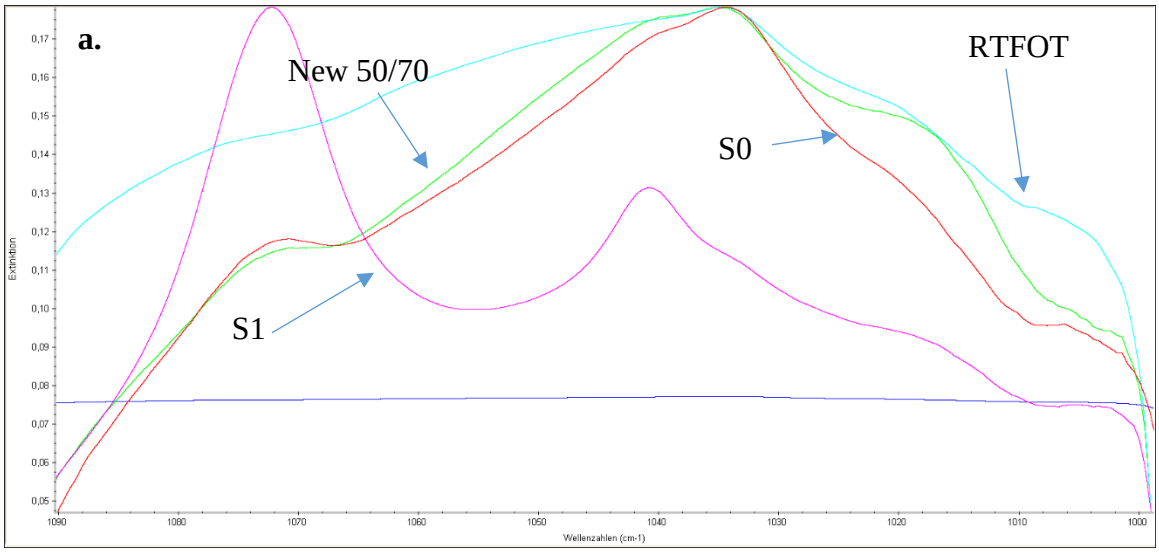

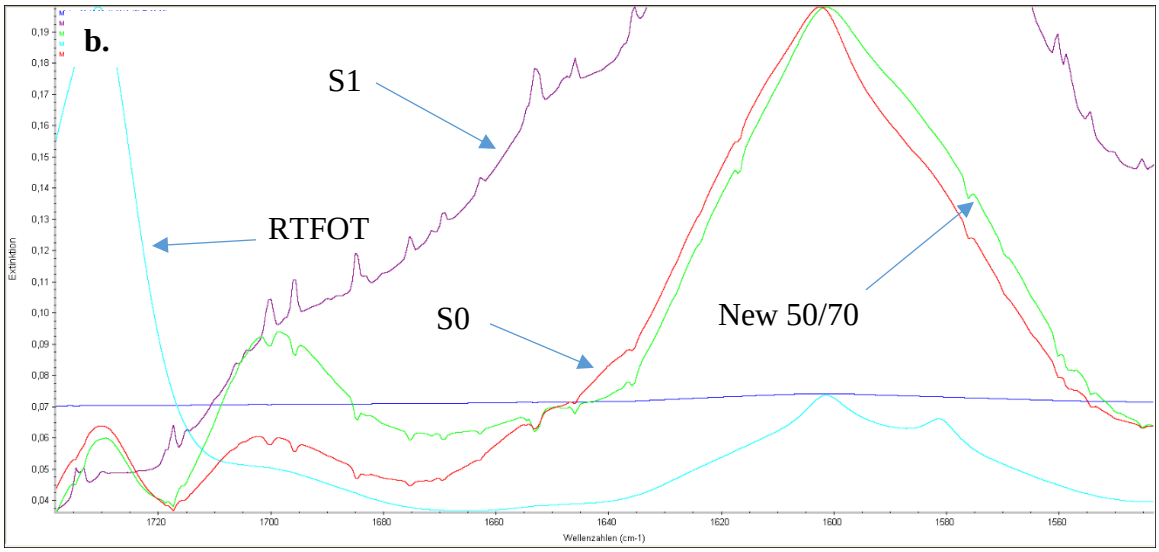

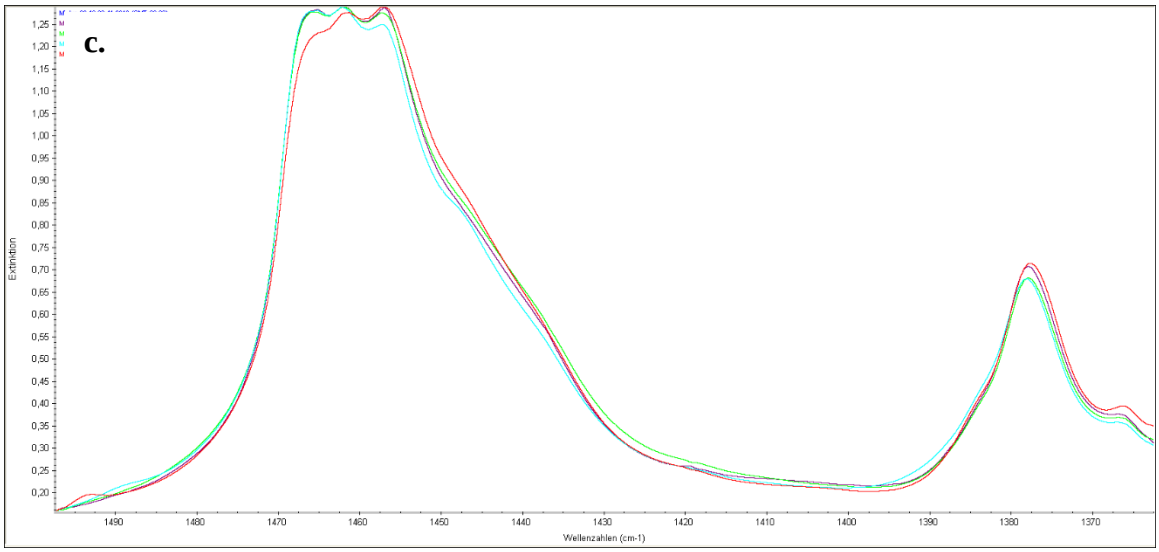

Legend:

50/70 = virgin bitumen grade 50/70 RTFOT = short-term aged bitumen

S0 = extracted bitumen from RAP only mix

S1 = extracted bitumen from mix of RAP and rejuvenator 1

Fig. 82: Fourier transform infrared spectroscopy (FTIR) spectrum of bitumen extracted from SMA 11 S mixes, **a.** at 1030/cm, **b.** at 1705/cm, and **c.** reference peaks 1375/cm and 1460/cm wavenumbers.

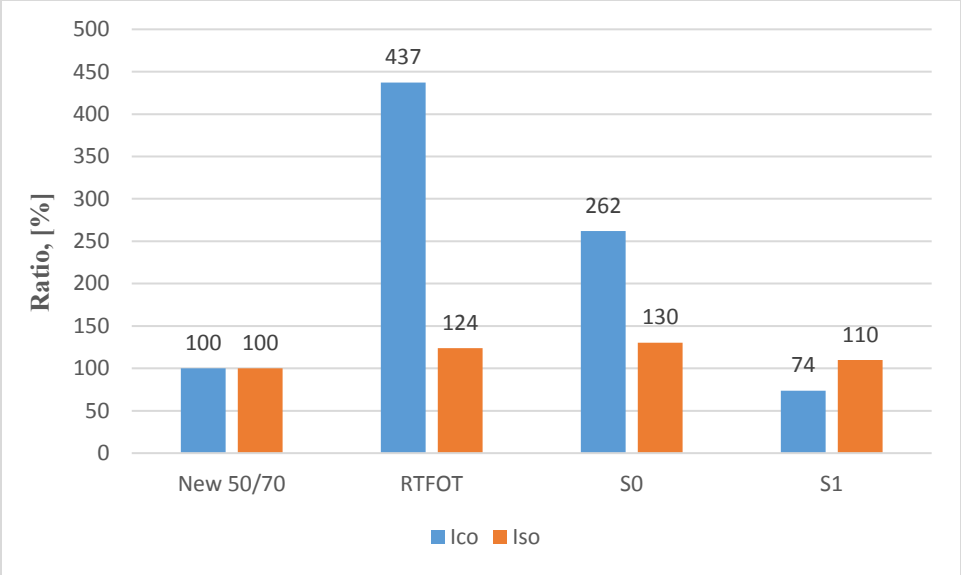

Legend:

New 50/70 = virgin bitumen grade 50/70 RTFOT = short-term aged bitumen

S0 = extracted bitumen from RAP only mix

S1 = extracted bitumen from mix of RAP and rejuvenator 1

Fig. 83: Indices of short- and long- term ageing as a ratio to reference (new) bitumen

6.8 Conclusion on the Impact of RAP and Rejuvenators on Asphalt Specimens' Properties

The use of RAP at higher contents (90%) is possible. The reuse process should include determining the bitumen content and physical properties (needle penetration and softening point ring and ball) as well as the aggregate gradation of the RAP. The reuse of RAP in high content is only possible in combination with the use of rejuvenators, whose amount should be determined according to the data collected regarding the bitumen properties in RAP. Additional new bitumen may be needed if the amount of bitumen in RAP and rejuvenator are insufficient to meet the Specification.

The rejuvenators utilized in this research showed an impact on the stiffness modulus of the asphalt with RAP. However, the extent of this effect differed based on the source and properties of the rejuvenator. The specimens produced by RAP only (without rejuvenator)

showed a higher stiffness modulus due to the impact of hardened bitumen in RAP. Fatigue resistance was reduced in asphalt-specimens containing rejuvenators compared to specimens containing only RAP (no rejuvenators). This indicates the role of rejuvenators in reducing the stiffness of the aged bitumen. The rutting resistance of the asphalt with RAP and rejuvenators was comparable to that of the new asphalt specimens for SMA 11 S mix. While, AC 16 T D mix showed different responses indicating that the mix design may reduce rutting resistance at higher temperatures (50 °C). Compared to the new mixes, the asphalt with RAP and rejuvenators exhibited enhanced resistance to failure temperature ($T_{failure}$), failure stresses (σ_{cry}) and tensile strength β_t (T) induced by low-temperatures.

The bitumen extracted from the asphalt variants with RAP and rejuvenator showed an increase in magnitudes of physical properties for needle penetration and decrease in softening point ring and ball due to the impact of rejuvenators. The rheological properties were similarly reduced in the bitumen extracted from the asphalt mix with rejuvenators compared to the oxidized bitumen. However, the rate of impact of rejuvenators was less on the sulfoxide group of the oxidized bitumen. Higher effect of rejuvenators used was detected on the carbonyl group. In addition, the RTFOT-aged bitumen showed higher indices of ageing (Ico and Iso) than did field-aged (RAP) bitumen.

Chapter VII

Conclusions and Recommendations

According to the results obtained, tests performed, materials used, equipment employed, literatures cited and laboratory conditions, the following can be concluded:

1) The use of a liquid oxidizing agent (hydrogen peroxide) to accelerate the ageing process of asphalt mixes resulted in a 10% increase in stiffness modulus at low temperatures or high-speed loadings. While, at high temperatures or low-speed loadings, there were marginal differences in stiffness compared to new asphalt mixes. The fatigue behavior of unaged and aged asphalt was calculated and compared according to the equations derived from fatigue test. Two points of initial elastic strain for heavy- and light-loadings (0.10‰ and 0.03‰ respectively) were selected to demonstrate the impact of ageing process. Compared to unaged mix, peroxide aged mix shows an increase in load cycles at heavy- and light-loading of 162% and 477% respectively.

2) The use of high temperature as an additional accelerated ageing method before or after ageing by peroxide affected the results concerning stiffness and fatigue but to a lower extent compared to peroxide ageing method only. This suggests that the use of peroxide alone is recommended to accelerate asphalt ageing. The peroxide concentration and soaking duration as well as pressure and subjection to the asphalt's maximum surface area represent important factors for achieving ideal test conditions.

3) The physical, chemical, and rheological properties of bitumen extracted from peroxide-aged mixes were comparable to long term-aged bitumen in the lab (PAV). This method of ageing can be used to simulate the ageing of pavement in service as well as to produce sufficient quantities of aged bitumen to evaluate bitumen properties.

4) Using ozone as an oxidizing gas resulted in a marginal increase in the stiffness modulus of asphalt of about 4% at low temperatures or high loading speeds. At high temperatures or over long loading times, there were no differences in stiffness between the reference and ozone-aged specimens. The fatigue resistance results showed no change compared with the new mixes, which was due to constraints in test conditions. To optimize the ozone test, the testing chamber needs to provide exposure to the maximum surface area of asphalt in order to oxidize the bitumen.

5) Although the test conditions were not ideal regarding ozone ageing. The properties of bitumen extracted from ozone-aged asphalt were in the range between bitumen short-term aged by RTFOT and long-term aged via PAV. Therefore, promising results can be obtained through this method of mimicking pavement ageing.

6) The method of accelerating asphalt ageing by storing asphalt for 4 h at 135 ºC and then for 288 h at 75 ºC showed results identical to those of peroxide-aged asphalt. These include the performance properties of asphalt (stiffness and fatigue) and properties of bitumen extracted from aged mixes. A temperature of 75 ºC was selected according to the recorded maximum temperature of pavement in the field.

7) The performance properties of the asphalt mixes with RAP for surface, full-depth and base course layers showed that it is possible to use 90% of RAP content in combination with rejuvenators. The properties of asphalt within an acceptable limit can be maintained for the specified layer. The determined test results of stiffness modulus, fatigue resistance, susceptibility to temperature variations, and rutting resistance are nearly comparable to the test results of new mixes. However, the rutting resistance of the full-depth layer was lower than that of the new mixes. The recommendation is to use these types of mixes for low-volume roads.

8) Rejuvenating agents 1, 2, and 3, which were used in the reuse process of RAP, obtained from the surface layer to produce the asphalt mix SMA 11 S. Dosage of 0.60%, 0.29%, and 0.37% by the mass of the total mix were selected of the rejuvenating agent 1, 2, and 3 respectively. The stiffness modulus decreases by 48%, 38%, and 42% at high temperatures. At low temperatures, a reduction of about 14%, 8% and 12% in the stiffness modulus respectively, were measured compared to the asphalt prepared with RAP only (S0). Resistance to fatigue cracking was enhanced in the SMA 11 S with RAP compared to the reference mix (S, New 30/45). This result evidenced by the shift in the slope of fatigue results at heavy- and light- loadings. For the reference mix, permanent deformation was 3.8% regardless of the bitumen type (30/45 and PmB 25/55-55 A) used. While, it was 3.3%, 4%, and 4.2% for the mixes S1, S2, and S3 respectively. Finally, the resistance to low-temperature behavior showed an increase in tensile strength of 0.7 MPa, 0.8 MPa, and 1.2 MPa for S1, S2, and S3 respectively. A decrease of fracture temperature was also measured compared to the reference mix (S, New 30/45). These indicate an increased resistance of the asphalt mix with RAP and rejuvenators to freezing temperatures.

9) The use of RAP at a content of 90% to produce a full-depth layer mix AC 16 T D in combination with rejuvenators is possible. The three rejuvenators 1, 2, and 3 at concentrations of 0.50%, 0.23%, and 0.30% of the total mix were selected respectively. Compared to the variant D0, the use of rejuvenators resulted in a decrease in stiffness modulus at low temperatures for the variants D1, D2, and D3 of about 12%, 8%, and 11% respectively. The decrease at high temperature is 32%, 40%, and 41% respectively. The fatigue resistance exhibited an enhancement in mixes with rejuvenating agent 1. While, the slope of the trend line was flatter for the mixes with rejuvenating agent 2 and 3 compared to the reference mix. The cumulative axial strain (permanent deformation) of the reference mix was 3.8%. For the mixes with rejuvenators D1, D2, and D3 the cumulative axial strain (permanent deformation) of 7.5%, 7.1%, and 7.2% were determined. The

cumulative axial strain increased significantly compared to the reference mix due to the aggregate variations in RAP. Other factors may affect the cumulative axial strain such as mixing and compacting temperatures, bitumen properties, volumetrics and filler content. These factors might not be contributed because reused mixes were prepared in comparable characteristics of the reference mix. There was an enhancement in the resistance to freezing stresses of asphalt mixes with all rejuvenating agents used in the study. The failure temperature of these mixes was around -35 ºC and of the reference mix was around -31 ºC.

10) The base-course layer mixes AC 22 T S with rejuvenators 1, 2, and 3 at concentrations of 0.4%, 0.18% and 0.25% of the total mix were produced and tested. The use of rejuvenators resulted in a reduction in stiffness modulus at low temperature of about 8% for the variant T1, and 10% for both of the variants T2 and T3 compared to the variant T0. The decrease in the stiffness modulus of the variants T1, T2, and T3 at a high temperature compared to the variant T0 was 27%, 41%, and 29% respectively. Fatigue resistances of reused variants were also decreased in response to the decrease in stiffness modulus.

11) The use of rejuvenators has noticeable impact on physical, chemical, and rheological properties of bitumen through the decrease in hardness of bitumen in RAP. This impact expressed by the increase in penetration and decrease in softening point of recovered bitumen from variants of RAP and rejuvenator. In addition, the decrease in complex modulus and increase in phase angle supports these findings. Additionaly, the results of chemical structure elements of bitumen (Ico and Iso) are inline with the physical and rheological results.

12) The use of mixes with RAP only (S0, D0, and T0) were less informative compared to the results collected from cores of old pavement regarding the performance characteristics. The decrease in stiffness modulus can be attributed to the high

viscousity of bitumen in RAP. The preparation method provides less bonding potential even with the use of high mixing temperature (130 °C), due to the hardened bitumen. Therefore, it is recommended to cut cores of samples from old pavements before milling to evaluate the performance properties and thus optimize the process of reusing RAP in asphalt.

Recommendations:

1) To optimize the accelerated ageing process with hydrogen peroxide, it is highly recommended to use the peroxide at a high concentration (40% to 60% or higher). Stainless-steel containers are recommended to avoid corrosion due to the oxidation process. It is also important to increase the surface area of asphalt granules subjected to the effects of peroxide. The use of a controlled pressure chamber is recommended to increase the efficiency of the oxidation process. However, safety should be considered in addition to the use of ventilation hood.

2) Already used in rubber testing, an ozone test chamber is recommended with modifications so that the asphalt granules are exposed to direct contact with the ozone flow in order to extremely oxidize the bitumen. This can be achieved by distributing asphalt granulates into different layers separated by perforated pans. Ozone concentration and exposure periods also represent important factors.

3) Use of a high RAP content (90%) in combination with suitable rejuvenator in the asphalt mix is recommended to reduce the need for new natural resources regarding aggregate and bitumen. In addition, the asphalt mixing temperature can also be reduced to mitigate the emission of fumes and CO_2. However, lab results need to be validated in-situ by constructing a test section to verify and address the weak points of the pavement with high RAP content.

Bibliography

1. AASHTO (2010) designation: T 315-10. *Standard method of test for determining the rheological properties of asphalt binder using a dynamic shear rheometer (DSR).*

2. Abutalib, N., Fini, H. F., Aflaki, S., and Abu-Lebdeh, T. M. (2015). *Investigating Effects of Application of Silica Fume to Reduce Asphalt Oxidative Ageing*. American Journal of Engineering and Applied Sciences. April.

3. Airey D. and Prathapa R. (2013). *Triaxial testing of asphalt*. Proceedings of the 18th International Conference on Soil Mechanics and Geotechnical Engineering, Paris.

4. Airey, G. D (1997). *Rheological characteristics of polymer modified and aged bitumens*. Ph.D. thesis submitted to the University of Nottingham.

5. Almeida, M.D., Gomes, J.P.C., and Antunes, M. L. (2010). *Mix design criteria for half warm recycling (HWMR)- case study*. Sustainable applications of construction and demolition recycled materials. May.

6. Bankowski, W. (2018). *Evaluation of Fatigue Life of Asphalt Concrete Mixtures with Reclaimed Asphalt Pavement*. Applied sciences, March.

7. Beale, J. M., Zhanping Y., Elham F., Boubacar Z., Chee Huei L., and Yoke K.Y. (2014). *Ageing Influence on Rheology Properties of Petroleum-Based Asphalt Modified with Biobinder*. American Society of Civil Engineers.

8. Behbahani, H., Nowbakht, S., Fazaeli, H., and Rahmani, J., (2009). *Effects of fiber type and content on the rutting performance of stone matrix asphalt.* Journal of applied sciences 9 (10): 1980-1984, ISSN 1812-5654, Asian Network for Scientific Information.

9. Behzadfar, E. (2014). *The Flow Properties of Bitumen In The Presence of CO_2*. Thesis submitted to University of British Columbia (Vancouver) for the degree of Ph.D. September.

10. Bressi, S., Alan C., Nicolas B., and André-Gilles D. (2015). *Impact of different ageing levels on binder rheology*. International Journal of Pavement Engineering, 09 February. At: **01:33**.

11. Button, J.W., Timothy B.A., Ronald C., Frank F., Gary L. F., Thomas P.H., Hicks, R.G., Huber, A.G., King, G.N., McDaniel, R.S., Newcomb, D.E., Nodes, J.E., Paul, H.R., Scherocman, J.A., Shuler, S., Takallou, H.B., Watson, D.E., Weigel, J.J. (2004). *New Simple Performance Tests for Asphalt Mixes*. Transportation research board E-circular, Number **E-C068**, September.

12. Byrne, D.A. (2005). *Recycling of asphalt pavements in new bituminous mixes*. Thesis submitted to Napier University, School of built environment, for the degree of Ph.D. October.

13. Campbell, P., and Wright, J. (1964). *Ozonation of Asphalt Flux*. I & EC Product Research and Development. Vol. **3** No. 3, September. pp 186-194.

14. Carlson IV, R.E. (2014). *Feasibility of using 100% recycled asphalt pavement mixtures for road construction*. Thesis submitted to the University of Iowa for the degree of Master of Science. December.

15. Ceylan, H., Sunghwan, K., and Kasthurirangan, G. (2007). *Hot Mix Asphalt Dynamic Modulus Prediction Models Using Neural Networks Approach*. Civil, Construction and Environmental Engineering Conference Presentations and Proceedings. Paper **29**.

16. Cheng, Y., Jinglin, T., Yubo, J., Qinglin, G., and Chao L. (2015). *Influence of Diatomite and Mineral Powder on Thermal Oxidative Ageing Properties of Asphalt*. Hindawi Publishing Corporation, Advances in Materials Science and Engineering, Article ID 947834, 10 pages.

17. Clyne, T.R., Xinjun, L., Mihai O. M., and Eugene L.S. (2003). *Dynamic and Resilient Modulus of Mn/DOT Asphalt Mixtures*. Minnesota Department of Transportation Office of Research Services. Final report.

18. Das, P.K., Romain, B., Niki, K., and Bjorrn, B. (2014). *On the oxidative ageing mechanism and its effect on asphalt mixtures morphology*. Materials and Structures. RILEM.

19. Dickinson, E. J., Nicholas, J. H., and Traube, S. B. (1958). *Physical factors affecting the absorption of oxygen by thin films of bituminous road binders*. J. app. Chem., **8**, October.

20. Dony, A., Layella, Z., Ivan D., Simon, P., Stephane, F.D., Delphine, S., Virginie, M., Jean, E.P., Thomas, G., Laurence, B., Nicolai, A., and Gueit, C. (2016). *MURE National project: FTIR spectroscopy study to assess ageing of asphalt mixtures*. E&E, 6th Eurasphalt & eurobitume congress, 1-3 June, Prague, Czech Republic.

21. Emmanuel O.E., and Dennis B.E. (2009). *Fatigue and rutting strain analysis of flexible pavements designed using CBR methods*. African Journal of Environmental Science and Technology Vol. 3 (**12**), pp. 412-421, December.

22. Erkens, S,. Porot, L., Glaser, R., and Glover, C. J., (2016). *Aging of bitumen and asphalt concrete comparing state of the practice and ongoing developments in the United*

States and Europe. In TRB 95th Annual meeting compendium of papers. (pp 1-12). [16-5770] Washington: Transportation Research Board (TRB).

23. Feng, Z.G., Hui-juan, B., Xin-jun, L., and Jian-ying, Y. (2015). *FTIR analysis of UV ageing on bitumen and its fractions. Materials and Structures*. RILEM.

24. FHWA-HIF-17-042. (2018). *Overview of Project Selection Guidelines for Cold In-place and Cold Central Plant Pavement Recycling. Office of Asset Management, Pavements, and Construction*. February.

25. Francken, L., Vanelstraete, A., and Verhasselt, A. (1997). *Long term ageing of pure and modified bitumen: Influence on the rheological properties and relation with the mechanical performance of asphalt mixtures*. pp. 1259-1278.

26. Gawel, I., Franciszek, C., and Jacek, K. (2016). *An environmental friendly anti-ageing additive to bitumen*. Construction and Building Materials **110**, 42–47.

27. Glover, C.J., Davidson, R.R., Chris, H.D., Yonghong, R., Pramitha, J., Knorr, D.B., and Sung H.J. (2002). *Development of A New Method for Assessing Asphalt Binder Durability with Field Validation*. Texas Transportation Institute, The Texas A&M University System. August.

28. Glover, I.C. (2007). *Wet and Dry Ageing of Polymer-Asphalt Blends: Chemistry and Performance.* Thesis submitted to Louisiana State University and Agricultural and Mechanical College for the degree of Ph.D. December.

29. Goetz, W.H., and Schaub, J. H. (1959). *Triaxial testing of bituminous mixtures*. Joint highway research project, Purdue University, Lafayette Indiana, March, No. **6**.

30. Golalipour, A. Jamshidi, E. Niazi, Y. Afsharikia, Z. and Khadem, M. (2012). *Effect of aggregate gradation on rutting of asphalt pavements.* Procedia – social and behavioral sciences 53 440-449.

31. Green, J. B., Yu, S.K.T., Pearson, C.D., and Reynolds, J.W. (1993). *Analysis of sulfur compound types in asphalt*. Energy & Fuels **7**(1), January.

32. Grossegger, D. (2015). *Investigation of aged, non-aged bitumen and their bitumen fractions*. Master thesis submitted to the Vienna University of Technology, Institute of materials chemistry.

33. Guo, X., Mingzhi, S., Wenting, D., and Shuang, C. (2016). *Performance Characteristics of Silane Silica Modified Asphalt*. Hindawi Publishing Corporation, Advances in Materials Science and Engineering, Volume 2016, Article ID 6731232, 7 pages.

34. Hagos, E. T. (2008). *The Effect of Ageing on Binder Properties of Porous Asphalt Concrete*. Thesis submitted to Section of Road and Railway Engineering, Faculty of Civil Engineering and Geosciences, Delft University of Technology for the degree of Ph.D. October.

35. Han, R. (2011). *Improvement to a Transport Model of Asphalt Binder Oxidation in Pavements: Pavement Temperature Modeling, Oxygen Diffusivity in Asphalt Binders and Mastics, and Pavement Air Void Characterization*. Ph.D. Submitted to the Office of Graduate Studies of Texas A&M University. May.

36. Harvey, J.T., John A.D., Bor-Wen, T., and Monismith, C.L. (1995). *Fatigue Performance of Asphalt Concrete Mixes and its Relationship to Asphalt Concrete Pavement Performance in California.* Asphalt Research Program: CAL/APT Program, Institute of Transportation Studies, University of California at Berkeley, Technical Task Report, July 94-Sept 95.

37. Heneash, U. (2013). *Effect of the repeated recycling on hot mix asphalt properties*. Thesis submitted to the University of Nottingham for the degree of Ph.D. May.

38. Hoang, L. N., and Le, T. H. (2018). *Effect of aggregate gradation on rutting of asphalt concrete by using a wheel tracking device in Vietnam.* Journal of the mechanica; behavior of materials. 20182007.

39. James, A.D., and Stewart, D. (1991). *The Use of Fatty Amine Derivatives to Slow Down the Age-Hardening Process in Bitumen*. Presented at the conference "The Chemistry of Bitumen" Rome, 671-684.

40. Jenkins, K.J., and Twagira, M.E. (2009). *Updating Bituminous Stabilized Materials Guidelines: Mix Design Report, Phase II Task 11: Durability: Ageing of bituminous binder*. Technical Memorandum, Sept.

41. Jung, S.H. (2006). *The Effects of Asphalt Binder Oxidation on Hot Mix Asphalt Concrete Mixture Rheology and Fatigue Performance*. Ph.D. thesis Submitted to the Office of Graduate Studies of Texas A&M University. August.

42. Kandhal, P. S., and Mallick, R. B. (1997). *Pavement recycling guidelines for state and local governments-participant's reference book*. National center for asphalt technology, Auburn University, December.

43. Katman, H.Y., Mohd, R.I., Mohamed, R.K., Mashaan, N.S., and Koting, S. (2015). *Evaluation of Permanent Deformation of Unmodified and Rubber-Reinforced SMA Asphalt Mixtures Using Dynamic Creep Test*. Hindawi Publishing Corporation, Advances in Materials Science and Engineering, Volume 2015, Article ID 247149, 11 pages.

44. Kim, O.K., Chris, A.B., James, E.W., Glenn, b. (1987). *Development of laboratory oxidative ageing procedures for asphalt cements and asphalt mixtures*. Transportation research board, annual meeting, January.

45. Kurtenbach, R., Jörg, K., Anita, N., and Peter, W. (2012). *Primary NO_2 emissions and their impact on air quality in traffic environments in Germany*. Environmental Sciences Europe 2012, 24:21.

46. Lamontagne, J., Dumas, P., Mouillet, V., and Kister, J. (2001). *Comparison by Fourier transform infrared (FTIR) spectroscopy of different ageing techniques: application to road bitumen*. Fuel **80**, 483–488.

47. Lefeuvre, Y., La Roche, C.D., and Piau, J.-M. (2005). *Asphalt material fatigue test under cyclic loading: the lengthening of samples as a way to characterize the material damage experiments and modelling*. Materials' and Structures, **38**, 115-119.

48. Lerfald, B.O. (2000). *Ageing and Degradation of Asphalt Pavements on Low Volume Roads*. Thesis submitted to the Faculty of Civil and Environmental Engineering,

    The Norwegian University of Science and Technology for the degree of Dr. Ing. February.

49. Likhterova, N.M., Lunin, V.V., V. N., Torkhovskii , Frantsuzov V.K., and Kalinicheva, O.N.(1999). *Effect of Ozonation And Strong Uv Radiation on The Rheological Properties of Atmospheric Resid And Liquid Asphalt*. Chemistry and Technology of Fuels and Oils, I1"ol. **35**, No. 5.

50. Lira, B., Ekbald, J., and Lundstroem, R. (2019). *Evaluation of asphalt rutting based on mixture aggregate gradation, road materials and pavement design.* DOI: 10.1080/14680629.2019.1683061.

51. Liu, X., Shaopeng, W., Ling, P., Yue, X., and Pan, P. (2014). *Fatigue Properties of Layered Double Hydroxides Modified Asphalt and Its Mixture*. Hindawi Publishing Corporation, Advances in Materials Science and Engineering, Volume 2014, Article ID 868404, 6 pages.

52. Lopes, M.D., Dan, Z., Emmanuel, C., Malal, K., Thomas, G., et al. (2012). *Characterization of ageing processes on the asphalt mixture surface*. 2nd International Symposium on, Asphalt Pavements et Environnement, Transportation Research Board, of The National Academies, Oct., France. 10p, ill., bibliogr. <hal-00849450>.

53. Lu, X., and Ulf, I. (2002). *Effect of ageing on bitumen chemistry and rheology*. Construction and building materials 16, 15-22.

54. Lu, X., Talon, Y., and Redelius, P., (2008). *Aging of bituminous binders- laboratory tests and field data.* Conference E&E At: Copenhagen, doi: 10.13140/2.1.4101.2487.

55. Lucena, M.C.C., Soares, S.A., Jorge, B.S. (2004). *Characterization and Thermal Behavior of Polymer-Modified Asphalt*. Materials research, Vol. **7**, No. 4, 529-534.

56. Mackiewicz, P., (2018). *Fatigue cracking in road pavement.* IOP conf. series: Materials Science and Engineering 356, 012014 doi: 10.1088/1757-899X/356/1/012014.

57. Malekzehtab, H. (2016). *Characterization of asphalt mixes with recycled asphalt pavement.* Thesis submitted to Curtin University for the degree of Ph.D. October.

58. Mashaan, N.S., and Mohamed, R.K. (2013). *Evaluation of Permanent Deformation of CRM-Reinforced SMA and Its Correlation with Dynamic Stiffness and Dynamic Creep.* Hindawi Publishing Corporation, The Scientific World Journal, Volume 2013, Article ID 981637, 7 pages.

59. Maxwell, A. S., Broughton, W. R., Dean, G., and Sims, G.D. (2005). *Review of accelerated ageing methods and lifetime prediction techniques for polymeric materials*. NPL Report DEPC MPR 016.

60. McDaniel, R. S., Soleymani, H., Michael, A., Turner, P., and Robert, P. (2000). *Recommended use of reclaimed asphalt pavement in the superpave mix design method*. National cooperative highway research program, transportation research board, national research council. October.

61. Melkonyan, A., and Patrick, W. (2013). *Ozone and its projection in regard to climate change.* Atmospheric Environment 67, 287-295.

62. Mohajeri, M. (2015). *Hot mix asphalt recycling, practices and principles*. Thesis submitted to Section of road and railway engineering, Faculty of civil engineering and geosciences, Delft University of technology. 28 January.

63. Pais, J. (2009). *Four-point bending, proceedings of the second workshop*. University of Minho, Portugal, September.

64. Paliukait, M., Audrius V., and Adam Z. (2014). *Evaluation of bitumen fractional composition depending on the crude oil type and production technology*. The 9th

International Conference "Environmental Engineering" 22–23 May, Vilnius, Lithuania.

65. Petersen, J.C. (2009). *A Review of the Fundamentals of Asphalt Oxidation Chemical, Physicochemical, Physical Property, and Durability Relationships*. Transportation Research Circular E-C140, October.

66. Poulikakos, L.D., Bernhard, H., Porot, L., Xiaohu, L., Fischer, H. and Kringos, N. (2016). *Impact of temperature on short- and long-term ageing of asphalt binders*. RILEM Technical Letters (2016) 1: 6 – 9.

67. Punith, V.S., Feipeng, X., and David W. (2013). *Performance characterization of half warm mix asphalt using foaming technology*. American society of civil engineers.

68. Raab, C., Ingrid C., Manfred N. P. (2017). *Ageing and performance of warm mix asphalt pavements*. Periodical offices of Changan University. July.

69. Rad, F.Y. (2018). *Evaluation of the Effect of Oxidative Ageing on Asphalt Mixtures for Pavement Performance Prediction*. Thesis submitted to North Carolina State University, March.

70. Reena, G.S., and Kaur, V. (2012). Characterization of Bitumen and Modified Bitumen (e-PMB) using FT-IR, Thermal and SEM techniques. Research Journal of Chemical Sciences, Vol. 2(8), 31-36, August.

71. Ryer, A. (1998*). Light measurement handbook*.

72. Safiuddin, M., Tighe, S. L., and Uzarowski, L. (2014). *Evaluation of stiffness to predict rutting resistance of hot-mix asphalt: a Canadian case study*. The Baltic jornal of road and bridge engineering. ISSN 1822-427X print / ISSN 1822-4288 online Volume 9(4): 283-296

73. Schvallinger, M. (2011). *Analyzing trends of asphalt recycling in France*. Master thesis in environmental strategies research SoM EX 2011-41, KTH Royal institute of technology, department of urban planning and environment, division of environmental strategies research – fms.

74. Seferoglu, A.G., Mehmet, T.S., and Muhammet, V. A. (2018). *Investigation of the Effect of Recycled Asphalt Pavement Material on Permeability and Bearing Capacity in the Base Layer*. Hindawi, Advances in Civil Engineering, Volume 2018, Article ID 2860213, 6 pages.

75. Sharew, Y.J. (2010). *Development of A Laboratory Ageing Method for Bitumen in Porous Asphalt*. A Thesis Submitted in partial fulfillment of the requirements for

the degree of Master of Science in Civil Engineering from the Road and Railways Engineering Department, Delft University of Technology, Delft, The Netherlands, August.

76. *Shell bitumen handbook Fifth edition*, 2003.

77. Sheng, Y., Li, H., Guo, P., Zhao, G., Chen, H., and Xiong, R. (2017). *Effect of fibers on mixture design of stone matrix asphalt.* MDPI, Appl. Sci., 7, 297; doi:10.3390/app7030297.

78. Steiner, D., Bernhard, H., Markus, H., Handle, F., Hinrich, G., Fussl, J. Eberhardsteinera, L., and Ronald, B. (2015). *Towards an optimised lab procedure for long-term oxidative ageing of asphalt mix specimen*. International Journal of Pavement Engineering.

79. Subramanian, M., and Hanson, F.V. (1996). *Compositional Analysis of Bitumen and Bitumen-Derived Products.* Journal of Chromatographic Science, Vol. 34, January.

80. Tan Y.Q., Wang, J.N., Feng, Z.L., and Zhou, X.Y. (2007). *Influence and Mechanism of Ultraviolet Ageing on Bitumen Performance*. Proceedings of the 26th Southern African Transport Conference (SATC 2007) 9 - 12 July.

81. Upreti, S.R., and Anil K.M. (2000). *Experimental Measurement of Gas Diffusivity in Bitumen: Results for Carbon Dioxide*. Ind. Eng. Chem. Res., **39**, 1080-1087.

82. Van Den Bergh, W. (2011). *The effect of ageing on the fatigue and healing properties of bituminous mortars*. Ph.D. thesis submitted to Delft University of Technology.

83. Verhasselt, A. (2005). *Report of the limited Round Robin Trial with the RCAT (Rotating Cylinder Ageing Test) method*. Belgian Road Research Centre, Brussels.

84. Willis, X.P. (2016). *Analysis of the use of Reclaimed Asphalt Pavement (RAP) in Europe*. Master of Science in Civil Engineering Transport Infrastructure submitted to Politecnico Di Milano.

85. Wright, S. (2010). *Asphalt Surface Ageing Prediction (ASAP) System*. Western Research Institute, September.

86. Wu, J. (2009). *The Influence of Mineral Aggregates and Binder Volumetrics on Bitumen Ageing*. Thesis submitted to the University of Nottingham for the degree of Doctor of Philosophy, May.

87. Wu, S., Ling, P., Gang, L., and Jiqing, Z. (2010). *Laboratory Study on Ultraviolet Radiation Ageing of Bitumen.* J. Mater. Civ. Eng. **22**:767-772.

88. Yousif, R.A., Ratnasamy, M., Salihudin, H., Fauzan, J., and Eltaher, A. (2015). *An overview of quantification of fatigue resistance of asphalt mixture using pre-aged binder*. WALIA journal **31**(S1): 125-132.

89. Yu, X., Ying, W., Yilin, L., and Long, Y. (2013). *The Effects of Salt on Rheological Properties of Asphalt after Long-Term Ageing*. Hindawi Publishing Corporation the Scientific World Journal, Volume 2013, Article ID 921090, 10 pages.

90. Zakaria, N.M., Nur, I.M., Yusoff, S.H., Khairul Anuar, M.N., and El-Shafie, A. (2014). *Measurements of the Stiffness and Thickness of the Pavement Asphalt Layer Using the Enhanced Resonance Search Method*. Hindawi Publishing Corporation, The Scientific World Journal, Volume 2014, Article ID 594797, 8 pages.

91. Zaumanis, M., Mallick, R. B., and Frank, R. (2015). *Evaluation of different recycling agents for restoring aged asphalt binder and performance of 100 % recycled asphalt*. Materials and structures, 48:2475-2488.

92. Zaumanis, M., Mallick, R.B., and Robert, F. (2016). *100% hot mix asphalt recycling: challenges and benefits*. Transportation Research Procedia **14,** 3493 – 3502.

93. Zhang, F., and Changbin, H. (2015). *The research for high-elastic modified asphalt*. J. of applied polymer science. February.

94. Zhang, H., Jianying, Y., Huacai, W., and Lihui, X. (2011). *Investigation of microstructures and ultraviolet ageing properties of organo-montmorillonite/SBS modified bitumen.* Materials chemistry and physics 129, 769-776.

95. Zhang, H.L., Wang, H.C., and Yu, J.Y. (2011a). *Effect of ageing on morphology of organo-montmorillonite modified bitumen by atomic force microscopy*. Journal of Microscopy, Vol. **242**, Pt 1, pp. 37–45.

Appendix A

Volumetric analysis of test specimens

Preliminary tests were conducted to determine the volumetric properties for every mix type used in this study, which was achieved by preparing Marshall specimens to determine bitumen content and air voids which meets the specification limits of every new mix. These limits were then used to produce slabs which must meet the pre-determined properties by calculating the compaction ratio of every slab compared with new mix. Slabs must meet the required compaction ratio ± 1% without exceeding air voids limits, and the difference between the maximum and minimum bulk-specific gravity must not exceed 0.03 g/cm^3. The slabs with compaction ratios outside of this range or exceeding air voids limits were excluded from the testing plan and regarded as failed slabs with the aid of a pre-programmed Excel sheet as well as specification limits and allowances. The cores or prisms were then produced and volumetric analysis was also determined, and specimens were grouped and sorted according to their bulk-specific gravity in order to test the specimens at similar volumetric properties. However, the compaction ratio differs from the original slab due to the coring, cutting, and grinding processes. The number of specimens employed in the testing program are summarized in tables A-1 and A-2 for the reusing and ageing phases respectively. Because the stiffness test is non-destructive, the same specimens were utilized in the fatigue test, which is destructive and therefore these specimens were excluded from the total number of samples.

Table A-1: Number of samples used in the testing plan of reusing phase.

Test	Mix type	New	Agent-1	Agent-2	Agent-3
Stiffness	SMA 11 S-30/45	12	12	12	12
	SMA 11 S-PMB	12	-	-	-
	AC 16 T D-50/70	12	12	12	12
	AC 22 T S-30/45	12	12	12	12
	AC 22 T S-50/70	12	-	-	-
Fatigue	SMA 11 S-30/45	9	9	9	9
	SMA 11 S-PMB	9	-	-	-
	AC 16 T D-50/70	9	9	9	9
	AC 22 T S-30/45	9	9	9	9
	AC 22 T S-50/70	9	-	-	-
Rutting	SMA 11 S-30/45	5	5	5	5
	SMA 11 S-PMB	5	-	-	-
	AC 16 T D-50/70	5	5	5	5
	AC 22 T S-30/45	5	5	5	5
	AC 22 T S-50/70	5	-	-	-
Low Temp.	SMA 11 S-30/45	15	15	15	15
	SMA 11 S-PMB	15	-	-	-
	AC 16 T D-50/70	15	15	15	15
	AC 22 T S-30/45	15	15	15	15
	AC 22 T S-50/70	15	-	-	-
	Total	160	96	96	96

Table A-2: Number of samples used in the ageing phase for AC 16 B S mix.

Test type	New	H2O2	O3	STA	STB	ST	LT
Stiffness test	12	12	2	12	12	12	12
Fatigue test	9	9	2	9	9	9	9
Total	12	12	2	12	12	12	12

Marshall specimens were prepared at different bitumen contents the bitumen content with air voids within limits were chosen. However, due to the significant number of samples, only specimen's optimum bitumen content is shown below in Tables A-3 to A-6 for SMA 11 S, AC 16 B S, AC 16 T D, and AC 22 T S mixes respectively.

A-3: Results of Marshall Specimens for *SMA 11 S* mix at optimum bitumen content.

Mischgutart/-sorte:	**SMA 11 S 30/45 @ 7.2%**			
Probenbezeichnung:		1	2	3
Mittelwert Probekörperhöhe	[mm]	62.6	61.5	62.3
Raumdichte rb (Einzelwerte)	[g/cm³]	2.445	2.442	2.442
Mittelwert Raumdichte rb, c	[g/cm³]	2.443		
Hohlraumgehalt V (Einzelwerte)	[Vol.-%]	2.7	2.8	2.8
Hohlraumgehalt V (Mittelwert)	[Vol.-%]	2.7		

A-4: Results of Marshall Specimens for *AC 16 B S* mix at optimum bitumen content.

Mischgutart/-sorte:	**AC 16 B S @ 5%**			
Probenbezeichnung:		1	2	3
Mittelwert Probekörperhöhe	[mm]	63.8	64.4	64.3
Raumdichte ρb (Einzelwerte)	[g/cm³]	2.435	2.438	2.440
Mittelwert Raumdichte ρb, c	[g/cm³]	2.438		
Hohlraumgehalt V (Einzelwerte)	[Vol.-%]	5.8	5.7	5.6
Hohlraumgehalt V (Mittelwert)	[Vol.-%]	5.7		

A-5: Results of Marshall Specimens for *AC 16 T D* mix at optimum bitumen content.

Mischgutart/-sorte:	**AC 16 T D @ 5.7%**			
Probenbezeichnung:		**1**	**2**	**3**
Mittelwert Probekörperhöhe	**[mm]**	**62.0**	**61.7**	**61.7**
Raumdichte ρb (Einzelwerte)	**[g/cm³]**	**2.481**	**2.493**	**2.499**
Mittelwert Raumdichte ρb, c	**[g/cm³]**	**2.491**		
Hohlraumgehalt V (Einzelwerte)	**[Vol.-%]**	**2.1**	**1.6**	**1.4**
Hohlraumgehalt V (Mittelwert)	**[Vol.-%]**	**1.7**		

A-6: Results of Marshall Specimens for *AC 22 T S* mix at optimum bitumen content.

Mischgutart/-sorte:	**AC 22 T S @ 4.5%**			
Probenbezeichnung:		**1**	**2**	**3**
Mittelwert Probekörperhöhe	**[mm]**	**61.8**	**61.4**	**61.9**
Raumdichte ρb (Einzelwerte)	**[g/cm³]**	**2.473**	**2.465**	**2.448**
Mittelwert Raumdichte ρb, c	**[g/cm³]**	**2.462**		
Hohlraumgehalt V (Einzelwerte)	**[Vol.-%]**	**5.7**	**6.0**	**6.7**
Hohlraumgehalt V (Mittelwert)	**[Vol.-%]**	**6.1**		

Appendix B

Stiffness modulus of asphalt mixtures

Stiffness modulus of asphalt mixes were performed at four temperatures (+20 °C, +10 °C, 0 °C, and -10 °C) and three frequencies (0,1,1.0 and 10.0 Hz), then Sigmoidal function was used to construct the master curve of results according to following equation:

$$y = y_0 + \frac{w}{1 + e^{-\left(\frac{x - x_0}{z}\right)}}$$

Where:

y: Stiffness modulus

y_0, *w*, *x*, x_0, and, *z*: regression parameters.

Regression parameters were determined by using solver package of Excel software so that minimum error is obtained.

Table B-1: Stiffness modulus of *AC 16 BS new mix*.

T	f	lEI_1	lEI_2	lEI_3	lEI		
[°C]	[Hz]	[MPa]	[MPa]	[MPa]	Mittelwert [MPa]	Standartabw. [MPa]	Variationskoeffizient
20	0.1	3,969	3,854	3,980	3,934	70	1.8
20	1.0	6,864	6,677	6,816	6,786	97	1.4
20	10.0	11,775	11,636	11,820	11,744	96	0.8
10	0.1	8,024	7,485	7,934	7,814	289	3.7
10	1.0	12,308	11,640	12,183	12,044	355	2.9
10	10.0	18,282	17,734	18,528	18,181	406	2.2
0	0.1	13,847	14,022	14,220	14,030	187	1.3
0	1.0	18,117	18,353	18,619	18,363	251	1.4
0	10.0	23,756	23,999	24,265	24,009	255	1.1
-10	0.1	19,690	21,423	20,002	20,372	924	4.5
-10	1.0	23,445	25,064	23,650	24,053	882	3.7
-10	10.0	27,965	29,833	28,295	28,698	997	3.5

Table B-2: Stiffness modulus of *AC 16 BS aged mix*.

T	f	lEI1	lEI2	lEI3	lEI		
[°C]	[Hz]	[MPa]	[MPa]	[MPa]	Mittelwert [MPa]	Standartabw. [MPa]	Variationskoeffizient
20	0.1	4,681	5,215	5,489	5,128	410,913	8.0
20	1.0	8,574	8,512	8,725	8,604	109,555	1.3
20	10.0	14,454	14,277	14,266	14,332	105,510	0.7
10	0.1	9,111	9,141	9,810	9,354	395,192	4.2
10	1.0	13,322	13,562	14,166	13,683	434,885	3.2
10	10.0	19,440	19,783	20,287	19,837	426,043	2.1
0	0.1	15,942	15,650	16,821	16,138	609,528	3.8
0	1.0	19,955	19,802	21,022	20,260	664,617	3.3
0	10.0	25,746	25,355	26,888	25,996	796,569	3.1
-10	0.1	23,153	22,584	23,307	23,015	380,834	1.7
-10	1.0	26,459	25,913	26,886	26,419	487,711	1.8
-10	10.0	30,126	30,512	31,888	30,842	926,194	3.0

Table B-3: Stiffness modulus values of *AC 16 BS reused RAP mix* using rejuvenator 1.

T	f	lEI1	lEI2	lEI3	lEI		
[°C]	[Hz]	[MPa]	[MPa]	[MPa]	Mittelwert [MPa]	Standartabw. [MPa]	Variationskoeffizient
20	0.1	2,972	2,405	2,604	2,660	288	10.8
20	1.0	4,849	4,617	4,520	4,662	169	3.6
20	10.0	8,476	7,138	8,113	7,909	692	8.7
10	0.1	4,817	3,866	4,551	4,411	491	11.1
10	1.0	7,792	6,403	7,460	7,218	725	10.0
10	10.0	12,647	10,241	12,088	11,658	1,259	10.8
0	0.1	10,470	8,530	10,122	9,707	1,034	10.7
0	1.0	13,931	11,542	13,484	12,986	1,270	9.8
0	10.0	18,811	15,866	18,259	17,645	1,565	8.9
-10	0.1	16,301	13,661	16,174	15,379	1,489	9.7
-10	1.0	19,501	16,446	19,160	18,369	1,674	9.1
-10	10.0	23,975	20,345	23,583	22,634	1,992	8.8

Table B-4: Stiffness modulus values of *AC 16 BS reused RAP mix* using rejuvenator 2.

T	f	lEI1	lEI2	lEI3	lEI		
[°C]	[Hz]	[MPa]	[MPa]	[MPa]	Mittelwert [MPa]	Standartabw. [MPa]	Variationskoeffizient
20	0.1	1,741	1,847	1,530	1,706	161	9.5
20	1.0	2,782	3,764	2,862	3,136	545	17.4
20	10.0	5,603	6,629	5,556	5,929	606	10.2
10	0.1	2,880	3,434	2,930	3,081	306	9.9
10	1.0	4,660	5,975	4,973	5,202	687	13.2
10	10.0	8,002	10,225	9,221	9,149	1,113	12.2
0	0.1	6,311	7,127	6,460	6,632	435	6.6
0	1.0	9,344	10,416	9,511	9,757	577	5.9
0	10.0	13,562	15,063	13,799	14,141	807	5.7
-10	0.1	11,593	13,412	12,030	12,345	950	7.7
-10	1.0	14,604	16,659	15,113	15,458	1,070	6.9
-10	10.0	18,736	20,847	19,200	19,594	1,109	5.7

Table B-5: Stiffness modulus values of *AC 16 B S reused RAP mix* using rejuvenator 3.

T	f	lEI1	lEI2	lEI3	lEI		
[°C]	[Hz]	[MPa]	[MPa]	[MPa]	Mittelwert [MPa]	Standartabw. [MPa]	Variationskoeffizient
20	0.1	2,317	1,875	2,247	2,146	238	11.1
20	1.0	3,763	3,412	4,897	4,024	776	19.3
20	10.0	7,138	6,475	7,597	7,070	564	8.0
10	0.1	3,627	3,553	3,869	3,683	165	4.5
10	1.0	6,342	5,569	6,486	6,132	493	8.0
10	10.0	10,749	9,595	11,203	10,515	829	7.9
0	0.1	7,566	7,071	7,946	7,527	439	5.8
0	1.0	11,130	10,397	11,528	11,018	574	5.2
0	10.0	16,028	15,002	16,462	15,830	750	4.7
-10	0.1	13,710	12,962	13,952	13,541	516	3.8
-10	1.0	17,158	16,552	17,290	17,000	394	2.3
-10	10.0	21,441	21,233	21,832	21,502	304	1.4

Table B-6: Regression parameters used in the *AC 16 BS* mixes

Reg. Para	New mix	Aged mix	Asphalt mix with rejuvenator 1	Asphalt mix with rejuvenator 2	Asphalt mix with rejuvenator 2
y0	-5,190.05	-44,144.98	-769.48	-631.09	-847.01
w	42,243.96	112,635.28	30,871.52	29,800.74	34,473.63
x0	2.08	0.75	3.09	3.81	3.96
z	2.32	6.42	1.93	1.93	2.11
Ea/R	25,000	25,000	25,000	25,000	25,000

Table B-7: Stiffness modulus master curve (T_0 = 20 °C) for *AC 16 BS new mix*.

			X	Y			Prozent Fehler-quadrat [%]
f	T	α T	log(α T*f)	Steifigkeitsmodul	Regression	Schätzung	
[Hz]	[K]	[-]	[Hz]	[MPa]	R	$(Y-R)^2$	
0.1	293.15	1.00	-1.000	5,128	4.550	334.353	5.79
1.0	293.15	1.00	0.000	8,604	8.893	83.941	1.45
10.0	293.15	1.00	1.000	14,332	13.276	1.115.455	19.32
0.1	283.15	20.32	0.308	9,354	10.242	787.933	13.65
1.0	283.15	20.32	1.308	13,683	14.626	888.600	15.39
10.0	283.15	20.32	2.308	19,837	18.981	732.627	12.69
0.1	273.15	515.03	1.712	16,138	16.391	64.164	1.11
1.0	273.15	515.03	2.712	20,260	20.719	210.994	3.65
10.0	273.15	515.03	3.712	25,996	24.946	1.102.943	19.10
0.1	263.15	16,685.19	3.222	23,015	22.893	14.914	0.26
1.0	263.15	16,685.19	4.222	26,419	27.050	397.997	6.89
10.0	263.15	16,685.19	5.222	30,842	31.041	39.419	0.68
					FQS:	5.773.345	100.00

Table B-8: Master curve (T_0 = 20 °C) *AC 16 BS reused RAP mix* using rejuvenator 1.

			X	Y			Prozent
f	T	α T	log(α T*f)	Steifigkeitsmodul	Regression	Schätzung	Fehler-
[Hz]	[K]	[-]	[Hz]	[MPa]	R	(Y-R)²	quadrat
							[%]
0.1	293.15	1.00	-1.000	2,660	2.546	13.177	0.45
1.0	293.15	1.00	0.000	4,662	4.419	59.024	2.00
10.0	293.15	1.00	1.000	7,909	7.051	736.337	24.91
0.1	283.15	20.32	0.308	4,411	5.145	538.657	18.23
1.0	283.15	20.32	1.308	7,218	8.019	641.748	21.71
10.0	283.15	20.32	2.308	11,659	11.598	3.667	0.12
0.1	273.15	515.03	1.712	9,707	9.392	99.243	3.36
1.0	273.15	515.03	2.712	12,986	13.177	36.589	1.24
10.0	273.15	515.03	3.712	17,645	17.151	243.960	8.25
0.1	263.15	16,685.19	3.222	15,379	15.215	26.941	0.91
1.0	263.15	16,685.19	4.222	18,369	19.088	517.493	17.51
10.0	263.15	16,685.19	5.222	22,634	22.438	38.720	1.31
					FQS:	2.955.561	100.00

Table B-9: Master curve (T_0 = 20 °C) *AC 16 BS reused RAP mix* using rejuvenator 2.

			X	Y			Prozent
f	T	α T	log(α T*f)	Steifigkeitsmodul	Regression	Schätzung	Fehler-
[Hz]	[K]	[-]	[Hz]	[MPa]	R	(Y-R)²	quadrat
							[%]
0.1	293.15	1.00	-1.000	1,706	1,653	2,817	0.13
1.0	293.15	1.00	0.000	3,136	3,013	15,180	0.72
10.0	293.15	1.00	1.000	5,929	5,016	833,916	39.32
0.1	283.15	20.32	0.308	3,081	3,554	223,790	10.55
1.0	283.15	20.32	1.308	5,203	5,783	336,214	15.85
10.0	283.15	20.32	2.308	9,149	8,762	150,187	7.08
0.1	273.15	515.03	1.712	6,633	6,897	69,994	3.30
1.0	273.15	515.03	2.712	9,757	10,156	158,808	7.49
10.0	273.15	515.03	3.712	14,141	13,904	56,471	2.66
0.1	263.15	16,685.19	3.222	12,345	12,032	97,777	4.61
1.0	263.15	16,685.19	4.222	15,459	15,867	166,572	7.85
10.0	263.15	16,685.19	5.222	19,594	19,499	9,172	0.43
					FQS:	2.,20,903	100.00

Table B-10 Master curve (T_0 = 20 °C) *AC 16 BS reused RAP mix* using rejuvenator 3.

			X	Y			Prozent Fehler-quadrat [%]
f	T	α T	log(α T*f)	Steifigkeitsmodul	Regression	Schätzung	
[Hz]	[K]	[-]	[Hz]	[MPa]	R	$(Y-R)^2$	
0.1	293.15	1.00	-1.000	2,146	2,145	2,32	0.00
1.0	293.15	1.00	0.000	4,024	3,722	91,485	2.75
10.0	293.15	1.00	1.000	7,070	5,950	1,254,821	37.78
0.1	283.15	20.32	0.308	3,683	4,333	422,208	12.71
1.0	283.15	20.32	1.308	6,132	6,783	423,518	12.75
10.0	283.15	20.32	2.308	10,516	9,965	303,466	9.14
0.1	273.15	515.03	1.712	7,528	7,982	206,747	6.22
1.0	273.15	515.03	2.712	11,018	11,435	173,857	5.23
10.0	273.15	515.03	3.712	15,831	15,384	199,592	6.01
0.1	263.15	16,685.19	3.222	13,541	13,410	17,151	0.52
1.0	263.15	16,685.19	4.222	17,000	17,470	220,753	6.65
10.0	263.15	16,685.19	5.222	21,502	21,412	8,010	0.24
FQS:						3,321,616	100.00

Table B-11: Stiffness modulus values of *SMA 11 S new mix* using 30/45 bitumen grade.

T	f	lEI1	lEI2	lEI3	lEI		
[°C]	[Hz]	[MPa]	[MPa]	[MPa]	Mittelwert [MPa]	Standartabw. [MPa]	Variationskoeffizient
20	0.1	3,122	2,388	2,343	2,617	437	16.7
20	1.0	4,708	4,360	4,375	4,481	197	4.4
20	10.0	9,482	8,412	8,352	8,748	636	7.3
10	0.1	5,949	5,321	5,336	5,535	358	6.5
10	1.0	9,511	8,816	8,841	9,056	394	4.4
10	10.0	14,961	14,241	14,332	14,511	392	2.7
0	0.1	11,800	11,149	11,721	11,556	355	3.1
0	1.0	15,588	15,246	15,643	15,492	215	1.4
0	10.0	21,079	20,516	21,187	20,927	360	1.7
-10	0.1	17,428	17,449	19,130	18,002	977	5.4
-10	1.0	20,661	21,064	22,621	21,448	1,035	4.8
-10	10.0	25,340	25,788	27,091	26,073	910	3.5

Table B-12: Stiffness modulus values of *SMA 11 S new mix* using PMB grade.

T	f	lEI1	lEI2	lEI3	lEI		
[°C]	[Hz]	[MPa]	[MPa]	[MPa]	Mittelwert [MPa]	Standartabw. [MPa]	Variationskoeffizient
20	0.1	1,364	1,562	1,516	1,480	104	7.0
20	1.0	2,610	3,029	2,838	2,825	210	7.4
20	10.0	5,379	5,889	5,660	5,642	255	4.5
10	0.1	3,128	3,384	3,322	3,278	134	4.1
10	1.0	5,724	6,206	6,017	5,982	243	4.1
10	10.0	10,203	11,031	10,605	10,613	414	3.9
0	0.1	7,997	8,017	7,775	7,929	134	1.7
0	1.0	11,878	12,198	11,728	11,934	240	2.0
0	10.0	17,347	18,028	17,261	17,545	420	2.4
-10	0.1	15,047	15,798	15,634	15,493	395	2.5
-10	1.0	18,936	19,523	19,713	19,390	405	2.1
-10	10.0	23,723	24,396	24,472	24,197	412	1.7

Table B-13: Stiffness modulus values of *SMA 11 S reused RAP mix* using rejuvenator 1.

T	f	lEI1	lEI2	lEI3	lEI		
[°C]	[Hz]	[MPa]	[MPa]	[MPa]	Mittelwert [MPa]	Standartabw.	Variationskoeffizient
20	0.1		1,988	1,858	1,951	82	4.2
20	1.0	3,409	3,414	3,219	3,347	111	3.3
20	10.0	6,373	6,388	6,059	6,273	186	3.0
10	0.1	3,733	3,992	3,782	3,835	138	3.6
10	1.0	6,231	6,707	5,967	6,301	375	6.0
10	10.0	11,184	10,945	10,267	10,798	476	4.4
0	0.1	7,083	7,705	6,897	7,228	423	5.9
0	1.0	10,545	11,425	10,357	10,775	570	5.3
0	10.0	15,828	16,872	15,516	16,072	710	4.4
-10	0.1	14,209	13,238	12,263	13,236	973	7.4
-10	1.0	18,039	17,293	16,014	17,115	1,024	6.0
-10	10.0	23,212	22,814	21,229	22,418	1,049	4.7

Table B-14: Stiffness modulus values of *SMA 11 S reused RAP mix* using rejuvenator 2.

T	f	lEI1	lEI2	lEI3	lEI		
[°C]	[Hz]	[MPa]	[MPa]	[MPa]	Mittelwert [MPa]	Standartabw. [MPa]	Variationskoeffizient
20	0.1	2,467	2,356	2,188	2,337	140	6.0
20	1.0	4,284	4,002	3,795	4,027	245	6.1
20	10.0	7,574	7,425	6,988	7,329	305	4.2
10	0.1	4,704	4,902	4,504	4,703	199	4.2
10	1.0	7,847	7,988	7,458	7,764	275	3.5
10	10.0	12,727	12,938	12,099	12,588	436	3.5
0	0.1	8,870	9,703	9,071	9,214	435	4.7
0	1.0	12,637	13,761	12,681	13,026	637	4.9
0	10.0	17,852	18,831	17,875	18,186	559	3.1
-10	0.1	15,815	15,904	14,912	15,543	549	3.5
-10	1.0	19,482	19,966	18,660	19,369	660	3.4
-10	10.0	24,495	24,139	23,352	23,995	585	2.4

Table B-15: Stiffness modulus values of *SMA 11 S reused RAP mix* using rejuvenator 3.

T	f	lEI1	lEI2	lEI3	lEI		
[°C]	[Hz]	[MPa]	[MPa]	[MPa]	Mittelwert [MPa]	Standartabw. [MPa]	Variationskoeffizient
20	0.1	2,122	2,295	2,289	2,235	98	4.4
20	1.0	3,738	3,965	3,892	3,865	116	3.0
20	10.0	6,888	7,240	7,143	7,090	182	2.6
10	0.1	4,555	4,626	4,744	4,641	95	2.1
10	1.0	7,467	7,826	7,660	7,651	180	2.3
10	10.0	12,093	12,214	12,343	12,216	125	1.0
0	0.1	9,060	9,283	9,168	9,170	112	1.2
0	1.0	12,639	12,814	12,830	12,761	106	0.8
0	10.0	17,701	17,850	17,969	17,840	134	0.8
-10	0.1	14,740	14,579	15,020	14,779	223	1.5
-10	1.0	18,168	18,269	18,580	18,339	215	1.2
-10	10.0	22,662	23,019	23,119	22,933	240	1.0

Table B-16: Regression parameters of Master Curve for *SMA 11 S* mixes

Reg. Para	New 30/45	New PMB	Reused mix, no.1	Reused mix, no.2	Reused mix, no.3
y_0	-2,312.59	-459.90	-1,833.88	-1,890.98	-2,374.78
w	35,070.42	31,410.17	43,888.11	36,488.45	35,359.43
x_0	2.58	3.28	4.75	3.39	3.27
z	1.90	1.53	2.39	2.10	2.18
E_a/R	25,000	25,000	25,000	25,000	25,000

Table B-17: Master curve (T_0 = 20 °C) for *SMA 11 S new mix* (30/45 bitumen grade).

			X	Y			Prozent Fehler-quadrat [%]
f	T	α_T	log(α_T*f)	Steifigkeitsmodul	Regression	Schätzung	
[Hz]	[K]	[-]	[Hz]	[MPa]	R	$(Y-R)^2$	
0.1	293.15	1.00	-1.000	2,618	2,307	96,366	3.72
1.0	293.15	1.00	0.000	4,481	4,854	138,981	5.36
10.0	293.15	1.00	1.000	8,749	8,314	188,748	7.28
0.1	283.15	20.32	0.308	5,535	5,823	82,551	3.18
1.0	283.15	20.32	1.308	9,056	9,552	245,989	9.49
10.0	283.15	20.32	2.308	14,511	13,958	305,991	11.80
0.1	273.15	515.03	1.712	11,557	11,273	80,263	3.10
1.0	273.15	515.03	2.712	15,492	15,819	106,927	4.12
10.0	273.15	515.03	3.712	20,927	20,286	410,802	15.84
0.1	263.15	16,685.19	3.222	18,002	18,148	21,202	0.82
1.0	263.15	16,685.19	4.222	21,449	22,353	818,346	31.56
10.0	263.15	16,685.19	5.222	26,073	25,762	96,694	3.73
					FQS:	2,592,865	100.00

Table B-18: Master curve (T_0 = 20 °C) for *SMA 11 S new mix* (PMB grade).

			X	Y			Prozent Fehler-quadrat [%]
f	T	α_T	log(α_T*f)	Steifigkeitsmodul	Regression	Schätzung	
[Hz]	[K]	[-]	[Hz]	[MPa]	R	(Y-R)²	
0.1	293.15	1.00	-1.000	1,481	1,357	15,234	1.35
1.0	293.15	1.00	0.000	2,826	2,851	621	0.05
10.0	293.15	1.00	1.000	5,643	5,331	97,104	8.59
0.1	283.15	20.32	0.308	3,278	3,494	46,577	4.12
1.0	283.15	20.32	1.308	5,982	6,340	127,647	11.30
10.0	283.15	20.32	2.308	10,613	10,422	36,511	3.23
0.1	273.15	515.03	1.712	7,930	7,845	7,156	0.63
1.0	273.15	515.03	2.712	11,935	12,360	181,241	16.04
10.0	273.15	515.03	3.712	17,545	17,430	13,334	1.18
0.1	263.15	16,685.19	3.222	15,493	14,939	306,425	27.12
1.0	263.15	16,685.19	4.222	19,391	19,911	270,948	23.98
10.0	263.15	16,685.19	5.222	24,197	24,033	27,020	2.39
					FQS:	1,129,825	100.00

Table B-19: Master curve (T_0 = 20 °C), *SMA 11 S reused RAP mix* using rejuvenator 1.

			X	Y			Prozent Fehler-quadrat [%]
f	T	α_T	log(α_T*f)	Steifigkeitsmodul	Regression	Schätzung	
[Hz]	[K]	[-]	[Hz]	[MPa]	R	(Y-R)²	
0.1	293.15	1.00	-1.000	1,952	1,804	21,698	0.76
1.0	293.15	1.00	0.000	3,347	3,466	14,013	0.49
10.0	293.15	1.00	1.000	6,273	5,743	281,381	9.86
0.1	283.15	20.32	0.308	3,836	4,096	67,773	2.38
1.0	283.15	20.32	1.308	6,302	6,585	80,227	2.81
10.0	283.15	20.32	2.308	10,799	9,798	1,000,646	35.08
0.1	273.15	515.03	1.712	7,228	7,794	320,181	11.22
1.0	273.15	515.03	2.712	10,776	11,298	273,136	9.57
10.0	273.15	515.03	3.712	16,072	15,435	405,900	14.23
0.1	263.15	16,685.19	3.222	13,237	13,343	11,365	0.40
1.0	263.15	16,685.19	4.222	17,115	17,715	359,136	12.59
10.0	263.15	16,685.19	5.222	22,418	22,287	17,189	0.60
					FQS:	2.852.651	100.00

Table B-20: Master curve (T_0 = 20 °C), *SMA 11 S reused RAP mix* using rejuvenator 2.

			X	Y			Prozent Fehler-quadrat [%]
f	T	α_T	log(α_T*f)	Steifigkeitsmodul	Regression	Schätzung	
[Hz]	[K]	[-]	[Hz]	[MPa]	R	(Y-R)²	
0.1	293.15	1.00	-1.000	2,337	2,143	37,469	2.16
1.0	293.15	1.00	0.000	4,027	4,188	25,949	1.50
10.0	293.15	1.00	1.000	7,329	6,986	117,941	6.81
0.1	283.15	20.32	0.308	4,703	4,966	69,009	3.98
1.0	283.15	20.32	1.308	7,764	8,005	57,923	3.34
10.0	283.15	20.32	2.308	12,588	11,770	669,282	38.62
0.1	273.15	515.03	1.712	9,215	9,447	54,173	3.13
1.0	273.15	515.03	2.712	13,026	13,445	174,956	10.10
10.0	273.15	515.03	3.712	18,186	17,750	189,701	10.95
0.1	263.15	16,685.19	3.222	15,544	15,632	7,847	0.45
1.0	263.15	16,685.19	4.222	19,369	19,919	302,147	17.43
10.0	263.15	16,685.19	5.222	23,995	23,832	26,646	1.54
					FQS:	1,733,050	100.00

Table B-21: Master curve (T_0 = 20 °C), *SMA 11 S reused RAP mix* using rejuvenator 3.

			X	Y			Prozent Fehler-quadrat [%]
f	T	α_T	log(α_T*f)	Steifigkeitsmodul	Regression	Schätzung	
[Hz]	[K]	[-]	[Hz]	[MPa]	R	(Y-R)²	
0.1	293.15	1.00	-1.000	2,235	2,010	50,651	2.31
1.0	293.15	1.00	0.000	3,865	4,091	51,240	2.33
10.0	293.15	1.00	1.000	7,090	6,865	50,561	2.30
0.1	283.15	20.32	0.308	4,642	4,870	52,231	2.38
1.0	283.15	20.32	1.308	7,651	7,860	43,721	1.99
10.0	283.15	20.32	2.308	12,217	11,476	548,612	24.98
0.1	273.15	515.03	1.712	9,170	9,255	7,202	0.33
1.0	273.15	515.03	2.712	12,761	13,061	90,089	4.10
10.0	273.15	515.03	3.712	17,840	17,091	561,157	25.55
0.1	263.15	16,685.19	3.222	14,780	15,115	112,779	5.13
1.0	263.15	16,685.19	4.222	18,339	19,103	584,293	26.60
10.0	263.15	16,685.19	5.222	22,933	22,723	44,055	2.01
					FQS:	2,196,597	100.00

Table B-22: Stiffness modulus values of *AC 16 T D new mix* using 50/70 bitumen grade.

T	f	lEI1	lEI2	lEI3	lEI		
[°C]	[Hz]	[MPa]	[MPa]	[MPa]	Mittelwert [MPa]	Standartabw. [MPa]	Variationskoeffizient
20	0.1	2,120	2,270	2,212	2,200	76	3.4
20	1.0	4,099	4,446	4,316	4,287	175	4.1
20	10.0	8,103	8,755	8,447	8,435	326	3.9
10	0.1	4,781	4,858	4,810	4,816	39	0.8
10	1.0	8,345	8,520	8,417	8,427	88	1.0
10	10.0	14,180	14,399	14,734	14,437	279	1.9
0	0.1	10,347	10,492	10,426	10,421	73	0.7
0	1.0	14,821	15,267	15,013	15,033	224	1.5
0	10.0	20,975	21,538	21,201	21,238	283	1.3
-10	0.1	19,345	19,337	18,895	19,192	258	1.3
-10	1.0	23,829	23,836	22,919	23,528	527	2.2
-10	10.0	28,911	29,052	27,834	28,599	666	2.3

Table B-23: Stiffness modulus of *AC 16 T D reused RAP mix* using rejuvenator 1.

T	f	lEI1	lEI2	lEI3	lEI		
[°C]	[Hz]	[MPa]	[MPa]	[MPa]	Mittelwert [MPa]	Standartabw. [MPa]	Variationskoeffizient
20	0.1	2,143	2,552	2,364	2,353	205	8.7
20	1.0	4,100	4,751	4,163	4,338	359	8.3
20	10.0	7,272	8,632	7,851	7,918	682	8.6
10	0.1	4,372	4,894	5,123	4,796	385	8.0
10	1.0	7,291	8,050	7,849	7,730	393	5.1
10	10.0	11,947	12,814	12,661	12,474	463	3.7
0	0.1	9,750	10,186	9,454	9,796	368	3.8
0	1.0	13,335	14,002	13,115	13,484	462	3.4
0	10.0	18,529	19,229	18,432	18,730	435	2.3
-10	0.1	15,498	16,326	16,362	16,062	489	3.0
-10	1.0	18,940	19,788	19,888	19,538	521	2.7
-10	10.0	23,642	24,381	24,758	24,260	568	2.3

Table B-24: Stiffness modulus of *AC 16 T D reused RAP mix* using rejuvenator 2.

T	f	lEI1	lEI2	lEI3	lEI		
[°C]	[Hz]	[MPa]	[MPa]	[MPa]	Mittelwert [MPa]	Standartabw. [MPa]	Variationskoeffizient
20	0.1	2,180	2,066	2,003	2,083	90	4.3
20	1.0	4,436	3,899	4,264	4,199	274	6.5
20	10.0	8,601	7,703	7,673	7,992	527	6.6
10	0.1	5,343	4,606	3,972	4,640	686	14.8
10	1.0	8,198	7,820	7,035	7,684	593	7.7
10	10.0	13,638	13,483	12,039	13,053	882	6.8
0	0.1	9,323	8,409	8,210	8,647	594	6.9
0	1.0	13,794	12,590	12,313	12,899	787	6.1
0	10.0	19,629	18,328	17,827	18,594	930	5.0
-10	0.1	16,260	15,089	15,262	15,537	632	4.1
-10	1.0	20,256	19,590	19,485	19,777	418	2.1
-10	10.0	25,750	25,099	24,935	25,261	431	1.7

Table B-25: Stiffness modulus of *AC 16 T D reused RAP mix* using rejuvenator 3.

T	f	lEI1	lEI2	lEI3	lEI		
[°C]	[Hz]	[MPa]	[MPa]	[MPa]	Mittelwert [MPa]	Standartabw. [MPa]	Variationskoeffizient
20	0.1	2,199	2,267	1,964	2,143	159	7.4
20	1.0	4,136	4,272	3,737	4,048	278	6.9
20	10.0	8,094	8,344	7,329	7,922	529	6.7
10	0.1	4,808	5,360	4,424	4,864	471	9.7
10	1.0	8,102	8,120	7,455	7,892	379	4.8
10	10.0	13,400	13,303	12,549	13,084	466	3.6
0	0.1	9,860	10,149	9,490	9,833	330	3.4
0	1.0	13,987	14,238	13,397	13,874	432	3.1
0	10.0	19,551	19,673	18,764	19,329	493	2.6
-10	0.1	15,871	16,363	15,588	15,940	392	2.5
-10	1.0	19,724	20,278	19,182	19,728	548	2.8
-10	10.0	24,619	25,202	24,232	24,684	488	2.0

Table B-26: Regression parameters of Master Curve for *AC 16 T D* mixes of all types.

Reg. Para	New 30/45	Reused mix, no.1	Reused mix, no.2	Reused mix, no.3
y_0	-1,539.39	-2,028.84	-4,139.73	-3,024.26
w	39,582.96	36,426.15	53,274.86	38,322.12
x_0	3.16	3.26	4.67	3.18
z	1.81	2.11	2.78	2.19
E_a/R	25,000	25,000	25,000	25,000

Table B-27: Master curve (T_0 = 20 °C) for *AC 16 T D new mix* (50/70 bitumen grade).

			X	Y			Prozent
f	T	α_T	log(α_T*f)	Steifigkeitsmodul	Regression	Schätzung	Fehler-
[Hz]	[K]	[-]	[Hz]	[MPa]	R	$(Y-R)^2$	quadrat
							[%]
0.1	293.15	1.00	-1.000	2,201	2,060	19,698	0.69
1.0	293.15	1.00	0.000	4,287	4,327	1,604	0.06
10.0	293.15	1.00	1.000	8,435	7,656	606,200	21.35
0.1	283.15	20.32	0.308	4,816	5,231	171,945	6.06
1.0	283.15	20.32	1.308	8,427	8,914	237,130	8.35
10.0	283.15	20.32	2.308	14,438	13,672	585,557	20.63
0.1	273.15	515.03	1.712	10,422	10,721	89,810	3.16
1.0	273.15	515.03	2.712	15,034	15,812	605,911	21.34
10.0	273.15	515.03	3.712	21,238	21,253	231	0.01
0.1	263.15	16,685.19	3.222	19,192	18,596	356,188	12.55
1.0	263.15	16,685.19	4.222	23,528	23,910	146,156	5.15
10.0	263.15	16,685.19	5.222	28,599	28,464	18,305	0.64
					FQS:	2,838,742	100.00

Table B-28: Master curve (T_0 = 20 °C), *AC 16 T D reused RAP mix* using rejuvenator 1.

			X	Y			Prozent
f	T	α_T	$\log(\alpha_T * f)$	Steifigkeitsmodul	Regression	Schätzung	Fehler-
[Hz]	[K]	[-]	[Hz]	[MPa]	R	$(Y-R)^2$	quadrat
							[%]
0.1	293.15	1.00	-1.000	2,353	2,230	15,168	0.73
1.0	293.15	1.00	0.000	4,338	4,361	523	0.03
10.0	293.15	1.00	1.000	7,918	7,251	445,799	21.44
0.1	283.15	20.32	0.308	4,796	5,167	137,702	6.62
1.0	283.15	20.32	1.308	7,730	8,297	320,998	15.44
10.0	283.15	20.32	2.308	12,474	12,127	120,134	5.78
0.1	273.15	515.03	1.712	9,797	9,770	705	0.03
1.0	273.15	515.03	2.712	13,484	13,816	110,058	5.29
10.0	273.15	515.03	3.712	18,730	18,114	379,464	18.25
0.1	263.15	16,685.19	3.222	16,062	16,007	3,013	0.14
1.0	263.15	16,685.19	4.222	19,539	20,256	514,775	24.76
10.0	263.15	16,685.19	5.222	24,260	24,085	30,817	1.48
					FQS:	2,079,162	100.00

Table B-29: Master curve (T_0 = 20 °C), *AC 16 T D reused RAP mix* using rejuvenator 2.

			X	Y			Prozent
f	T	α_T	$\log(\alpha_T * f)$	Steifigkeitsmodul	Regression	Schätzung	Fehler-
[Hz]	[K]	[-]	[Hz]	[MPa]	R	$(Y-R)^2$	quadrat
							[%]
0.1	293.15	1.00	-1.000	2,083	1,982	10,103	0.22
1.0	293.15	1.00	0.000	4,200	4,220	399	0.01
10.0	293.15	1.00	1.000	7,992	7,080	832,651	18.08
0.1	283.15	20.32	0.308	4,640	5,031	152,934	3.32
1.0	283.15	20.32	1.308	7,684	8,094	167,551	3.64
10.0	283.15	20.32	2.308	13,053	11,809	1,549,169	33.65
0.1	273.15	515.03	1.712	8,647	9,517	757,004	16.44
1.0	273.15	515.03	2.712	12,899	13,479	336,578	7.31
10.0	273.15	515.03	3.712	18,595	17,949	416,374	9.04
0.1	263.15	16,685.19	3.222	15,537	15,710	29,871	0.65
1.0	263.15	16,685.19	4.222	19,777	20,357	336,636	7.31
10.0	263.15	16,685.19	5.222	25,261	25,140	14,834	0.32
					FQS:	4,604,110	100.00

Table B-30: Master curve (T_0 = 20 °C), *AC 16 T D reused RAP mix* using rejuvenator 3.

			X	Y			Prozent
f	T	α_T	log(α_T*f)	Steifigkeitsmodul	Regression	Schätzung	Fehler-
[Hz]	[K]	[-]	[Hz]	[MPa]	R	$(Y-R)^2$	quadrat
							[%]
0.1	293.15	1.00	-1.000	2,143	1,941	40,787	1.32
1.0	293.15	1.00	0.000	4,048	4,262	45,818	1.48
10.0	293.15	1.00	1.000	7,922	7,331	349,122	11.29
0.1	283.15	20.32	0.308	4,864	5,127	69,042	2.23
1.0	283.15	20.32	1.308	7,892	8,426	284,366	9.20
10.0	283.15	20.32	2.308	13,084	12,378	498,496	16.12
0.1	273.15	515.03	1.712	9,833	9,955	14,903	0.48
1.0	273.15	515.03	2.712	13,874	14,099	50,617	1.64
10.0	273.15	515.03	3.712	19,329	18,445	781,868	25.28
0.1	263.15	16,685.19	3.222	15,941	16,320	143,605	4.64
1.0	263.15	16,685.19	4.222	19,728	20,601	762,510	24.66
10.0	263.15	16,685.19	5.222	24,684	24,458	51,157	1.65
					FQS:	3,092,295	100.00

Table B-31: Stiffness modulus values of *AC 22 T S new mix* using 30/45 bitumen grade.

T	f	lEI1	lEI2	lEI3	lEI		
[°C]	[Hz]	[MPa]	[MPa]	[MPa]	Mittelwert	Standartabw.	Variationskoeffizient
20	0.1	5,190	4,855	5,392	5,146	271	5.3
20	1.0	8,736	8,325	9,029	8,697	354	4.1
20	10.0	14,875	14,176	15,316	14,789	575	3.9
10	0.1	11,509	10,149	10,910	10,856	682	6.3
10	1.0	16,183	14,920	15,614	15,572	633	4.1
10	10.0	23,559	21,612	22,551	22,574	974	4.3
0	0.1	18,214	16,848	17,104	17,389	726	4.2
0	1.0	22,583	20,792	21,654	21,676	896	4.1
0	10.0	28,478	26,698	27,881	27,686	906	3.3
-10	0.1	23,427	24,916	23,040	23,794	990	4.2
-10	1.0	27,324	28,699	26,887	27,637	946	3.4
-10	10.0	32,302	33,839	31,867	32,669	1.036	3.2

Table B-32: Stiffness modulus values of *AC 22 T S new mix* using 50/70 bitumen grade.

T	f	lEI1	lEI2	lEI3	lEI		
[°C]	[Hz]	[MPa]	[MPa]	[MPa]	Mittelwert [MPa]	Standartabw. [MPa]	Variationskoeffizient
20	0.1	4,261	3,757	4,500	4,173	379	9.1
20	1.0	7,673	6,777	7,630	7,360	505	6.9
20	10.0	13,460	12,221	13,406	13,029	700	5.4
10	0.1	8,134	8,080	7,990	8,068	73	0.9
10	1.0	12,692	12,511	12,499	12,567	108	0.9
10	10.0	19,786	19,091	19,157	19,345	384	2.0
0	0.1	15,600	14,890	14,026	14,839	788	5.3
0	1.0	20,709	19,315	18,983	19,669	916	4.7
0	10.0	27,234	25,345	25,478	26,019	1,054	4.1
-10	0.1	22,915	21,410	22,127	22,151	753	3.4
-10	1.0	26,509	25,346	26,159	26,005	597	2.3
-10	10.0	31,780	30,621	31,876	31,426	699	2.2

Table B-33: Stiffness modulus values of *AC 22 T S reused RAP mix* using rejuvenator 1.

T	f	lEI1	lEI2	lEI3	lEI		
[°C]	[Hz]	[MPa]	[MPa]	[MPa]	Mittelwert [MPa]	Standartabw. [MPa]	Variationskoeffizient
20	0.1	3,677	3,831	4,024	3,844	174	4.5
20	1.0	6,199	6,437	6,590	6,408	197	3.1
20	10.0	10,342	10,700	10,689	10,577	204	1.9
10	0.1	7,460	7,387	6,438	7,095	570	8.0
10	1.0	10,881	10,645	9,288	10,271	860	8.4
10	10.0	16,183	15,675	13,536	15,131	1,405	9.3
0	0.1	12,485	11,895	10,691	11,690	914	7.8
0	1.0	16,130	15,546	13,730	15,135	1,252	8.3
0	10.0	21,509	20,533	18,220	20,087	1,689	8.4
-10	0.1	17,906	17,903	17,611	17,806	169	1.0
-10	1.0	21,709	21,284	20,753	21,248	479	2.3
-10	10.0	26,937	26,114	25,665	26,238	645	2.5

Table B-34: Stiffness modulus values of *AC 22 T S reused RAP mix* using rejuvenator 2.

T	f	lEI1	lEI2	lEI3	lEI		
[°C]	[Hz]	[MPa]	[MPa]	[MPa]	Mittelwert [MPa]	Standartabw. [MPa]	Variationskoeffizient
20	0.1	2,918	3,477	3,235	3,210	280	8.7
20	1.0	4,976	5,895	5,622	5,497	472	8.6
20	10.0	8,976	10,465	9,842	9,761	748	7.7
10	0.1	5,392	5,299	5,970	5,553	364	6.5
10	1.0	8,669	8,550	9,398	8,872	459	5.2
10	10.0	14,159	14,004	14,623	14,262	322	2.3
0	0.1	11,205	10,700	11,387	11,097	356	3.2
0	1.0	15,437	15,022	15,313	15,257	213	1.4
0	10.0	21,431	20,720	20,695	20,948	418	2.0
-10	0.1	16,581	16,490	17,399	16,823	501	3.0
-10	1.0	20,743	20,220	20,717	20,560	295	1.4
-10	10.0	26,161	25,378	25,894	25,811	398	1.5

Table B-35: Stiffness modulus values of *AC 22 T S reused RAP mix* using rejuvenator 3.

T	f	lEI1	lEI2	lEI3	lEI		
[°C]	[Hz]	[MPa]	[MPa]	[MPa]	Mittelwert [MPa]	Standartabw. [MPa]	Variationskoeffizient
20	0.1	3,247	3,162	3,567	3,325	214	6.4
20	1.0	5,215	5,759	6,163	5,712	476	8.3
20	10.0	9,800	10,284	10,711	10,265	456	4.4
10	0.1	6,868	5,802	6,861	6,510	613	9.4
10	1.0	10,097	9,384	10,307	9,929	484	4.9
10	10.0	14,879	14,959	15,357	15,065	256	1.7
0	0.1	9,204	8,816	8,806	8,942	227	2.5
0	1.0	12,449	12,211	11,623	12,094	425	3.5
0	10.0	17,386	16,971	15,839	16,732	801	4.8
-10	0.1	17,761	18,160	17,019	17,646	579	3.3
-10	1.0	21,845	21,509	19,521	20,958	1,256	6.0
-10	10.0	27,555	25,379	24,137	25,690	1,730	6.7

Table B-36: Regression parameters of Master Curve for *AC 22 T S* mixes of all types.

Reg. Para	New 30/45	New 50/70	Reused RAP mix, no.1	Reused RAP mix, no.2	Reused RAP mix, no.3
y_0	-18,046.50	-5,926.09	-14,191.33	-2,697.07	-10,918.93
w	63,477.47	48,219.84	100,172.92	39,809.21	872,912.39
x_0	0.87	2.31	7.42	3.15	25.85
z	3.25	2.44	5.53	2.32	6.58
E_a/R	25,000	25,000	25,000	25,000	25,000

Table B-37: Master curve (T_0 = 20 °C) for *AC 22 T S new mix* (30/45 bitumen grade).

			X	Y			Prozent
f	T	α_T	log(α_T*f)	Steifigkeitsmodul	Regression	Schätzung	Fehler-
[Hz]	[K]	[-]	[Hz]	[MPa]	R	$(Y-R)^2$	quadrat
							[%]
0.1	293.15	1.00	-1.000	5,146	4,797	121,689	1.39
1.0	293.15	1.00	0.000	8,697	9,458	579,484	6.61
10.0	293.15	1.00	1.000	14,789	14,313	226,893	2.59
0.1	283.15	20.32	0.308	10,856	10,943	7,513	0.09
1.0	283.15	20.32	1.308	15,572	15,813	57,844	0.66
10.0	283.15	20.32	2.308	22,574	20,585	3,957	45.16
0.1	273.15	515.03	1.712	17,389	17,764	140,95	1.61
1.0	273.15	515.03	2.712	21,676	22,435	575,746	6.57
10.0	273.15	515.03	3.712	27,686	26,729	914,530	10.44
0.1	263.15	16,685.19	3.222	23,794	24,684	791,798	9.04
1.0	263.15	16,685.19	4.222	27,637	28,732	1,199,033	13.68
10.0	263.15	16,685.19	5.222	32,669	32,233	190,014	2.17
					FQS:	8,762,746	100.00

Table B-38: Master curve (T_0 = 20 °C) for *AC 22 T S new mix* (50/70 bitumen grade).

			X	Y			Prozent
f	T	α_T	log(α_T*f)	Steifigkeitsmodul	Regression	Schätzung	Fehler-
[Hz]	[K]	[-]	[Hz]	[MPa]	R	(Y-R)²	quadrat
							[%]
0.1	293.15	1.00	-1.000	4,173	3,917	65,445	0.90
1.0	293.15	1.00	0.000	7,360	7,521	25,804	0.36
10.0	293.15	1.00	1.000	13,029	11,833	1,429	19.74
0.1	283.15	20.32	0.308	8,068	8,781	507,810	7.01
1.0	283.15	20.32	1.308	12,567	13,274	499,654	6.90
10.0	283.15	20.32	2.308	19,345	18,154	1,417	19.56
0.1	273.15	515.03	1.712	14,839	15,218	144,175	1.99
1.0	273.15	515.03	2.712	19,669	20,149	229,976	3.17
10.0	273.15	515.03	3.712	26,019	24,919	1,210,650	16.71
0.1	263.15	16,685.19	3.222	22,151	22,628	228,138	3.15
1.0	263.15	16,685.19	4.222	26,005	27,174	1,367,426	18.88
10.0	263.15	16,685.19	5.222	31,426	31,082	118,382	1.63
					FQS:	7,244,396	100.00

Table B-39: Master curve (T_0 = 20 °C) *AC 22 T S reused RAP mix* using rejuvenator 1.

			X	Y			Prozent
f	T	α_T	log(α_T*f)	Steifigkeitsmodul	Regression	Schätzung	Fehler-
[Hz]	[K]	[-]	[Hz]	[MPa]	R	(Y-R)²	quadrat
							[%]
0.1	293.15	1.00	-1.000	3,844	3,728	13,428	0.45
1.0	293.15	1.00	0.000	6,409	6,547	19,216	0.64
10.0	293.15	1.00	1.000	10,577	9,681	802,341	26.71
0.1	283.15	20.32	0.308	7,095	7,479	147,513	4.91
1.0	283.15	20.32	1.308	10,271	10,710	192,179	6.40
10.0	283.15	20.32	2.308	15,131	14,248	781,147	26.01
0.1	273.15	515.03	1.712	11,690	12,102	169,592	5.65
1.0	273.15	515.03	2.712	15,135	15,759	389,027	12.95
10.0	273.15	515.03	3.712	20,087	19,691	156,837	5.22
0.1	263.15	16,685.19	3.222	17,807	17,734	5,254	0.17
1.0	263.15	16,685.19	4.222	21,249	21,793	296,154	9.86
10.0	263.15	16,685.19	5.222	26,239	26,063	30,790	1.03
					FQS:	3,003,48	100.00

Table B-40: Master curve (T_0 = 20 °C), *AC 22 T S reused RAP mix* using rejuvenator 2.

			X	Y			Prozent
f	T	α_T	log(α_T*f)	Steifigkeitsmodul	Regression	Schätzung	Fehler-
[Hz]	[K]	[-]	[Hz]	[MPa]	R	(Y-R)²	quadrat
							[%]
0.1	293.15	1.00	-1.000	3,210	3,008	40,798	0.60
1.0	293.15	1.00	0.000	5,498	5,451	2,187	0.03
10.0	293.15	1.00	1.000	9,761	8,594	1,363,049	19.92
0.1	283.15	20.32	0.308	5,554	6,344	625,253	9.14
1.0	283.15	20.32	1.308	8,872	9,697	679,61	9.93
10.0	283.15	20.32	2.308	14,262	13,632	396,496	5.79
0.1	273.15	515.03	1.712	11,097	11,228	16,984	0.25
1.0	273.15	515.03	2.712	15,257	15,330	5,243	0.08
10.0	273.15	515.03	3.712	20,949	19,599	1,820,688	26.61
0.1	263.15	16,685.19	3.222	16,823	17,513	474,976	6.94
1.0	263.15	16,685.19	4.222	20,560	21,720	1,344,654	19.65
10.0	263.15	16,685.19	5.222	25,811	25,541	73,074	1.07
					FQS:	6,843,020	100.00

Table B-41: Master curve (T_0 = 20 °C), *AC 22 T S reused RAP mix* using rejuvenator 3.

			X	Y			Prozent
f	T	α_T	log(α_T*f)	Steifigkeitsmodul	Regression	Schätzung	Fehler-
[Hz]	[K]	[-]	[Hz]	[MPa]	R	(Y-R)²	quadrat
							[%]
0.1	293.15	1.00	-1.000	3,325	3,595	72,852	0.35
1.0	293.15	1.00	0.000	5,712	5,931	47,771	0.23
10.0	293.15	1.00	1.000	10,265	8,634	2,660,638	12.77
0.1	283.15	20.32	0.308	6,510	6,722	44,775	0.21
1.0	283.15	20.32	1.308	9,929	9,549	144,845	0.70
10.0	283.15	20.32	2.308	15,065	12,816	5,058,162	24.28
0.1	273.15	515.03	1.712	8,942	10,812	3,495,405	16.78
1.0	273.15	515.03	2.712	12,094	14,274	4,752,889	22.82
10.0	273.15	515.03	3.712	16,732	18,270	2,366,015	11.36
0.1	263.15	16,685.19	3.222	17,647	16,243	1,969,953	9.46
1.0	263.15	16,685.19	4.222	20,958	20,540	175,416	0.84
10.0	263.15	16,685.19	5.222	25,690	25,486	41,658	0.20
					FQS:	20,830,385	100.00

Appendix C

Fatigue results

Cylindrical samples cored from prepared slabs were tested by indirect tensile stress at 10 Hz and 20 ºC till failure at three strain levels. Number of cycles when crack initiates (N_{macro}) then determined as change in energy ratio happens. Decrease in stiffness modulus can be determined as well (Fig. C-1). Tabels C-2 to C-28 contain the details of fatigue test.

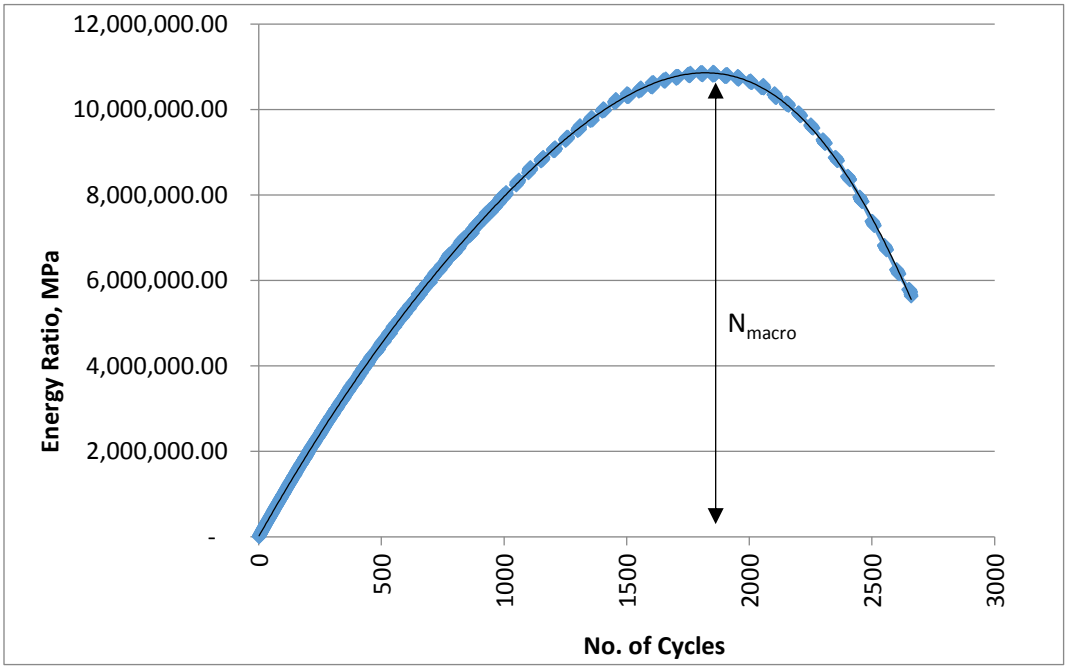

Figure C-1: determination of number of cycles at failure in the fatigue test.

Table C-1: Results of fatigue test of new *AC 16 B S* mix.

Aspaltmaterial:			AC 16 B S					Bitumen:		30/45
Durchmesser [mm]:			100							
Rohdichte ρ_m [g/cm³]:			2.585				Raumdichte ρ_b [g/cm³]:			2.438
Querdehnzahl μ [-]:			0.2984							
Pk-Nr. [-]	hohe [mm]	ρ_b [g/cm³]	V [Vol.-%]	T [°C]	f [Hz]	s_u [MPa]	s_o [MPa]	IEI [MPa]	$e_{el.\ anf}$ [‰]	N_{Makro} [-]
A-1	39.9	2.465	4.6	20	10	0.035	0.800	11,926	0.147	1,853
J-1	40.0	2.465	4.6				0.800	11,301.	0.131	2,453
S-2	40.0	2.457	5.0				0.800	10,019	0.124	3,206
D-2	39.9	2.478	4.1			0.035	0.350	11,132	0.054	24,007
R-1	40.0	2.506	3.1				0.350	12,388	0.048	27,500
S-2	40.1	2.466	4.6				0.350	11,114	0.054	69,509
B-2	40.0	2.472	4.4			0.035	0.200	12,264	0.026	542,854
I-1	40.0	2.497	3.4				0.200	12,893	0.024	772,020
I-2	39.9	2.486	3.8				0.200	12,710	0.025	358,194

Table C-2: Results of fatigue test of aged *AC 16 B S* mix using peroxide.

Aspaltmaterial:			AC 16 B S					Bitumen:		30/45
Durchmesser [mm]:			100							
Rohdichte ρ_m [g/cm³]:			2.585				Raumdichte ρ_b [g/cm³]:			2.438
Querdehnzahl μ [-]:			0.2984	H_2O_2 concentration 35% for 168 h						
Pk-Nr. [-]	hohe [mm]	ρ_b [g/cm³]	V [Vol.-%]	T [°C]	f [Hz]	s_u [MPa]	s_o [MPa]	IEI [MPa]	$e_{el.\ anf}$ [‰]	N_{Makro} [-]
Pe-02	39.8	2.477	4.2	20	10	0.035	0.800	13,114	0.109	4,257
Pe-11	40.0	2.478	4.1				0.800	13,267	0.104	9,108
Pe-08	40.0	2.472	4.5				0.800	12,854	0.114	6,405
Pe-21	40.1	2.479	3.9			0.035	0.350	13,457	0.089	16,001
Pe-34	40.0	2.484	3.7				0.350	14,037	0.085	19,625
Pe-04	39.9	2.498	3.7				0.350	13,647	0.084	16,038
Pe-16	40.0	2.471	4.5			0.035	0.200	13,611	0.057	90,004
Pe-19	40.0	2.472	4.5				0.200	13,847	0.053	101,568
Pe-23	40.1	2.487	3.9				0.200	14,317	0.056	115,421

Table C-3: Results of fatigue test of aged *AC 16 B S* mix using peroxide + short-term ageing.

Aspaltmaterial:			AC 16 B S					Bitumen:		30/45
Durchmesser [mm]:			100							
Rohdichte ρ_m [g/cm³]:			2.585				Raumdichte ρ_b [g/cm³]:			2.438
Querdehnzahl μ [-]:			0.2984							
					STA: H_2O_2 concentration 35% for 168 h +					
					short-term ageing at 135 ºC for 4 h					
Pk-Nr. [-]	hohe [mm]	ρ_b [g/cm³]	V [Vol.-%]	T [°C]	f [Hz]	s_u [MPa]	s_o [MPa]	IEI [MPa]	$e_{el,\ anf}$ [‰]	N_{Makro} [-]
AA-3	40.0	2.471	4.4	20	10	0.035	0.800	13,547	0.102	5,802
AA-5	40.0	2.469	4.5				0.800	13,114	0.106	5,602
AB-3	40.1	2.477	4.2				0.800	13,374	0.103	5,617
AB-2	40.0	2.482	4.0			0.035	0.350	13,084	0.083	15,000
AA-1	39.9	2.482	4.0				0.350	13,228	0.078	19,006
AA-4	40.0	2.479	4.1				0.350	12,957	0.080	17,225
AA-2	39.8	2.492	3.6			0.035	0.200	13,748	0.043	163,510
AB-1	40.1	2.482	4.0				0.200	14,487	0.037	436,505
AB-5	40.0	2.484	3.9				0.200	14,297	0.040	286,882

Table C-4: Results of fatigue test of aged *AC 16 B S* mix using short-term ageing + peroxide.

Aspaltmaterial:			AC 16 B S					Bitumen:		30/45
Durchmesser [mm]:			100							
Rohdichte ρ_m [g/cm³]:			2.585				Raumdichte ρ_b [g/cm³]:			2.438
Querdehnzahl μ [-]:			0.2984							
					STB: short-term ageing at 135 ºC for 4 h +					
					H_2O_2 concentration 35% for 168 h					
Pk-Nr. [-]	hohe [mm]	ρ_b [g/cm³]	V [Vol.-%]	T [°C]	f [Hz]	s_u [MPa]	s_o [MPa]	IEI [MPa]	$e_{el,\ anf}$ [‰]	N_{Makro} [-]
SB-13	39.8	2.481	4.0	20	10	0.035	0.800	12,891	0.088	5,102
SB-14	39.9	2.478	4.1				0.800	13,214	0.093	4,725
SB-22	40.0	2.477	4.2				0.800	12,827	0.097	4,105
SB-11	39.8	2.479	4.1			0.035	0.350	12,927	0.091	10,310
SB-21	40.0	2.484	3.9				0.350	12,884	0.070	14,000
SB-25	39.9	2.502	3.2				0.350	13,417	0.066	34,500
SB-12	39.8	2.486	3.8			0.035	0.200	13,847	0.042	202,506
SB-23	40.0	2.479	4.1				0.200	14,255	0.044	175,030
SB-24	39.9	2.488	3.8				0.200	14,084	0.036	247,084

Table C-5: Results of fatigue test of aged *AC 16 B S* mix using short-term ageing.

Aspaltmaterial:			AC 16 B S					Bitumen:		30/45
Durchmesser [mm]:			100							
Rohdichte ρ_m [g/cm³]:			2.585				Raumdichte ρ_b [g/cm³]:			2.438
Querdehnzahl μ [-]:			0.2984							
					ST: short-term ageing at 135 ºC for 4 h					
Pk-Nr. [-]	hohe [mm]	ρ_b [g/cm³]	V [Vol.-%]	T [°C]	f [Hz]	s_u [MPa]	s_o [MPa]	IEI [MPa]	$e_{el, anf}$ [‰]	N_{Makro} [-]
ST-13	40.0	2.472	4.4	20	10	0.035	0.800	11,841	0.114	3,960
ST-15	40.1	2.477	4.2				0.800	12,414	0.109	4,710
ST-23	40.0	2.469	4.5				0.800	12,084	0.112	4009
ST-22	40.0	2.480	4.1			0.035	0.350	12,241	0.088	12,601
ST-24	39.9	2.479	4.1				0.350	12,657	0.067	22,503
ST-25	39.9	2.488	3.8				0.350	12,877	0.058	67,002
ST-11	40.0	2.491	3.6			0.035	0.200	12,844	0.045	141,066
ST-12	40.0	2.488	3.8				0.200	13,354	0.052	114,494
ST-34	40.1	2.486	3.8				0.200	13,884	0.042	150,195

Table C-6: Results of fatigue test of aged *AC 16 B S* mix using long-term ageing.

Aspaltmaterial:			AC 16 B S					Bitumen:		30/45
Durchmesser [mm]:			100							
Rohdichte ρ_m [g/cm³]:			2.585				Raumdichte ρ_b [g/cm³]:			2.438
Querdehnzahl μ [-]:			0.2984							
					LT: short-term ageing at 135 ºC for 4 h +					
					long-term ageing at 75 ºC for 244 h					
Pk-Nr. [-]	hohe [mm]	ρ_b [g/cm³]	V [Vol.-%]	T [°C]	f [Hz]	s_u [MPa]	s_o [MPa]	IEI [MPa]	$e_{el, anf}$ [‰]	N_{Makro} [-]
LT-11	40.1	2.468	4.5	20	10	0.035	0.800	12,444	0.113	4,958
LT-32	40.0	2.474	4.3				0.800	12,847	0.092	5,622
LT-33	40.0	2.475	4.3				0.800	13,119	0.098	6,659
LT-24	40.0	2.481	4.0			0.035	0.350	13,497	0.091	10,659
LT-34	40.0	2.479	4.1				0.350	12,859	0.087	12,608
LT-35	40.0	2.481	4.0				0.350	12,577	0.094	11,307
LT-21	39.8	2.477	4.2			0.035	0.200	13,566	0.062	58,507
LT-22	39.8	2.484	3.9				0.200	14,222	0.052	116,294
LT-31	40.0	2.476	4.2				0.200	13,811	0.043	156,202

Table C-7: Results of fatigue test of aged *AC 16 B S* mix using Ozone.

Aspaltmaterial:			AC 16 B S					Bitumen:		30/45
Durchmesser [mm]:			100							
Rohdichte ρ_m [g/cm³]:			2.585				Raumdichte ρ_b [g/cm³]:			2.438
Querdehnzahl μ [-]:			0.2984							
					O_3: concentration 20 ppm and humidity 50% for 300 h					
Pk-Nr. [-]	hohe [mm]	ρ_b [g/cm³]	V [Vol.-%]	T [°C]	f [Hz]	s_u [MPa]	s_o [MPa]	IEI [MPa]	$e_{el, anf}$ [‰]	N_{Makro} [-]
O-1	39.9	2.472	4.4			0.035	0.800	11,937	0.089	8,204
O-2	39.9	2.478	4.1				0.200	12,622	0.074	13,805
				20	10					

Table C-8: Results of fatigue test of aged *AC 16 B S* mix with rejuvenator 1.

Aspaltmaterial:			AC 16 B S					Bitumen:		30/45
Durchmesser [mm]:			100					Rejuvenator:		1
Rohdichte ρ_m [g/cm³]:			2.585				Raumdichte ρ_b [g/cm³]:			2.438
Querdehnzahl μ [-]:			0.2984							
Pk-Nr. [-]	hohe [mm]	r_b [g/cm³]	V [Vol.-%]	T [°C]	f [Hz]	s_u [MPa]	s_o [MPa]	IEI [MPa]	$e_{el, anf}$ [‰]	N_{Makro} [-]
B1-11	40.0	2.471	4.4				0.800	7,051	0.121	3,550
B1-32	39.8	2.468	4.5			0.035	0.800	8,501	0.101	4,656
B1-33	39.8	2.475	4.3				0.800	7,722	0.111	3,948
B1-14	40.1	2.466	4.6				0.350	7,919	0.052	42,000
B1-15	40.1	2.470	4.4	20	10	0.035	0.350	7,990	0.060	50,008
B1-31	39.8	2.461	4.8				0.350	8,025	0.055	55,886
B1-22	40.1	2.472	4.4				0.200	8,582	0.037	451,503
B1-23	40.1	2.469	4.5			0.035	0.200	8,322	0.035	374,984
B1-35	40.0	2.477	4.2				0.200	8,771	0.033	510,996

Table C-9: Results of fatigue test of *AC 16 B S* mix with rejuvenator 2.

Aspaltmaterial:			AC 16 B S					Bitumen:		30/45
Durchmesser [mm]:			100					Rejuvenator:		2
Rohdichte ρ_m [g/cm³]:			2.585				Raumdichte ρ_b [g/cm³]:			2.438
Querdehnzahl μ [-]:			0.2984							
Pk-Nr. [-]	hohe [mm]	ρ_b [g/cm³]	V [Vol.-%]	T [°C]	f [Hz]	s_u [MPa]	s_o [MPa]	IEI [MPa]	$e_{el, anf}$ [‰]	N_{Makro} [-]
B2-13	40.2	2.473	4.3	20	10	0.035	0.800	5,403	0.100	8,956
B2-24	40.0	2.479	4.1				0.800	5,503	0.100	9,009
B2-33	40.1	2.500	3.3				0.800	5,402	0.108	6,395
B2-11	40.2	2.488	3.8			0.035	0.350	6,185	0.088	13,206
B2-12	40.2	2.480	4.1				0.350	7,464	0.055	34,504
B2-22	40.0	2.481	4.0				0.350	7,599	0.065	36,485
B2-15	40.3	2.477	4.2			0.035	0.200	6,675	0.037	151,504
B2-23	40.0	2.480	4.1				0.200	7,220	0.034	126,920
B2-25	40.0	2.484	3.9				0.200	7,714	0.032	215,324

Table C-10: Results of fatigue test of aged *AC 16 B S* mix with rejuvenator 3.

Aspaltmaterial:			AC 16 B S					Bitumen:		30/45
Durchmesser [mm]:			100					Rejuvenator:		3
Rohdichte ρ_m [g/cm³]:			2.585				Raumdichte ρ_b [g/cm³]:			2.438
Querdehnzahl μ [-]:			0.2984							
Pk-Nr. [-]	hohe [mm]	ρ_b [g/cm³]	V [Vol.-%]	T [°C]	f [Hz]	s_u [MPa]	s_o [MPa]	IEI [MPa]	$e_{el, anf}$ [‰]	N_{Makro} [-]
B3-24	40.0	2.469	4.5	20	10	0.035	0.800	6,204	0.212	482
B3-13	40.3	2.487	3.8				0.800	6,424	0.109	5,706
B3-12	40.3	2.480	4.1				0.800	6,332	0.110	4,158
B3-11	40.3	2.479	4.1			0.035	0.350	7,224	0.056	39,003
B3-22	39.8	2.480	4.1				0.350	6,844	0.069	40,000
B3-25	40.0	2.477	4.2				0.350	6,627	0.061	32,000
B3-31	40.0	2.481	4.0			0.035	0.200	7,311	0.042	117,019
B3-21	39.8	2.477	4.2				0.200	7,548	0.039	210,988
B3-33	40.0	2.477	4.2				0.200	7,277	0.037	136,558

Table C-11: Results of fatigue test of new *SMA 11 S* mix with bitumen grade 30/45

Aspaltmaterial:			SMA 11 S					Bitumen:		30/45
Durchmesser [mm]:			100							
Rohdichte ρ_m [g/cm³]:			2.585				Raumdichte ρ_b [g/cm³]:			2.438
Querdehnzahl μ [-]:			0.2984							
Pk-Nr. [-]	hohe [mm]	ρ_b [g/cm³]	V [Vol.-%]	T [°C]	f [Hz]	s_u [MPa]	s_o [MPa]	IEI [MPa]	$e_{el, anf}$ [‰]	N_{Makro} [-]
L-5	40.0	2.494	0.7	20	10	0.035	0.600	7,470	0.145	1,651
L-1	40.5	2.496	0.6				0.600	7,892	0.138	3,401
D-2	39.9	2.493	0.8				0.600	8,702	0.125	3,702
L-4	40.0	2.494	0.7			0.035	0.400	8,250	0.085	21,007
D-4	40.0	2.499	0.5				0.400	8,245	0.085	18,508
A-4	40.0	2.490	0.9				0.400	8,939	0.078	30,006
L-2	40.0	2.491	0.8			0.035	0.250	8,891	0.046	100,501
D-3	40.3	2.503	0.4				0.250	9,208	0.044	139,303
A-2	40.0	2.487	1.0				0.250	9,570	0.043	199,509

Table C-12: Results of fatigue test of new *SMA 11 S* mix with SBS bitumen 25/55-55 A

Aspaltmaterial:			SMA 11 S					Bitumen:		PMB
Durchmesser [mm]:			100							
Rohdichte ρ_m [g/cm³]:			2.525				Raumdichte ρ_b [g/cm³]:			2.461
Querdehnzahl μ [-]:			0.2984							
Pk-Nr. [-]	hohe [mm]	ρ_b [g/cm³]	V [Vol.-%]	T [°C]	f [Hz]	s_u [MPa]	s_o [MPa]	IEI [MPa]	$e_{el, anf}$ [‰]	N_{Makro} [-]
E-4	40.0	2.492	1.3	20	10	0.035	0.600	5,082	0.195	1,554
C-5	40.2	2.491	1.3				0.600	4,785	0.207	1,250
C-1	40.1	2.490	1.4				0.600	4,907	0.202	1,159
C-3	40.0	2.496	1.1			0.035	0.400	5,855	0.103	8,003
A-3	39.9	2.490	1.4				0.400	5,859	0.102	8,506
A-1	39.8	2.485	1.6				0.400	5,438	0.115	11,502
C-2	40.1	2.484	1.6			0.035	0.250	5,863	0.037	99,005
A-5	39.7	2.482	1.7				0.250	5,652	0.039	250,505
E-1	40.0	2.491	1.3				0.250	5,724	0.039	200,000

Table C-13: Results of fatigue test of RAP of surface layer without rejuvenator (S0)

Aspaltmaterial:			SMA 11 S					Bitumen:		
Durchmesser [mm]:			100							
Rohdichte ρ_m [g/cm³]:			2.495				Raumdichte ρ_b [g/cm³]:			2.419
Querdehnzahl μ [-]:			0.2984							
Pk-Nr. [-]	hohe [mm]	ρ_b [g/cm³]	V [Vol.-%]	T [°C]	f [Hz]	s_u [MPa]	s_o [MPa]	IEI [MPa]	$e_{el, anf}$ [‰]	N_{Makro} [-]
S01-4	40.0	2.455	1.6	20	10	0.035	0.600	9,764	0.150	6,252
S01-5	40.0	2.455	1.6				0.600	9,928	0.129	9,004
S03-4	40.1	2.452	1.7				0.600	9,844	0.133	8,888
S01-3	40.3	2.456	1.6			0.035	0.400	10,819	0.119	14,410
S01-2	40.3	2.467	1.1				0.400	10,887	0.091	44,410
S02-2	39.8	2.466	1.2				0.400	10,777	0.094	39,500
S01-1	40.2	2.461	1.4			0.035	0.250	10,195	0.068	273,003
S02-5	40.0	2.467	1.1				0.250	10,307	0.066	251,547
S02-3	39.8	2.463	1.3				0.250	10,618	0.063	349,747

Table C-14: Results of fatigue test of asphalt mix with rejuvenator 1 of SMA 11 S mix (S1)

Aspaltmaterial:			SMA 11 S					Bitumen:		30/45
Durchmesser [mm]:			100					Rejuvenator:		1
Rohdichte ρ_m [g/cm³]:			2.499				Raumdichte ρ_b [g/cm³]:			2.424
Querdehnzahl μ [-]:			0.2984							
Pk-Nr. [-]	hohe [mm]	ρ_b [g/cm³]	V [Vol.-%]	T [°C]	f [Hz]	s_u [MPa]	s_o [MPa]	IEI [MPa]	$e_{el, anf}$ [‰]	N_{Makro} [-]
S11-2	40.0	2.474	1.0	20	10	0.035	0.600	6,499	0.141	4,107
S11-1	40.0	2.474	1.0				0.600	6,419	0.111	9,555
S11-3	40.0	2.477	0.9				0.600	6,238	0.146	3,410
S11-5	39.5	2.476	0.9			0.035	0.400	6,900	0.080	32,904
S12-1	39.8	2.464	1.4				0.400	6,844	0.080	58,007
S12-3	39.8	2.476	0.9				0.400	6,611	0.094	49,785
S11-4	39.5	2.465	1.4			0.035	0.250	6,430	0.039	1,216,506
S12-5	39.8	2.471	1.1				0.250	6,742	0.045	542,367
S12-4	40.0	2.471	1.1				0.250	6,112	0.041	496,977

Table C-15: Results of fatigue test of asphalt mix with rejuvenator 2 of SMA 11 S mix (S2)

Aspaltmaterial:			SMA 11 S					Bitumen:		30/45
Durchmesser [mm]:			100					Rejuvenator:		2
Rohdichte ρ_m [g/cm³]:			2.497				Raumdichte ρ_b [g/cm³]:			2.422
Querdehnzahl μ [-]:			0.2984							
Pk-Nr. [-]	hohe [mm]	ρ_b [g/cm³]	V [Vol.-%]	T [°C]	f [Hz]	s_u [MPa]	s_o [MPa]	IEI [MPa]	$e_{el, anf}$ [‰]	N_{Makro} [-]
S12-3	40.2	2.464	1.3	20	10	0.035	0.600	7,138	0.128	9,007
S12-2	40.2	2.464	1.3				0.600	7,611	0.119	10,406
S22-3	40.0	2.472	1.0				0.600	6,884	0.122	8,500
S12-1	40.2	2.477	0.8			0.035	0.400	7,308	0.096	24,952
S12-5	40.2	2.475	0.9				0.400	6,886	0.079	70,109
S22-1	40.0	2.469	1.1				0.400	7,111	0.088	29,000
S12-4	40.2	2.464	1.3			0.035	0.250	7,471	0.043	999,009
S22-2	40.0	2.474	0.9				0.250	7,655	0.046	870,010
S22-5	40.1	2.478	0.8				0.250	7,448	0.041	831,498

Table C-16: Results of fatigue test of asphalt mix with rejuvenator 3 of SMA 11 S mix (S3)

Aspaltmaterial:			SMA 11 S					Bitumen:		30/45
Durchmesser [mm]:			100					Rejuvenator:		3
Rohdichte ρ_m [g/cm³]:			2.501				Raumdichte ρ_b [g/cm³]:			2.429
Querdehnzahl μ [-]:			0.2984							
Pk-Nr. [-]	hohe [mm]	ρ_b [g/cm³]	V [Vol.-%]	T [°C]	f [Hz]	s_u [MPa]	s_o [MPa]	IEI [MPa]	$e_{el, anf}$ [‰]	N_{Makro} [-]
S13-2	39.2	2.478	0.9	20	10	0.035	0.600	6,851	0.150	6,105
S13-3	39.2	2.470	1.2				0.600	7,093	0.146	6,510
S23-1	39.8	2.468	1.3				0.600	7,291	0.145	4,826
S13-1	39.2	2.474	1.1			0.035	0.400	7,336	0.098	19,557
S13-5	40.0	2.480	0.8				0.400	7,501	0.073	32,960
S23-3	39.8	2.475	1.1				0.400	7,444	0.088	20,159
S13-4	40.0	2.479	0.9			0.035	0.250	7,311	0.060	246,722
S23-5	40.0	2.475	1.0				0.250	7,766	0.064	419,877
S23-2	39.8	2.475	1.0				0.250	7,748	0.062	381,184

Table C-17: Results of fatigue test of new *AC 16 T D* mix

Aspaltmaterial:			AC 16 T D					Bitumen:		50/70
Durchmesser [mm]:			100							
Rohdichte ρ_m [g/cm³]:			2.534				Raumdichte ρ_b [g/cm³]:			2.491
Querdehnzahl μ [-]:			0.2984							
Pk-Nr. [-]	hohe [mm]	ρ_b [g/cm³]	V [Vol.-%]	T [°C]	f [Hz]	s_u [MPa]	s_o [MPa]	IEI [MPa]	$e_{el, anf}$ [‰]	N_{Makro} [-]
503-2	40.2	2.508	1.0	20	10	0.035	0.500	8,046	0.111	5,208
503-3	40.0	2.510	0.9				0.500	8,541	0.105	5,202
503-5	39.8	2.510	0.9				0.500	8,147	0.101	4,253
501-2	40.0	2.512	0.9			0.035	0.360	8,305	0.076	17,500
501-3	40.0	2.508	1.0				0.360	8,275	0.076	13,003
501-4	40.0	2.514	0.8				0.360	8,705	0.072	16,001
502-2	40.2	2.511	0.9			0.035	0.300	10,432	0.048	240,502
502-3	40.2	2.505	1.1				0.300	10,673	0.048	175,503
502-4	40.2	2.514	0.8				0.300	10,512	0.048	204,003

Table C-18: Results of fatigue test of RAP of binder layer without rejuvenator (D0)

Aspaltmaterial:			AC 16 T D					Bitumen:		50/70
Durchmesser [mm]:			100							
Rohdichte ρ_m [g/cm³]:			2.520				Raumdichte ρ_b [g/cm³]:			2.463
Querdehnzahl μ [-]:			0.2984							
Pk-Nr. [-]	hohe [mm]	ρ_b [g/cm³]	V [Vol.-%]	T [°C]	f [Hz]	s_u [MPa]	s_o [MPa]	IEI [MPa]	$e_{el, anf}$ [‰]	N_{Makro} [-]
D01-2	40.2	2.476	1.7	20	10	0.035	0.500	10,999	0.132	7,200
D01-3	39.8	2.477	1.7				0.500	10,981	0.133	9,410
D01-5	39.8	2.470	2.0				0.500	10,706	0.129	10,010
D02-2	40.0	2.477	1.7			0.035	0.360	11,117	0.09	33,000
D01-4	40.2	2.474	1.8				0.360	11,333	0.102	25,509
D02-3	40.1	2.469	2.0				0.360	11,424	0.096	22,000
D01-1	40.2	2.470	2.0			0.035	0.300	10,641	0.065	192,009
D02-1	39.8	2.481	1.5				0.300	11,417	0.064	340,044
D02-4	40.1	2.477	1.7				0.300	11,627	0.055	253,555

Table C-19: Results of fatigue test of asphalt mix with rejuvenator 1 of *AC 16 T D* mix (D1)

Aspaltmaterial:			AC 16 T D					Bitumen:		50/70
Durchmesser [mm]:			100					Rejuvenator:		1
Rohdichte ρ_m [g/cm³]:			2.522				Raumdichte ρ_b [g/cm³]:			2.477
Querdehnzahl μ [-]:			0.2984							
Pk-Nr. [-]	hohe [mm]	ρ_b [g/cm³]	V [Vol.-%]	T [°C]	f [Hz]	s_u [MPa]	s_o [MPa]	IEI [MPa]	$e_{el,\ anf}$ [‰]	N_{Makro} [-]
592-4	39.8	2.500	0.9	20	10	0.035	0.500	7,719	0.143	3,601
592-5	39.8	2.505	0.7				0.500	7,747	0.143	3,502
593-1	40.2	2.495	1.1				0.500	7,723	0.143	3,550
592-2	40.4	2.496	1.0			0.035	0.360	8,285	0.084	34,000
593-3	40.2	2.501	0.8				0.360	7,955	0.086	32,148
593-5	40.0	2.499	0.9				0.360	7,984	0.085	33,458
592-1	40.4	2.497	1.0			0.035	0.300	7,591	0.067	127,507
593-2	40.2	2.496	1.0				0.300	7,664	0.068	134,685
593-4	40.0	2.495	1.1				0.300	7,617	0.065	129,504

Table C-20: Results of fatigue test of asphalt mix with rejuvenator 2 of *AC 16 T D* mix (D2)

Aspaltmaterial:			AC 16 T D					Bitumen:		50/70
Durchmesser [mm]:			100					Rejuvenator:		2
Rohdichte ρ_m [g/cm³]:			2.519				Raumdichte ρ_b [g/cm³]:			2.469
Querdehnzahl μ [-]:			0.2984							
Pk-Nr. [-]	hohe [mm]	ρ_b [g/cm³]	V [Vol.-%]	T [°C]	f [Hz]	s_u [MPa]	s_o [MPa]	IEI [MPa]	$e_{el,\ anf}$ [‰]	N_{Makro} [-]
D22-2	39.5	2.502	0.7	20	10	0.035	0.500	7,997	0.115	6,759
D22-3	39.2	2.502	0.7				0.500	7,946	0.117	8,654
D23-1	39.8	2.499	0.8				0.500	7,647	0.120	5,832
D22-1	39.2	2.495	1.0			0.035	0.360	7,529	0.096	15,355
D22-4	39.5	2.496	0.9				0.360	8,178	0.052	76,502
D23-2	39.8	2.492	1.1				0.360	7,894	0.077	33,666
D22-5	39.5	2.492	1.1			0.035	0.300	7,896	0.042	222,005
D23-4	40.0	2.496	0.9				0.300	7,611	0.037	190,272
D23-5	40.0	2.492	1.1				0.300	8,214	0.040	277,669

Table C-21: Results of fatigue test of asphalt mix with rejuvenator 3 of *AC 16 T D* mix (D3)

Aspaltmaterial:			AC 16 T D					Bitumen:		50/70
Durchmesser [mm]:			100					Rejuvenator:		3
Rohdichte ρ_m [g/cm³]:			2.525				Raumdichte ρ_b [g/cm³]:			2.479
Querdehnzahl μ [-]:			0.2984							
Pk-Nr. [-]	hohe [mm]	ρ_b [g/cm³]	V [Vol.-%]	T [°C]	f [Hz]	s_u [MPa]	s_o [MPa]	IEI [MPa]	$e_{el, anf}$ [‰]	N_{Makro} [-]
590-2	40.0	2.499	1.0	20	10	0.035	0.500	6,713	0.135	3,709
590-5	40.2	2.502	0.9				0.500	6,545	0.142	10,502
595-3	40.0	2.498	1.1				0.500	6,822	0.135	7,453
590-1	40.0	2.505	0.8			0.035	0.360	6,276	0.084	42,869
590-3	39.8	2.499	1.0				0.360	6,019	0.084	58,007
595-5	40.0	2.499	1.0				0.360	6,111	0.052	49,785
590-4	40.2	2.502	0.9			0.035	0.300	6,447	0.036	648,002
595-1	40.0	2.495	1.2				0.300	6,574	0.035	542,367
595-2	40.0	2.496	1.1				0.300	6,388	0.035	610,548

Table C-22: Results of fatigue test of new *AC 22 T S* mix with bitumen grade 30/45

Aspaltmaterial:			AC 22 T S					Bitumen:		30/45
Durchmesser [mm]:			150							
Rohdichte ρ_m [g/cm³]:			2.623				Raumdichte ρ_b [g/cm³]:			2.462
Querdehnzahl μ [-]:			0.2984							
Pk-Nr. [-]	hohe [mm]	ρ_b [g/cm³]	V [Vol.-%]	T [°C]	f [Hz]	s_u [MPa]	s_o [MPa]	IEI [MPa]	$e_{el, anf}$ [‰]	N_{Makro} [-]
G-1	60.1	2.541	3.1	20	10	0.035	0.900	14,394	0.116	3,404
I-2	60.1	2.505	4.5				0.900	14,606	0.114	1,659
J-2	60.1	2.535	3.4				0.900	15,235	0.109	2,758
D-2	60.1	2.526	3.7			0.035	0.650	16,090	0.074	16,508
A-2	60.1	2.522	3.9				0.650	17,403	0.068	13,002
H-2	60.1	2.516	4.1				0.650	15,823	0.075	13,010
D-1	60.1	2.529	3.6			0.035	0.350	16,184	0.038	478,104
C-1	60.1	2.529	3.6				0.350	16,132	0.038	463,502
A-1	60.1	2.525	3.7				0.350	16,599	0.037	837,005

Table C-23: Results of fatigue test of new *AC 22 T S* mix with bitumen grade 50/70

Aspaltmaterial:			AC 22 T S					Bitumen:		50/70
Durchmesser [mm]:			150							
Rohdichte ρ_m [g/cm³]:			2.625				Raumdichte ρ_b [g/cm³]:			2.484
Querdehnzahl μ [-]:			0.2984							
Pk-Nr. [-]	hohe [mm]	ρ_b [g/cm³]	V [Vol.-%]	T [°C]	f [Hz]	s_u [MPa]	s_o [MPa]	IEI [MPa]	$e_{el, anf}$ [‰]	N_{Makro} [-]
F-1	60.3	2.519	4.0	20	10	0.035	0.900	11,772	0.125	906
G-1	60.1	2.516	4.2				0.900	11,892	0.124	1,053
B-1	60.1	2.516	4.2				0.900	12,022	0.122	953
B-2	60.0	2.512	4.3			0.035	0.650	12,223	0.058	15,010
E-2	60.0	2.524	3.8				0.650	12,329	0.057	17,510
K-1	60.1	2.535	3.4				0.650	13,558	0.052	40,002
A-2	60.5	2.518	4.1			0.035	0.350	12,515	0.029	313,502
G-2	60.1	2.509	4.4				0.350	12,534	0.028	388,504
H-1	60.5	2.519	4.0				0.350	13,508	0.026	279,005

Table C-24: Results of fatigue test of RAP from base layer without rejuvenator (T0)

Aspaltmaterial:			AC 22 T S					Bitumen:		
Durchmesser [mm]:			150							
Rohdichte ρ_m [g/cm³]:			2.595				Raumdichte ρ_b [g/cm³]:			2.429
Querdehnzahl μ [-]:			0.2984							
Pk-Nr. [-]	hohe [mm]	ρ_b [g/cm³]	V [Vol.-%]	T [°C]	f [Hz]	s_u [MPa]	s_o [MPa]	IEI [MPa]	$e_{el, anf}$ [‰]	N_{Makro} [-]
T01-4	59.9	2.465	5.0	20	10	0.035	0.900	12,670	0.092	9,953
T02-4	59.8	2.468	4.9				0.900	12,710	0.106	7,777
T02-2	60.0	2.468	4.9				0.900	12,558	0.096	8,888
T01-3	60.0	2.463	5.1			0.035	0.650	12,555	0.078	33,501
T01-1	59.2	2.480	4.4				0.650	11,359	0.058	95,109
T02-5	59.8	2.463	5.1				0.650	12,107	0.066	87,254
T01-2	59.2	2.468	4.9			0.035	0.350	12,126	0.043	129,004
T02-1	60.0	2.478	4.5				0.350	12,104	0.040	181,374
T02-3	60.0	2.480	4.4				0.350	11,855	0.036	242,814

Table C-25: Results of fatigue test of asphalt mix with rejuvenator 1 of *AC 22 T S* mix (T1)

Aspaltmaterial:			AC 22 T S					Bitumen:		30/45
Durchmesser [mm]:			150					Rejuvenator:		1
Rohdichte ρ_m [g/cm³]:			2.606				Raumdichte ρ_b [g/cm³]:			2.441
Querdehnzahl μ [-]:			0.2984							
Pk-Nr. [-]	hohe [mm]	ρ_b [g/cm³]	V [Vol.-%]	T [°C]	f [Hz]	s_u [MPa]	s_o [MPa]	IEI [MPa]	$e_{el, anf}$ [‰]	N_{Makro} [-]
T31-1	59.2	2.502	4.0	20	10	0.035	0.900	8,723	0.096	2,501
T21-1	59.5	2.509	3.7				0.900	8,478	0.095	2,507
T11-1	59.3	2.508	3.8				0.900	10,838	0.091	3,351
T11-2	59.3	2.509	3.7			0.035	0.650	11,842	0.032	75,423
T41-1	60	2.516	3.5				0.650	11,973	0.033	84,001
T51-2	59.8	2.516	3.5				0.650	12,043	0.032	85,017
T31-2	59.2	2.508	3.8			0.035	0.350	10,448	0.038	111,000
T51-1	59.8	2.519	3.3				0.350	12,133	0.036	124,812
T41-2	60	2.509	3.7				0.350	13,439	0.029	133,508

Table C-26: Results of fatigue test of asphalt mix with rejuvenator 2 of *AC 22 T S* mix (T2)

Aspaltmaterial:			AC 22 T S					Bitumen:		30/45
Durchmesser [mm]:			150					Rejuvenator:		2
Rohdichte ρ_m [g/cm³]:			2.602				Raumdichte ρ_b [g/cm³]:			2.445
Querdehnzahl μ [-]:			0.2984							
Pk-Nr. [-]	hohe [mm]	ρ_b [g/cm³]	V [Vol.-%]	T [°C]	f [Hz]	s_u [MPa]	s_o [MPa]	IEI [MPa]	$e_{el, anf}$ [‰]	N_{Makro} [-]
T32-2	60.2	2.505	3.7	20	10	0.035	0.900	9,150	0.097	2,454
T22-2	60.5	2.516	3.3				0.900	8,486	0.087	9,359
T42-2	59.8	2.509	3.6				0.900	8,777	0.092	7,851
T22-1	60.5	2.517	3.3			0.035	0.650	8,319	0.072	21,405
T12-2	60.0	2.500	3.9				0.650	7,803	0.067	42,756
T12-1	60.0	2.500	3.9				0.650	9,946	0.035	57,760
T32-1	60.2	2.509	3.6			0.035	0.350	10,560	0.021	1,333,506
T42-1	59.8	2.519	3.2				0.350	9,944	0.026	492,373
T52-2	60.0	2.498	4.0				0.350	10,243	0.028	386,975

Table C-27: Results of fatigue test of asphalt mix with rejuvenator 3 of *AC 22 T S* mix (T3)

Aspaltmaterial:			AC 22 T S					Bitumen:		30/45
Durchmesser [mm]:			150					Rejuvenator:		3
Rohdichte ρ_m [g/cm³]:			2.605				Raumdichte ρ_b [g/cm³]:			2.446
Querdehnzahl μ [-]:			0.2984							
Pk-Nr. [-]	hohe [mm]	ρ_b [g/cm³]	V [Vol.-%]	T [°C]	f [Hz]	s_u [MPa]	s_o [MPa]	IEI [MPa]	$e_{el, anf}$ [‰]	N_{Makro} [-]
T43-1	60.0	2.499	4.1	20	10	0.035	0.900	7,798	0.104	1,405
T53-2	59.7	2.508	3.7				0.900	7,666	0.094	5,942
T23-2	59.9	2.503	3.9				0.900	9,653	0.101	4,654
T53-1	59.6	2.503	3.9			0.035	0.650	9,733	0.083	25,447
T13-2	60.0	2.501	4.0				0.650	10,278	0.079	12,405
T43-2	60.0	2.517	3.4				0.650	9,882	0.086	12,005
T33-2	59.8	2.509	3.7			0.035	0.350	8,086	0.049	91,501
T33-1	59.8	2.517	3.4				0.350	7,965	0.049	103,510
T23-1	59.5	2.517	3.4				0.350	8,840	0.035	657,198

Appendix D

Results of low temperature behavior

Table D-1: Uniaxial tension stress test (UTST) of new SMA 11 S mix with virgin bitumen 30/45

Pk. Nr.	E-1	E-2	F-2	Average
Raumdichte ρ_b [g/cm³]:	2.481	2.491	2.495	
Width, [mm]	40.1	40.0	40.0	
Length, [mm]	160.1	159.8	159.6	
Spannung bei -40 °C [kPA]	-	-	-	
Spannung bei -35 °C [kPA]	-	-	-2,104.31	
Spannung bei -30 °C [kPA]	-	-1,872.15	-2,282.22	
Spannung bei -25 °C [kPA]	-4,665.09	-3,230.94	-4,086.91	3,994.32
Spannung bei -20 °C [kPA]	-3,293.47	-2,427.48	-2,732.14	
Spannung bei -15 °C [kPA]	-2,065.12	-1,383.66	-1,581.74	
Spannung bei -10 °C [kPA]	-1,214.65	-709.08	-839.30	921.01
Spannung bei -5 °C [kPA]	-669.62	-329.15	-406.72	
Spannung bei 0 °C [kPA]	-370.75	-115.85	-189.21	
Spannung bei 5 °C [kPA]	-203.53	-65.82	-82.44	117.26
Spannung bei 10 °C [kPA]	-113.97	-32.60	-34.27	
Spannung bei 15 °C [kPA]	-53.97	-14.94	-14.09	
Spannung bei 20 °C [kPA]	-2.45	-3.12	-3.18	2.92
Failure point				
max. Spannung [Mpa]	4.678	3.707	4.126	4.171
Temperatur [°C]	-25.1	-24.8	-25.2	-25.0
Zeilenzähler	16,272	16,161	16,335	

Table D-2: Thermal stress restrained specimen test (TSRST) of new SMA 11 S mix with virgin bitumen 30/45

Temperature, [ºC]	-25			-10		
Pk-Nr.	F-1	F-5	J-5	H-3	H-4	H-5
Width, [mm]	40.3	40.2	40.1	40.1	40.1	40.1
Length, [mm]	160.1	160.2	159.8	159.7	159.9	159.8
Raumdichte ρ_b [g/cm³]:	2.490	2.490	2.493	2.500	2.487	2.484
Maximale Zugfestigkeit [Mpa]	3.934	4.141	4.186	5.744	5.611	5.472
Maximale Bruchdehnung [%]	0.02	0.02	0.02	0.04	0.04	0.04
Zeilenzähler max. Bruchd.	322	718	731	724	804	724
Temperature, [ºC]	5			20		
Pk-Nr.	E-5	F-3	H-2	E-3	E-4	H-1
Width, [mm]	40.0	40.1	40.0	40.1	40.2	40.2
Length, [mm]	160.0	160.1	159.9	159.7	159.6	160.0
Raumdichte ρ_b [g/cm³]:	2.480	2.498	2.489	2.488	2.493	2.487
Maximale Zugfestigkeit [Mpa]	3.944	4.198	4.166	0.958	0.868	0.915
Maximale Bruchdehnung [%]	0.31	0.30	0.28	0.64	0.74	0.74
Zeilenzähler max. Bruchd.	949	1,698	849	1,077	1,075	1,581

Table D-3: Uniaxial tension stress test (UTST) of new SMA 11 S mix with virgin bitumen PMB

Pk. Nr.	D-4	I-1	I-5	Average
Raumdichte ρ_b [g/cm³]:	2.480	2.481	2.471	
Width, [mm]	40.1	40.3	40.1	
Length, [mm]	160.2	160.1	159.9	
Spannung bei -40 °C [kPA]	-	-	-	
Spannung bei -35 °C [kPA]	431.36	237.73	-	
Spannung bei -30 °C [kPA]	-4,052.81	-4,019.65	-4,002.03	
Spannung bei -25 °C [kPA]	-2,629.20	-2,526.96	-2,659.38	2,605.18
Spannung bei -20 °C [kPA]	-1,545.93	-1,528.64	-1,554.26	
Spannung bei -15 °C [kPA]	-817.21	-822.61	-815.75	
Spannung bei -10 °C [kPA]	-385.56	-413.90	-386.95	395.47
Spannung bei -5 °C [kPA]	-178.71	-208.33	-182.31	
Spannung bei 0 °C [kPA]	-74.55	-96.47	-80.57	
Spannung bei 5 °C [kPA]	-29.98	-51.51	-32.21	37.90
Spannung bei 10 °C [kPA]	-10.88	-27.29	-17.08	
Spannung bei 15 °C [kPA]	-0.64	-15.50	-13.13	
Spannung bei 20 °C [kPA]	0.96	-4.78	1.40	0.81
Failure point				Average
max. Spannung [Mpa]	4.354	4.372	4.522	4.416
Temperatur [°C]	-31.1	-31.3	-32.1	-31.5
Zeilenzähler	18,413	18,509	18,813	

Table D-4: Thermal stress restrained specimen test (TSRST) of new SMA 11 S mix with virgin bitumen PMB

Temperature, [ºC]	-25			-10		
Pk-Nr.	K-2	K-4	L-4	L-2	L-3	L-5
Width, [mm]	40.1	40.2	40.0	40.1	40.1	40.1
Length, [mm]	159.8	160.2	159.8	159.6	160.2	159.7
Raumdichte ρ_b [g/cm³]:	2.478	2.480	2.479	2.488	2.480	2.466
Maximale Zugfestigkeit [Mpa]	4.888	4.596	5.191	6.038	6.717	5.964
Maximale Bruchdehnung [%]	0.02	0.02	0.02	0.07	0.10	0.08
Zeilenzähler max. Bruchd.	689	710	740	909	811	1,626
Temperature, [ºC]	5			20		
Pk-Nr.	I-3	K-1	L-1	D-5	I-2	I-4
Width, [mm]	40.1	40.3	40.0	40.2	40.1	40.0
Length, [mm]	159.8	159.8	159.6	159.8	160.1	160.0
Raumdichte ρ_b [g/cm³]:	2.493	2.471	2.471	2.469	2.494	2.484
Maximale Zugfestigkeit [Mpa]	2.659	2.538	2.605	0.538	0.559	0.603
Maximale Bruchdehnung [%]	0.37	0.34	0.39	1.09	0.98	0.93
Zeilenzähler max. Bruchd.	820	842	851	1,481	1,203	1,313

Table D-5: Uniaxial tension stress test (UTST) of SMA 11 S mix with RAP and rejuvenator 1

Pk. Nr.	S 21-5	S 31-3	S 41-3	Average
Raumdichte ρ_b [g/cm³]:	2.423	2.423	2.42	
Width, [mm]	39.7	39.8	39.8	
Length, [mm]	162.5	161.0	160.3	
Spannung bei -40 °C [kPA]	-	-	-	
Spannung bei -35 °C [kPA]	-	-66.97	42.01	
Spannung bei -30 °C [kPA]	-	492.77	338.85	
Spannung bei -25 °C [kPA]	-4,275.87	-4,318.98	-4,430.19	4,341.68
Spannung bei -20 °C [kPA]	-2,956.89	-2,944.70	-3,010.41	
Spannung bei -15 °C [kPA]	-1,851.09	-1,851.79	-1,912.03	
Spannung bei -10 °C [kPA]	-1,086.36	-1,078.45	-1,104.91	1,089.91
Spannung bei -5 °C [kPA]	-567.73	-581.83	-609.02	
Spannung bei 0 °C [kPA]	-288.15	-284.84	-281.74	
Spannung bei 5 °C [kPA]	-156.89	-162.76	-168.38	162.67
Spannung bei 10 °C [kPA]	-60.60	-63.46	-72.26	
Spannung bei 15 °C [kPA]	-23.77	-26.03	-27.80	
Spannung bei 20 °C [kPA]	8.55	7.46	5.41	7.14
Failure point				
max. Spannung [Mpa]	5.048	5.060	4.970	5.026
Temperatur [°C]	-28.2	-28.1	-27.4	-27.9
Zeilenzähler	17,412	17,326	17,120	

Table D-6: Thermal stress restrained specimen test (TSRST) of SMA 11 S mix RAP and rejuvenator 1

Temperature, [ºC]	-25			-10		
Pk-Nr.	S 31-5	S 31-4	S 41-2	S 21-4	S 31-2	S 41-1
Width, [mm]	39.8	39.8	39.9	39.7	39.8	39.9
Length, [mm]	161.8	161.2	160.8	161.9	160.1	161.0
Raumdichte ρ_b [g/cm³]:	2.421	2.421	2.425	2.421	2.426	2.416
Maximale Zugfestigkeit [Mpa]	4.663	5.433	4.617	5.454	6.894	6.692
Maximale Bruchdehnung [%]	0.02	0.02	0.02	0.04	0.06	0.06
Zeilenzähler max. Bruchd.	561	1,275	652	692	735	717
Temperature, [ºC]	5			20		
Pk-Nr.	S 21-1	S 21-2	S 41-5	S 21-3	S 31-1	S 41-4
Width, [mm]	39.8	39.8	39.9	39.6	39.8	39.8
Length, [mm]	160.0	160.7	159.7	161.0	160.0	160.0
Raumdichte ρ_b [g/cm³]:	2.418	2.426	2.419	2.427	2.413	2.424
Maximale Zugfestigkeit [Mpa]	4.104	4.304	4.409	1.423	1.405	1.408
Maximale Bruchdehnung [%]	0.23	0.23	0.23	0.50	0.47	0.52
Zeilenzähler max. Bruchd.	791	784	742	824	788	893

Table D-7: Uniaxial tension stress test (UTST) of SMA 11 S mix with RAP and rejuvenator 2

Pk. Nr.	S 52-2	S42-5	S32-4	Average
Raumdichte ρ_b [g/cm³]:	2.412	2.418	2.422	
Width, [mm]	39.5	39.5	39.5	
Length, [mm]	158.4	159.6	158.8	
Spannung bei -40 °C [kPA]	-	-	-	
Spannung bei -35 °C [kPA]	-	-	-126.52	
Spannung bei -30 °C [kPA]	-	-	-24.37	
Spannung bei -25 °C [kPA]	-4,543.90	-	-4,408.33	4543.90
Spannung bei -20 °C [kPA]	-3,129.11	-3,122.30	-2,995.20	
Spannung bei -15 °C [kPA]	-1,949.30	-1,918.41	-1,838.53	
Spannung bei -10 °C [kPA]	-1,126.22	-1,095.84	-1,049.77	1090.61
Spannung bei -5 °C [kPA]	-589.26	-576.64	-531.54	
Spannung bei 0 °C [kPA]	-291.24	-289.11	-257.08	
Spannung bei 5 °C [kPA]	-134.30	-106.15	-102.28	114.24
Spannung bei 10 °C [kPA]	-61.33	-56.74	-51.66	
Spannung bei 15 °C [kPA]	-27.49	-24.63	-19.36	
Spannung bei 20 °C [kPA]	-2.58	2.12	6.18	1.91
Failure point				Average
max. Spannung [Mpa]	4.885	4.408	4.542	4.612
Temperatur [°C]	-26.5	-24.7	-25.7	-25.6
Zeilenzähler	16,807	16,134	16,500	

Table D-8: Thermal stress restrained specimen test (TSRST) of SMA 11 S mix RAP and rejuvenator 2

Temperature, [ºC]	-25			-10		
Pk-Nr.	S32-5	S42-3	S42-4	S32-2	S52-4	S52-6
Width, [mm]	39.5	39.8	39.8	39.6	39.4	39.5
Length, [mm]	158.9	159.3	159.5	158.7	159.0	159.1
Raumdichte ρ_b [g/cm³]:	2.415	2.420	2.416	2.420	2.421	2.414
Maximale Zugfestigkeit [Mpa]	5.201	4.752	4.292	6.306	6.736	6.419
Maximale Bruchdehnung [%]	0.02	0.02	0.02	0.05	0.05	0.05
Zeilenzähler max. Bruchd.	627	645	1,091	706	721	688
Temperature, [ºC]	5			20		
Pk-Nr.	S42-2	S42-6	S52-3	S32-3	S52-1	S52-5
Width, [mm]	39.5	39.6	39.9	39.6	39.8	39.4
Length, [mm]	159.2	159.4	158.6	158.9	158.2	158.8
Raumdichte ρ_b [g/cm³]:	2.409	2.422	2.419	2.427	2.407	2.416
Maximale Zugfestigkeit [Mpa]	4.894	4.866	4.977	1.421	1.545	1.576
Maximale Bruchdehnung [%]	0.254	0.253	0.200	0.548	0.507	0.516
Zeilenzähler max. Bruchd.	817	1,381	799	910	870	870

Table D-9: Uniaxial tension stress test (UTST) of SMA 11 S mix with RAP and rejuvenator 3

Pk. Nr.	S 43-5	S 53-2	S 53-3	Average
Raumdichte ρ_b [g/cm³]:	2.423	2.416	2.420	
Width, [mm]	39.6	39.4	39.8	
Length, [mm]	158.4	160.2	160.1	
Spannung bei -40 °C [kPA]	-	-	-	
Spannung bei -35 °C [kPA]	-	-	-	
Spannung bei -30 °C [kPA]	-	-	-	
Spannung bei -25 °C [kPA]	-4,399.60	-	-4,425.57	4,412.59
Spannung bei -20 °C [kPA]	-2,939.65	-3,204.23	-3,044.13	
Spannung bei -15 °C [kPA]	-1,779.19	-2,033.35	-1,888.55	
Spannung bei -10 °C [kPA]	-986.93	-1,155.83	-1,051.88	1,064.88
Spannung bei -5 °C [kPA]	-504.89	-610.11	-554.42	
Spannung bei 0 °C [kPA]	-238.32	-305.57	-268.75	
Spannung bei 5 °C [kPA]	-107.76	-96.30	-103.97	102.68
Spannung bei 10 °C [kPA]	-56.54	-68.96	-56.913	
Spannung bei 15 °C [kPA]	-27.94	-29.23	-26.27	
Spannung bei 20 °C [kPA]	0.91	2.99	3.34	2.411
Failure point				Average
max. Spannung [Mpa]	4.906	3.919	4.762	4.529
Temperatur [°C]	-26.9	-22.7	-26.5	-25.4
Zeilenzähler	16,924	15,418	16,762	

Table D-10: Thermal stress restrained specimen test (TSRST) of SMA 11 S mix RAP and rejuvenator 3

Temperature, [ºC]	-20			-10		
Pk-Nr.	S 33-4	S 43-4	S 53-4	S 43-2	S 43-6	S 53-6
Width, [mm]	39.4	39.3	39.7	39.5	39.7	39.4
Length, [mm]	158.8	158.4	159.9	158.4	158.8	159.7
Raumdichte ρ_b [g/cm³]:	2.421	2.419	2.422	2.424	2.418	2.417
Maximale Zugfestigkeit [Mpa]	4.871	3.223	4.704	6.720	7.088	6.644
Maximale Bruchdehnung [%]	0.02	0.01	0.02	0.05	0.06	0.05
Zeilenzähler max. Bruchd.	612	509	611	872	812	747
Temperature, [ºC]	5			20		
Pk-Nr.	S 33-5	S 33-6	S 53-1	S 33-3	S 43-3	S 53-5
Width, [mm]	39.8	39.4	39.5	39.6	39.5	39.5
Length, [mm]	158.8	158.7	160.2	158.9	158.4	159.8
Raumdichte ρ_b [g/cm³]:	2.418	2.417	2.424	2.419	2.426	2.416
Maximale Zugfestigkeit [Mpa]	4.819	4.886	4.595	1.462	1.354	1.510
Maximale Bruchdehnung [%]	0.25	0.22	0.23	0.58	0.65	0.62
Zeilenzähler max. Bruchd.	857	832	1,482	921	991	968

Table D-11: Uniaxial tension stress test (UTST) of new AC 16 T D mix with virgin bitumen 50/70

Pk. Nr.	504-1	505-2	505-3	Average
Raumdichte ρ_b [g/cm³]:	2.512	2.509	2.511	
Width, [mm]	49.7	49.7	49.7	
Length, [mm]	159.5	160.2	161.4	
Spannung bei -40 °C [kPA]	-	-	-	
Spannung bei -35 °C [kPA]	-	-	-	
Spannung bei -30 °C [kPA]	-5,066.79		-4,870.37	
Spannung bei -25 °C [kPA]	-3,280.15	-3,451.79	-3,204.83	3,312.26
Spannung bei -20 °C [kPA]	-1,933.73	-1,983.22	-1,819.24	
Spannung bei -15 °C [kPA]	-974.62	-1,032.06	-910.52	
Spannung bei -10 °C [kPA]	-431.99	-470.36	-395.38	432.57
Spannung bei -5 °C [kPA]	-165.93	-182.54	-151.63	
Spannung bei 0 °C [kPA]	-71.76	-70.35	-59.75	
Spannung bei 5 °C [kPA]	-32.29	-33.54	-24.17	29.99
Spannung bei 10 °C [kPA]	-14.11	-19.12	-10.51	
Spannung bei 15 °C [kPA]	-6.54	-11.42	-4.53	
Spannung bei 20 °C [kPA]	-0.62	2.51	5.34	2.41
Failure point				
max. Spannung [Mpa]	5.717	5.104	5.062	5.295
Temperatur [°C]	-32.0	-29.8	-30.8	-30.9
Zeilenzähler	18,736	17,970	18,311	

Table D-12: Thermal stress restrained specimen test (TSRST) of new AC 16 T D mix with virgin bitumen 50/70

Temperature, [ºC]	-25			-10		
Pk-Nr.	506-1	506-2	506-4	504-4	505-5	506-5
Width, [mm]	49.6	49.6	49.6	49.7	49.3	49.6
Length, [mm]	161.0	160.5	160.5	159.5	161.6	160.0
Raumdichte ρ_b [g/cm³]:	2.509	2.510	2.513	2.512	2.519	2.505
Maximale Zugfestigkeit [Mpa]	6.535	6.232	5.705	7.333	6.628	7.241
Maximale Bruchdehnung [%]	0.02	0.02	0.02	0.08	0.06	0.07
Zeilenzähler max. Bruchd.	790	773	758	923	872	918
Temperature, [ºC]	5			20		
Pk-Nr.	504-3	505-4	506-3	504-2	504-5	505-1
Width, [mm]	49.6	49.6	49.6	49.7	49.6	49.9
Length, [mm]	159.5	161.1	160.5	159.5	159.5	161.5
Raumdichte ρ_b [g/cm³]:	2.512	2.517	2.507	2.512	2.505	2.515
Maximale Zugfestigkeit [Mpa]	3.601	3.405	3.581	0.683	0.736	0.625
Maximale Bruchdehnung [%]	0.34	0.35	0.37	0.85	0.87	1.28
Zeilenzähler max. Bruchd.	910	905	905	1,127	1,125	1,455

Table D-13: Uniaxial tension stress test (UTST) of AC 16 T D mix with RAP and rejuvenator 1

Pk. Nr.	D41-1	D41-3	D61-1	Average
Raumdichte ρ_b [g/cm³]:	2.487	2.489	2.476	
Width, [mm]	49.5	49.5	49.6	
Length, [mm]	159.5	159.5	159.0	
Spannung bei -40 °C [kPA]	-	-	-	
Spannung bei -35 °C [kPA]	-	-	-5,619.76	
Spannung bei -30 °C [kPA]	-4,259.64	-	-4166.90	
Spannung bei -25 °C [kPA]	-2,893.36	-1451.38	-2794.29	2,379.68
Spannung bei -20 °C [kPA]	-1,830.07	-1836.14	-1837.71	
Spannung bei -15 °C [kPA]	-1,058.85	-1078.71	-1058.10	
Spannung bei -10 °C [kPA]	-574.24	-575.19	-591.95	580.46
Spannung bei -5 °C [kPA]	-321.04	-296.64	-288.56	
Spannung bei 0 °C [kPA]	-137.44	-148.87	-166.86	
Spannung bei 5 °C [kPA]	-73.68	-71.90	-71.56	72.38
Spannung bei 10 °C [kPA]	-36.93	-36.08	-36.24	
Spannung bei 15 °C [kPA]	-14.39	-16.34	-14.59	
Spannung bei 20 °C [kPA]	-0.37	4.11	6.42	3.39
Failure point				
max. Spannung [Mpa]	5.550		5.674	5.612
Temperatur [°C]	-34.4		-35.5	-34.3
Zeilenzähler	19638	14947	20025	

Table D-14: Thermal stress restrained specimen test (TSRST) of AC 16 T D mix with RAP and rejuvenator 1

Temperature, [ºC]	-25			-10		
Pk-Nr.	D61-2	D61-3	failed	D51-3	failed	failed
Width, [mm]	49.7	49.7		49.6		
Length, [mm]	159.4	159.4		159.6		
Raumdichte ρ_b [g/cm³]:	2.490	2.495		2.491		
Maximale Zugfestigkeit [Mpa]	5.245	4.796		6.935		
Maximale Bruchdehnung [%]	0.02	0.02		0.06		
Zeilenzähler max. Bruchd.	856	730		1,062		
Temperature, [ºC]	5			20		
Pk-Nr.	D41-4	D41-5	failed	D41-2	D51-2	D61-5
Width, [mm]	49.5	49.5		49.5	49.8	49.9
Length, [mm]	159.5	159.5		159.5	159.7	160
Raumdichte ρ_b [g/cm³]:	2.481	2.488		2.496	2.483	2.474
Maximale Zugfestigkeit [Mpa]	3.511	3.436		1.111	1.073	1.108
Maximale Bruchdehnung [%]	0.27	0.26		0.63	0.53	0.59
Zeilenzähler max. Bruchd.	1,490	860		960	849	929

Table D-15: Uniaxial tension stress test (UTST) of AC 16 T D mix with RAP and rejuvenator 2

Pk. Nr.	D22-2	D32-5	D42-5	Average
Raumdichte ρ_b [g/cm³]:	2.505	2.500	2.508	
Width, [mm]	49.5	49.4	49.5	
Length, [mm]	160.7	159.9	160.0	
Spannung bei -40 °C [kPA]	-	-	-	
Spannung bei -35 °C [kPA]	-4,987.18	-	-5,009.30	
Spannung bei -30 °C [kPA]	-3,518.96	-3,588.45	-2,992.54	
Spannung bei -25 °C [kPA]	-2,088.13	-2,261.51	-2,056.06	2,088.13
Spannung bei -20 °C [kPA]	-1,241.62	-1,298	-974.38	
Spannung bei -15 °C [kPA]	-586.44	-691.21	-470.64	
Spannung bei -10 °C [kPA]	-223.66	-324.22	-210.89	252.93
Spannung bei -5 °C [kPA]	-116.71	-138.34	-121.06	
Spannung bei 0 °C [kPA]	-54.35	-71.24	-49.20	
Spannung bei 5 °C [kPA]	-34.11	-37.41	-28.41	33.31
Spannung bei 10 °C [kPA]	-20.32	-21.58	-17.95	
Spannung bei 15 °C [kPA]	-11.54	-12.52	-10.03	
Spannung bei 20 °C [kPA]	1.69	-0.16	1.04	0.86
Failure point				avg
max. Spannung [Mpa]	5.499	4.671	5.620	5.264
Temperatur [°C]	-36.3	-34.1	-36.1	-35.5
Zeilenzähler	20,648	19,519	21,955	

Table D-16: Thermal stress restrained specimen test (TSRST) of AC 16 T D mix with RAP and rejuvenator 2

Temperature, [ºC]	-25			-10		
Pk-Nr.	D22-3	D32-4	D42-4	D32-3	D42-1	D42-3
Width, [mm]	49.5	49.5	49.4	49.7	49.7	49.7
Length, [mm]	160.8	159.6	160.0	159.2	160.4	160.0
Raumdichte ρ_b [g/cm³]:	2.507	2.503	2.501	2.505	2.503	2.501
Maximale Zugfestigkeit [Mpa]	6.395	6.260	6.373	7.044	7.673	7.506
Maximale Bruchdehnung [%]	0.03	0.03	0.03	0.09	0.12	0.12
Zeilenzähler max. Bruchd.	911	1,541	853	1,014	1,046	1,065
Temperature, [ºC]	5			20		
Pk-Nr.	D32-1	D32-2	D42-2	D22-1	D22-4	D22-5
Width, [mm]	49.4	49.3	49.8	49.4	49.6	49.4
Length, [mm]	158.5	158.8	160.4	161.0	160.5	160.5
Raumdichte ρ_b [g/cm³]:	2.507	2.505	2.501	2.518	2.500	2.496
Maximale Zugfestigkeit [Mpa]	3.296	2.849	3.075	0.794	0.758	0.750
Maximale Bruchdehnung [%]	0.39	0.19	0.42	0.96	1.06	1.26
Zeilenzähler max. Bruchd.	1,015	756	1,678	1,217	1,365	1,524

Table D-17: Uniaxial tension stress test (UTST) of AC 16 T D mix with RAP and rejuvenator 3

Pk. Nr.	D23-3	D23-5	D53-1	Average
Raumdichte ρ_b [g/cm³]:	2.494	2.492	2.491	
Width, [mm]	49.0	49.0	49.3	
Length, [mm]	160.0	160.0	159.3	
Spannung bei -40 °C [kPA]	-	-	-	
Spannung bei -35 °C [kPA]	-5,577.86	-	-5,821.57	
Spannung bei -30 °C [kPA]	-3,813.77	-3,370.39	-4,253.16	
Spannung bei -25 °C [kPA]	-2,493.76	-2,126.37	-2,602.90	2,407.68
Spannung bei -20 °C [kPA]	-1,382.65	-1,310.40	-1,492.64	
Spannung bei -15 °C [kPA]	-685.64	-687.94	-775.92	
Spannung bei -10 °C [kPA]	-313.75	-323.37	-368.51	335.21
Spannung bei -5 °C [kPA]	-124.26	-137.66	-162.78	
Spannung bei 0 °C [kPA]	-55.97	-62.46	-68.58	
Spannung bei 5 °C [kPA]	-24.89	-30.98	-34.57	30.15
Spannung bei 10 °C [kPA]	-12.58	-16.33	-19.31	
Spannung bei 15 °C [kPA]	-5.12	-8.94	-10.96	
Spannung bei 20 °C [kPA]	0.92	1.71	1.15	1.26
Failure point				
max. Spannung [Mpa]	5.898	3.832	6.129	5.287
Temperatur [°C]	-37.0	-31.9	-36.1	-35.0
Zeilenzähler	20,600	18,709	20,239	

Table D-18: Thermal stress restrained specimen test (TSRST) of AC 16 T D mix with RAP and rejuvenator 3

Temperature, [ºC]	-25			-10		
Pk-Nr.	D33-3	D53-2	D53-3	D23-4	D33-2	D33-4
Width, [mm]	49.2	49.0	49.0	49.6	49.8	49.8
Length, [mm]	158.6	158.2	157.3	160.0	158.6	158.5
Raumdichte ρ_b [g/cm³]:	2.496	2.490	2.490	2.491	2.496	2.489
Maximale Zugfestigkeit [Mpa]	5.672	7.419	7.289	6.088	6.366	7.317
Maximale Bruchdehnung [%]	0.02	0.03	0.03	0.06	0.08	0.11
Zeilenzähler max. Bruchd.	834	954	932	960	1,003	1,010
Temperature, [ºC]	5			20		
Pk-Nr.	D23-1	D33-5	D53-5	D23-2	D33-1	D53-4
Width, [mm]	49.0	49.7	49.3	49.0	49.0	49.8
Length, [mm]	160.0	158.3	157.3	160.0	159.5	158.5
Raumdichte ρ_b [g/cm³]:	2.486	2.504	2.487	2.487	2.495	2.489
Maximale Zugfestigkeit [Mpa]	3.307	3.023	3.436	0.798	0.714	0.882
Maximale Bruchdehnung [%]	0.39	0.33	0.37	1.41	1.31	1.14
Zeilenzähler max. Bruchd.	954	866	1,062	1,667	1,550	1,899